Università degli Studi del Piemonte Orientale

"Amedeo Avogadro"

Dipartimento di Scienze e Innovazione Tecnologica

Dottorato di Ricerca in Scienze Chimiche

DEVELOPMENT AND VALIDATION OF ANALYTICAL METHODS BASED ON MASS-SPECTROMETRY FOR THE DETERMINATION OF BIO-ACTIVE MOLECULES

Dott. ssa Rita Mastroianni

Relatore: Prof. Emilio Marengo

Coordinatore dottorato: Prof. Domenico Osella

XXVIII Ciclo (A.A. 2012-2015)

The work presented in this thesis was carried out entirely in the Mass Spectrometry Laboratory, NBE Bioanalytics Department, Merck Serono, Colleretto Giacosa (Turin), Italy.

A tutte le persone che mi amano

Contents

Acronyms and abbreviations

2D:	Two Dimensional
3D:	Three Dimensional
Å:	Angstrom
AA:	Amino acids
ACN:	Acetonitrile
ACS:	American Chemical Society
ADAs:	Anti-Drug Antibodies
ADC:	Antibody Drug Conjugates
AGC:	Automatic Gain Control
AIF:	All Ion Fragmentation
amu:	atomic mass unit
AN:	Analyte
APCI:	Atmospheric Pressure Chemical Ionization
BEH:	Ethylene Bridged Hybrid
BIAS%:	Accuracy percent
BSA:	Bovine Serum Albumin
$CaCl_2$:	Calcium Chloride
CAD:	Collisionally Activated Dissociation
CE:	Collision Energy
CH_3CN :	Acetonitrile
CI:	Chemical Ionization
Conc.:	Concentration
CSH:	Charged Surface Hybrid
CV%:	Coefficient Variation Percent
CXP:	Cell Exit Potential

Da:	Dalton
DAR:	Drug to Antibody Ratio
DBK:	Double Blank
DC:	Direct Current
DNA:	Deoxyribonucleic acid
Dp:	Diameter of particles
DP:	Declustering Potential
DTT:	D-L Dithiothreitol
EGFR:	Epidermal Growth Factor Receptor
EI:	Electronic Impact
EMA:	European Medicines Agency
EP:	Entrance Potential
Fab:	Fragment antigen-binding
Fc:	Fragment, crystallizable
FDA:	Food and Drug Administration
FTMS:	Fourier Transform Mass Spectrometry
FWHM:	Full Width at Half Maximum
GC-MS:	Gas Chromatography-Mass Spectrometry
GLP:	Good Laboratory Practice
HC:	Heavy Chain
HCD:	Higher Energy Collision Dissociation
HER2:	Human Epidermal growth factor Receptor 2
HETP:	Height Equivalent to a Theoretical Plate
HPLC:	High Performance Liquid Chromatography
$HCOONH_4$:	Ammonium Formate
HFBA:	HeptaFluoroButyric Acid
HPA:	HydroxyPropylAmide
ICH:	International Conference on Harmonization
i.d.:	Internal Diameter

ID:	Identity
IS:	Internal Standard
IAA:	Iodoacetic acid
IAM:	Iodoacetamide
IT:	Ion Trap
IgG:	Immunoglobulin G
IL-17 A/F:	Interleukin 17 type A and F
LC:	Light Chain
LC-MS/MS:	Liquid Chromatography-Mass Spectrometry/Mass Spectrometry
LTQ:	Linear Trap Quadrupole
LLOQ:	Lower Limit Of Quantitation
kV:	kiloVolt
M:	Molar
mAb(s):	monoclonal Antibody (ies)
MALDI:	Matrix-Assisted Laser Desorption/Ionisation
MCX:	Mixed Cation Exchange
mer:	monomer
mM:	milliMolar
mmu:	millimass unit
MeOH:	Methanol
min:	minutes
MOA:	Mechanism Of Action
MPA:	Mobile Phase A
MPB:	Mobile Phase B
MRM:	Multiple Reaction Monitoring
ms:	millisecond
MSIA:	Mass Spectrometry Immuno Assay
m/z:	mass to charge
MW:	Molecular Weight

Nb:	Nanobody
NCE:	Normalized Collision Energy
NH_3 (NH_4OH):	Ammonium hydroxide 33% in Water
nL:	nanoLiter
Nom.	Nominal
PBS:	Phosphate Buffered Saline
PK:	PharmacoKinetic
p-ESI:	positive ElectroSpray Ionization
pI:	Isoelectric point
PNGasF:	Peptide N-Glycosidase (from flavobacterium)
PPT:	Protein Precipitation Technique
Q (1, 2 or 3):	First, Second and Third quadrupole
QC:	Quality Control
r:	correlation coefficient
R:	Coefficient of determination of a linear regression
Reag.Ph.Eur.:	Reagent European Pharmacopoeia
RF:	Radio Frequency
rpm:	revolutions per minute
RSLC:	Rapid Separation Liquid Chromatography
RT:	Room Temperature
RT:	Redox Titration
SCX:	Strong Cation Exchange
SD:	Standard Deviation
S/N:	Signal to Noise Ratio
SPE:	Solid Phase Extraction
SS:	Spiked Sample
STD:	Standard
T:	Temperature
T:	Aqueous Titration

T-DM1:	antibody–drug conjugate trastuzumab emtansine
TFA:	Trifluoroacetic Acid
TIC:	Total Ion Current
TQ:	Triple Quadrupole
TRIS-HCl:	Tris (hydroxymethyl) aminomethane hydrochloride
UHPLC:	Ultra High Performance Liquid Chromatography
UPLC:	Ultra Performance Liquid Chromatography
ULOQ:	Upper Limit Of Quantitation
V:	Volt
Vol.:	Volume
VS:	Validation Sample

1. Introduction

Liquid Chromatography-Mass Spectrometry (LC-MS) technology, including conventional LC-tandem Mass Spectrometry (MS/MS) and LC-High-Resolution Accurate Mass Spectrometry (HR/AMS), is emerging as an important strategy for analysis of therapeutic proteins, nanobodies, monoclonal antibodies (mAbs), antibody - drug - conjugates (ADC) and peptides in biological samples.

Development of LC-MS/MS bioanalytical methods is a key point in ensuring accurate, selective and sensitive quantification of bio-molecules in toxicokinetic and pharmacokinetic studies.

Currently, the two main techniques to quantify biomolecules (therapeutic proteins, peptides etc.) are immunoassay and LC-MS/MS.

Immunoassay methods have historically been the only platform available for the bioanalysis of large molecules offering several advantages: the ability to measure low concentrations of molecules, minimal sample preparation and high-throughput platforms.

However, this technique often suffers from poor linear quantification ranges and requires specific antibodies to be raised to the target analyte, which can be expensive and time consuming.

Additionally, interferences from homologous peptide and high-abundance proteins in the sample can affect the selectivity of the immunoassay methods.

MS-based technology is now providing alternative approaches with inherent characteristics that complement immunoassay technique: a truly orthogonal detection principle, based on the physicochemical properties of the target protein analyte or proteotypic peptide sequences present in its primary structure and a potentially greater tolerance for interferences from other proteins (e.g., anti-drug antibodies, ADAs) which may be present[1].

The aim of this PhD, carried out in Merck Serono laboratories, was to develop and qualify/validate bioanalytical methods for determining bio-active molecules using the LC-MS platform.

[1] The AAPS Journal, Vol. 17, No. 1, January 2015 (© 2014), doi 10.1208/s12248-014-9685-5

It is also important to validate, in a Good Laboratory Practice (GLP) environment, the systems, materials and processes that have to be applied to conduct pre-clinical study. This means that all the process parameters will be evaluated, optimized and validated for long-term process usage in a regulated environment and eventually transferred to other studies.

Chapter I

1. Bioanalysis

Bioanalysis is a sub-discipline of analytical chemistry covering the quantitative measurement of xenobiotics (drugs and their metabolites, and biological molecules in unnatural locations or concentrations) and biotics (macromolecules, proteins, DNA, large molecule drugs and metabolites) in biological systems.

The focus of bioanalysis in the pharmaceutical industry is to provide a quantitative measure of the active drug and/or its metabolite(s) for the purpose of pharmacokinetics, toxicokinetics, bioequivalence and exposure–response (pharmacokinetics/pharmacodynamics) studies. Bioanalysis also applies to drugs used for illicit purposes, forensic investigations, anti-doping testing in sports, and environmental concerns.

Bioanalysis was traditionally thought of in terms of measuring small molecule drugs. However, the past twenty years have seen an increase in biopharmaceuticals (e.g. proteins and peptides), which have been developed to address many of the same diseases as small molecules. These larger biomolecules have presented their own unique challenges to quantification[2].

Modern drugs are more potent and have required more sensitive bioanalytical assays to accurately and reliably determine these drugs at lower concentrations. This has driven improvements in technology and analytical methods.

1.1. Bioanalytical techniques

Bioanalytical techniques, as the name suggests, are the analytical tools to study biological molecules, and non-biological molecules involved with life, such as drugs and biological processes. These tools are routinely used to identify, estimate, purify, and characterize

[2] Booth, Brian P (2009-04-03). "Welcome to Bioanalysis" (PDF). Bioanalysis 1 (1): 1–2. doi:10.4155/bio.09.4. Retrieved 2010-05-13.

biomolecules. Quantification of molecules in biological samples is at the heart of bioanalysis and is routinely used to diagnose various diseases and metabolic disorders.

Bioanalytical methods are also used to detect drugs and their metabolites in biological samples. Initially, nonspecific assays were used to quantify drugs in biological samples. Evolution of existing assays, advancement in instrumentation, and introduction of newer techniques have made it possible to distinguish drug molecules and their closely related metabolites in complex biological specimens.

Identification and quantification of analytes is perhaps the most common application of bioanalytical methods. Various diseases and disorders including cancers are diagnosed by estimating the levels of characteristic biomarkers in a particular tissue or organ.

Qualitative analysis tells us about the presence or absence of an analyte in a sample. Absence of an analyte, however, may be due to concentrations below the detection level of the bioanalytical technique used. Qualitative analyzes are used where detection of an analyte is sufficient to take a further course of action. In certain cases, however, it is important to estimate the concentration of the analyte. A quantitative analysis would allow the determination of the actual amount of substance present in the sample.

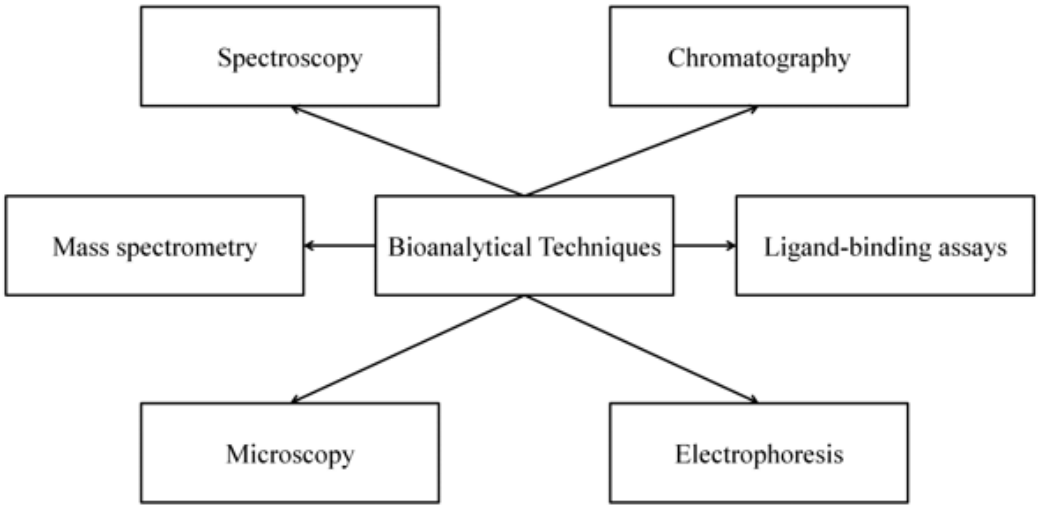

Figure 1: *Various bioanalytical methods*

Chapter II

1. Introduction to Mass Spectrometry

Currently, mass spectrometry technology is the most important approach in analytical methods thanks to the several advantages it offers, among which high sensitivity, detection limits, selectivity, speed and diversity of application.

In analytical chemistry, the most recent applications are generally oriented towards biochemical problems, such as proteome, metabolome, high throughput in drug discovery and metabolism, and so on. Other analytical applications are routinely applied in pollution control, food control, forensic science, natural products or process monitoring.

Mass spectrometry progressed extremely rapidly between 1995 and 2005. This progress has led to the advent of entirely new instruments. New atmospheric pressure sources were developed, existing analyzers were perfected and new hybrid instruments were made by new combinations of analyzers. This has led to the development of new applications. New high-throughput mass spectrometry was developed to meet the needs of proteomics, metabolomics and other 'omics'[3].

1.1. Principles

The first step in the mass spectrometric analysis of compounds is the production of gas - phase ions of the compound, for example by electron ionization:

$$M + e^- \longrightarrow M^{\bullet +} + 2e^-$$

Figure 2: Electron ionization

This molecular ion normally undergoes fragmentations.

[3] Edmond de Hoffmann and Vincent Stroobant, Mass Spectrometry, Principle and Application, Third Edition

Because it is a radical cation with an odd number of electrons, it can fragment to give either a radical and an ion with an even number of electrons, or a molecule and a new radical cation:

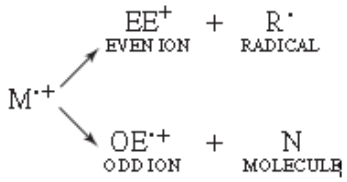

***Figure 3**: Type of ions generated by electron ionization*

These two types of ions have different chemical properties. Each primary product ion derived from the molecular ion can, in turn, undergo fragmentation, and so on. All these ions are separated in the mass spectrometer according to their mass-to-charge ratio, and are detected in proportion to their abundance. A mass spectrum of the molecule is thus produced. It provides this result as a plot of ion abundance versus mass-to-charge ratio.

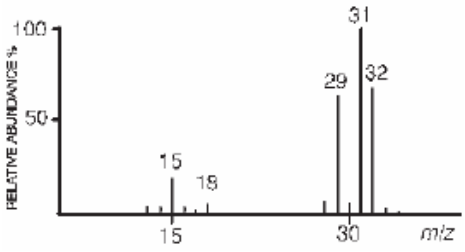

m/z	Relative abundance (%)	*m/z*	Relative abundance (%)
12	0.33	28	6.3
13	0.72	29	64
14	2.4	30	3.8
15	13	31	100
16	0.21	32	66
17	1.0	33	0.73
18	0.9	34	~ 0.1

***Figure 4**: Example of mass spectrometry data*

As illustrated in **Figure 4** mass spectra can be presented as a bar graph or as a table. In either presentation, the most intense peak is called the base peak and is arbitrarily assigned the relative abundance of 100 %. The abundances of all the other peaks are given their proportionate values, as percentages of the base peak. Many existing publications label the y axis of the mass spectrum as number of ions, ion counts or relative intensity. Most of the

positive ions have a charge corresponding to the loss of only one electron, but for large molecules, multiple charged ions also can be obtained. Ions are separated and detected according to the mass-to-charge ratio.

There are different ways to define and thus to calculate the mass of an atom, molecule or ion. For stoichiometric calculations, chemists use the average mass calculated using the atomic weight, which is the weighted average of the atomic masses of the different isotopes of each element in the molecule. In mass spectrometry, the nominal mass or the mono-isotopic mass is generally used. The nominal mass is calculated using the mass of the predominant isotope of each element rounded to the nearest integer value that corresponds to the mass number, also called nucleon number. But the exact masses of isotopes are not exact whole numbers. They differ slightly from the summed mass values of their constituent particles that are protons, neutrons and electrons. These differences, which are called the mass defects, are equivalent to the binding energy that holds these particles together.

Consequently, every isotope has a unique and characteristic mass defect. The mono-isotopic mass, which takes into account these mass defects, is calculated by using the exact mass of the most abundant isotope for each constituent element.

The difference between the average mass, the nominal mass and the mono-isotopic mass can amount to several Da, depending on the number of atoms and their isotopic composition. The type of mass determined by mass spectrometry depends largely on the resolution and accuracy of the analyzer. Let us consider CH_3Cl as an example. Actually, chlorine atoms are mixtures of two isotopes, whose exact masses are respectively 34.968 Da and 36.965.

Their relative abundances are 75.77% and 24.23 %. The atomic weight of chlorine atoms is the balanced average: (34.968…×0.7577+36.965…×0.2423) =35.453 Da.

The average mass of CH_3Cl is [12.011… + (3×1.00) + 35.453…] = 50.4878 Da, whereas its mono-isotopic mass is [12.000 + (3×1.007…) + 34.968852…] = 49.992 327 u. When the mass of CH_3Cl is measured with a mass spectrometer, two isotopic peaks will appear at their respective masses and relative abundances. Thus, two mass-to-charge ratios will be observed with a mass spectrometer. The first peak will be at m/z (34.968…+12.000+3×1.007….) = 49.992.

The mass-to-charge value of the second peak will be (36.965…+12.000+3×1.007….) = 51.989. To better explain the differences between monoisotopic mass and average mass we could imagine two simple alkane molecules ($C_{20}H_{42}$ and $C_{100}H_2O_2$)[4].

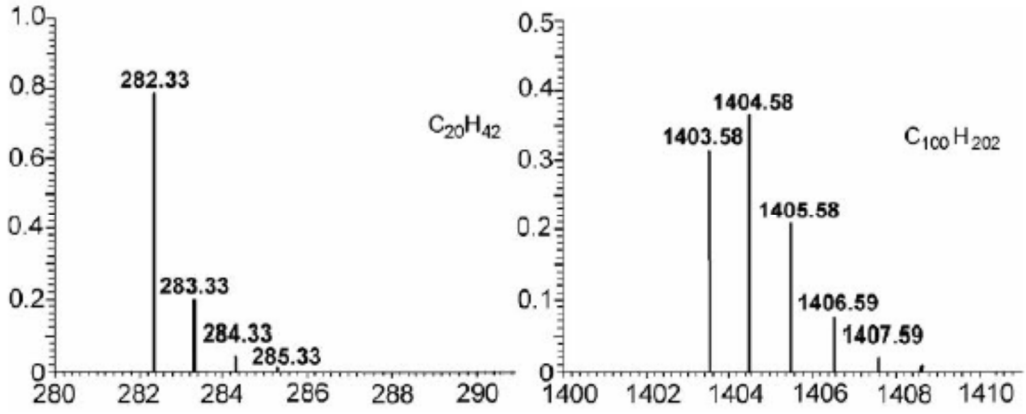

***Figure 5**: The monoisotopic mass is the lightest mass of the isotopic pattern whereas the average mass, used by chemists in stoichiometric calculations, is the balanced mean value of all the observed masses.*

1.2. Mass Spectrometer Instruments

The instrument consists of three major components:

1. Ion Source: for producing gaseous ions from the substance being studied.

2. Analyzer: for resolving the ions into their characteristic mass components according to their mass-to-charge ratio.

3. Detector System: for detecting the ions and recording the relative abundance of each of the resolved ionic species.

[4] Edmond de Hoffmann and Vincent Stroobant, Mass Spectrometry, Principle and Application, Third Edition

In addition, a sample introduction system is necessary to admit the samples to be studied to the ion source while maintaining the high vacuum requirements (~10^{-6} to 10^{-8} mm of mercury) of the technique; and a computer is required to control the instrument, acquire and manipulate data, and compare spectra to reference libraries.

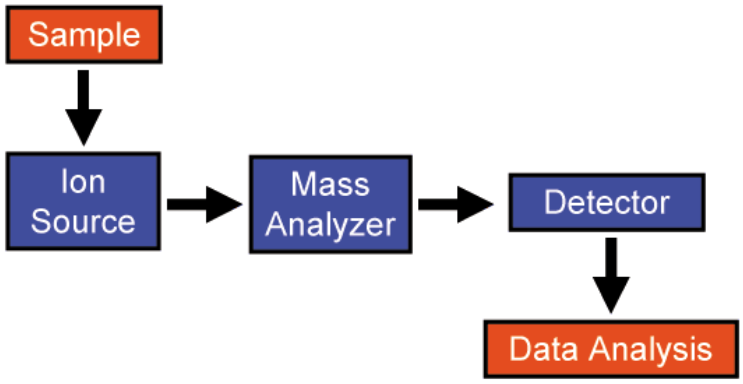

***Figure 6**: Components of a Mass Spectrometer*

With all the above components, a mass spectrometer should always perform the following processes:

1. Produce ions from the sample in the ionization source.
2. Separate these ions according to their mass-to-charge ratio in the mass analyzer.
3. Eventually, fragment the selected ions and analyze the fragments in a second analyzer.
4. Detect the ions emerging from the last analyzer and measure their abundance with the detector that converts the ions into electrical signals.
5. Process the signals from the detector that are transmitted to the computer and control the instrument using feedback[5].

[5] Edmond de Hoffmann and Vincent Stroobant, Mass Spectrometry, Principle and Application, Third Edition

This Ph.D. involved working mainly with triple quadrupole mass analyzers (Ab Sciex 5500 Triple Quadrupole™) and, for one project, with the Orbitrap (Orbitrap Elite™, Thermo Fischer) and the Q-Exactive Plus Hybrid Quadrupole-Orbitrap™ (Thermo Fischer), which will be described in detail in the following paragraphs.

1.3. The ESI Ion Source

Mass spectrometers use an ion source to generate ions, then sort and identify those ions in the mass analyzer according to their m/z ratios. Different types of ion sources commonly used include, among others, electrospray ionization (ESI) and atmospheric pressure chemical ionization (APCI).

The electrospray ionization technique (ESI) (**Figure 7**) is a method to generate highly charged droplets from which ions are ejected by an ion evaporation process. Ion Spray is an improved version of electrospray, in which droplets are created by both a high electric field and a pneumatic nebulization which allows higher liquid flow rates to be employed and produces a more stable ion current.

The mechanism by which ions can be emitted from a liquid into the gas phase was first proposed in 1976[6] and the term Ion Evaporation was applied to the process. Experimental evidence combined with a theoretical model suggested that, as a charged droplet evaporates, a critical point may be reached at which it is kinetically and energetically possible for ions at the surface of the liquid to “evaporate”.

The details of the process are independent of how the droplets are originally formed or how they are originally charged. A charged droplet contains the solvent plus both positive and negative ions, with ions of one polarity being dominant, the difference being the net charge.

The excess ions are those which were originally present in the liquid being sprayed. If there are enough excess ions, and the droplet evaporates far enough, a critical field is reached at which ions are emitted from the surface. The rate of ion emission depends on the solvation energies of the individual ions so that one type of ion may preferentially evaporate if it has lower solvation energy.

[6] Iribarne, J.V. and Thomson, B.A. (1976). On the Evaporation of Small Ions from Charged Droplets. J. Chem. Phys. 64, 2287.

In both electrospray and ion spray, an electric field is generated at the tip of the sprayer by applying a high voltage directly to the sprayer. Ions of one polarity are preferentially drawn into the drops by the electric field as they are separated from the bulk liquid.

Electrospray and ion-spray operate both with flow from 1 – 5 µl/min to 1 mL/min[7].

The ions observed are created by the addition of a proton (a hydrogen ion) and denoted $[M+H]^+$ or of another cation such as sodium ion, $[M+Na]^+$, or the removal of a proton, $[M-H]^-$. Multiply charged ions such as $[M+2H]^{2+}$ are often observed. For large macromolecules, there can be many charge states, occurring with different frequencies; the charge can be as great as, $[M+25H]^{25+}$ for example.

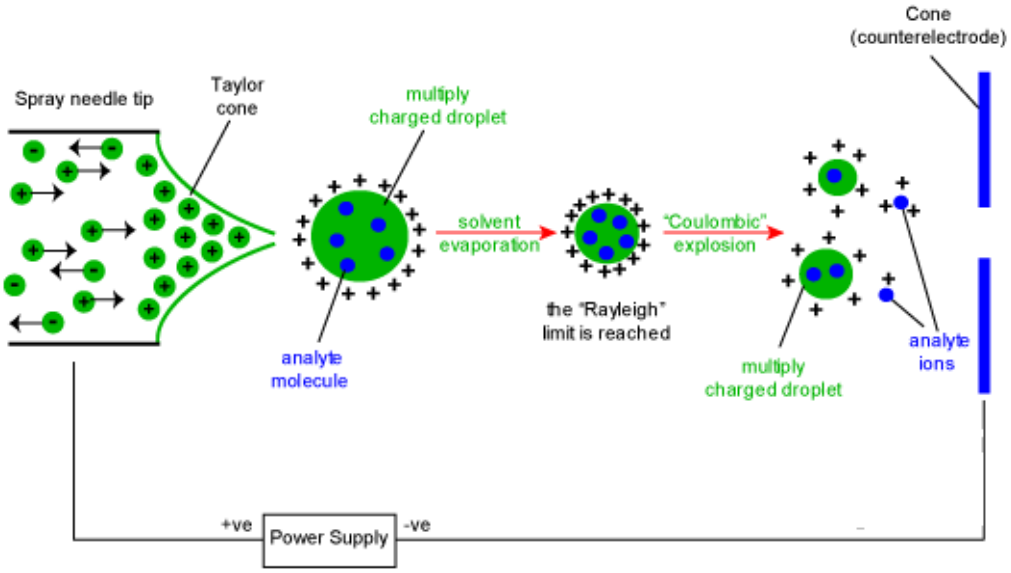

Figure 7: *Scheme of an ESI interface*

1.4. The Quadrupole Mass Analyzer

The quadrupole analyzer is a device which uses the stability of the trajectories in oscillating electric fields to separate ions according to their m/z ratios. Quadrupole analyzers are made up of four rods of circular or, ideally, hyperbolic section (**Figure 8**).

The rods must be perfectly parallel.

[7] The API Book, Perkin-Elmer Sciex Instruments. 1994.

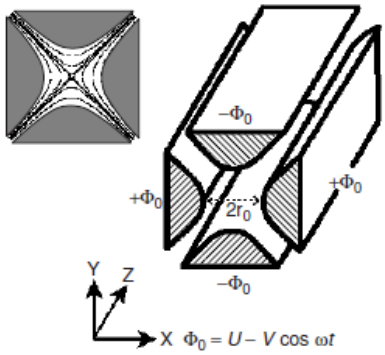

Figure 8: *Quadrupole with hyperbolic rods and applied potentials. The equipotential lines are represented above, on the left.*

A positive ion entering the space between the rods will be drawn towards a negative rod. If the potential changes sign before it discharges itself on this rod, the ion will change direction. The principle of the quadrupole was described by Paul and Steinwegen at Bonn University, in 1953. They started from research work on the strong focusing of ions carried out in 1951 in Athens by the electrical engineer Christophilos.

Ions travelling along the z axis are subjected to the influence of a total electric field made up of a quadrupolar alternative field superimposed on a constant field resulting from the application of the potentials upon the rods:

$\Phi 0 = + (U - V \cos \omega t)$ and $- \Phi 0 = - (U - V \cos \omega t)$

In this equation, $\Phi 0$ represents the potential applied to the rods, ω the angular frequency (in radians per second = $2\pi v$, where v is the frequency of the RF field), U is the direct potential and V is the 'zero-to-peak' amplitude of the RF voltage. Typically, U will vary from 500 to 2000V and V from 0 to 3000V (from -3000 to +3000V peak to peak).

The ions accelerated along the z axis enter the space between the quadrupole rods and maintain their velocity along this axis. However, they are submitted to accelerations along x and y that result from the forces induced by the electric fields.

The equations of motion of an ion accelerated through the x axis of a quadrupole lead to the following equations:

$$U = a_u \frac{m}{z} \frac{\omega^2 r_0^2}{8e} \quad \text{and} \quad V = q_u \frac{m}{z} \frac{\omega^2 r_0^2}{4e}$$

The last terms of both the U and V equations is a constant for a given quadrupole instrument, as they operate at constant ω. We see that switching from one m/z to another results in a

proportional multiplication of a_u and q_u (stability areas), which means changing the scale of the drawing in U, V coordinates.

Figure 9 represents in a U, V diagram the areas A obtained with different masses. We can see in this diagram that scanning along a line maintaining the U/V ratio constant allows the successive detection of the different masses. So long as the line keeps going through stability areas, then the higher the slope, the better the resolution[8] .

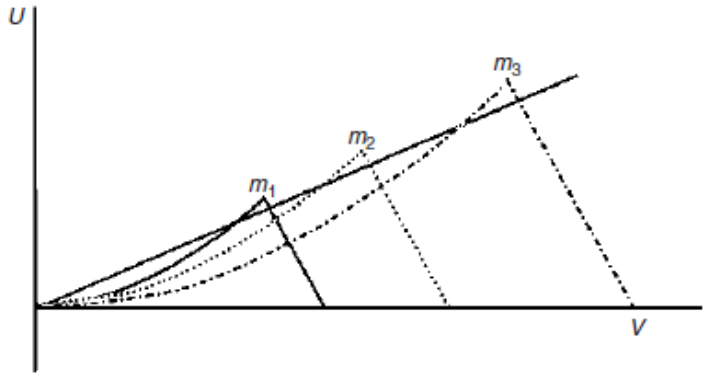

***Figure 9**: Stability areas as a function of U and V for ions with different masses (m1 < m2 < m3). Changing U linearly as a function of V, we obtain a straight operating line that allows us to observe those ions successively. A line with a higher slope would give us a higher resolution, so long as it goes through the stability areas. Keeping U=0 (no direct potential) we obtain zero resolution. All of the ions have a stable trajectory so long as V is within the limits of their stability area. Reproduced (modified) from March R.E. and Hughes R.J., Quadrupole Storage Mass Spectrometry, Wiley, New York, 1989, with permission.*

1.4.1. The Triple Quadrupole Mass Analyzer

The quadrupole is one type of mass analyzer. It is the component of the instrument responsible for filtering sample ions, based on their m/z ratio. A quadrupole mass analyzer is essentially a mass filter that is capable of transmitting only the ion of choice. The mass spectrum is obtained by scanning through the mass range of interest over time. The quadrupole consists of four parallel metal rods. Each opposing rod pair is connected electrically and a radio frequency (RF) voltage is applied between one pair of rods, and the other. A direct current (DC) voltage is then superimposed on the RF voltage. Ions travel down the quadrupole between the rods. Only ions of a certain m/z will reach the detector for a given ratio of voltages: other ions have unstable trajectories and will collide with the rods.

[8] Hoffmann E (2007) Mass spectrometry: principles and application 3rd edition

In liquid chromatography-mass spectrometry or gas chromatography-mass spectrometry they serve as exceptionally high specificity detectors.

A linear series of three quadrupoles can be used, known as “triple quadrupole” mass spectrometer. The first (Q1) and third (Q3) quadrupoles act as mass filters, and the middle (Q2) quadrupole is employed as a collision cell.

This collision cell is an RF only quadrupole (non-mass filtering) using Ar or N_2 gas (~10^{-3}torr) to induce collisional dissociation of selected precursor ions from Q1. Subsequent fragments are passed through to Q3 where they may be filtered or scanned.

This process allows for the study of fragments (product ions) which are crucial in structural identification. For example, the Q1 may be set to "filter" for a drug ion of a known mass, which is fragmented in Q2. The third quadrupole (Q3) can then be set to scan the entire m/z range, giving information on the sizes of the fragments made. Thus, the structure of the original ion can be deduced[9] (**Figure 10**).

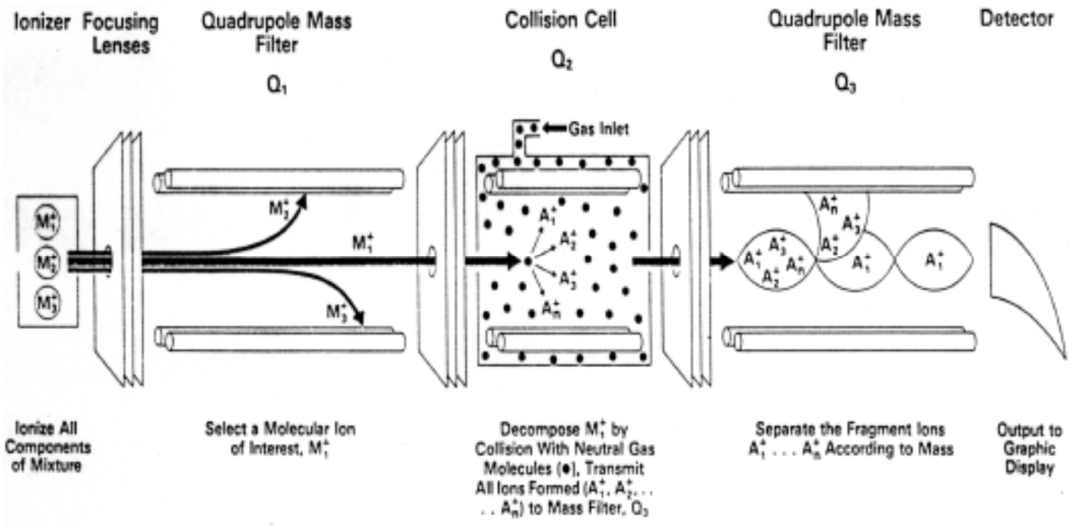

Figure 10: *An example of Triple Quadrupole*

Quadrupole instruments typically have unit mass resolution throughout the mass range.

[9] M.Vincenti. MS/MS Triple Quadrupole Analyzers MSn Ion Trap Analyzers, Acquisitions Methods, Scuola Nazionale di Spettrometria di Massa, Parma.

In a triple quadrupole mass spectrometer, there are several types of experiment that can be performed. The figures show a schematic representation of four common types of MS/MS experiment:

Product ion scan.

In this case, the precursor ion is focused in Q1 (MS1) and transferred into Q2 (MS2), the collision cell, where it interacts with a collision gas and fragments. The fragments are then measured by scanning Q3. This results in the typical MS/MS spectrum and is the method most commonly employed with ESI ionization and/or LC-MS, description in **Figure 11 A**.

Precursor ion scan.

In this case Q3 is held to measure the occurrence of a particular fragment ion and Q1 (MS1) is scanned. This results is a spectrum of precursor ions that result in that particular product ion, which is especially useful when used with EI or CI ionization and/or GC-MS, description in **Figure 11 B**.

Neutral loss scan.

In this case Q1 (MS1) is scanned as in precursor ion scan but this time Q3 is also scanned to produce a spectrum of precursor ions that undergo a particular neutral loss. Again this mode is especially useful for EI and CI ionization, description in **Figure 11 C.**

Multiple Reaction Monitoring.

Also in this case, the precursor ion is focused in Q1 (MS1) and transferred into Q2 (MS2), the collision cell, where it interacts with a collision gas and fragments. Q3 (CID) is held to measure a particular fragment ion, description in **Figure 11 D**.

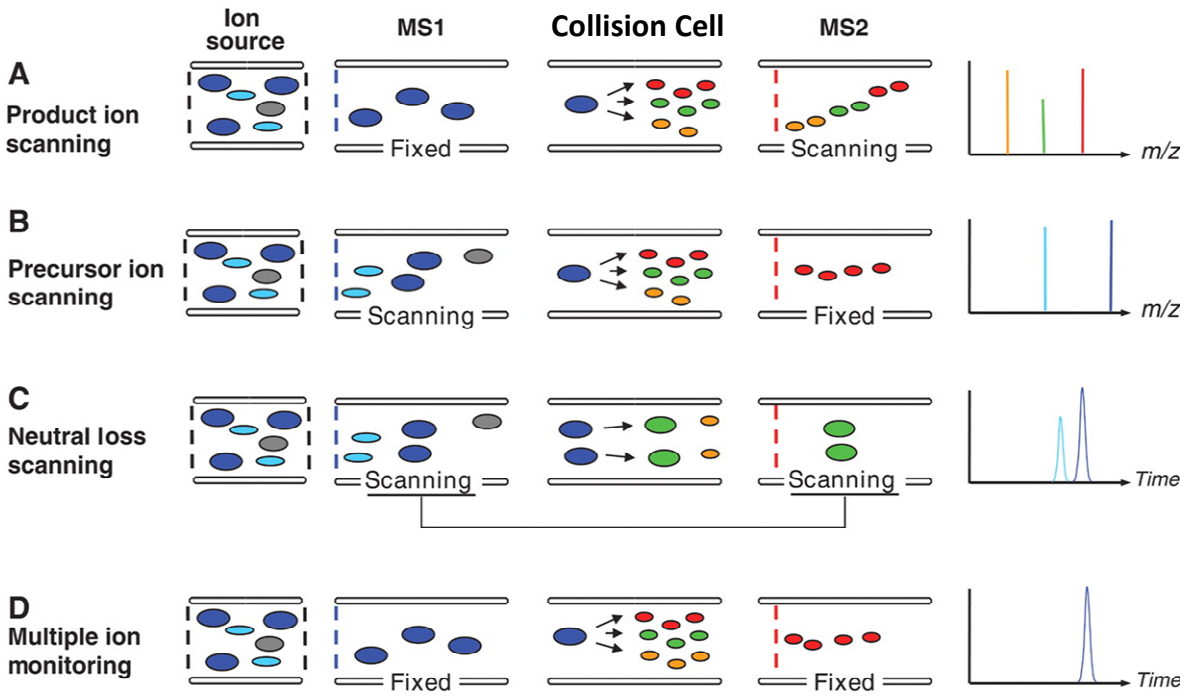

***Figure 11**: Scheme of the main type of triple quadrupole experiments*

1.5. The Ion trap

An ion trap is a device that uses an oscillating electric field to store ions. The ion trap works by using an RF quadrupolar field that traps ions in two or three dimensions. An ion trap mass spectrometer may incorporate a Penning trap (Fourier transform ion cyclotron resonance), Paul trap or Kingdon trap.

A Penning trap stores charged particles using a strong homogeneous axial magnetic field to confine particles radially and a quadrupole electric field to confine the particles axially[10].

A Paul trap is a type of quadrupole ion trap that uses static direct current (DC) and radio frequency (RF) oscillating electric fields to trap ions (**Figure 12**). Paul traps are commonly used as a component of a mass spectrometer. The invention of the 3D quadrupole ion trap itself is attributed to Wolfgang Paul who shared the Nobel Prize in Physics in 1989 for this work.

[10] Brown, L.S., Gabrielse, G.(1986). Rev. of Modern Physics58: 233

The trap consists of two hyperbolic metal electrodes with their foci facing each other and a hyperbolic ring electrode halfway between the other two electrodes. Ions are trapped in the space between these three electrodes by the oscillating and static electric fields.

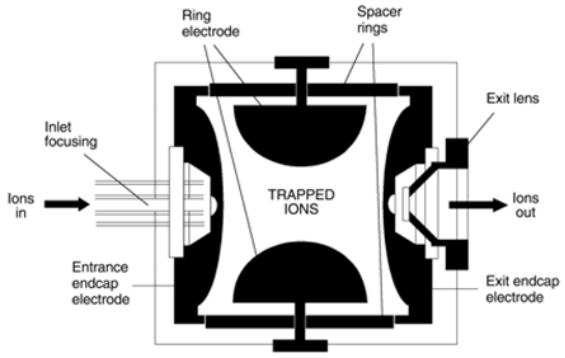

***Figure 12**: Schematic view of a 3D ion trap*

A Kingdon trap consists of a thin central wire and an outer cylindrical electrode. A static applied voltage results in a radial logarithmic potential between the electrodes. In a Kingdon trap there is no potential minimum to store the ions; however, they are stored with a finite angular momentum about the central wire and the applied electric field in the device allows for the stability of the ion trajectories[11]. It consists of a thin central wire, an outer cylindrical electrode and isolated end cap electrodes at both ends. A static applied voltage results in a radial logarithmic potential between the electrodes. In 1981, Knight introduced a modified outer electrode that included an axial quadrupole term that confines the ions on the trap axis.

1.5.1. The Orbitrap

The Orbitrap mass analyzer bears a similarity to an earlier ion storage device, the Kingdon trap, as well as to two types of ion-trapping mass analyzers, the Paul trap (quadrupole ion trap), and the Fourier transform ion cyclotron resonance instrument. The first step in the set of inventions that led to the Orbitrap was the implementation of orbital trapping, a method of ion trapping, which can itself be used for mass analysis. The orbitrap mass analyzer (which can also be considered a refined Knight-style Kingdon trap) is composed of a spindle-like central electrode and a barrel-like outer electrode (**Figure 13**). A DC voltage is applied

[11] Major, Fouad G (2005). Springer. ISBN 3-540-22043-7

between the two axially symmetric electrodes, resulting in the following electrostatic potential distribution[12],[13],[14]

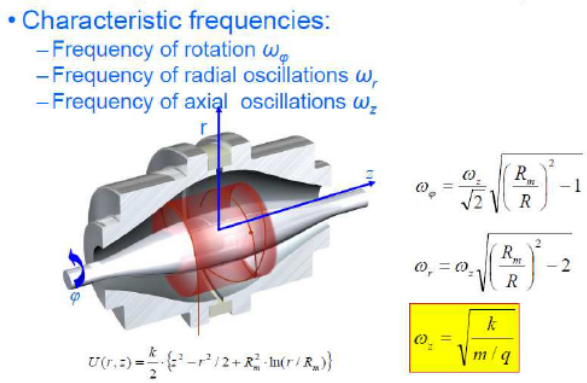

Figure 13: *Equations that rule the Orbital trap, the axial oscillation directly depends on the mass to charge ratio of the ions (J. Mass Spectrom. 2005; 40: 430–443)*

Ions are injected into the orbitrap after the voltage on the central electrode is turned on (typically 50–90 msec) but before the voltage has reached its final value. Consequently, as the ions enter the orbitrap they experience a monotonic increase in electric field strength, a process termed ‘‘electrodynamic squeezing’’[15],[16]. This has the effect of contracting the radius of the ion cloud, as well as pulling the ion packet closer to the z-axis (i.e., reducing the rotational radius), thereby preventing collisions with the outer electrode as the packets begin their axial oscillations. The risetime of the field strength (typically 20–100 msec) determines the trapped m/z range.

Since ions of different m/z values are injected at different times, with larger m/z ions arriving later, electrodynamics squeezing results in larger final amplitude of axial oscillation as well as larger mean orbital radius for ions of larger m/z ratio. Both effects will tend to increase the induced ion image current for larger m/z, although this effect may be partially or completely offset by the dependence on the axial frequency.

---

[12] Major, Fouad G (2005). Springer. ISBN 3-540-22043-7

[13] Gillig KJ et al. (1996) Int J Mass Spectrom 157,129–147

[14] Makarov A (1999) Mass spectrometer. US Patent 5,886,346

[15] Makarov A (2000). Anal Chem 72, 1156–1162

[16] Hu Q et al. (2007) J Am Soc Mass Spectrom 18, 980–983

Squeezing is stopped when there is no more possibility of losing ions to collisions with the outer electrode, which is maintained at virtual ground. After ions of all m/z values have entered the orbitrap, the voltage on the central electrode and deflector is held constant to prevent mass shifts during detection.

The deflector is switched to a voltage level that compensates for fringing fields caused by the injection slot. This is necessary to ensure that ions experience the harmonic axial potential throughout the volume of the orbitrap, thereby minimizing differences in frequency for ions of a given m/z value, which in turn could result in mass errors, peak splitting and lower resolution. After both the central electrode and deflector voltages are stabilized, image current detection may take place.

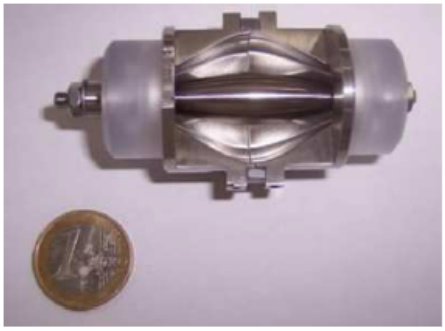

***Figure 14**: Real dimension of Orbital trap. Provided by Thermo Fisher Scientific*.

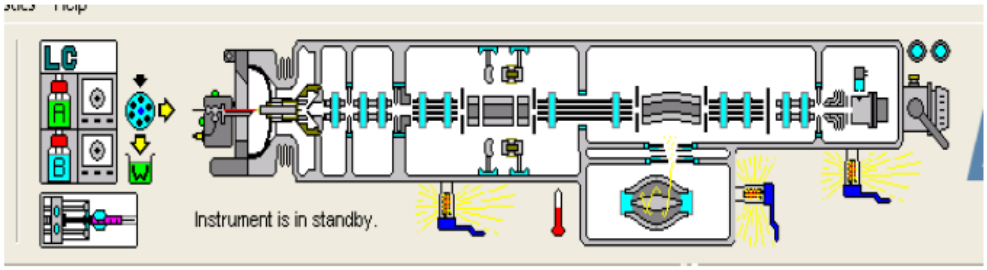

***Figure 15**: Schematic representation of the LTQ XL Orbitrap Picture obtained from LTQ Tune software, Thermo Fisher Scientific*

The high mass accuracy (better than 1 ppm with internal calibration), resolving power (up to 150,000) and MS^n capabilities of the LTQ-Orbitrap™ make it a valuable instrument for chemical analysis.

1.5.2. The Q-Exactive

Taking advantage of the small size of the Orbitrap analyzer a standalone benchtop instrument termed “Exactive” has been introduced mainly for small molecule applications. However, because of the absence of mass selection, its use in proteomics is limited to non-mass selective fragmentation of the entire mass range (called “All Ion Fragmentation” (AIF) on this instrument[17]).

A quadrupole Exactive instrument or “Q Exactive” would be able to select ions virtually instantaneously because of the fast switching times of quadrupoles and it would be able to fragment peptides in HCD mode on a similarly fast time scale.

Furthermore, because of the small size and mature technology used in current quadrupole mass filters, this analyzer combination should have a small footprint and be particularly robust.

Finally, the ability to separate “in space” and analyze MS and MS/MS ranges at high resolution in the Orbitrap analyzer offers the promise of enabling efficient multiplexed-scan modes not currently applied in proteomics research using trapping instruments.

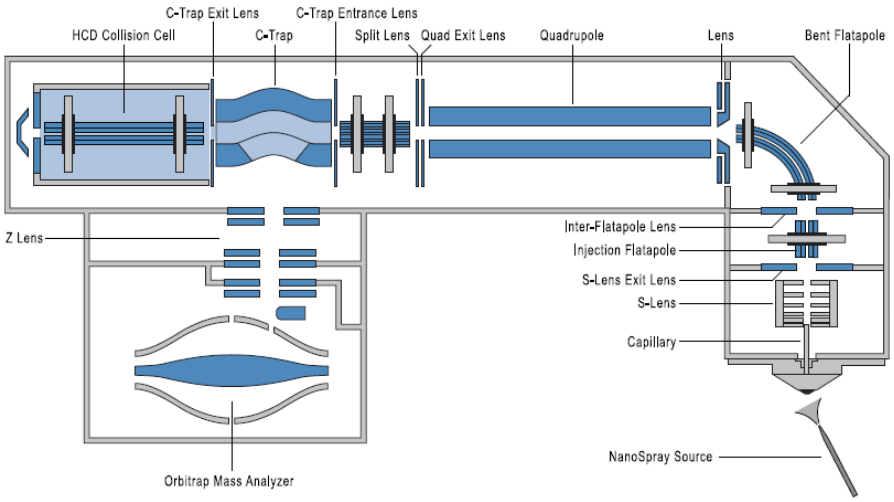

***Figure 16**: Construction details of the Q Exactive. This instrument is based on the Exactive platform but incorporates an S-lens, a mass selective quadrupole, and an HCD collision cell directly interfaced to the C-trap. Note that the drawing is not to scale.*

[17] Annette Michalski, Eugen Damoc§, Jan-Peter Hauschild§, Oliver Lange, Andreas Wieghaus, Alexander Makarov, Nagarjuna Nagaraj, Juergen Cox, Matthias Mann, and Stevan Horning, June 3, 2011, doi:10.1074/mcp.M111.011015

2. Liquid Chromatography – Mass Spectrometry

LC/MS is a hyphenated technique, combining the separation power of HPLC, with the detection power of Mass Spectrometry. Even with a very sophisticated MS instrument, HPLC is still useful to remove the interferences from the sample that would impact the ionization.
Its application is oriented towards the separation, general detection and potential identification of chemicals of particular masses in the presence of other chemicals (i.e., in complex mixtures), e.g., natural products from natural-products extracts, and pure substances from mixtures of chemical intermediates. Preparative LC-MS systems can be used for rapid mass-directed purification of specific substances from such mixtures that are important in basic research, and pharmaceutical, agrochemical, food, and other industries.

2.1. Ultra Performance Liquid Chromatography (UPLC™)

High performance liquid chromatography (HPLC) is a proven technique that has been used in laboratories worldwide over the past 30-plus years. One of the primary drivers for the growth of this technique has been the evolution of packing materials used to effect the separation. The underlying principles of this evolution are governed by the van Deemter equation, which is an empirical formula that describes the relationship between linear velocity (flow rate) and plate height (HETP or column efficiency). Since particle size is one of the variables, a van Deemter curve can be used to investigate chromatographic performance. According to the van Deemter equation, as the particle size decreases to less than 2.5 µm, not only is there a significant gain in efficiency, but the efficiency does not diminish at increased flow rates or linear velocities. By using smaller particles, speed and peak capacity (number of peaks resolved per unit time in gradient separations) can be extended to new limits, termed **Ultra Performance Liquid Chromatography™**, or UPLC™. The technology takes full advantage of chromatographic principles to run separations using columns packed with smaller particles and/or higher flow rates for increased speed, with superior resolution and sensitivity. **Figure 17** shows a stability indicating assay of five related substances accomplished in about one minute, proving that the resolving power of UPLC is not compromised even at high speed.

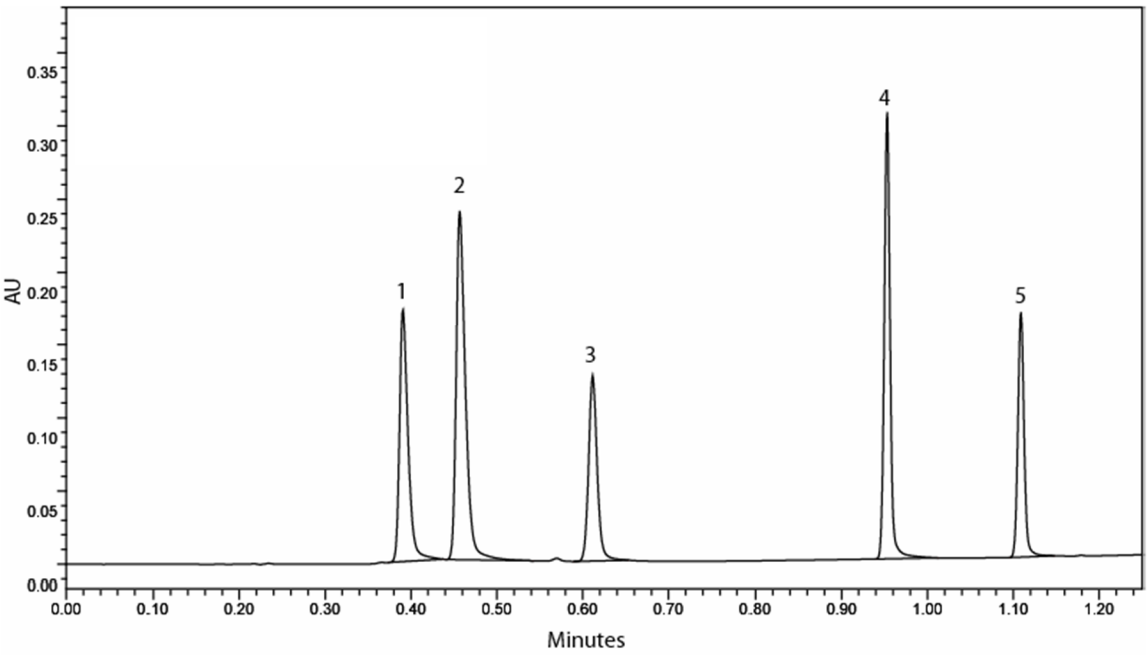

Figure 17: *UPLC separation of five substances (Source: Waters)*

Smaller particles provide not only increased efficiency, but also the ability to work at increased linear velocity without a loss of efficiency, providing both resolution and speed. Efficiency is the primary separation parameter behind UPLC™ since it relies on the same selectivity and retentivity as HPLC. In the fundamental resolution (Rs) equation:

$$Rs = \underbrace{\frac{\sqrt{N}}{4}}_{\text{System Efficiency}} \underbrace{\left(\frac{\alpha - 1}{\alpha}\right)}_{\text{Selectivitv}} \underbrace{\left(\frac{k}{k+1}\right)}_{\text{Retentivitv}}$$

resolution is proportional to the square root of N. But since N is inversely proportional to particle size (dp):

$$N \propto \frac{1}{dp}$$

as the particle size is lowered by a factor of three, from, for example, 5 µm (HPLC-scale) to 1.7 µm (UPLC-scale), N is increased by three and resolution by the square root of three or 1.7. N is also inversely proportional to the square of the peak width:

$$N \propto \frac{1}{\omega^2}$$

This illustrates that the narrower the peaks are, the easier they are to separate from each other. Also, peak height is inversely proportional to the peak width:

$$H \propto \frac{1}{\omega}$$

So as the particle size decreases to increase N and subsequently Rs, an increase in sensitivity is obtained, since narrower peaks are taller peaks. Narrower peaks also mean more peak capacity per unit time in gradient separations, desirable for many applications, e.g., peptide maps. Still another equation comes into play when migrating toward smaller particles:

$$F_{opt} \propto \frac{1}{dp}$$

This relationship also is revealed from the van Deemter plot. As particle size decreases, the optimum flow Fopt to reach maximum N increases. But since back pressure is proportional to flow rate, smaller particle sizes require much higher operating pressures, and a system properly designed to capitalize on the efficiency gains. A system that can both reliably deliver the requisite pressures and that can maintain the separation efficiency of the small particles with tightly managed volumes. Higher resolution and efficiency can be leveraged even further, however, when analysis speed is the primary objective. Efficiency is proportional to column length and inversely proportional to the particle size:

$$N \propto \frac{L}{dp}$$

Therefore, the column can be shortened by the same factor as the particle size without loss of resolution. Using a flow rate three times higher due to the smaller particles and shortening the column by one third (again due to the smaller particles), the separation is completed in 1/9 the time while maintaining resolution[18].

[18] Michael E. Swartz, Ph.D. Waters Corporation, Milford, Massachusetts, “Ultra Performance Liquid Chromatography (UPLC): An Introduction” (SEPARATION SCIENCE REDEFINED MAY 2005)

2.2. Nano Liquid Chromatography[19]

Intrinsic sensitivity of the analytical method applied to the analysis of biomolecules, generally liquid chromatography–mass spectrometry, needs to be enhanced. Miniaturization of LC system and its interfacing with MS results in the necessary increase in sensitivity. Nano LC is at the heart of this gain in sensitivity.

History has a tendency to repeat itself. In the 1990s, genomics led to the development of an array of dedicated analytical techniques to solve the challenges in DNA identification. During the past decade, the identification and quantification of proteins and peptides in biological fluids, also known as proteomics, has necessitated similar developments. Although polymerase chain reaction (PCR) is used in genomics to amplify the amount of DNA and increase the signal above the limit of detection, it is not applicable to proteomics. Therefore, the intrinsic sensitivity of the analytical method applied to the analysis of biomolecules, generally liquid chromatography–mass spectrometry (LC–MS), needs to be enhanced. The miniaturization of LC systems that led to the development of nano LC and its interfacing with MS is at the heart of this gain in sensitivity.

The analysis of samples as complex as those in proteomics consists of multiple steps (sampling, sample pretreatment, separation and detection, and data analysis) in which nano LC is applied as a routine part before tandem MS detection. This installment of "Innovations in HPLC" reflects on the principles, development, and current state of nano LC instrumentation.

Miniaturization of LC Systems

Theory

A reduction in column internal diameter results in less chromatographic dilution and, consequently, increased concentration of the injected sample on the high performance liquid

[19] Nano LC: Principles, Evolution, and State-of-the-Art of the Technique, Oct 01, 2011, By Evert-Jan Sneekes, Laurent Rieux, Remco Swart, LCGC North AmericaVolume 29, Issue 10

chromatography (HPLC) system. The chromatographic dilution (D) of the sample, when injected on a LC system, is expressed by the following equation:

$$D = \frac{C_o}{Cmax} \frac{-\mathcal{E}_T \pi r^2 (1+k)\sqrt{2\pi LH}}{V\ inj}$$

where C_o is the initial compound concentration in a sample (before injection into the LC system); C *max* is the final compound concentration at the peak maximum; $\mathcal{E}$ is the column porosity; r is the column radius; k is the retention factor; L is the column length; H is the column plate height; and V *inj* is the sample volume injected.

D increases proportionally with the square of the column radius and with the square root of the length of the column. Thus, a reduction in column diameter results in a significantly lower dilution factor, thereby increasing the concentration in the eluted peak.

Though this formula applies to isocratic elution conditions, its consequences are commonly extrapolated to gradient elution conditions. Under gradient elution conditions, dilution is partly counteracted by increasing the strength of the mobile phase over time. However, the gain in sensitivity of this effect is far smaller than what is gained by decreasing the column internal diameter. The gain in sensitivity (f) resulting from the use of a LC column with a smaller internal diameter can be approximated by the following relation:

$$f = \frac{{d_1}^2}{{d_2}^2}, \mathrm{d_1 > d_2}$$

where d_1 and d_2 are the diameters of the conventional and nano LC columns, respectively.

Therefore, downscaling the column used in an analytical method from 4.6 mm i.d. to 75 µm i.d. should result in an almost 4000-fold gain in sensitivity. However, such an increase in sensitivity is not readily achieved because reducing the column internal diameter has practical consequences for the entire setup.

Chapter III

1. Protein Therapeutics

Once a rarely used subset of medical treatments, protein therapeutics have increased dramatically in number and frequency of use since the introduction of the first recombinant protein therapeutic - human insulin - 25 years ago. Protein therapeutics already have a significant role in almost every field of medicine. Proteins have the most dynamic and diverse role of any macromolecule in the body, catalyzing biochemical reactions, forming receptors and channels in membranes, providing intracellular and extracellular scaffolding support, and transporting molecules within a cell or from one organ to another. It is currently estimated that there are 25,000–40,000 different genes in the human genome, and with alternative splicing of genes and post-translational modification of proteins (for example, by cleavage, phosphorylation, acylation and glycosylation), the number of functionally distinct proteins is likely to be much higher. Viewed from the perspective of disease mechanisms, these estimates pose an immense challenge to modern medicine, as disease may result when any one of these proteins contains mutations or other abnormalities, or is present in an abnormally high or low concentration. Viewed from the perspective of therapeutics, however, these estimates represent a tremendous opportunity in terms of harnessing protein therapeutics to alleviate disease. At present, more than 130 different proteins or peptides are approved for clinical use by the US Food and Drug Administration (FDA), and many more are in development.

Protein therapeutics have several advantages over small-molecule drugs. First, proteins often serve a highly specific and complex set of functions that cannot be mimicked by simple chemical compounds. Second, because the action of proteins is highly specific, there is often less potential for protein therapeutics to interfere with normal biological processes and cause adverse effects. Third, because the body naturally produces many of the proteins that are used as therapeutics, these agents are often well tolerated and are less likely to elicit immune responses. Fourth, for diseases in which a gene is mutated or deleted, protein therapeutics can provide effective replacement treatment without the need for gene therapy, which is not currently available for most genetic disorders. Fifth, the clinical development and FDA

approval time of protein therapeutics may be faster than that of small-molecule drugs. A study published in 2003 showed that the average clinical development and approval time was more than 1 year faster for 33 protein therapeutics approved between 1980 and 2002 than for 294 small-molecule drugs approved during the same time period. Last, because proteins are unique in form and function, companies are able to obtain far-reaching patent protection for protein therapeutics. The last two advantages make proteins attractive from a financial perspective compared with small-molecule drugs.

Recombinant proteins can have several further benefits compared with non-recombinant proteins. First, transcription and translation of an exact human gene can lead to a higher specific activity of the protein and a decreased chance of immunological rejection. Second, recombinant proteins are often produced more efficiently and inexpensively, and in potentially limitless quantity.

There are now many examples in which proteins have been used successfully therapeutically. Nonetheless, potential protein therapies that have failed far outnumber the successes so far, in part owing to a number of challenges that are faced in the development and use of protein therapeutics. First, protein solubility, route of administration, distribution and stability are all factors that can hinder the successful application of a protein therapy. Proteins are large molecules with both hydrophilic and hydrophobic properties that can make entry into cells and other compartments of the body difficult, and the half-life of a therapeutic protein can be drastically affected by proteases, protein-modifying chemicals or other clearance mechanisms.

A second important challenge is that the body may mount an immune response against the therapeutic protein. In some cases, this immune response can neutralize the protein and can even cause a harmful reaction in the patient.

An appreciation of the many therapeutic uses of proteins may be facilitated by categorizing such therapies according to their mechanism of action:

Group I: enzymes and regulatory proteins. Protein therapeutics in this group function by a classic paradigm in which a specific endogenous protein is deficient, and the deficit is then remedied by treatment with exogenous protein. These proteins are used in a range of conditions, from providing lactase in patients lacking this gastrointestinal enzyme to replacing vital blood-clotting factors such as factor VIII and factor IX in hemophiliacs. A classic example is the use of insulin for the treatment of diabetes.

Group II: targeted proteins. The binding specificity of monoclonal antibodies and immunoadhesins can be exploited in numerous ways using recombinant DNA technology. Many protein therapeutics of this Group use the antigen recognition sites of immunoglobulin (Ig) molecules or the receptor-binding domains of native protein ligands to guide the immune system to destroy specifically targeted molecules or cells.

Group III: protein vaccines. As recombinant DNA technology was being developed, great strides were also being made in understanding the molecular mechanisms that allow the immune system to protect the body against infectious diseases and cancer. Immune-cell activation is mediated by antigen-presenting cells, which display on their surface specific oligopeptides that are derived from proteins found in foreign organisms or cancer cells. By specifically injecting the appropriate immunogenic (but non-pathogenic) protein components of a microorganism, vaccines can hopefully be created that provide immunity in an individual without exposing the individual to the risks of infection or toxic reaction.

Group IV: protein diagnostics. Proteins classified in Group IV are not used to treat disease, but purified and recombinant proteins used for medical diagnostics (both in vivo and in vitro) are mentioned here because they are invaluable in the decision-making process that precedes the treatment and management of many diseases.
A classic example of an in vivo diagnostic is the purified protein derivative (PPD) test, which determines whether an individual has been exposed to antigens from Mycobacterium tuberculosis[20].

[20] Nature Reviews Drug Discovery 7, 21-39 (January 2008) | doi:10.1038/nrd2399

2. Mass Spectrometry applied to Protein Analysis

Mass spectrometry is a central analytical technique for protein research and for the study of biomolecules in general. Driven by the need to identify, characterize, and quantify proteins at ever increasing sensitivity and in ever more complex samples, a wide range of new mass spectrometry–based analytical platforms and experimental strategies have emerged. Mass spectrometry was restricted for a long time to small and thermostable compounds because of the lack of effective techniques to softly ionize and transfer the ionized molecules from the condensed phase into the gas phase without excessive fragmentation.

The development in the late 1980s of two techniques for the routine and general formation of molecular ions of intact biomolecules - electrospray ionization (ESI) and matrix assisted laser desorption/ionization (MALDI) - dramatically changed this situation and made polypeptides accessible to mass spectrometric analysis. This catalyzed the development of new mass analyzers and complex multistage instruments [for instance, hybrid quadrupole time-of-flight (Q-Q-ToF) and tandem time-of-flight (ToF-ToF) instruments] designed to tackle the challenges of protein and proteome analysis. Mass spectrometers are used either to measure simply the molecular mass of a polypeptide or to determine additional structural features including the amino acid sequence or the site of attachment and type of posttranslational modifications. In the former case, single-stage mass spectrometers are used, acting essentially as balances to weigh molecules. In the latter case, after the initial mass determination, specific ions are selected and subjected to fragmentation through collision. In such experiments, referred to as tandem mass spectrometry, detailed structural features of the peptides can be inferred from the analysis of the masses of the resulting fragments.

Although no proteomic strategies are currently capable of completely and routinely analyzing a proteome, the techniques are robust and their potential for complete proteome analysis is increasing rapidly. Moreover, the analysis of specific subproteomes, such as the proteins contained in organelles or subcellular fractions, has become routine. Proteomic studies also differ in their objectives. Many studies are descriptive, focusing on the identification of the proteins in a sample and the characterization of their post-translational modifications. More recently, quantitative measurements of either absolute protein quantities or quantitative changes of proteins between samples have been performed. Virtually every mass spectrometry–based proteomic workflow consists of three distinct stages: (I) Protein samples

are isolated from their biological source and optionally fractionated. The final protein sample is then digested and the resulting peptide sample is further fractionated. (II) The peptides are subjected to qualitative and quantitative mass-spectrometric analysis. (III) The large data sets generated are analyzed by suitable software tools to deduce the amino acid sequence and, if applicable, the quantity of the proteins in a sample. The peptide identity is assigned to the MS/MS spectra through database searching, which is performed according to established guidelines to generate consistent results. A subsequent statistical analysis of the search results is critical to ensure confidence in the identifications.

MS analysis of substantially purified proteins

This approach is exemplified by the original proteomic approach: two-dimensional (2D) gel electrophoresis followed by the mass-spectrometric identification of the protein(s) in a single gel spot (**Figure 18A**). The targeted proteins are digested and identified by mass spectrometry, usually peptide mass fingerprinting using a MALDIToF instrument. More recently, variants of this approach have been developed in which various combinations of sequential electrophoretic or chromatographic separation methods are combined to achieve sufficient peak capacity to resolve complex samples. Quantification is achieved at the protein level by comparing the signal intensities of identical proteins in different samples. The strength of these methods is their ability to resolve related proteins, such as differentially modified forms, and the low degree of complexity of the samples generated for mass spectrometry analysis. The methods suffer from limited dynamic range, insufficient power to resolve proteomes, and limited sample throughput. Furthermore, important classes of proteins, including membrane proteins, are difficult to analyze by these methods, which are best suited for the analysis of protein samples of limited complexity and for studies where specific proteins need to be extensively characterized.

MS analysis of complex peptide mixtures

In this method, also referred to as shotgun proteomics, complex protein samples are digested, and the resulting peptide samples are extensively fractionated and analyzed by automated MS/MS, typically using rapidly scanning analyzers such as IT (Ion Trap) mass spectrometers (**Figure 18B**). Protein samples analyzed by this method include complete cell lysates or tissue extracts, subcellular fractions, isolated organelles, or other subproteomes. If samples are labeled with stable isotopes, the ratio of signal intensities of differentially labeled but chemically identical analytes can be used to determine accurately their relative abundance in

different samples. Multiple analyses can be performed concomitantly by using tandem mass tags. Alternately, the absolute quantity of peptide can be determined by adding calibrated amounts of isotopically labeled peptides into the sample before the MS analysis. The strength of the shotgun approach is its conceptual and experimental simplicity, increased proteomic coverage compared with the method described above, and accurate quantification. The shotgun method suffers from limited dynamic range, informatics challenges related to inferring peptide and protein sequence identities from the large number of acquired mass spectra, a high redundancy, and the enormous complexity of the generated peptide samples. These limitations have been addressed, in part, by the use of fractionation that reduces the complexity of the peptide sample. Popular fractionation methods target information-rich subsets of the proteome, such as the cysteine-containing peptides, phosphorylated peptides, or glycosylated peptides. Shotgun proteomics is most suitable for the rapid identification of the components of complex sample mixtures and for the comparative quantitative analysis of the proteins contained in different samples. Because the connection between the peptides that are analyzed in the mass spectrometer and the protein(s) from which the peptides originate is lost during proteolysis, this approach is less well suited for the extensive characterization of proteins with multiple modifications.

Comparative pattern analysis

Comparative peptide pattern analysis (**Figure 18C**) is conceptually similar to the 2D gel electrophoresis method in that 2D patterns of features are generated for each sample, and the patterns are compared to identify quantitative or qualitative changes. Such features are then further characterized, for example, by sequencing or by determining their post-translationally modified state. However, in MS-based pattern analysis methods, protein samples are proteolyzed, fractionated, and the resulting peptides are analyzed by LC/MS. The two dimensions to describe a peptide ion are chromatographic elution time and mass. Quantification of the detected features is achieved by integrating the ion counts of each signal. The main advantage of this method is that all the features that are detectable by MS can be quantified. This is in contrast with the shotgun methods, in which only identified peptides are quantified. However, in practice, it is extraordinarily challenging to generate highly reproducible patterns and to develop software tools that reliably match related patterns. Such analyses result in a list of features that represents putative peptide ions, with the following attributes: mass-to-charge ratio (m/z), charge state, elution time, and ion intensity. The peptides that need to be sequenced (for instance, features indicating different

expression between two samples) are included in a list and then submitted to a new, directed mass-spectrometric experiment to collect MS/MS spectra of these features exclusively. This type of analysis is also well suited for the MALDI/MS/MS platform, because the samples are ‘‘immobilized’’ on the sample plate and can therefore be interrogated sequentially and without any time constraints.

Hypothesis-driven strategies

It can be expected that incremental improvements in instrument performance will continue to translate into more sensitive, faster, and more reliable proteomic analyses. However, it is not clear whether such advances will be sufficient to eliminate the major bottlenecks encountered in the current proteomics approaches. It has been argued before that proteomics needs to undergo a paradigm shift to reach the goal of robustly and globally analyzing proteomes. The essence of this shift is the transformation of proteomics from a mode where in every experiment the proteome is rediscovered, to a mode in which the information from prior proteomic experiments is used to guide the present experiments. Specifically, it can be anticipated that extensive (complete) proteome maps containing all the peptides of a species that are observable by mass spectrometry will be generated and that future strategies will aim at the targeted, non-redundant analysis of information-rich peptides. For mass spectrometry instrumentation and strategy, this shift of paradigm requires the development of instruments and data acquisition protocols that support the fast, sensitive, and robust analysis of previously generated lists of target peptides. Databases that allow the extraction of peptides that uniquely identify a specific protein or a specific modified form of a protein and that are easily detectable by mass spectrometry are just emerging. It can be anticipated that biological hypotheses will generate lists of proteins that need to be characterized and quantified in a particular study. Such lists of proteins can then be submitted to the database to produce the minimal set of peptides required to test the hypothesis. This set of peptides can then be measured by targeted methods, including MRM (**Figure 18D**). The directed nature of this approach allows the mass spectrometer to focus on a non-redundant set of targets and therefore leads to a substantial gain in throughput and sensitivity. By adding calibrated, isotopically labeled reference peptides, precise quantitative information can be obtained[21].

[21] Bruno Domon and Ruedi Aebersold, SCIENCE VOL 312 14 APRIL 2006

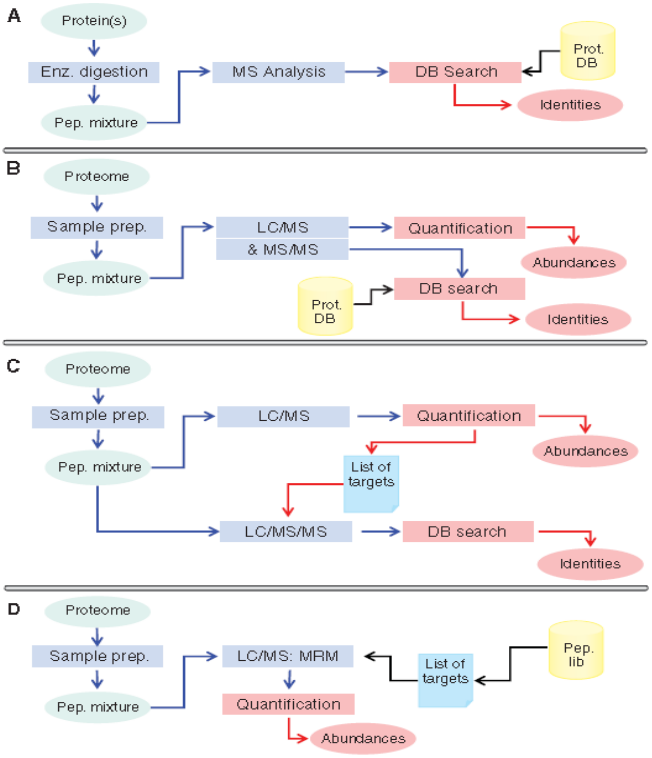

***Figure 18**: Proteomics strategies. (A) Identification of simple protein (prot.) mixtures from 2D gel electrophoresis or pull-down experiments is carried out by enzymatic (enz.) digestion and by mass spectrometry analysis of the resulting peptides (pep.) (in ESI or MALDI mode). Peptide masses allows their identification (and that of the parent proteins) using peptide mass fingerprinting (PMF). Additional MS/MS data are also used for the peptide identification. (B) Random protein identification and quantification, also referred to as shotgun proteomics, couples identification and quantification of specific peptides in a sample. Selected peptides are subjected to product ion scanning in a tandem mass spectrometer. The precursor ions are selected randomly, and typically only a fraction of the precursor ions detected are selected (undersampling). The ion intensities in MS1 are used to quantify the analytes by relating the signal intensity of the selected analyte to the signal intensity of a suitable reference molecule (frequently, a reference peptide labeled with heavy stable isotopes). (C) Quantification-driven identification decouples quantification and identification of peptides. In a first step, peptides that quantitatively differ between samples are detected by comparing the MS1 peptide patterns (mass versus chromatographic retention time) between samples, allowing for a more extensive analysis of the peptide patterns. Candidate peptides that show interesting quantitative properties are subjected to MS/MS sequencing in a second step using an inclusion list resulting from the primary analysis. (D) Hypothesis-driven peptide identification measures with high precision the abundance of a series of predetermined peptides. The targeted peptides, usually identified from previous experiments, are subjected to MRM. Accurate quantification is achieved by adding a suitable calibrated reference peptide[22].*

[22] Bruno Domon and Ruedi Aebersold, SCIENCE VOL 312 14 APRIL 2006

Chapter IV

1. The Nanobody® ALX-0761 project

Th17 cells and IL-17 are associated with the pathology of many human inflammatory and autoimmune disorders like psoriasis, rheumatoid arthritis (RA) and multiple sclerosis and have proved to play an important role in animal models mimicking these and other auto-immune disorders. Although IL-17A is the most characterized family member, its closest relative IL-17F has similar biological activity and possibly even a non-redundant role in vivo. Both exist in homo- and hetero-dimeric forms.

Therefore, targeting both IL-17A and F could provide a more effective way to block inflammatory responses. To this purpose, a trivalent Nanobody ALX-0761 was developed comprising an N-terminal IL-17F specific moiety, a C-terminal moiety that binds both IL-17A and F and a central building block binding to albumin for plasma half-life extension. The subunits are fused head-to-tail with a 9 amino acid glycine/serine linker. ALX- 0761 binds to IL-17A and IL-17F with picomolar affinities. The three Nanobody building blocks are both human and cynomolgus monkey cross-reactive.

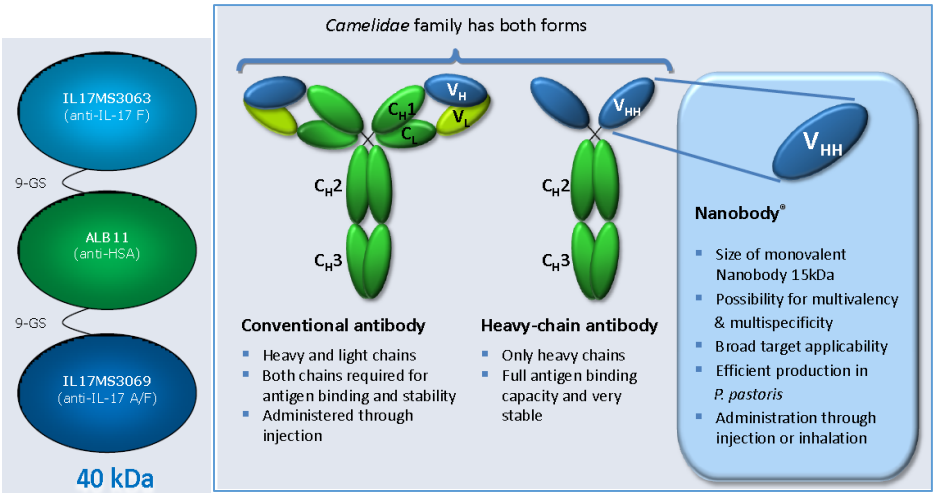

***Figure 19**: Conventional antibody and innovative Nanobody characteristics*

The aim of this project was to verify the method feasibility of ALX-0761 quantitation in human serum.

The steps followed during the method development were:

I. Qualitative analysis of tryptic peptides and investigation on the peptide pattern to find the unique signature peptide by High Resolution Mass Spectrometry Technology (HRMS)

II. To define a sample processing strategy for quantitative analysis of the signature peptide

1.1. Material and methods

Standards, chemicals and reagents

ALX-0761* Nanobody anti IL-17 A/F Drug product was produced by MS-Aubonne Site, Switzerland and provided by Merck Serono, Guidonia Montecelio Site. Acetonitrile (LiChrosolv®, Reag. Ph. Eur., gradient grade for liquid chromatography), 2-Propanol (LiChrosolv®, gradient grade for liquid chromatography), Methanol (LiChrosolv®, Reag. Ph. Eur., gradient grade for liquid chromatography), Formic Acid (Emsure® ACS, Reag. Ph. Eur., 98-100% for analysis). Ammonia Solution 32% (extra pure), Trypsin from porcine pancreas (Type IX-S), Iodoacetamide, IAM (BioUltra, ≥ 99% NMR), D-L Dithiothreitol, DTT (BioUltra, ≥ 99.5% RT), Calcium Chloride dihydrate (Reagent Plus® ≥99%), Ammonium bicarbonate (BioUltra, ≥ 99.5% T), Ammonium formiate (for mass spectrometry, ≥ 99.0%), Phosphate Buffered Saline, PBS (BioPerformance Certified for molecular biology pH 7.4), Urea (for electrophoresis gel) and Heptafluorobutyric acid (for ion chromatography ≥ 99.5% GC). RapiGest was from (Waters Corporation Milford, MA). Ultrapure water was from a Millipore Milli-Q system (Merck Millipore, Billerica, MA). Human Serum was purchased from Charles River Laboratories.

***ALX-0761 Nanobody** compound is composed of 378 amino acids with a Molecular Weight of 40111.2 Da and a theoretical pI of 5.81.

LC–MS Equipment

The LC–MS analyses were performed using two technologies: (I) an LTQ Orbitrap XL Hybrid Ion Trap-Orbitrap™ Mass Spectrometer (Thermo Fisher Scientifics, MA, USA) interfaced with a micro-LC Ultimate 3000™ (Dionex corporation, CA, USA) for the preliminary qualitative experiments and (II) a Q-Exactive Plus Hybrid Quadrupole-Orbitrap™ Mass Spectrometer (Thermo Fisher Scientifics, MA, USA) interfaced with a nano-LC Ultimate 3000™ (Thermo Fisher Scientifics, MA, USA) for the quantitative experimental part. Excalibur software version 3.0 was used for data acquisition and data processing.

1.2. Method development

The technical approach followed was:

- BLAST search to reveal uniqueness
- Tryptic digestion of Nanobody (no matrix)
- LC-HRMS to determine most intense peptides and to reveal chromatographic and mass spectrometric behavior
- MS/MS on most intense peptides (+1, +2, +3)
- Choice of the optimal signature peptide

1.2.1. Qualitative experimental part

A preliminary investigation was performed to identify and confirm, using the Orbitrap™ technology, tryptic peptides from the longest peptide No.5. UniProtKB/Swiss-Prot software processing was used to run a sequence similarity search and to drive the research of the signature peptide (**Table 1**).

N	AA position (a-IL17-NB)	Length	AA Sequence	N. Matches in UniProt DB
1	1-26	26	Peptide 1	0
2	37-46	9	Peptide 2	0
3	65-78	14	Peptide 3	> 25
4	80-96	17	Peptide 4	0
5	112-285	174	Peptide 5	NA
6	292-305	14	Peptide 6	>25
7	314-332	19	Peptide 7	> 25
8	334-351	18	Peptide 8	0
9	368-378	11	Ppetide 9	> 25

***Table 1**: AA sequences and human proteome (*Specific sequences have been removed for confidentiality reasons)*

Prior to conducting the experimental part we also verified, using ExPASy software (Peptide Cutter tool), the positions of cleavage sites for the longest unique peptide, Peptide No.5 (**Table 2** and **Figure 20**):

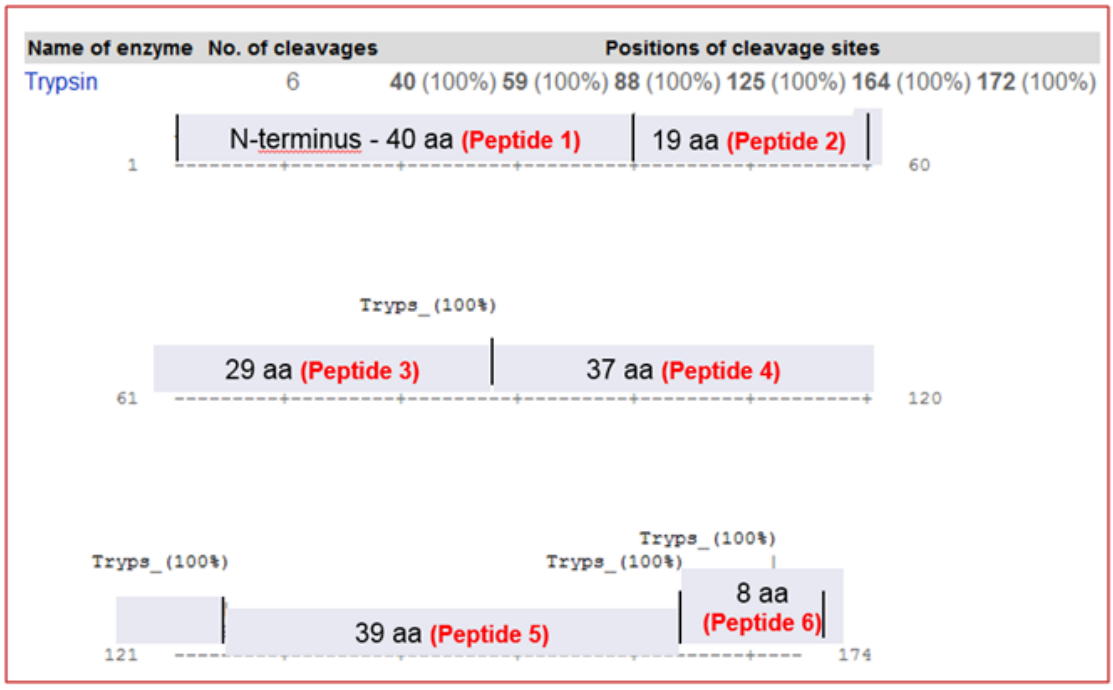

***Figure 20:** Trypsin on Peptide No.5*

N	AA position (a-IL17-NB)	Length	AA Sequence	N. Matches in UniProt DB	Comment
1	112-151	40	Peptide 1	NA	N-terminus peptide
2	152-170	19	Peptide 2	0	+2
3	171-197	29	Peptide 3	0	not detected: maybe due to pyroglutammic N-terminus formation
4	200-236	28	Peptide 4	0	+2 or +3
5	237-275	39	Peptide 5	0	+2 or +3
6	276-283	8	Peptide 6	0	C-terminus, +1

***Table 2**: Tryptic peptide analysis from Peptide No.5. Protein Blast algorithm used.*

A Full MS scan experiment at 100,000 of resolution (FWHM, Full Width at Half Maximum) was conducted in order to obtain confirmation of the predicted tryptic peptides (**Figure 21**). The chromatographic column was a Biobasic™ C4 (Thermo Scientific), 0.18 x 150 mm, 5 µm, 300 Å. A gradient from 10% B to 90% B (mobile phase B: acetonitrile containing 0.1% of formic acid) was run in 100 minutes.

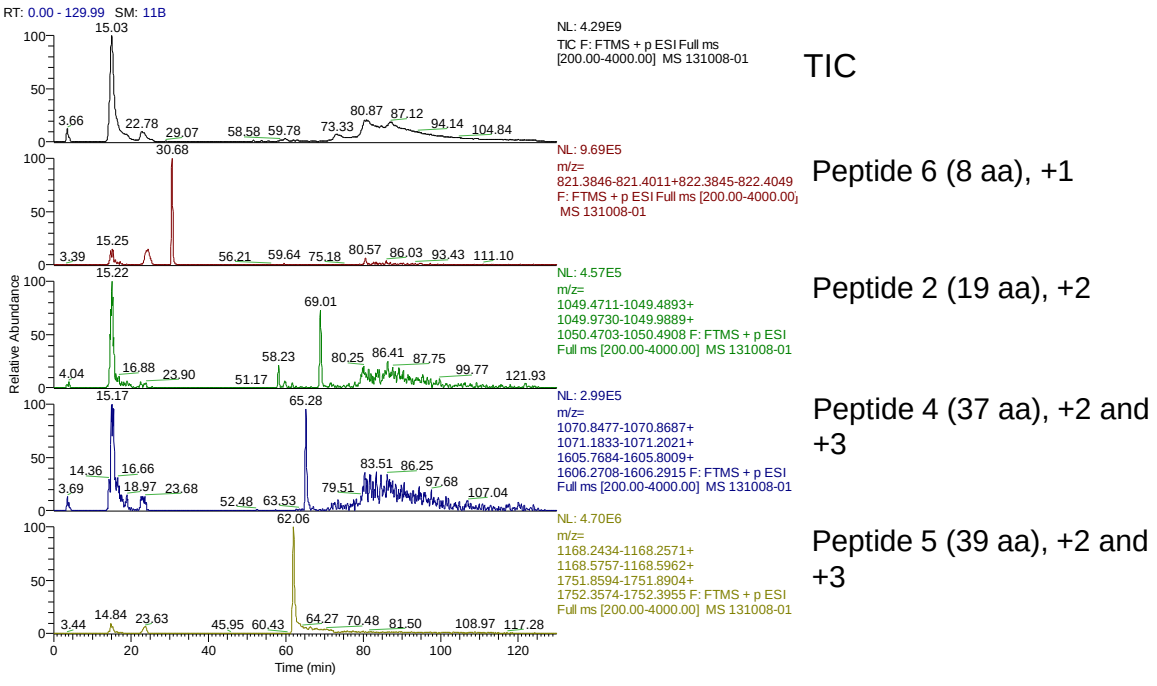

***Figure 21**: Full MS (100,000 Resolution, FWHM) scan for tryptic peptide analysis*

A preliminary conclusion on this experimental part was that the peptides analyzed are not present in the human proteome and therefore could be selective sequences. It was investigated whether they could be targeted by enzymatic cleavage and have suitable properties for quantification (pI, MW, stability, MS sensitivity…).

The best in class peptides were tryptic peptides coming from Peptide No.5 (see **Table 2**) with the 19-mer and 8-mer sequences:

1. **peptide 2 (19 aa)**
2. **peptide 6 (8 aa)**

Subsequently, an additional analysis was performed on the other sequences from trypsin cleavage (see **Table 1**). The only unique sequence (i.e. not coming from the peptide No.5) after trypsin cleavage was (**Figure 22**) peptide 1:

- MW (av.): 1868
- pI = 4.4

Additionally, this peptide displayed a very good pI and high MS intensity.

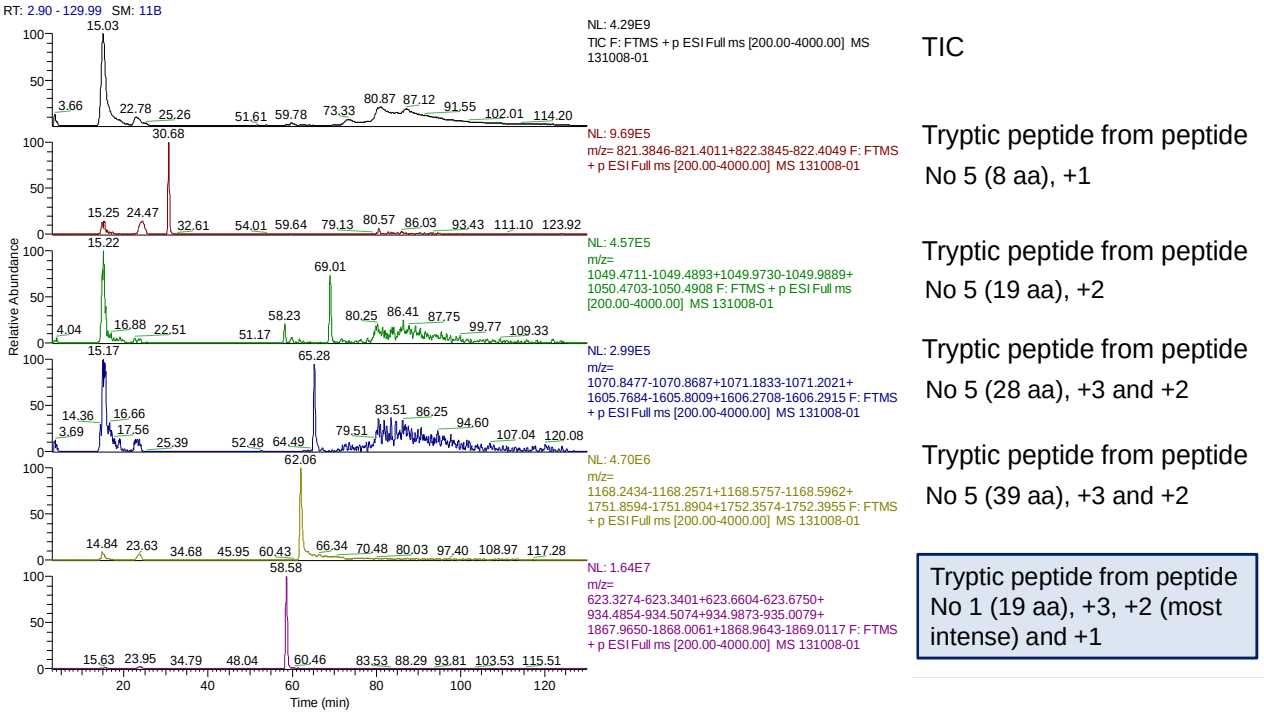

Figure 22: *Full MS (100,000 Resolution, FWHM) scan of Unique Tryptic peptide analysis.*

1.2.2. Quantitative experimental part (LC-MS optimization)

The MS/MS quantitative experimental part was conducted using a Q-Exactive™ mass spectrometry in order to achieve better sensitivity and selectivity on the signature peptides. The experimental part began by optimizing the appropriate LC-MS conditions for the N-terminus tryptic peptide (**Peptide 1, 19 aa**).

The tryptic sample injected during this first step was prepared applying the following procedure:

400.0 µL of 100 mM Tris-HCl at pH 8 containing 0.05% of RapiGest™ (*) and 51.0 µL of DTT (conc. 30.0 mg/mL in 100 mM Tris-HCl pH 8, equivalent to 20.8 mM in the final sample) were added to 28.0 µL of Anti IL-17 Nb at 60.0 µg/mL concentration prepared in PBS. The reaction was conducted at 60°C, shaking at 750 rpm for 30 min.

Then 64.0 µL of IAA (92.0 mg/mL in 100 mM Tris-HCl pH 8, to reach 58.7 mM final concentration in the sample) were added to the sample. The reaction was conducted at 37°C with shaking at 750 rpm for 60 min and in the dark in order to avoid IAA photodegradation.

The final step was to add 10.0 µL of 55 mM $CaCl_2$ (to reach a 1 mM final concentration in the sample) and 5.0 µL of trypsin (10.0 mg/mL in H_2O). The digestion was conducted over night (16 hours) at 37°C with shaking at 750 rpm.

The digestion was stopped by adding formic acid to obtain a final acidic concentration of 1%.

(*): The patented RapiGest™ SF Surfactant (Waters supplier) is a reagent used to enhance enzymatic digestion of proteins, both in-gel and in-solution. RapiGest SF helps solubilize proteins, making them more susceptible to enzymatic cleavage without inhibiting enzyme activity. Unlike other commonly used denaturants, such as SDS or urea, RapiGest SF does not modify peptides or suppress protease activity. It is compatible with enzymes such as Trypsin, Lys-C, Asp-N, Glu-C, PNGaseF and other enzymes.

- Compatible for LC and MS analysis
- Improves efficiency and speed of digestion
- Degraded at low pH and removed from the sample
- Simplifies preparation protocols and improves throughput of analysis

Chromatography was performed by using a Thermo Scientific EASY-spray™ column PepMap RSLC, C18 2 µm, 100 Å, 75 µm x 25 cm. Mobile phases A and B were, respectively, water containing 0.1% of formic acid and acetonitrile containing 0.1% formic acid.

The mass spectrometer conditions were:

- spray voltage capillary 2 kV;
- capillary temperature 300°C;
- S-Lens RF level 100
- scan range 200-3000 amu;
- R 70000;
- AGC $1e^6$ and maximum ion time 100 ms.

The injection volume was 0.1 µL and the column temperature was set at 60°C. The chromatographic gradient was:

Time (min)	% B	Flow (µL/min)
0.0	20	0.300
0.5	20	0.300
20.0	80	0.300
21.0	95	0.300
25.0	95	0.300
26.0	20	0.300
40.0	20	0.300

Figure 23: *Chromatographic gradient used to run the digested sample*

Before injection, the digested sample was diluted 10 times with water containing 0.1% of formic acid.

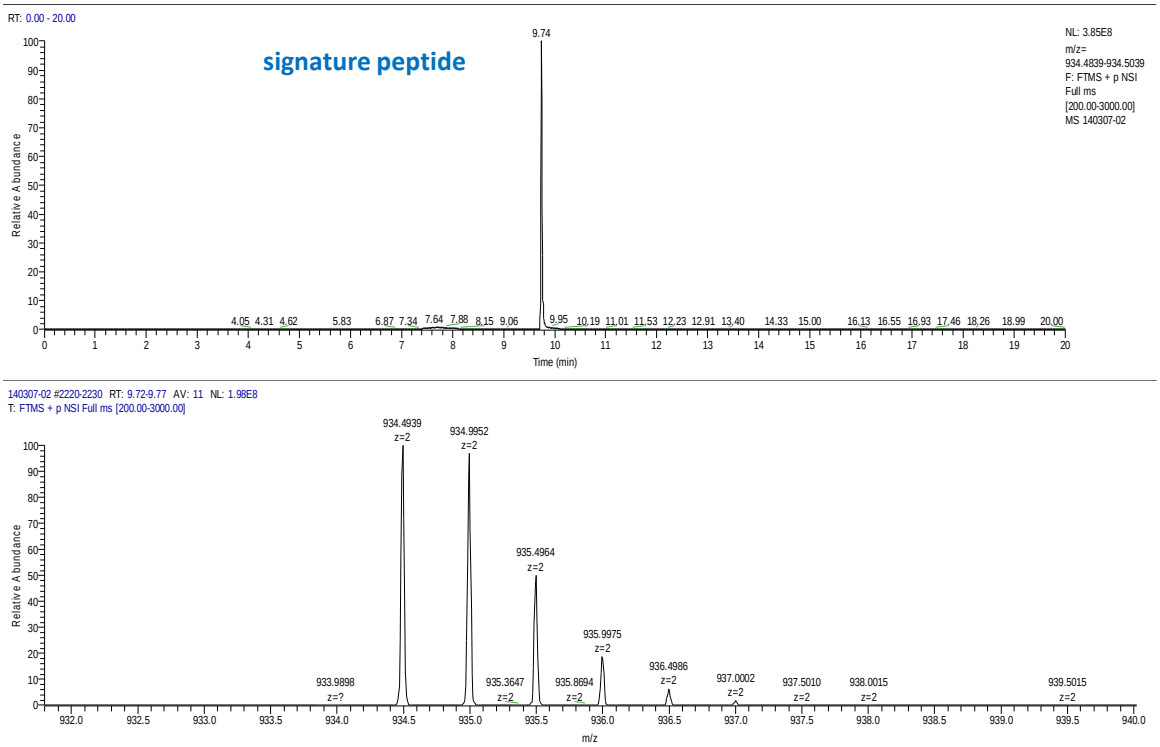

Figure 24: *Extracted ion chromatogram (m/z 934.4939, width 0.02 mmu) from a Full MS experiment of a protein standard (10.0 µg/mL) digested in buffer and diluted 10 times before injection*

After this preliminary investigation on LC-MS conditions for the signature peptide, the chromatographic gradient was modified (see **Table 3**) in order to obtain a shorter run time but maintaining the required selectivity and reproducibility of the method. The column length was changed from 250 mm to 150 mm.

	time (min)	B%	flow (µL/min)
	0.0	10	0.300
%B/min	1.0	10	0.300
2.86	15.0	50	0.300
	16.0	95	0.500
	21.0	95	0.500
eq.time	21.1	10	0.500
11 min	31.0	10	0.500
	32.0	10	0.300

Table 3: *Gradient used to obtain a shorter run time*

10 injections of a digested standard prepared in buffer and matrix (at a concentration of 5.0 µg/mL) were run using the gradient reported in **Table 3**. The CV (%) calculated on the areas

was below 6% and 8% for standard in buffer and in matrix, respectively, and the retention time was reproducible over the ten injections.

The second step of the experimental part was to optimize the sample processing strategy.

The strategy adopted was to selectively cleave the analyte by limiting trypsin cleavage to more flexible or exposed (analyte) chains without performing any reduction or alkylation.

Protein	Buffer/Additive	No Reduction	No Alkylation	Trypsin	Incubation
Serum sample spiked at different protein conc. (final volume 100.0 µL)	900 µL of 50 mM NH_4HCO_3 + 1 mM $CaCl_2$ + 1 M Urea	No DTT	No IAA	Trypsin (Sigma)	37°C, 16h

The advantages of this approach were:

I. Reduction of interferences from the matrix (reduced sample complexity)

II. Improved sensitivity/selectivity in MS

III. More efficicient removal of partially digested proteins or disulfide-linked digested peptides by SPE and/or by the LC step

IV. New opportunity to use disulfide-linked digested peptides as a new kind of signature peptides that contain a 3D-structural feature

V. Streamlining sample digestion by eliminating the reduction and alkylation steps,

while the only disadvantages could be associated to incomplete digestion that could impact method sensitivity.

The selective digestion was performed as described in the following protocol:

- aliquot 100.0 µL of sample spiked at different analyte concentrations
- add 900.0 µL of 50 mM NH_4HCO_3+1 mM $CaCl_2$+1 M Urea solution
- add trypsin to the sample (ratio trypsin:protein w/w 1:20)
- keep the sample overnight (16 hours) at T=37°C, shaking at 750 rpm

- stop digestion by lowering the pH of the reaction to below pH 4 by adding formic acid (final formic acid concentration 1%)

Figure 25 shows clearly abundant interference clusters in the fully digested tryptic human matrix and how these interferences are lower in the selectively cleaved human matrix.

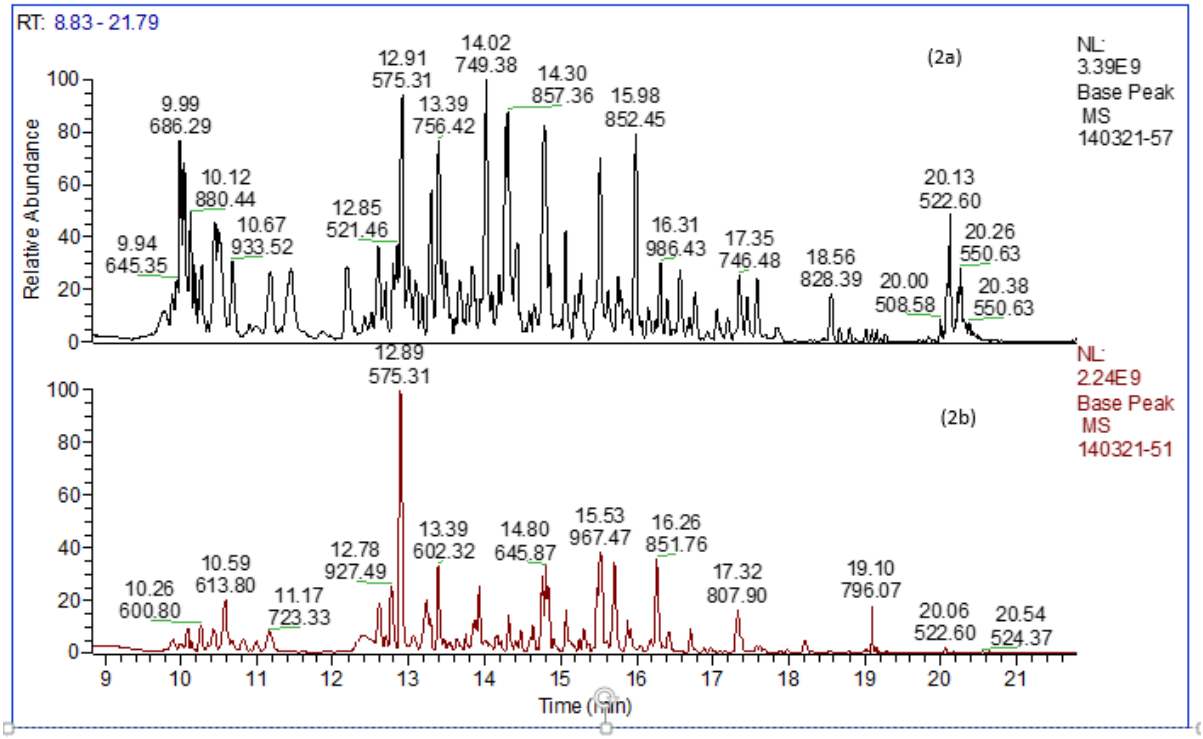

***Figure 25**: A representative Full Scan mass spectrum of tryptic human matrix. Full Denaturation (2a) vs. Selected Digestion (2b).*

Subsequently, different ratios of trypsin to sample and dilution buffer with and without 1 M Urea were tested in order to set the best conditions for Selective Digestion (**Figure 26**). The best conditions found, in term of signal intensity, were obtained using 1 M Urea and trypsin/sample ratio of 1 : 200.

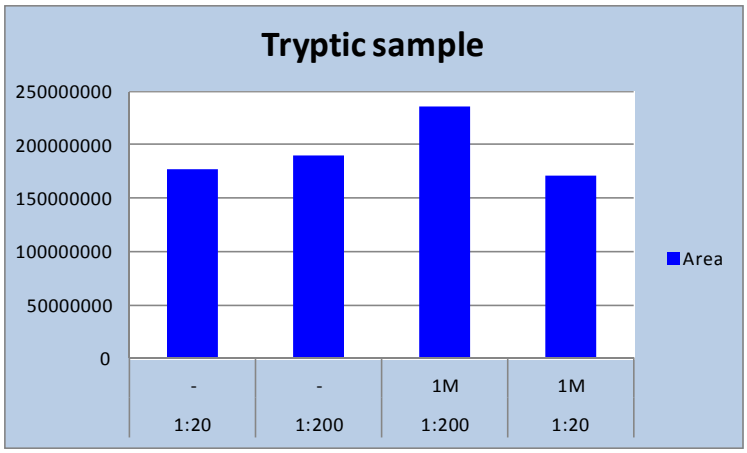

***Figure 26**: Areas of signature peptide at different trypsin/protein ratios (w/w) and with and without 1 M Urea*

The third step was to set up the extraction method. A combination of two extractions was tested during the sample preparation phase: a preliminary clean-up on the intact protein using:

1) customized SCX plate with 1000 Å pore size to avoid dimensional exclusion effects due to the presence, in the serum matrix, of analyte-natural ligand complexes that have large hydrodynamics volumes (>180 Å) or alternatively

2) An Immobilized-Protein G Spin Plate in order to eliminate the most abundant IgG present in the serum and a second extraction (see procedure **3**) performed on the digested sample using a Polymeric Reversed SPE plate.

1) **<u>SCX (Strong Cation Exchange SPE, 60 mg sorbent mass, pore size 1000Å, Glyce Corp.) procedure</u>:**

- Equilibration: 1.0 mL of 10 mM $HCOONH_4$ pH 2.8
- Loading: 100.0 µL of sample diluted 10 times with 10 mM $HCOONH_4$ pH 2.8 (collected and analyzed)
- Washing: 1.0 mL of 10 mM $HCOONH_4$ pH=2.8 (collected and analyzed)
- Elution (four conditions):

  Elution 1 (condition 1): 50 mM Tris pH 8,

  Elution 2 (condition 2): 5% of NH_3 in 60% Methanol

Elution 3 (condition 3): 5% of NH_3 in 80% Methanol

Elution 4 (condition 4): 5% of NH_3 in 100% Methanol

Each fraction was collected and analyzed in order to evaluate the % of methanol necessary to eluate the protein of interest.

2) <u>Immobilized-Protein G Spin Plate(*) (Thermo Scientific) procedure</u>:

- Equilibration: 400.0 µL of PBS buffer, centrifuge 1 min at 1000 g
- Loading: 200.0 µL of sample diluted 2 times with PBS with shaking at 450 rpm for 30 min.
- Elution: centrifuge 1min at 1000 g

(*) The Thermo Scientific Pierce Protein G Agarose Spin Plate for IgG Screening allows quick purification and screening of antibodies. It consists of purified native Protein A that has been covalently immobilized at high density onto high-quality cross-linked 6% beaded agarose (CL-6B). Among the many available varieties of immobilized Protein A affinity resins, this one provides the most versatile combination of chromatographic features for high yield and high purity purification of whole IgG from mammalian serum samples. The agarose beads have physical and chemical properties suitable for many affinity purification systems.

3) <u>Reversed Phase (RP) SPE (Oasis HLB* 96-well plate, 60mg sorbent mass, Waters) procedure</u>:

- Equilibration: 1.0 mL of MeOH, 1.0 mL of water with 0.1% of formic acid
- Loading: tryptic sample from selective digestion procedure
- Washing: 1.0 mL of 10 mM $HCOONH_4$ pH = 2.8
- Elution: 500.0 µL of H_2O/CH_3CN : 1/1 containing 1% of formic acid

<u>Results</u>: Preliminary clean-up steps (1 or 2) performed on intact molecule did not show any improvements in sample recovery and purification (**Figure 27**) and the development was dismissed because this technology turned out to be specifically designed for qualitative/proteomic experiments rather than for quantitative bioanalysis.

Since the desired results could not be achieved with sample purification before the enzymatic reaction, post-reaction purification was applied by using the RP-SPE plates only.

(*) Oasis HLB is an all-purpose, strongly hydrophilic, water-wettable polymer with a unique hydrophilic-lipophilic balance. It is made from a specific ratio of two monomers, the hydrophilic N-vinylpirrolidone and the lipophilic divinylbenzene. This reversed-phase sorbent is ideal for acidic, basic and neutral analytes and features stability at extremes pH values in a wide range of solvents.

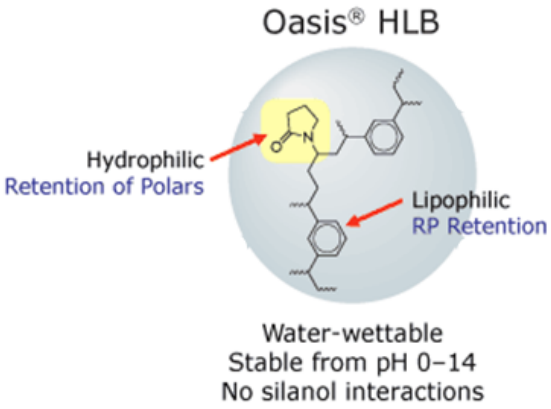

Functional group of HLB Phase

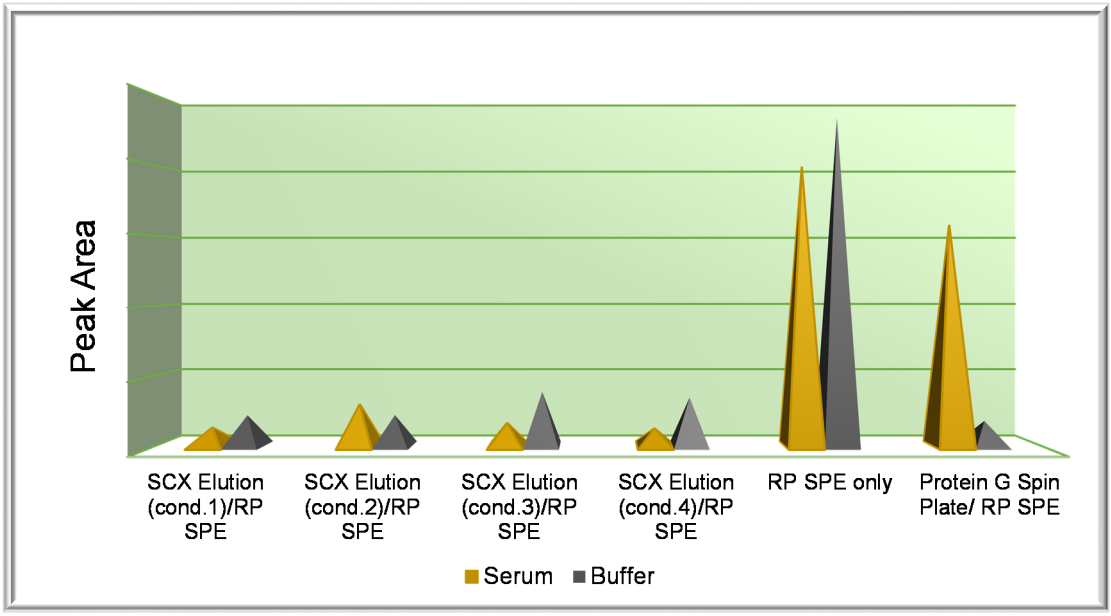

***Figure 27**: Comparison between preliminary and secondary purification followed by SPE RP vs. secondary purification only (intact protein standard concentration 100.0 µg/mL)*

To obtain the required LLOQ, we introduced the evaporation step on the sample eluted from the SPE plate. The sample was then dried and reconstituted using 50.0 µL of a mixture H_2O/CH_3CN : 1/1 containing 0.1% of formic acid. This allowed injection of 0.1 µL of sample into the nanoUHPLC-MS/MS system.

During the method development phase, an interfering species was detected at the same retention time as the target peptide (see **Figure 28**).

Even if the high MS resolution allowed distinction between the two species and correct quantification of the analyte, it was necessary to chromatographically separate them in order to improve sensitivity (**Figure 29**).

This meant introducing an ion pairing molecule in the mobile phases, heptafluorobutyric acid.

Despite the continuing dominance of trifluoroacetic acid (TFA) as the anionic ion-pairing reagent of choice for peptide separations by reversed-phase high-performance liquid chromatography (RP-HPLC)[23], HFBA was used as ion pairing agent in order to reduce the strong ion soppression effect induced by TFA.

Using this approach an LLOQ of 600.0 ng/mL corresponding to 28.0 ng/mL of the target peptide was achieved.

[23] J Chromatogr A 2005 Jul 1;1080(1):68-75

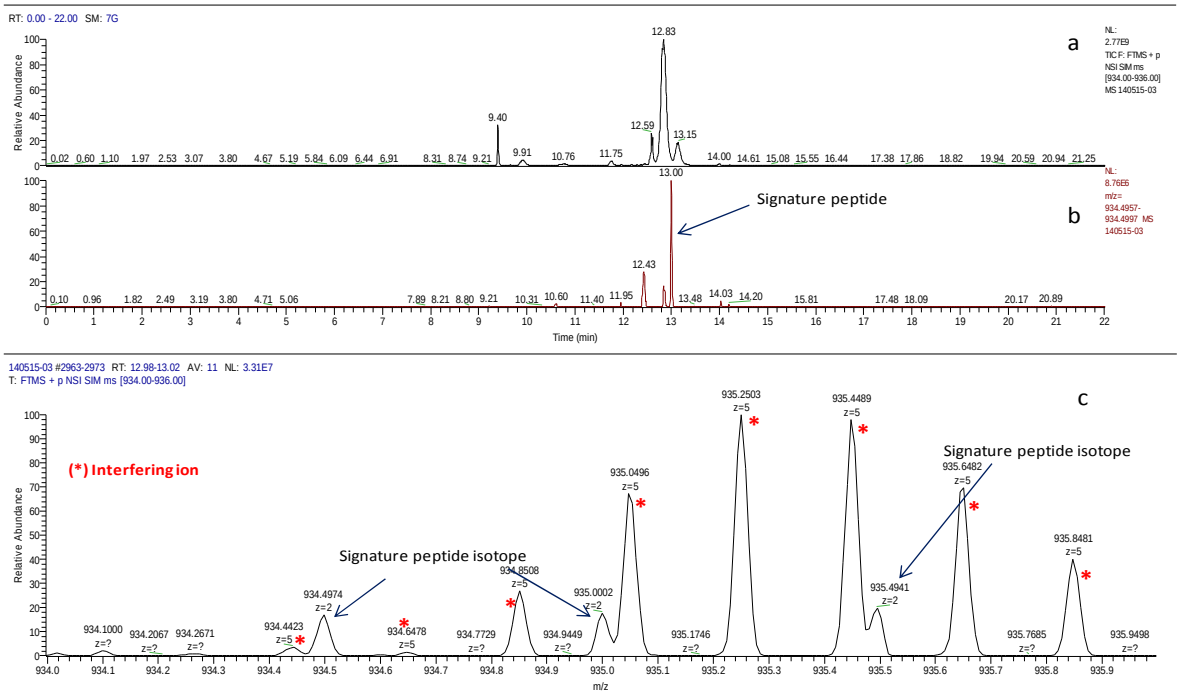

***Figure 28**: (a) total ion chromatogram from a SIM MS experiment (m/z range: 934-936); (b) Extracted ion chromatogram of m/z signature peptide from a SIM MS experiment (c) mass spectrum of the chromatographic peak at a retention time of 13.00 min*

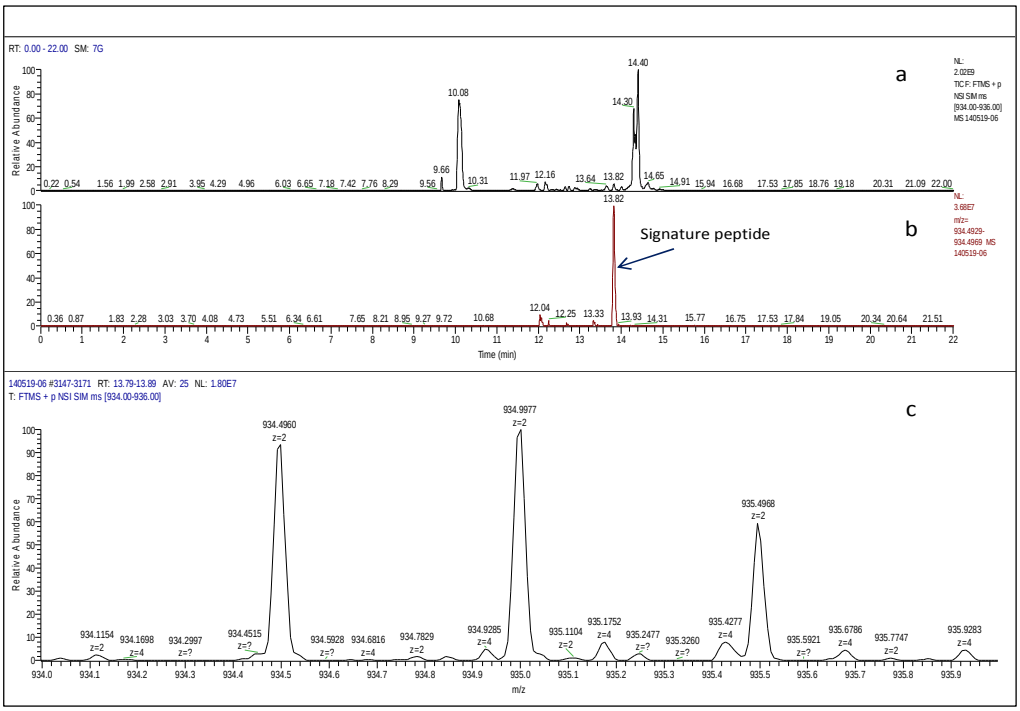

***Figure 29**: (a) total ion chromatogram from a SIM MS experiment (m/z range: 934-936); (b) Extracted ion chromatogram of m/z signature peptide from a SIM MS experiment (c) mass spectrum of the chromatographic peak at a retention time of 13.82 min.*

Sample: standard digested in matrix at a final concentration of 10.0 µg/mL.

1.2.3. Final Chromatographic and Mass Spectrometric conditions

The experiments carried out during the method set-up provided useful analytical information in order to proceed with the subsequent experiments.

Linearity was tested under the following final LC-MS/MS conditions:

- UHPLC Ultimate3000™, NanoSystem (Dionex)
- Analytical column: C18 PepMap™ 75µm x 15cm x 3µm (Thermo)
  - *gradient flow 300 nL/min, column heater 50°C*
  - *32 min. run time (Peptide Retention Time: 14.7)*
  - *MPA: 999:1 water:formic acid (v:v) + 0.01 HFBA*
  - *MPB: 999:1 ACN:formic acid (v:v) + 0.01 HFBA*

- Q-Exactive Plus™ (Thermo Scientific)
- EasySpray™ (nano flow)
- Experiment:
  - Targeted-MS^2 at 35,000 of resolution
  - Extracted Ions for quantitation (isolation width 5 ppm):

m/z 934.4972^{+2} → m/z 343.1606^{+1} (b3 ion)
→ m/z 456.2445^{+1} (b4 ion)
→m/z 586.3299^{+1} (y6 ion)
→m/z 1097.6053^{+1} (y12 ion)
→m/z 1184.6367^{+1} (y13 ion)
→m/z 1313.6808^{+1} (y14 ion)
→m/z 1412.7470^{+1} (y15 ion)

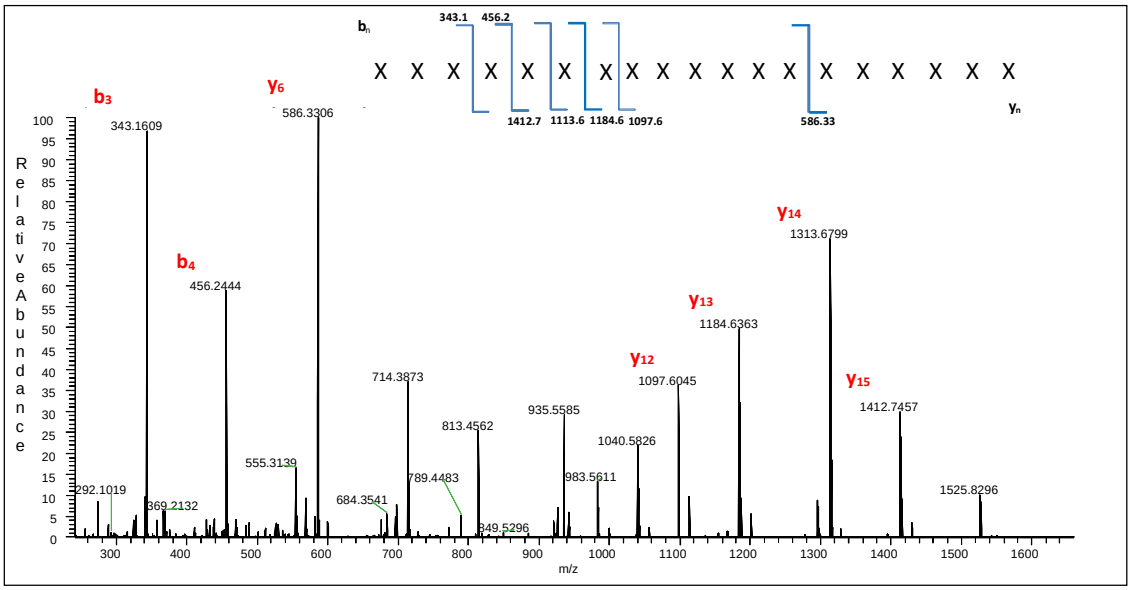

Figure 30: *Selection of m/z fragments for signature peptide used for quantitative assay*

**A specific sequence has been removed for confidentiality reasons*

Nano Source Interface (NSI) Parameters:

Spray voltage: 2kV,

Capillary temperature: 300°C

S-lens RF level: 100

Targeted-MS^2 parameters:

Scan range: 200 – 1700 m/z

Resolution: 35000

Polarity: Positive

AGC: $2e^5$

Maximum inject time: 100 ms

Parent isolation window: 4

NCE: 30

1.2.4. Linearity

In the early phases of method development, the lower limit of quantitation of the target peptide (LLOQ) was set at 70.0 ng/mL. No interfering m/z traces were detected in the matrix samples. Good linearity was achieved from the LLOQ (70.0 ng/mL) to the highest evaluated concentration, ULOQ (4.7 µg/mL), using a linear regression peak area with a $1/x^2$ weighting factor (**Figure 31**).

After optimization of chromatographic conditions as described in the "Chromatographic and mass spectrometric conditions" section, the linearity range was set from 28.0 ng/mL (LLOQ) to 233.0 ng/mL (ULOQ), with good linearity (**Figure 32**). Therefore the sum of the most intense and selective product m/z signal is recommended for low level quantitation (see **Figure 30**).

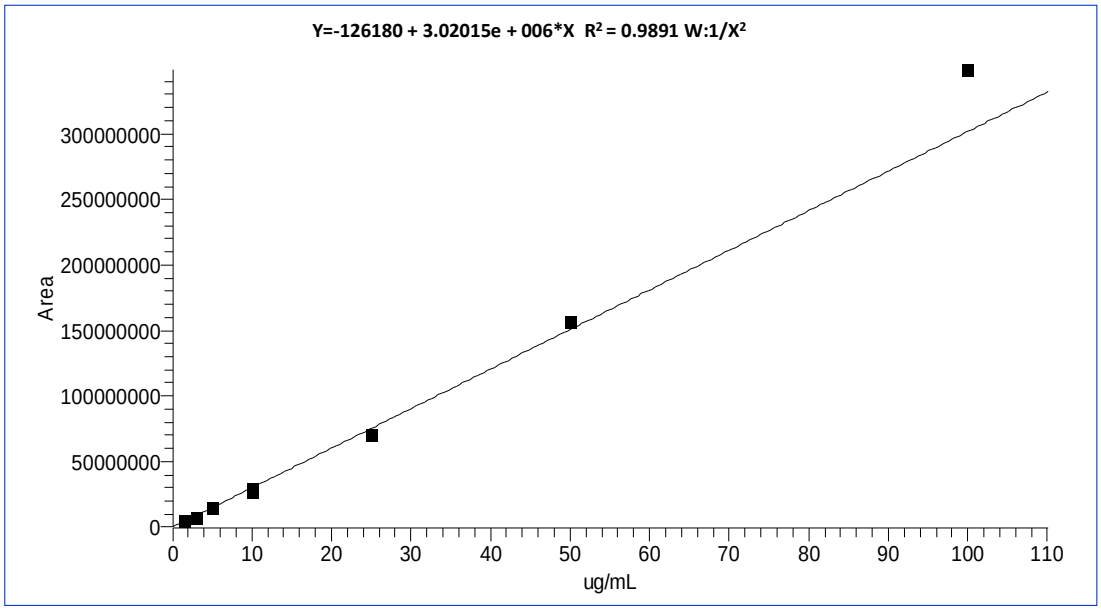

Figure 31: *The preliminary calibration curve of target peptide (concentration expressed as total protein)*

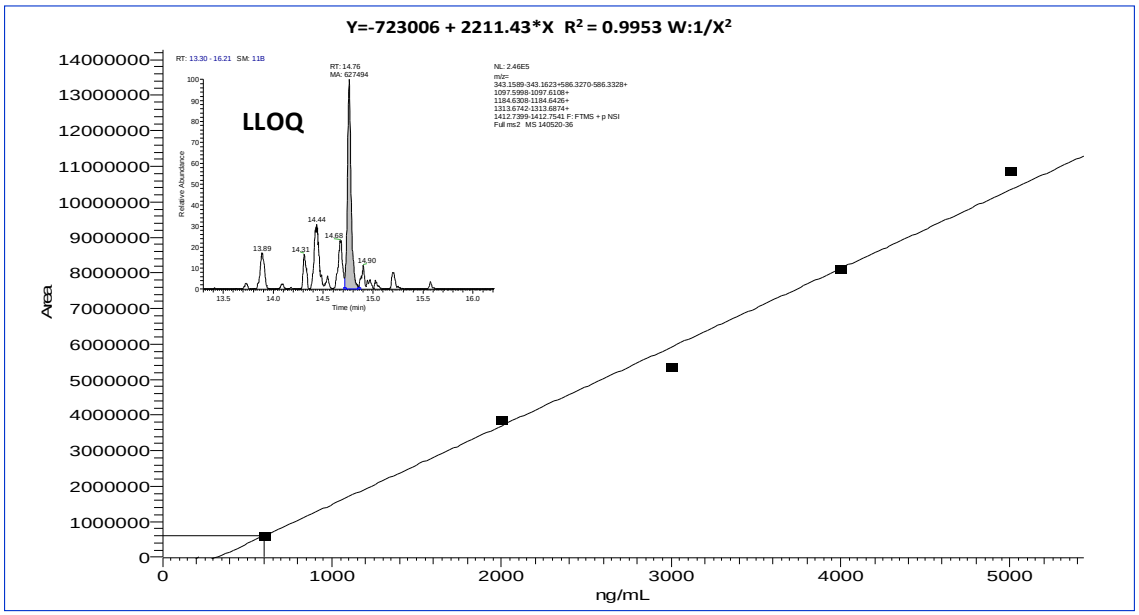

Figure 32: *The final calibration curve of target peptide (concentration expressed as total protein)*

1.3. Discussion

A selective, sensitive method for the quantitation of the biotherapeutic protein ALX-0761 was developed.

Advanced LC-MS technology and appropriate sample clean-up allowed quantification of low levels of target surrogate peptide.

The next step will be to introduce an isotopically labeled Internal Standard in order to further reduce variability and to finally evaluate the validability of the method according to GLP bioanalytical method validation guidances.

Chapter V

1. The anti-EGFR mAbs mixture project

Modification of the epidermal growth factor receptor (EGFR; ErbB1) pathway system has been reported to correlate with human malignancies. Increase in ligand production, receptor over-expression, receptor mutations, and/or cross-talk with other receptor systems are the most frequent modifications involved[24], [25], [26].

These changes have been linked to the development and maintenance of a malignant phenotype and correlated to poor clinical prognosis[27]. For this reason, the EGFR is an attractive target for anticancer therapy[28].

To date, four EGFR targeting agents (cetuximab, panitumumab, gefitinib and erlotinib) from two distinct drug classes have received FDA approval[29].

These include mAbs directed against the extracellular ligand-binding domain of EGFR and small molecule tyrosine kinase inhibitors (TKIs) directed against the cytosolic catalytic domain of the EGFR. Although selected patients receive clear benefit from anti-EGFR mAbs, overall single agent response rates are in the order of 10% [28].

When two mAbs against distinct receptor epitopes are combined, rapid and more efficient receptor internalization is observed, followed by EGFR degradation[30].

---

[24] Peghini PL, Iwamoto M, Raffeld M, Chen YJ, Goebel SU, Serrano J, Jensen RT, Clin Cancer Res. 2002 Jul;8(7):2273-85

[25] Damstrup L, Kuwada SK, Dempsey PJ, Brown CL, Hawkey CJ, Poulsen HS, Wiley HS, Coffey RJ Jr, Br J Cancer. 1999 Jun;80(7):1012-9.

[26] Wong AJ, Ruppert JM, Bigner SH, Grzeschik CH, Humphrey PA, Bigner DS, Vogelstein B., Proc Natl Acad Sci U S A. 1992 Apr 1;89(7):2965-9

[27] Arteaga CL, J Clin Oncol. 2001 Sep 15;19(18 Suppl):32S-40S

[28] Mendelshon J, Baselga J, Epidermal growth factor receptor targeting in cancer, Semin Oncol, (2006), 3(4):369-85

[29] Wheeler DL, Dunn EF, Harari PM, Nat Rev Clin Oncol. 2010 Sep;7(9):493-507. doi: 10.1038/nrclinonc.2010.97. Epub 2010 Jun 15

[30] Friedman LM1, Rinon A, Schechter B, Lyass L, Lavi S, Bacus SS, Sela M, Yarden Y, Proc Natl Acad Sci U S A. 2005 Feb 8;102(6):1915-20. Epub 2005 Jan 31

Mixed antibody treatment is also more effective than single Abs in inhibiting signaling and tumor growth in tissue culture and animal models[31],[32].

Anti-EGFR is a novel therapeutic antibody mixture product comprising two unmarketed mAbs, anti-EGFR mAb A and anti-EGFR mAb B, targeting the EGFR. In previous preclinical proof-of-concept studies, Anti-EGFR antibody mixture was shown to elicit superior cancer cell growth inhibition activities compared with marketed anti-EGFR mAbs[33].

When used together, anti-EGFR mAb A and anti-EGFR mAb B cross link epidermal growth factor receptor and the EGFR is rapidly internalized and undergoes degradation. Alone, these mAbs are unable to effectively induce degradation of EGFR and inhibit tumor growth. Anti-EGFR mAb A and anti-EGFR mAb B are thought to work synergistically. The antibodies bind to different epitopes on the EGFR and their cooperation shows a statistically significant improvement on tumor growth inhibition over non-synergistic use of the antibodies.

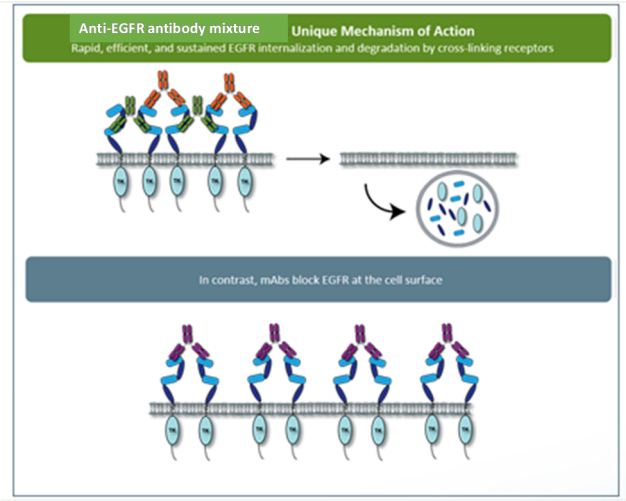

***Figure 33**: Anti-EGFR mAbs Mixture: Unique Mechanism of Action*

[31] Ben-Kasus T, Schechter B, Lavi S, Yarden Y, Sela M, Proc Natl Acad Sci U S A, 2009, 106(9):3294-9

[32] Spangler JB, Neil JR, Abramovitch S, Yarden Y, White FM, Lauffenburger DA, Wittrup KD, Proc Natl Acad Sci U S A, (2010), 107(30):13252-7

[33] Niels Jørgen Østergaard Skartved, Helle Jane Jacobsen, Mikkel Wandahl Pedersen, Pernille Foged Jensen, Jette Wagtberg Sen, Thomas Jørgensen, Adam Hey and Michael Kragh., August 8, 2011; DOI: 10.1158/1078-0432.CCR-11-1209

1.1. Aim of the anti-EGFR mAbs mixture project

The aim of the project was to develop and validate a bioanalytical method for the quantitation of the anti-EGFR antibody mixture in monkey serum samples by LC/MS to support the clinical development of this drug.

The validation was conducted according to GLP principles[34], and to FDA[35] and EMA[36] Guidelines for Bioanalytical Method Validation.
The two major challenges for this project were: 1) to establish acceptance limits and quality requirements for the method, since FDA/EMA guidelines for bioanalytical method validation did not cover the field of an LC/MS method for the quantitation of a protein therapeutic and 2) the requirement in advanced preclinical development to determine the single PK profiles of each component independently.

From this analysis it should be possible to understand how the relative distribution ratio of anti-EGFR mAb A (mAb A) and anti-EGFR mAb B (mAb B) in the central compartment is modified or maintained, to correlate it to any safety issues, and finally to grasp further pharmacology insights into the mode of action of the mixture itself[37]. It is clear that, given mAbs sequence similarities and any binding partners already present in the serum or that may appear (e.g. ADA) during an in-vivo assessment, the bioanalytical method needs more stringent selectivity and sensitivity. To mitigate this problem the analytical strategy was based on a LC-MS bottom-up method that allows quantitation of two signature peptides specific for each mAb and a third signature peptide that is common to both the mAbs but located on a different part of the mAb molecules, in a single run analysis. Comparison of the concentrations of the three peptides can further enhance the LC-MS intrinsic selectivity and provide further insight into the degradation status of the two molecules.

---

[34] OECD Principles on Good Laboratory Practice

[35] FDA (U.S. Food and Drug Administration), Guidance for Industry, Bioanalytical Method Validation, 2013

[36] EMA (European Medicines Agency): Guideline on bioanalytical method validation, 2011

[37] Skartved NJ, Jacobsen HJ, Pedersen MW, Jensen PF, Sen JW, Jørgensen TK, Hey A, Kragh M, Clin Cancer Res, (2011), 17(18):5962-72

These are the steps followed during project development:

- Identification of the best cleavage approach
- Evaluation of method selectivity, sensitivity and specificity
- Study feasibility
- Validation
- Preliminary investigation using MSIA technology

1.1.1. Material and methods

Proteins, chemicals and reagents

Labeled Peptide Internal Standards - Stable isotope-labeled amino acids, [13C6 15N] Leucine and [13C5 15N] Valine (> 97% by HPLC assay) were purchased from Bachem (Bubendorf, Switzerland). Acetonitrile (LiChrosolv®, Reag. Ph. Eur, gradient grade for liquid chromatography), 2-Propanol (LiChrosolv®, gradient grade for liquid chromatography), Methanol (LiChrosolv®, Reag. Ph. Eur, gradient grade for liquid chromatography), Formic Acid (Emsure® ACS, Reag. Ph. Eur., 98-100% for analysis) were purchased from Merck Millipore (Merck KGaA, Darmstadt, Germany). Ammonia Solution 32% (extra pure), Trypsin from porcine pancreas (Type IX-S), Iodoacetamide, IAA (BioUltra, ≥99% NMR), D-L Dithiothreitol, DTT (BioUltra, ≥99.5% RT), Calcium Chloride dihydrate (Reagent Plus® ≥99%), Ammonium bicarbonate (BioUltra, ≥99.5% T), Urea (for electrophoresis gel) and Phosphoric acid (85 wt. % in H_2O, 99.99% trace metals basis) were purchased from Sigma–Aldrich (St. Louis, MO). Ultrapure water was from a Millipore Milli-Q system (Merck Millipore, Billerica, MA).

LC–MS/MS equipment

The UPLC–MS/MS analyses were performed by an Acquity UPLC™ (Waters Corporation Milford, MA) system consisting of Binary Solvent Manager, Sample Manager, Sample Organizer and Column oven. An Acquity UPLC CSH™ (Charged Surface Hybrid) C18 column (2.1 × 150 mm, 1.7 μm particle size; Waters, Milford, MA, USA) was used for the separation.

The UPLC system was interfaced with an AB SCIEX TripleQuad™ 5500 mass spectrometer (AB SCIEX, Toronto, Canada) used as the detector. Analyst software v.1.5.1 was used for data acquisition and processing.

1.1.2. Method development

The bottom-up approach starts with the selection of the optimal signature peptides for each monoclonal antibody, which should have an amino acid sequence unique to the candidate protein and should be easily detectable by mass spectrometry.

The signature peptide must have several important characteristics. First of all, it should be distinguishable from other more abundant proteins or from matrix ions. Secondly, the ionization must be sufficiently efficient to produce abundant ions in the mass spectrum. Finally, as the quantification is carried out on one single peptide for one protein, this peptide must uniquely identify the targeted protein.

The enzyme selected for the cleavage was trypsin since this enzyme was able to provide peptides with well distributed length and charge, and at least 3 to 4 peptide pairs for heavy as well as light chains specific for each mAb Fab part. From these, the selectivity analysis conducted by the BLAST suite revealed the candidate signature peptides. These findings are reported in **Figure 34** and **Figure 35** for the mAb Fab parts.

The *in-silico* analysis regarding the shared mAb Fc parts are reported in **Figure 36**. As described by Furlong et al., these tryptic peptides can be used to obtain the concentration of a humanized mAb in non-human matrices.

mAb	Sequence	# of aa	MW Da	pI	"Macaca fascicularis BLASTP"	"Homo sapiens BLASTP"	Identity (%) vs. HC of the other mAb
Anti-EGFR mAb A	EVQLQQPGSELVRPGASVK	19	2022.2	6.24	OK	OK	78.9
Anti-EGFR mAb A	ASGYTFTSYWMHWVK	15	1864.1	8.55	OK	"Not OK" Chain B, Mature Metal Chelatase Catalytic Antibody With Hapten pdb|3FCT|B	93.3
Anti-EGFR mAb A	QRPGQGLEWIGNIYPGSR	18	2028.2	8.75	OK	OK	82.4
Anti-EGFR mAb A	ATLTVDTSSSTAYMQLSSLTSEDSAVYYCTR	31	3352.6	4.03	OK	OK	90.3
Anti-EGFR mAb A	NGDYYVSSGDAMDYWGQGTSVTVSSASTK	29	3034.1	3.93	OK	OK	80.0
Anti-EGFR mAb B	QVQLQQPGAELVEPGGSVK	19	1964.2	4.53	OK	"Not OK" Chain B, Anti-Blood Group A Fv pdb|1JV5|B"	78.9
Anti-EGFR mAb B	ASGYTFTSHWMHWVK	15	1838.0	8.65	OK	OK	93.3
Anti-EGFR mAb B	QRPGQGLEWIGEINPSSGR	19	2081.2	6.14	OK	OK	82.4
Anti-EGFR mAb B	SSSTAYMQFSSLTSEDSAVYYCVR	24	2682.9	4.37	OK	OK	91.7
Anti-EGFR mAb B	YYGYDEAMDYWGQGTSVTVSSASTK	25	2766.9	4.03	OK	OK	80.0

***Figure 34**: Result summary of the in-silico selection process for Fab Heavy Chains (HC). "OK" and "Not OK" mean "no match" or "match", respectively, for known protein sequences present in monkey or human proteome. When a match is present, some examples of proteins containing that exact sequence are listed. The level of identity with the corresponding peptide in the same region on the other mAb is reported (I to L not considered) as Identity (%) score. The average MW, and calculated isoelectric point (pI) are also reported for each peptide*

mAb	Sequence	# of aa	MW Da	pI	"Macaca fascicularis BLASTP"	"Homo sapiens BLASTP"	Identity (%) vs. LC of the other mAb
Anti-EGFR mAb A	DIQMTQTTSSLSASLGDR	18	1911.0	4.21	OK	"Not OK Chain A, Anti-Blood Group A Fv, pdb|1JV5|A, pdb|1IKF|L, pdb|3U0W|L"	50.0
Anti-EGFR mAb A	TSQDIGNYLNWYQQKPDGTVK	21	2455.6	5.63	OK	OK	NA
Anti-EGFR mAb A	LLIYYTSR	8	1028.2	8.59	OK	"Not OK", immunoglobulin VL region=humanized bispecific antibody [human, Peptide Recombinant, 107 aa, gb|AAB24132.1|"	NA
Anti-EGFR mAb A	LHSGVPSR	8	851.9	9.76	Not OK	Not OK	NA
Anti-EGFR mAb B	DIVMTQAAFSNPVTLGTSASISCR	24	2469.8	5.83	OK	"Not OK, anti-GlcNAc antibody variable region:SUBUNIT=light chain prf||1911357B"	50.0
Anti-EGFR mAb B	FSSSGSGTDFTLR	13	1361.4	5.84	OK	OK	NA
Anti-EGFR mAb B	VEAEDVGVYYCAQNLELPYTFGGGTK	26	2824.1	4.00	OK	OK	NA

***Figure 35**: Result summary of the in-silico selection process for Fab Light Chains (LC). "OK" and "Not OK" mean no match or match, respectively, for known protein sequences present in monkey or human proteome. When a match is present, some examples of proteins containing that exact sequence are listed. The level of identity with the corresponding peptide in the same region on the other mAb is reported (I to L not considered) as Identity (%) score. The average MW, and calculated isoelectric point (pI) are also reported for each peptide*

Peptide	Sequence	Human chain subclass	# of aa	MW (Av.), Da	pI
LC-1	TVAAPSVFIFPPSDEQLK	NA	18	1946.2	4.37
LC-2	SGTASVVCLLNNFYPR	NA	16	1740.9	7.94
LC-3	VDNALQSGNSQESVTEQDSK	NA	20	2136.1	3.92
LC-4	DSTYSLSSTLTLSK	NA	14	1502.6	5.83
HC-1	TPEVTCVVVDVSHEDPEVK	IgG1	19	2082.3	4.17
HC-2	FNWYVDGVEVHNAK	IgG1	14	1677.8	5.32
HC-3	VVSVLTVLHQDWLNGK	IgG1, IgG4	16	1808.1	6.71
HC-4	GFYPSDIAVEWESNGQPENNYK	IgG1, IgG2, IgG4	22	2544.6	4.00
HC-5	TTPPVLDSDGSFFLYSK	IgG1	17	1874.0	4.21

***Figure 36**: List of common tryptic Fc peptides from mAb A and mAb B [38]. None of them is present in monkey serum*

1.1.2.1. Optimization of experimental conditions and selection of signature peptides

The method set-up was thoroughly investigated in order to obtain the most selective peptides, the best SPE conditions and the appropriate chromatographic conditions for the separation of the signature peptides. During this phase, different SPE cartridges and different solvent mixtures were tested to obtain acceptable results in term of sensitivity, robustness, reproducibility and selectivity. Initially two signature peptides, anti-EGFR mAb A HC-3 and anti-EGFR mAb B HC-3, coming from paired regions were monitored and analyzed using a BEH C18 Column (1 x 100 mm, 1.7 µm, Waters), given their very intense MS signal. Unfortunately the anti-EGFR mAb A HC-3 peptide (QRPGQGLEWIGNIYPGSR) from anti-EGFR mAb A, did not show sufficient selectivity and sensitivity on different MRM transitions when monitored in a biological matrix, while the anti-EGFR mAb B HC-3 peptide (QRPGQGLEWIGEINPSSGR) from anti-EGFR mAb B showed acceptable selectivity and sensitivity in the biological matrix (**Figure 37**).

Modifications in chromatographic conditions (including column length) and SPE purification were not able to solve the issue with anti-EGFR mAb A HC-3 peptide. Of the other anti-EGFR mAb A peptides, anti-EGFR mAb A HC-1 peptide (EVQLQQPGSELVRPGASVK) was found to be the second choice in term of sensitivity.

[38] Furlong MT, Zhao S, Mylott W, Jenkins R, Gao M, Hegde V, Tamura J, Tymiak A, Jemal M, Dual universal peptide approach to bioanalysis of human monoclonal antibody protein drug candidates in animal studies, Bioanalysis, 2013, 5(11):1363-76

Therefore its selectivity was investigated and considered to be sufficient in matrix samples (**Figure 38**). In order to improve anti-EGFR mAb A HC-1 peptide sensitivity, a CSH™ (Charger Surface Hybrid) C18 column and some gradient modifications were introduced (see LC-MS/MS equipment and Chromatographic and mass spectrometric conditions section, respectively). With these modifications, anti-EGFR mAb A HC-1 peptide could be selected as mAb signature peptide.

The 1.7 µm Charged Surface Hybrid (CSH™) particle is a Waters third generation hybrid particle technology. Based on Waters Ethylene Bridged Hybrid (BEH™) particle technology, CSH particles incorporate a low level surface charge, designed to improve sample loadability and peak asymmetry in low-ionic-strength mobile phases, while maintaining the mechanical and chemical stability inherent in BEH™ particle technology.

The increased and improved loadability possible with CSH™ Technology permits the separation, identification and quantitation of closely eluting impurities or degradants.

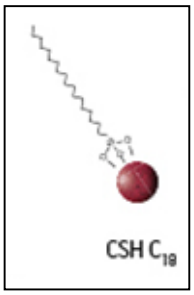

Two types of Solid Phase Extraction plates were tested: HLB (Hydrophilic-Lipophilic-Balanced) Oasis® Plate (polymeric reversed-phase, 30 mg sorbent mass, from Waters) and MCX Oasis® Plate (Mixed Mode Cation eXchange, polymeric phase, 30 mg sorbent mass, from Waters).

The most selective extraction was obtained using the MCX Oasis® plate. The MCX plate is composed of a strong sulfonic (HSO_3) group bonded onto the poly (divinylbenzene-co-N-polyvinyl-pyrrolidone) copolymer in order to give cation-exchange functionalities. This phase is stable from pH 0-14.

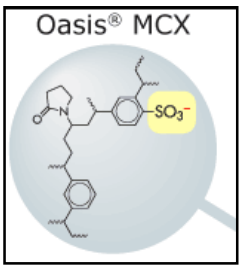

Functional group of MCX Phase

Additionally, quantitation of a signature peptide coming from the common region of the two monoclonal antibodies was introduced. This strategy was applied in order to confirm the analytical response from anti-EGFR mAb A HC-1-peptide and anti-EGFR mAb B HC-3-peptide (**Figure 39**).

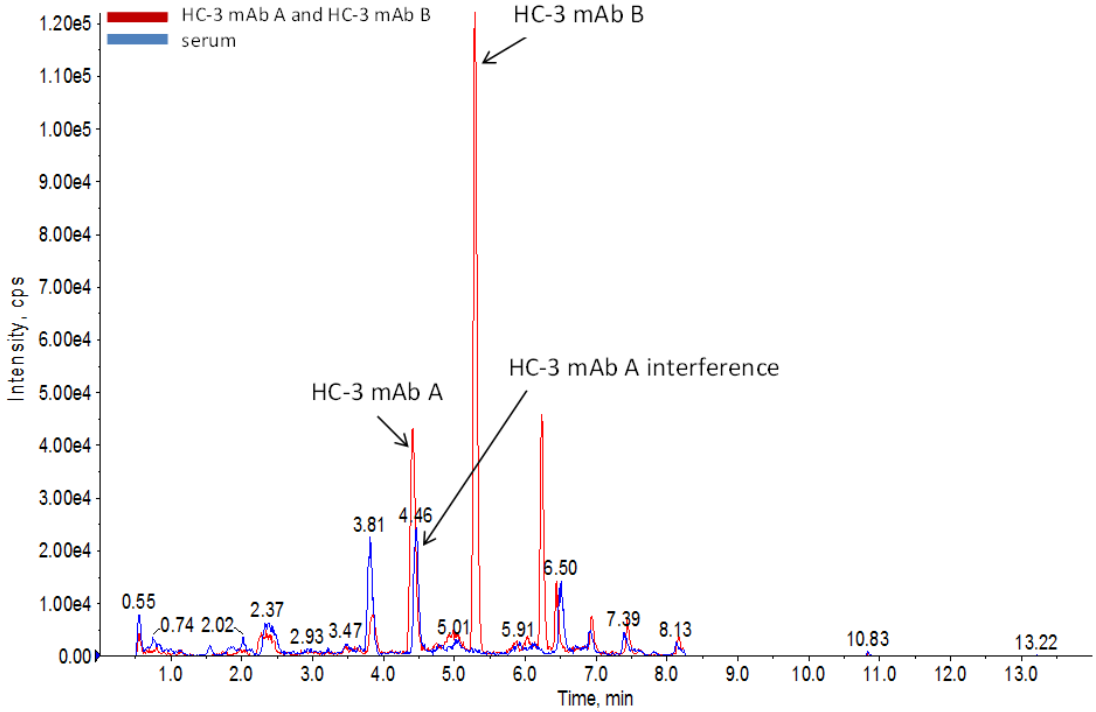

***Figure 37**: A representative MRM chromatogram showing anti-EGFR mAb A and anti-EGFR mAb B response in spiked monkey serum and ion interference at anti-EGFR mAb A retention time in monkey serum*

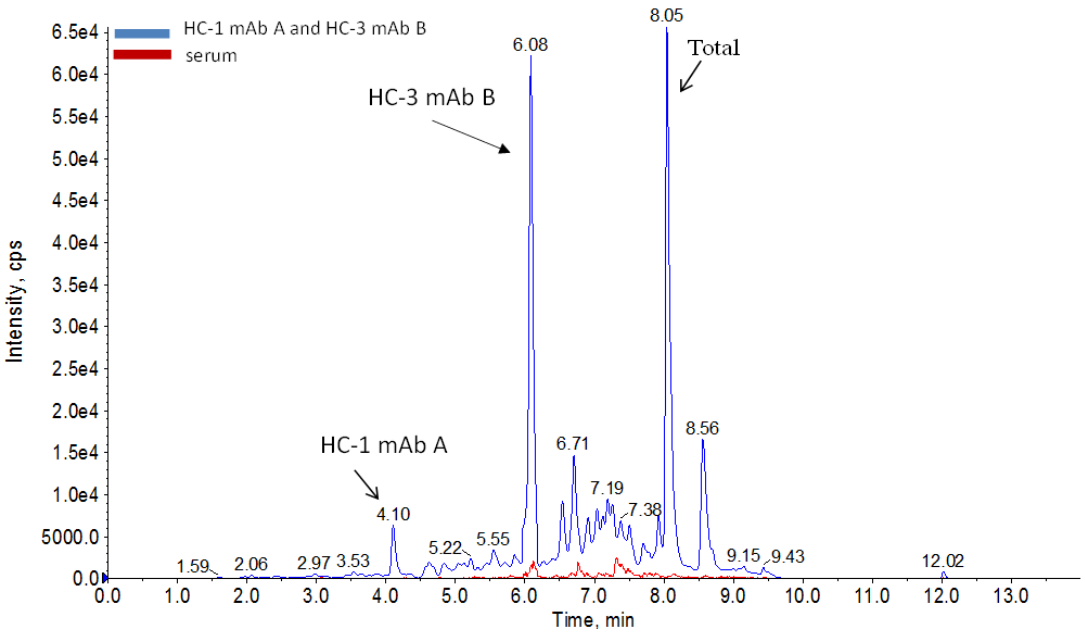

***Figure 38**: A representative MRM chromatogram showing anti-EGFR mAb A HC-1 signature peptide response and the selectivity obtained for this peptide*

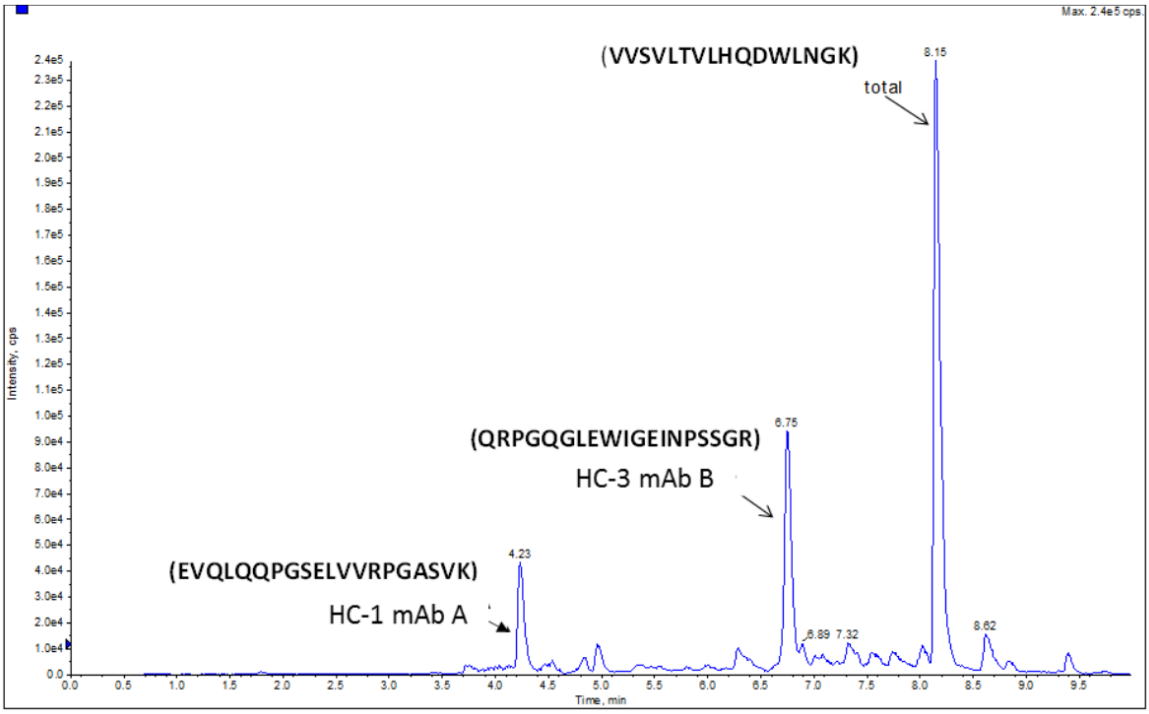

***Figure 39**: A representative MRM chromatogram showing anti-EGFR mAb A-HC-1 from anti-EGFR mAb A, anti-EGFR mAb B-HC-3 from anti-EGFR mAb B and total mAbs response in spiked monkey serum*

1.1.2.2. Monoclonal antibodies-spiked serum samples

Stock solutions of monoclonal antibodies mAb A and mAb B were prepared in ammonium bicarbonate buffer 100 mM at a concentration of 1 mg/mL, separately. Protein-spiked serum samples were prepared by diluting protein stock solutions into blank serum followed by further serial dilution in blank serum to obtain the final concentrations desired. mAb A and mAb B calibration standard concentrations were 150.0, 250.0, 500.0, 1000.0, 2500.0, 5000.0, 7500.0 and 10000.0 ng/mL for the method performance evaluation runs (for the total signature peptide the concentration levels are twice those listed); VS concentrations for all mAb analytes were 150.0, 450.0, 1500.0, 8500.0 and 10000.0 ng/mL. The anti-EGFR mAb A IS, anti-EGFR mAb B IS and total mAbs IS working solutions were prepared at a concentration of 5.00 µg/mL, 2.50 µg/mL and 2.50 µg/mL, respectively.

1.1.2.3. Serum sample digestion

Serum samples (50.0 µL) were transfered to 96-well polypropylene microplates prior to sample preparation. Anti-EGFR mAb A, Anti-EGFR mAb B and total mAbs Internal standards (5.0 µL), 2M Urea solution (700.0 µL), 250 mM DTT solution (70.0 µL) were

added to each well followed by vortex mixing at 750 rpm for 30 min. at 60°C. 0.5 M IAA solution (45.0 µL) was added to each well followed by vortex mixing at 750 rpm for 45 min. at RT. 87.5 mM calcium chloride (10.0 µL) solution and trypsin solution at 15.0 mg/mL concentration (85.0 µL) were added to each well followed by vortex mixing at 750 rpm for 40 min. at 60°C.

1.1.2.4. Sample clean-up

SPE: The digests of the serum samples were mixed with 15.0 µL of phosphoric acid (85%, %W/V) and then loaded onto the Oasis® MCX SPE 96-well plate, sorbent mass 30 mg. The samples were washed sequentially with 2.0 mL of 2% formic acid in water, 1.0 mL of 10% methanol and 1.0 mL of 5% ammonium hydroxide in water. The analytes were eluted with 1.0 mL of 5% ammonium hydroxide in 60/40 methanol/water and then dried down. The dried samples were reconstituted into 150.0 µL of 1% formic acid in water and analyzed by LC–MS/MS.

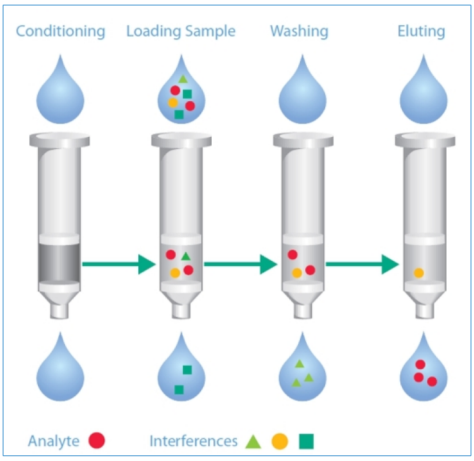

Figure 40: *Typical step of the SPE method*

1.1.2.5. Chromatographic and mass spectrometric conditions

A gradient solvent system consisting of mobile phase A (0.1% formic acid in water), and mobile phase B (0.1% formic acid in acetonitrile) was used. The column temperature was set at 45°C. The gradient was as follows: 0-0.5 min 10% B; 0.5–5.0 min 10–18% B; 5.0–8.5 min 30% B; 8.6-10.6 min 95%B; 10.7–16.5 min 10%B. The flow rate was 0.3 mL/min, and the injection volume was 20.0 µL. The mass spectrometer was operated in ESI positive mode. The following parameters were used: curtain gas 30 psi; ion source gas 1, 45 psi; ion

source gas 2, 50 psi; desolvation temperature 450°C; ion-spray voltage 5200 V. The MRM channels monitored for the surrogate peptides and their labeled IS are listed in **Table 4**. The dwell time for each MRM channel was 50 ms.

Peptide	Precursor ion (*m/z*)	Product ion (*m/z*)
HC-3- mAb B	694.4 $[M+3H]^{3+}$	916.5 y_9^{+1} ion
HC-3-mAb B	694.4 $[M+3H]^{3+}$	866.5 b_8^{+1} ion
HC-1- mAb A	674.7 $[M+3H]^{3+}$	648.8 y_{13}^{+2} ion
HC-1-mAb A	674.7 $[M+3H]^{3+}$	712.9 y_{14}^{+2} ion
HC-1-mAb A	674.7 $[M+3H]^{3+}$	777.0 y_{15}^{+2} ion
HC-3-total	603.3 $[M+3H]^{3+}$	805.4 y_{14}^{+2} ion
HC-3- mAb B IS	696.7 $[M+3H]^{3+}$	859.4 y_8^{+1} ion
HC-1- mAb A IS	677.3 $[M+3H]^{3+}$	715.4 y_{14}^{+2} ion
HC-3-total IS	605.3$[M+3H]^{3+}$	807.4 y_{14}^{+2} ion

Table 4: *MRM transitions for targeted peptides*

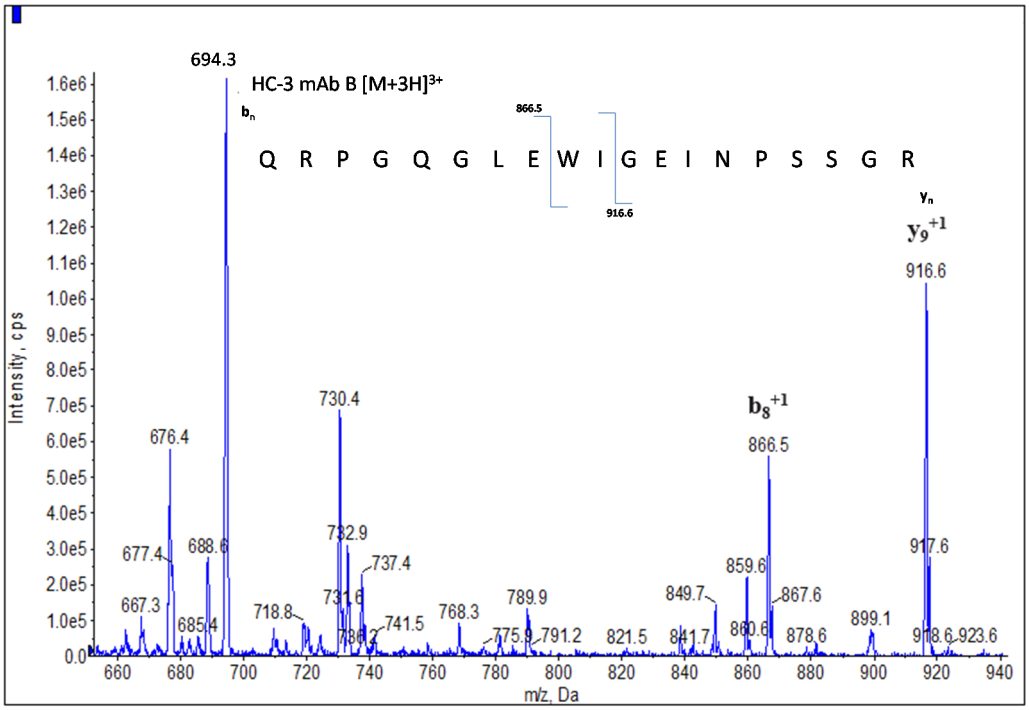

Figure 41*: Precursor ion and product ions selected for HC-3 mAb B*

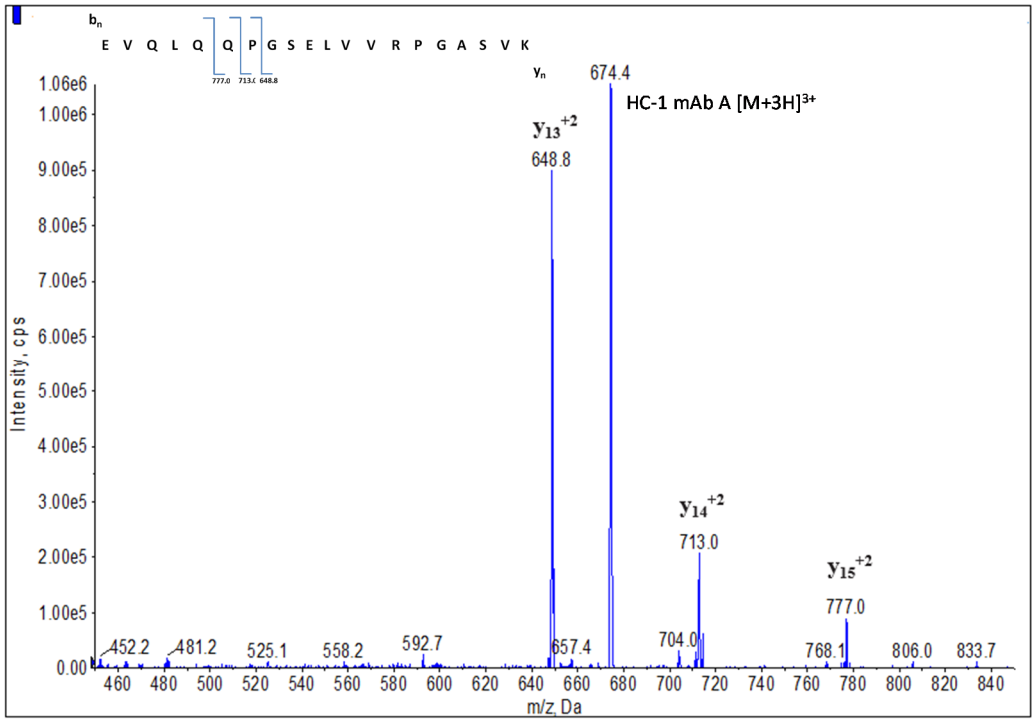

***Figure 42**: Precursor ion and product ions selected for HC-1 mAb A*

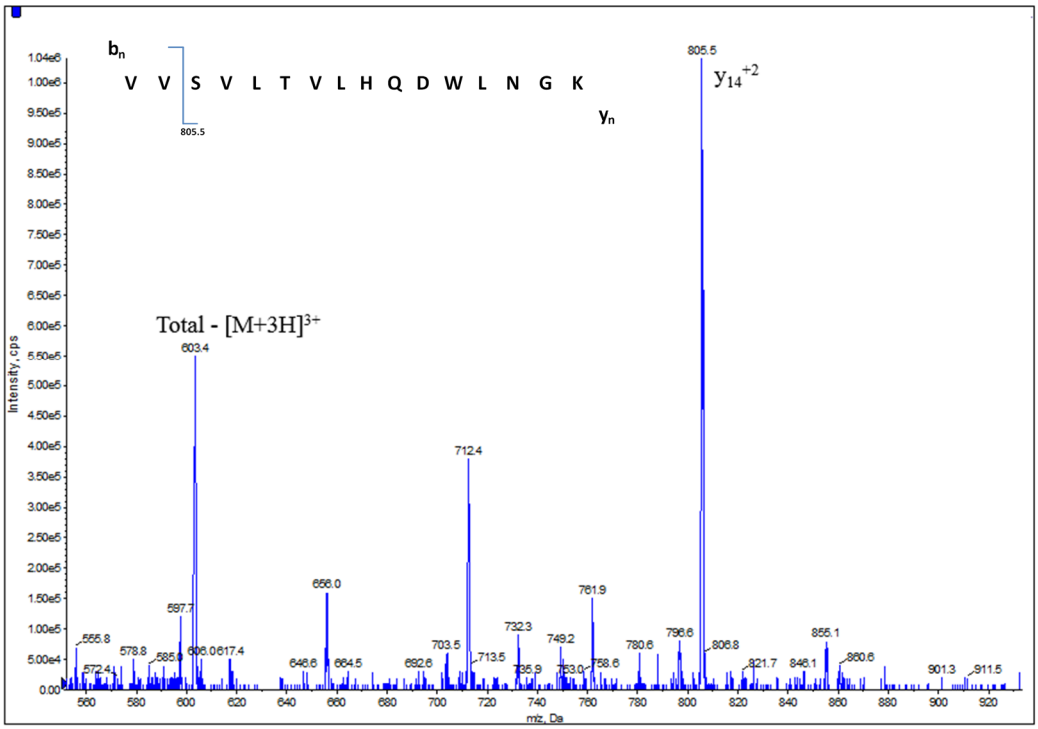

***Figure 43**: Precursor ion and product ion selected for Total mAbs*

1.2. Method validation

The method was validated by evaluating linearity, sensitivity, selectivity, accuracy and precision and matrix effect according to the recent industry guidelines adopting white paper suggestions[39],[40],[41]. For both the mAb analytes, a single calibration curve range and a single QC/VS concentration set were analyzed using the same LC method that incorporated all surrogate peptides.

1.2.1. Selectivity, specificity and sensitivity

Selectivity and specificity assessments were performed by evaluating potential analyte traces in different types of serum sample: a) zero sample; b) five different blank matrix sources; c) LLOQ prepared in five different matrix sources in six replicates each; d) mAb B at ULOQ concentration level spiked in the mAb A calibration standard curve from STD1 to STD 4 (the most critical concentrations to be determined) and vice-versa. No analyte ions were found in the blank serum samples or in the zero samples, which indicated that serum matrices and the IS do not interfere with the determination of either monoclonal antibodies or total mAbs. The lower limit of detection was 150.0 ng/mL for both the surrogate peptides (from mAb B and mAb A) and 300.0 ng/mL for the total surrogate peptide (common region of the two mAbs) with a S/N ratio above 5, which represented a concentration of about 1.00 nM, 1.00 nM and 2.00 nM of analytes (about 20.00 fmol, 20.00 fmol and 40.00 fmol) injected on the column for QRPGQGLEWIGEINPSSGR, EVQLQQPGSELVRPGASVK and VVSVLTVLHQDWLNGK peptides, respectively. Both monoclonal antibodies at LLOQ level met the required accuracy (%BIAS ± 25%) and precision (%CV ≤ 25%) criteria in all the sources of matrices tested and in all the signature peptides considered (**Table 5**). The total mAb determination was performed at LLOQ + 25.0% only during preliminary experiments.

---

[39] Bioanalysis. 2012 Sep;4(18):2213-26. doi: 10.4155/bio.12.205

[40] EMA, Guideline on bioanalytical method validation, 2011, Rev.1 Cor:1-23

[41] FDA, Guidance for Industry: Bioanlytical Method Validation, 2001, 1-25

It was also demonstrated that a high concentration (ULOQ) of one monoclonal antibody does not affect the response of the second monoclonal antibody at low concentrations, and vice-versa (specificity). Moreover, the accuracy (%) of the total mAbs quantified (sum of one mAb spiked at ULOQ level and the second one spiked at low levels, and vice-versa) gave confirmation of the method consistency (**Table 6**).

ANTI-EGFR MONOCLONAL ANTIBODY B					
Parameters	**Matrix 1**	**Matrix 2**	**Matrix 3**	**Matrix 4**	**Matrix 5**
Mean Conc.(µg/mL)	157.4	161.1	163.6	142.0	167.8
BIAS (%)	4.9	7.4	9.1	-5.3	11.9
SD	11.7	21.0	27.4	18.7	28.4
CV (%)	7.4	13.0	16.7	13.2	16.9
ANTI-EGFR MONOCLONAL ANTIBODY A					
Parameters	**Matrix 1**	**Matrix 2**	**Matrix 3**	**Matrix 4**	**Matrix 5**
Mean Conc.(µg/mL)	169.9	150.0	169.2	135.8	172.9
BIAS (%)	13.3	0.0	12.8	-9.5	15.3
SD	33.6	27.7	26.4	9.7	10.5
CV (%)	19.8	18.5	15.6	7.1	6.1

***Table 5**: Selectivity of the LC-MS/MS analysis of mAb B and mAb A spiked at LLOQ in five different monkey serum lots*

Sample	Nominal Conc.(ng/mL)	mAb A Calculated Conc. (ng/mL)	mAb A Accuracy (%)	mAb A Calculated Conc. (ng/mL)	mAb B Accuracy (%)	mAb B at ULOQ	mAb A at ULOQ	Sum of mAb A and mAb B at ULOQ	Sum of mAb B and mAb A at ULOQ	Total calculated conc. (ng/mL)	Accuracy (%)
SET 1											
Std1	**150.0**	158.0	105.3	--	--	11051.6	--	11209.6	--	11120.5	99.2
Std2	**250.0**	263.0	105.2	--	--	10426.9	--	10689.9	--	11502.6	107.6
Std3	**500.0**	590.0	118.0	--	--	10491.9	--	11081.9	--	12180.1	109.9
Std4	**1000.0**	1146.6	114.7	--	--	10154.0	--	11300.6	--	12687.6	112.3
SET 2											
Std1	**150.0**	--	--	161.6	107.7	--	11730.0	--	11891.6	12320.1	105.0
Std2	**250.0**	--	--	239.0	95.6	--	13011.3	--	13250.3	12249.6	94.1
Std3	**500.0**	--	--	434.3	86.9	--	14181.3	--	14615.6	9934.2	**70.1**
Std4	**1000.0**	--	--	997.4	99.7	--	10596.9	--	11594.3	12312.7	116.2

Sample	mAb A and B Nominal Conc.(ng/mL)	mAb B Calculated Conc.(ng/mL)	mAb A Calculated Conc. (ng/mL)	Sum of mAb A and mAb B Calculated Conc. (ng/mL)	Total mAbs Calculated Conc. (ng/mL)	Accuracy (%)
VS-LLOQ_1	150.0	165.8	141.5	307.2	301.6	98.2
VS-LLOQ_2	150.0	167.1	144.6	311.7	288.6	92.6
VS-LLOQ_3	150.0	173.1	162.1	335.3	290.1	86.5
VS-LLOQ_4	150.0	164.6	117.2	281.8	288.8	102.5
VS-LLOQ_5	150.0	152.4	152.2	304.6	297.7	97.7
VS-LLOQ_6	150.0	125.5	160.0	285.5	310.9	108.9
VS-LLOQ_7	150.0	141.8	148.9	290.7	263.1	90.5
VS-LLOQ_8	150.0	162.0	153.6	315.6	264.0	83.6
VS-LLOQ_9	150.0	162.5	156.7	319.2	313.8	98.3
VS-LLOQ_10	150.0	150.7	164.1	314.7	266.1	84.5
VS-LLOQ_11	150.0	152.6	158.2	310.7	267.0	85.9
VS-Low_1	450.0	498.5	460.1	958.5	942.4	98.3
VS-Low_2	450.0	509.0	490.1	999.1	1074.1	107.5
VS-Low_3	450.0	479.4	469.8	949.2	1016.4	107.1
VS-Low_4	450.0	530.8	477.9	1008.7	956.2	94.8

Sample	mAb A and B Nominal Conc.(ng/mL)	mAb B Calculated Conc.(ng/mL)	mAb A Calculated Conc. (ng/mL)	Sum of mAb A and mAb B Calculated Conc. (ng/mL)	Total mAbs Calculated Conc. (ng/mL)	Accuracy (%)
VS-Low_5	450.0	511.5	513.8	1025.3	1120.3	109.3
VS-Low_6	450.0	447.1	479.5	926.7	1007.3	108.7
VS-Low_7	450.0	414.8	450.2	865.0	783.9	90.6
VS-Low_8	450.0	462.6	458.4	921.0	873.7	94.9
VS-Low_9	450.0	393.5	424.1	817.6	1019.4	124.7
VS-Low_10	450.0	446.2	523.4	969.6	1124.5	116.0
VS-Low_11	450.0	461.5	377.6	839.1	1072.3	**127.8**
VS-Medium_1	1500.0	DEV	DEV	DEV	DEV	**DEV**
VS-Medium_2	1500.0	1701.1	1837.1	3538.3	3181.9	89.9
VS-Medium_3	1500.0	1634.9	1750.2	3385.1	3569.9	105.5
VS-Medium_4	1500.0	1717.1	1782.8	3499.9	3593.0	102.7
VS-Medium_5	1500.0	1706.7	1614.5	3321.1	3235.2	97.4
VS-Medium_6	1500.0	1475.4	1632.8	3108.2	2586.1	83.2
VS-Medium_7	1500.0	1524.1	1389.1	2913.1	2789.6	95.8
VS-Medium_8	1500.0	1443.1	1424.3	2867.4	2832.3	98.8
VS-Medium_9	1500.0	1697.3	1497.9	3195.1	3387.2	106.0
VS-Medium_10	1500.0	1698.5	1722.1	3420.6	3285.3	96.0
VS-Medium_11	1500.0	1875.6	1792.7	3668.3	3591.1	97.9
VS-High_1	8500.0	8401.0	8187.5	16588.5	15863.2	95.6
VS-High_2	8500.0	8948.2	9003.0	17951.2	16840.3	93.8
VS-High_3	8500.0	8501.8	8986.3	17488.1	17506.2	100.1
VS-High_4	8500.0	8797.9	8114.8	16912.7	19210.4	113.6
VS-High_5	8500.0	8881.8	8691.8	17573.6	18023.8	102.6
VS-High_6	8500.0	8191.7	8791.02	16982.8	14244.0	83.9
VS-High_7	8500.0	8800.2	8909.84	17710.0	15840.6	89.4
VS-High_8	8500.0	8421.5	9575.83	17997.4	14445.5	80.3
VS-High_9	8500.0	8429.3	8714.6	17143.8	17328.8	101.1
VS-High_10	8500.0	8183.6	9253.3	17436.9	16197.1	92.9
VS-High_11	8500.0	8406.3	8774.3	17180.6	16795.2	97.8
VS-ULOQ_1	10000.0	11091.2	13600.9	24692.1	22622.1	91.6
VS-ULOQ_2	10000.0	11414.5	11984.6	23399.1	24885.9	106.4
VS-ULOQ_3	10000.0	10760.8	11311.2	22072.0	21742.9	98.5
VS-ULOQ_4	10000.0	11190.5	12435.0	23625.5	22692.7	96.1
VS-ULOQ_5	10000.0	11018.2	14001.5	25019.7	24498.1	97.9
VS-ULOQ_6	10000.0	10099.1	11867.0	21966.1	16253.0	**74.0**
VS-ULOQ_7	10000.0	11463.1	11306.4	22769.5	20383.4	89.5
VS-ULOQ_8	10000.0	11299.2	10712.1	22011.3	17992.2	81.7
VS-ULOQ_9	10000.0	11412.3	11301.9	22714.2	23017.8	101.3
VS-ULOQ_10	10000.0	11870.9	11608.8	23479.7	24067.1	102.5
VS-ULOQ_11	10000.0	10427.4	11056.1	21483.5	21557.2	100.3

Table 6: *Evaluation of total mAbs accuracies when compared to the sum of individual mAbs measured concentrations. DEV stands for deviation from the sample preparation procedure. Set1 and Set2 also report the specificity experiment results where one mAb at ULOQ was spiked over a*

concentration curve of the other mAb. The last column reports the accuracy (%) of the calculated total mAb concentrations where the nominal concentration was assumed to be the sum of the individual mAbs calculated concentrations. Out of accuracy acceptance criteria [i.e. Accuracy (%) ± 20% and Accuracy (%) ± 25% at LLOQ level] are shown in red.

1.2.2. Assessment of matrix effect

Matrix effect assessment was conducted using the post-extraction spike method. It quantitatively assesses matrix effects by comparing the response of the surrogate peptides in neat solvent to the response of the surrogate peptide spiked into a blank matrix sample that has gone through the sample preparation process. The monoclonal antibodies, at QC-Low and QC-High level concentrations, were spiked in five different monkey serum sources in order to investigate also the matrix effect values among different lots of serum. The results reported in **Table 7** show that there is no significant matrix effect on either analyte.

ANTI-EGFR MONOCLONAL ANTIBODY B				
Parameters	**AN/IS Area ratio in samples spiked after extraction**		**AN/IS Area ratio in neat solvent**	
	VS Low 450.0 ng/mL	**VS High 8500.0 ng/mL**	**VS Low 450.0 ng/mL**	**VS High 8500.0 ng/mL**
Mean Area Ratio	0.658	9.66	0.501	9.39
Normalized Matrix Effect	1.3	1.0		
n	5	5	5	5
ANTI-EGFR MONOCLONAL ANTIBODY A				
Parameters	**AN/IS Area ratio in samples spiked after extraction**		**AN/IS Area ratio in neat solvent**	
	VS Low 450.0 ng/mL	**VS High 8500.0 ng/mL**	**VS Low 450.0 ng/mL**	**VS High 8500.0 ng/mL**
Mean Area Ratio	0.334	5.13	0.275	5.92
Normalized Matrix Effect	1.2	0.9		
n	5	5	5	5

Table 7: *Matrix effect of the LC-MS/MS analysis of mAb B and mAb A in monkey serum*

1.2.3. Accuracy and Precision

Accuracy and precision were determined in one run of intra-batch and three runs of inter-batch serum samples containing mAb A, mAb B and the total mAbs at five concentration levels (LLOQ, VS-Low, VS-Medium, VS-High and ULOQ).

The intra-batch relative mean accuracy of back-calculated concentrations of the VS compared with theoretical ones ranged from 2.4% to 12.7%, from -6.3% to 16.4% and from -2.2% to 16.4% for QRPGQGLEWIGEINPSSGR peptide (mAb B), EVQLQQPGSELVRPGASVK peptide (mAb A) and for VVSVLTVLHQDWLNGK (total mAbs), respectively. It should be noted that one QC at the medium concentration level was out of the acceptable limit of the assay for both the analytes but was excluded from the calculation since it was an outlier (known sample processing error).

The intra-assay precision (%CV) ranged from 2.2 to 4.6, from 4.3 to 11.7 and from 2.0 to 7.4 for QRPGQGLEWIGEINPSSGR peptide (mAb B), EVQLQQPGSELVRPGASVK peptide (mAb A) and VVSVLTVLHQDWLNGK (total), respectively (**Table 8**). As shown in **Table 9**, for QRPGQGLEWIGEINPSSGR peptide (mAb B), inter-assay accuracy (%Bias) of less than 10.9% and inter-assay precision (%CV) of less than 9% were achieved. For peptide EVQLQQPGSELVRPGASVK (mAb A), inter-assay accuracy (%Bias) of less than 9.6% and inter-assay precision (%CV) of less than 11.1% were achieved, while for VVSVLTVLHQDWLNGK (total mAbs) inter-assay accuracy (%Bias) was less than 11.0% and inter-assay precision (%CV) less than 12.3%.

The accuracy and precision of all the peptides are well below the 20% (25% for VS at LLOQ level) acceptance criteria typically used in LC–MS/MS applied to large molecule bioanalysis.

ANTI-EGFR MONOCLONAL ANTIBODY B					
Parameters	**VS LLOQ 150.0 ng/mL**	**VS Low 450.0 ng/mL**	**VS Medium 1500.0 ng/mL**	**VS High 8500.0 ng/mL**	**VS ULOQ 10000.0 ng/mL**
Mean Conc. (ng/mL)	164.6	505.8	1690.0	8706.2	11095.0
Accuracy (%BIAS)	9.7	12.4	12.7	2.4	10.9
SD	7.6	18.8	37.3	241.2	239.2
Precision (%CV)	4.6	3.7	2.2	2.8	2.2
n	5	5	4*	5	5
ANTI-EGFR MONOCLONAL ANTIBODY A					
Parameters	**VS LLOQ 150.0 ng/mL**	**VS Low 450.0 ng/mL**	**VS Medium 1500.0 ng/mL**	**VS High 8500.0 ng/mL**	**VS ULOQ 10000.0 ng/mL**
Mean Conc. (ng/mL)	143.5	482.3	1746.1	8596.7	9372.9
Accuracy (%BIAS)	-4.3	7.2	16.4	1.1	-6.3
SD	16.7	20.7	94.8	425.9	771.4
Precision (%CV)	11.7	4.3	5.4	5.0	8.2
n	5	5	4*	5	5
TOTAL					
Parameters	**VS LLOQ 300.0 ng/mL**	**VS Low 900.0 ng/mL**	**VS Medium 3000.0 ng/mL**	**VS High 17000.0 ng/mL**	**VS ULOQ 20000.0 ng/mL**
Mean Conc. (ng/mL)	293.4	1021.9	3395.0	17488.8	23288.3
Accuracy (%BIAS)	-2.2	13.5	13.2	2.9	16.4
SD	5.9	76.0	216.6	1256.3	1341.9
Precision (%CV)	2.0	7.4	6.4	7.2	5.8
n	5	5	4*	5	5
**One outlier of a set of five values, excluded from the statistic calculation*					

***Table 8**: Intra-assay accuracy and precision of the LC-MS/MS analysis of mAb B, mAb A and total mAbs in monkey serum*

ANTI-EGFR MONOCLONAL ANTIBODY B					
Parameters	**VS LLOQ 150.0 ng/mL**	**VS Low 450.0 ng/mL**	**VS Medium 1500.0 ng/mL**	**VS High 8500.0 ng/mL**	**VS ULOQ 10000.0 ng/mL**
Mean Conc. (ng/mL)	156.2	468.6	1647.4	8542.1	11095.2
Accuracy (%BIAS)	4.1	4.2	9.8	0.5	10.9
SD	13.6	42.4	131.3	270.3	504.6
Precision (%CV)	8.7	9.0	8.0	3.2	4.5
n	11	11	10*	11	11
ANTI-EGFR MONOCLONAL ANTIBODY A					
Parameters	**VS LLOQ 150.0 ng/mL**	**VS Low 450.0 ng/mL**	**VS Medium 1500.0 ng/mL**	**VS High 8500.0 ng/mL**	**VS ULOQ 10000.0 ng/mL**
Mean Conc. (ng/mL)	152.8	465.9	1644.3	8818.4	10428.8
Accuracy (%BIAS)	0.6	3.5	9.6	3.7	4.3
SD	13.2	40.5	160.4	419.1	1158.5
Precision (%CV)	8.8	8.7	9.8	4.8	11.1
n	11	11	10*	11	11
TOTAL MONOCLONAL ANTIBODIES					
Parameters	**VS LLOQ 300.0 ng/mL**	**VS Low 900.0 ng/mL**	**VS Medium 3000.0 ng/mL**	**VS High 17000.0 ng/mL**	**VS ULOQ 20000.0 ng/mL**
Mean Conc. (ng/mL)	286.5	999.1	3205.2	16572.3	21792.0
Accuracy (%BIAS)	-4.5	11.0	6.8	-2.5	9.0
SD	18.9	104.5	360.3	1475.0	2687.7
Precision (%CV)	6.6	10.9	11.2	8.9	12.3
n	11	11	10*	11	11

***Table 9**: Inter-assay accuracy and precision of the LC-MS/MS analysis of mbA B, mAb A and total mAbs in monkey serum (*Outlier value from the intra-batch assay, excluded from the statistic calculation).*

1.2.4. Standard Curve

The calibration curves of mAb A, mAb B and total mAbs in monkey serum were generated automatically by using the algorithm classic of Analyst software. For each assay, the calibration curve was fitted with the following equation: y = Ax + B (regression weight 1/x). The linear dynamic range evaluated was between 150.0 ng/mL and 10000.0 ng/mL for mAb A and mAb B, and from 300.0 ng/mL to 20000.0 ng/mL for total mAbs. Individual standard curve concentration data in monkey serum are shown in Table 10. With the exception of a single mAb B calibration point, the deviations of the back-calculated concentrations from their nominal values were all within ± 20% (within ± 25% at LLOQ) for all the surrogate peptides. The correlation coefficients (r) from three batches of calibration samples were 0.999, between 0.993 and 0.999 and 0.999 for QRPGQGLEWIGEINPSSGR peptide (mAb B), EVQLQQPGSELVRPGASVK (mAb A) and VVSVLTVLHQDWLNGK (total mAbs), respectively (**Figure 44**). These results indicated that this LC-MS method can provide

sensitive, specific, selective, precise and accurate analysis of mAb A, mAb B and total mAbs in monkey serum. Therefore it met the validation criteria set by Health Authority guidelines, industry best practice and opinion leaders' white papers in bioanalytical method validation.

ANTI-EGFR MONOCLONAL ANTIBODY B						
Nominal conc. (ng/mL)	**Calculated conc.(ng/mL)**	**Accuracy (%Bias)**	**Calculated conc.(ng/mL)**	**Accuracy (%Bias)**	**Calculated conc.(ng/mL)**	**Accuracy (%Bias)**
150.0	136.4	-9.0	155.4	3.6	146.8	-2.1
250.0	271.0	8.4	228.9	-8.5	151.4	*Dev
500.0	506.5	1.3	516.7	3.3	549.2	9.8
1000.0	1064.2	6.4	1060.6	6.1	980.0	-2.0
2500.0	2302.6	-7.9	2457.1	-1.7	2421.1	-3.2
5000.0	5098.9	2.0	4769.3	-4.6	4582.0	-8.4
7500.0	7092.6	-5.4	7390.1	-1.5	7835.3	4.5
10000.0	10427.8	4.3	10321.9	3.2	10135.6	1.4
ANTI-EGFR MONOCLONAL ANTIBODY A						
Nominal conc. (ng/mL)	**Calculated conc.(ng/mL)**	**Accuracy (%Bias)**	**Calculated conc.(ng/mL)**	**Accuracy (%Bias)**	**Calculated conc.(ng/mL)**	**Accuracy (%Bias)**
150.0	141.1	-5.9	152.6	1.7	128.8	-14.1
250.0	265.5	6.2	222.7	-10.9	222.4	-11.0
500.0	436.1	-12.8	513.3	2.7	584.6	16.9
1000.0	1147.0	14.7	1119.4	11.9	1122.2	12.2
2500.0	2721.4	8.9	2428.7	-2.9	2466.2	-1.4
5000.0	4489.4	-10.2	4730.4	-5.4	4855.1	-2.9
7500.0	6643.5	-11.4	7646.6	2.0	7514.5	0.2
10000.0	11056.0	10.6	10086.2	0.9	10006.2	0.1
TOTAL MONOCLONAL ANTIBODIES						
Nominal conc. (ng/mL)	**Calculated conc.(ng/mL)**	**Accuracy (%Bias)**	**Calculated conc.(ng/mL)**	**Accuracy (%Bias)**	**Calculated conc.(ng/mL)**	**Accuracy (%Bias)**
300.0	290.1	-3.3	297.9	-0.7	240.1	-20.0
500.0	527.1	5.4	486.3	-2.7	349.4	*Dev
1000.0	935.2	-6.5	1039.0	3.9	1101.4	10.1
2000.0	2140.5	7.0	2156.1	7.8	2250.6	12.5
5000.0	4707.9	-5.8	4589.8	-8.2	4977.7	-0.4
10000.0	10526.8	5.3	9673.2	-3.3	9922.9	-0.8
15000.0	14727.5	-1.8	15267.2	1.8	14693.3	-2.0
20000.0	19944.9	-0.3	20290.7	1.5	20114.1	0.6

**Dev: Deviation from nominal concentration*

***Table 10**: Individual standard curve concentration data of the LC-MS/MS analysis of mAb B, mAb A and total mAbs in monkey serum*

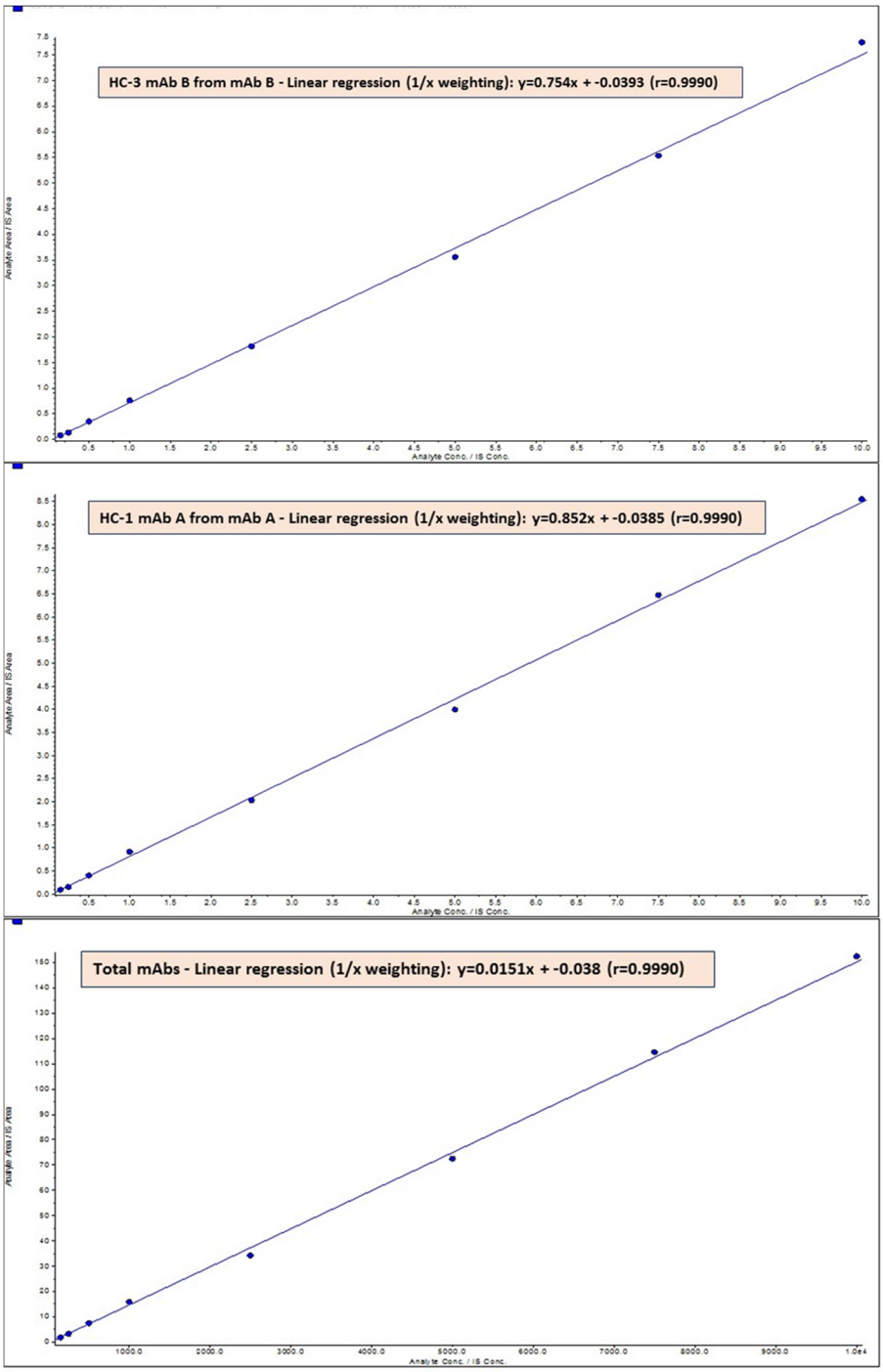

***Figure 44**: A representative linearity response of mAb B HC-3 from mAb B, mAb A HC-1 from mAb A and total mAbs signature peptides*

1.3. Discussion

In-silico analysis led to the selection of 3-4 candidate signature peptides specific for each mAb, which were then tested using LC-MS to assess sensitivity and selectivity in the real matrix. One additional constraint was the decision to select, as far as possible, tryptic peptide pairs deriving from homologous mAb regions. This was taken to allow for the possibility of differential in vivo degradation on different parts of the mAbs. Selecting peptides from paired regions would normalize the measured concentration by leveling off possible differential metabolic effects.

This was not entirely possible, since the sensitivity and selectivity for the N-terminus anti-EGFR mAbs B candidate were not ideal. Nevertheless, the two selected specific peptides derive from Heavy Chain N-terminus regions of the mAbs and to a certain extent metabolism is expected to impact similarly on these parts.

Since the quantitative method had to be developed in a non-human matrix and mAbs belong to the h-IgG1 class, it was hypothesized that a further improvement could be the quantitation of peptide(s) not present in monkey matrix but common to the two mAbs. This had already been reported by Furlong et al.[42] but in our work the investigation was extended. This was done for the total quantitation of the mAbs, but also attempting a comparison between the concentrations from the mAbs specific signature peptides and the concentration obtained from non-specific peptides. The added value lies not only in the consistency of the concentrations obtained, but in the help it can provide in understanding more completely the metabolic fate of the mAbs themselves.

To this end, first of all the method had to proven (for each of the three signature peptides independently) to be robust, sensitive and specific enough to meet design requirements. This was successfully demonstrated by assessing linearity, accuracy and precision, sensitivity,

[42] Furlong MT, Zhao S, Mylott W, Jenkins R, Gao M, Hegde V, Tamura J, Tymiak A, Jemal M, Dual universal peptide approach to bioanalysis of human monoclonal antibody protein drug cand dates in animal studies, Bioanalysis, 2013, 5(11):1363-76

selectivity, specificity, and matrix effect according to GLP industry guidelines for each of the three signature peptides.

Upon this solid basis, we were then able to confirm that the total mAbs concentration in spiked monkey serum samples is consistent with the sum of the specific single concentrations from the two mAbs within the same accuracy criteria that were applied in method performance assessment, i.e. Accuracy (%) ±20%; ±25% for LLOQ level (**Table 6**): 94.5% of the results met the acceptance criteria. Of course this should be further verified in incurred samples, and in spiked incurred samples to have a more complete picture of the applicability of the principle. This will be done when samples from *in-vivo* studies can be analyzed.

Chapter VI

1. MSIA Technology

An alternative sample preparation approach could be the Mass Spectrometric Immuno Assay (MSIA) technique.

MSIA is a hybrid technique that combines immunoaffinity protein analyte purification with high sensitive mass spectrometric detection.

The MSIA Platform is able to capture any byotinylated molecules. Streptavidin is covalently linked to a porous monolithic solid support in the distal end of the MSIA pipette tips. Analytes are enriched by the immobilized streptavidin-biotin conjugated complex, washed, and eluted to provide concentrated MS-ready samples.

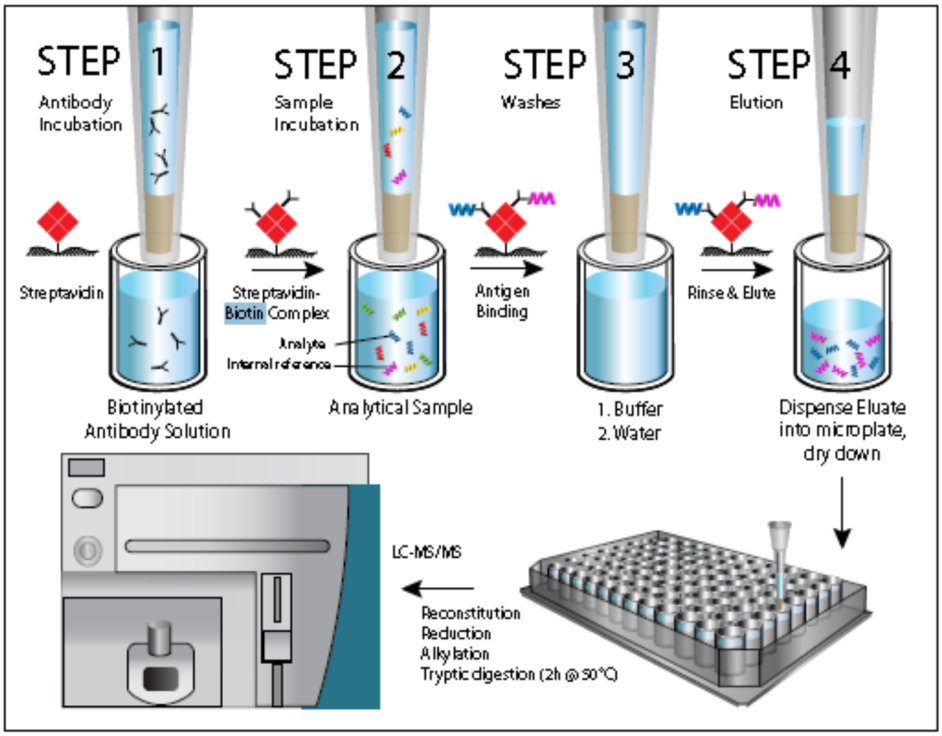

Figure 45: *Scheme of MSIA technology workflow*

1.1. MSIA Method Development

This technique was applied to the mixure of **anti-EGFR monoclonal antibody A** and **anti-EGFR monoclonal antibody B** in order to obtain a more sensitive, robust and reproducible method by combining the performance characteristics of traditional ligand binding assays with the benefits of MS detection.

The first experiment conducted in order to start the investigation on the best MSIA conditions was:

Experiment I:

- **Pre-Analytical**

To enable the Streptavidin MSIA tips to have a specific affinity for Goat Anti-Human IgG, each of the micro-columns was loaded with 125.0 µL of 0.06 and 0.10 mg/mL Biotin anti-IgG Fc conjugate antibody. This was accomplished by following the steps provided in **Figure 46** utilizing an electronic 12-channel pipette.

STEP 1: BIOTINYLATED ANTIBODY (Goat Anti-Human IgG-Fc specific) LOADING

Materials:

Wash Buffer 1/2- Dilution Buffer: PBS (Phosphate Saline Buffer, pH 7.2)

Step	Description	Microtiter Plate Volume (µL)	Mixing Cycle Volume (µL)	No. of mixing cycle iterations	Approx. Allotted time per step
1	Wash buffer	200	175	10	20 seconds
2	Biotinylated Ab Solution	125	100	500	14 minutes
3	Wash buffer	200	175	10	20 seconds

Figure 46: *Biotinylated Antibody Loading/Workflow for Electronic 12-Channel Pipette*

Workflow:

1. Dispense 200.0 µL Wash 1 in Row 1 (Mixing Cycle Vol: 175, Number of mix iterations: 10, vel up/down:1 – blow out)
2. Dispense 125.0 µL of Biotinylated Antibody: 0.06 /0.10 mg/mL in DB (row 2) (Cycle Vol: 100, Number of mix iterations: 500, vel up/down:1 – blow out)
3. Dispense 200.0 µL Wash 3 in Row 3 (Mixing Cycle Vol: 175, Number of mix iterations: 10, vel up/down:1 – blow out)

STEP 2: SAMPLE ANALYTE LOADING

Materials:

Wash Buffer 1/2- Dilution Buffer: PBS (Phosphate Saline Buffer, pH 7.2)

Step	Description	Microtiter Plate Volume (µL)	Mixing Cycle Volume (µL)	No. of mixing cycle iterations	Approx. Allotted time per step
1	Wash buffer	200	175	10	20 seconds
2	Analytical sample	50	175	500	~19 minutes
3	Wash buffer	200	175	10	20 seconds
4	Water	200	175	10	20 seconds
5	Water	200	175	10	20 seconds

***Figure 47**: Sample analyte load workflow for Electronic 12-Channel Pipette*

Workflow:

1. Dispense 200.0 µL Wash 1 in Row 4 (Mixing Cycle Vol: 175, Number of mix iterations: 10, vel up/down:1 – blow out)
2. 50.0 µL of sample diluted 1:5 in Wash Buffer – Dispense 250.0 µL in Row5 (Mixing Cycle Vol: 175, Number of mix iterations: 999, vel up/down:1 – blow out)
3. Dispense 200.0 µL Wash 2 in Row 6 (Mixing Cycle Vol: 175, Number of mix iterations: 10, vel up/down:1 – blow out)
4. Dispense 200.0 µL Water in Row 7 (Mixing Cycle Vol: 175, Number of mix iterations: 10, vel up/down:1 – blow out)
5. Dispense 200.0 µL Water in Row 8 (Mixing Cycle Vol: 175, Number of mix iterations: 10, vel up/down:1 – blow out)

STEP 3: SAMPLE ANALYTE ELUTION

Following the selective capture of anti-EGFR mAb A and B with the anti-IgG-Fc-derivatized Streptavidin MSIA, each device was treated with 100 µL of the Elution Solvent liberating the analyte.

Materials:

Acetonitrile for LCMS

TFA

1. Elution: dispense 100.0 µL of 33% ACN containing 0.4% of TFA in each well (Mixing Cycle Vol: 50, Number of mix iterations: 100, vel up/down:1 – blow out)

NB: Both the standard solution and the elution solvent are added with 100.0 µg/mL of BSA (Bovin Serum Albumin), in order to prevent non-specific binding to the labware.

Sample tested: sample prepared in duplicate at 10.0 µg/mL in 0.1 M ammonium bicarbonate buffer with BSA at 100.0 µg/mL.

Two different concentrations of biotinylated Goat Anti-human IgG to bind the tips (from Southern Biotech) were tested: 0.06 mg/mL e 0.10 mg/mL.

The samples purified by MSIA and dried were then dissolved in 250.0 µL of 0.1 M ammonium bicarbonate and digested by adding 50.0 µL of 8.0 mg/mL trypsin in 0.1 M ammonium bicarbonate for 40 min at 60°C in a termomixer shaker:

The reaction was stopped by adding 600.0 µL of o-phosphoric acid (assay 4.25%) and purified using the following **SPE protocol (Oasis® MCX SPE plate)**:

- Conditioning: 500.0 µL x 2 of methanol
- Equilibrate: 500.0 µL x 2 of H_2O
- Loading: the pre-treated sample as described above
- Wash 1: 1.0 mL x 2 of H_2O containing 2% of Formic Acid
- Wash 2: 0.5 mL x 2 of 10% methanol containing 2% of Formic Acid
- Wash 3: 0.5 mL x 2 of H_2O containing 5% of NH_4OH
- Elution: 500.0 µL x 2 of 60% methanol containing 5% of NH_4OH
- Evaporation by using the *Low Boiling Point* program at 40°C due to the methanol percentage and then using the *AQUEOUS* NH_3 program at 50°C.

The sample was dissolved in 150.0 µL of water containing 1% of formic acid and injected into the LC-MS/MS system (Acquity UPLC™ Waters - AB Sciex TripleQuad™ 5500 mass spectrometer, Analyst software v.1.5.1 for data acquisition and data reprocessing).

mAb B	Analyte Peak Area	Mean	% Recovery
Std_Ref_1	659502.5		
Std_Ref_2	585263.6	622383.1	
MSIA STD_set1_1	47516.5		
MSIA STD_set1_2	43161.3	45338.9	7.3
MSIA STD_set2_1	41608.6		
MSIA STD_set2_2	38514.4	40061.5	6.4
mAb A	Analyte Peak Area	Mean	% Recovery
Std_Ref_1	1632545.1		
Std_Ref_2	1445270.6	1538907.9	
MSIA STD_set1_1	168785.8		
MSIA STD_set1_2	155436.6	162111.2	10.5
MSIA STD_set2_1	152704.0		
MSIA STD_set2_2	134862.1	143783.1	9.3
Total mAbs	Analyte Peak Area	Mean	% Recovery
Std_Ref_1	1481059.6		
Std_Ref_2	1269962.5	1375511.1	
MSIA STD_set1_1	128151.8		
MSIA STD_set1_2	120280.6	124216.2	9.0
MSIA STD_set2_1	123047.0		
MSIA STD_set2_2	104929.8	113988.4	8.3

***Table 11*:** *Recovery of set 1 and set 2 from different biotinylated antibody concentrations used in the MSIA extraction protocol.*

Set 1: 0.06 mg/mL biotinylated antibody
Set 2: 0.10 mg/mL biotinylated antibody

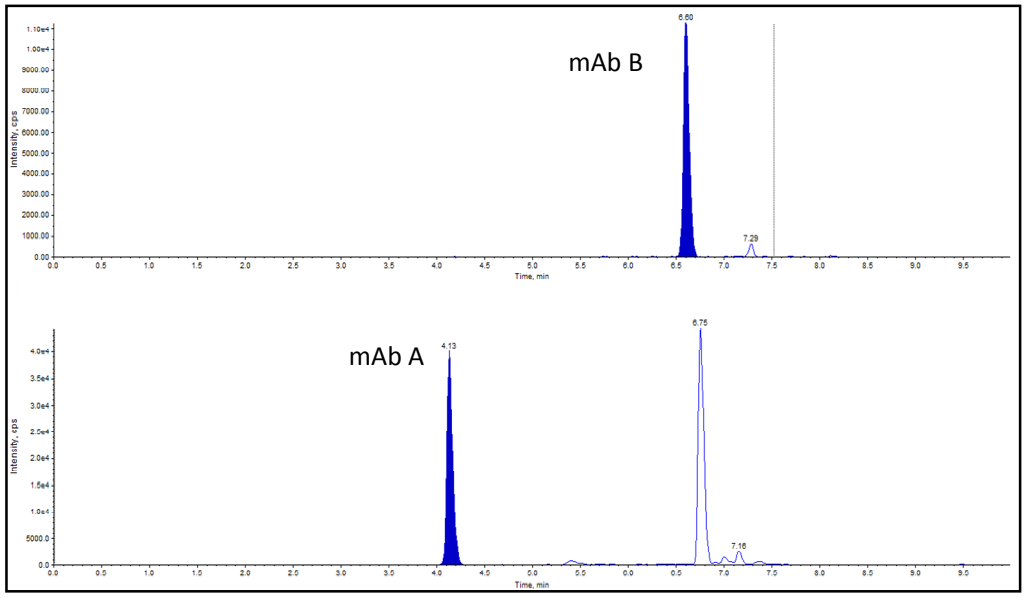

Figure 48: *A representative MRM chromatogram from MSIA protocol*

Results: the results showed very poor recovery (see **Table 11**) and it was therefore decided to test three different concentrations of biotinylated Goat Anti-Human IgG.

Experiment II:

The second step was to apply the MSIA protocol modified on the basis of the results obtained in experiment 1. A spiked sample (10.0 µg/mL for each peptide) in monkey serum was tested. Three different concentrations of biotinylated Goat Anti-Human IgG to bind the tips were tested: 0.02-0.04 and 0.06 mg/mL (identified as Set 1, Set 2 and Set 3 in the experiment performed, see **Table 12**).

Two replicates were analyzed for each condition and concentration. The samples were dried, digested with trypsin and purified via SPE as described in experiment I.

NB: The elution solvent was added with 100.0 µg/mL of BSA, in order to prevent non-specific binding to the labware.

A change was made at point 2 of step 1:

STEP 1: BIOTINYLATED ANTIBODY LOADING

Materials:

Wash Buffer 1/2- DB: PBS (Phosphate Buffered Saline, pH 7.2)

Worflow:

1. Dispense 200.0 µL Wash 1 in Row 1(Mixing Cycle Vol: 175, Number of mix iterations: 10, vel up/down:1 – blow out)
2. Dispense 125.0 µL of Biotinylated Antibody: 0.02 – 0.04 – 0.06 mg/mL in DB (Row 2) (Cycle Vol: 100, Number of mix iterations: 999, vel up/down:1 – blow out)
3. Dispense 200.0 µL Wash 2 in Row 1 (Mixing Cycle Vol: 175, Number of mix iterations: 10, vel up/down:1 – blow out)

mAb A	Analyte peak Area	Mean	Recovery (%) [a]
Set1_DBK_1	286.8		
Set1_DBK_2	0.0		
Set1_Std1	36107.3		
Set1_Std2	28988.1	32547.7	**5.2**
Set2_DBK_1	0.0		
Set2_DBK_2	0.0		
Set2_Std1	39008.9		
Set2_Std2	42702.6	40855.8	**6.6**
Set3_DBK_1	0.0		
Set3_DBK_2	0.0		
Set3_Std1	39040.2		
Set3_Std2	40684.7	39862.5	**6.4**
mAb B	**Analyte peak Area**	**Mean**	**Recovery (%) [a]**
Set1_DBK_1	0.0		
Set1_DBK_2	0.0		
Set1_Std1	58829.5		
Set1_Std2	49067.1	53948.3	**3.5**
Set2_DBK_1	226.0		
Set2_DBK_2	0.0		
Set2_Std1	66075.1		
Set2_Std2	72511.6	69293.4	**4.5**
Set3_DBK_1	0.0		
Set3_DBK_2	317.6		
Set3_Std1	71536.5		
Set3_Std2	76336.5	73936.5	**4.8**
Total mAbs	**Analyte peak Area**	**Mean**	**Recovery (%) [a]**
Set1_DBK_1	2374.6		
Set1_DBK_2	649.6		
Set1_Std1	87713.3		
Set1_Std2	59862.2	73787.8	**5.4**
Set2_DBK_1	386.2		
Set2_DBK_2	0.0		
Set2_Std1	77771.4		
Set2_Std2	74645.1	76208.3	**5.5**
Set3_DBK_1	357.7		
Set3_DBK_2	0.0		
Set3_Std1	57620.5		
Set3_Std2	77792.3	67706.4	**4.9**

Table 12: *Results for Set 1, Set 2 and Set 3 samples.*

Set 1: 0.02 mg/mL biotinylated antibody

Set 2: 0.04 mg/mL biotinylated antibody

Set 3: 0.06 mg/mL biotinylated antibody

[a]Recovery (%): the recovery was calculated using the data related to the experiment I (***Table 11***: *Recovery of set 1 and set 2 from different biotinylated antibody concentrations used in the MSIA extraction protocol*)

Results: the samples prepared using the biotinylated antibody at 0.04 and 0.06 mg/mL showed a higher response than samples prepared using biotinylated antibody at 0.02 mg/mL, but the recovery was generally very low.

Additionally, the replicates of mAb A and mAb B prepared using biotinylated antibody at 0.04 and 0.06 mg/mL were more reproducible while the total mAbs replicates were more reproducible using biotinylated antibody at 0.04 mg/mL.

Experiment III:

On the basis of the results obtained in experiment II and even if the recovery was low, the MSIA protocol described above was applied to analyze samples with a lower concentration. The purpose of this experiment was to verify the applicability of this method to lower concentrations.

The samples tested were blank matrix-anti-EGFR antibody mixture at 0.150, 1.00 and 10.0 µg/mL for each peptide. The biotinylated Goat Anti-Human IgG to bind the tips was tested at 0.05 mg/mL, with 100.0 µg/mL BSA and without BSA. The dried samples were then processed and analyzed.

	Sample Name	Sample Type	Analyte Concentration (ng/mL)	Analyte Peak Area (counts)	Calculated Concentration (ng/mL)	Accuracy (%)
	1 Set1_DBK	Double Blank	0.0	0.0	N/A	N/A
	2 Set1_Std1	Standard	150.0	1984.9	150.0	100.0
	3 Set1_Std4	Standard	1000.0	17469.6	1000.0	100.0
mAb A	4 Set1_Std8	Standard	10000.0	41995.1	2346.3	23.5
	7 Set1_DBK	Double Blank	0.0	0.0	N/A	N/A
	8 Set2_Std1	Standard	150.0	3022.2	150.0	100.0
	9 Set2_Std4	Standard	1000.0	15312.3	1000.0	100.0
	10 Set2_Std8	Standard	10000.0	48390.2	3287.7	32.9
	1 Set1_DBK	Double Blank	0.0	0.0	N/A	N/A
	2 Set1_Std1	Standard	150.0	4987.0	150.0	100.0
	3 Set1_Std4	Standard	1000.0	30963.3	1000.0	100.0
mAb B	4 Set1_Std8	Standard	10000.0	79482.5	2587.1	25.9
	7 Set1_DBK	Double Blank	0.0	78.7	4.3	N/A
	8 Set2_Std1	Standard	150.0	4571.5	150.0	100.0
	9 Set2_Std4	Standard	1000.0	30785.2	1000.0	100.0
	10 Set2_Std8	Standard	10000.0	101275.1	3287.7	32.9
	1 Set1_DBK	Double Blank	0.0	0.0	N/A	N/A
	2 Set1_Std1	Standard	300.0	3681.6	300.0	100.0
Total mAbs	3 Set1_Std4	Standard	2000.0	26327.1	2000.0	100.0
	4 Set1_Std8	Standard	20000.0	80054.2	6033.3	25.9
	7 Set1_DBK	Double Blank	0.0	0.0	N/A	N/A
	8 Set2_Std1	Standard	300.0	5642.3	300.0	100.0
	9 Set2_Std4	Standard	2000.0	27931.1	2000.0	100.0
	10 Set2_Std8	Standard	20000.0	62005.8	4598.9	23.0

***Table 13**: Accuracy of the three tested concentrations in set 1 and set 2 samples. Set 1 was prepared with BSA and set 2 without BSA. N/A=Not Applicable.*

Results: the back-calculated concentration of the standards was accurate for Std 1 and Std 4 (good proportionality observed within the peak areas) while Std 8 showed a non-linear response. This was probably due to some extraction issue.

No significant differences were observed between samples prepared with BSA and without BSA (for mAb A and mAb B) while a significant difference was observed for Total mAbs. In this case the presence of BSA resulted in a better respons in term of accuracy.

Experiment IV:

To standardize the process, the use of internal standard was introduced to analyze a calibration curve prepared by applying the MSIA protocol used in experiment III.

The calibration points tested were: 50.0 – 75.0 – 150.0 – 300.0 – 500.0 – 750.0 – 1000.0 and 2500.0 ng/mL for each peptide and in duplicate.

The biotinylated Goat Anti-Human IgG to bind the tips was tested at 0.05 mg/mL, with 100.0 µg/mL BSA.

	Sample Name	Sample Type	Analyte Concentration (ng/mL)	Analyte Peak Area (counts)	IS Peak Area (counts)	Calculated Concentration (ng/mL)	Accuracy (%)
	1 Std_1	Standard	50.0	658.1	60749.0	51.8	103.6
mAb B	2 Std_2	Standard	75.0	842.2	54591.9	69.8	93.0
	3 Std_3	Standard	150.0	2253.2	62132.8	151.3	100.9
	4 Std_4	Standard	300.0	5667.2	79810.9	287.2	95.7
	5 Std_5	Standard	500.0	11744.4	74648.5	625.0	125.0
	6 Std_6	Standard	750.0	15294.3	87520.0	693.1	92.4
	7 Std_7	Standard	1000.0	19104.0	84559.3	893.3	89.3
	1 Std_1	Standard	50.0	2247.6	60749.0	52.7	105.4
mAb A	2 Std_2	Standard	75.0	2603.1	54591.9	69.1	92.1
	3 Std_3	Standard	150.0	5453.2	62132.8	130.5	87.0
	4 Std_4	Standard	300.0	18727.1	79810.9	355.7	118.6
	5 Std_5	Standard	500.0	27292.9	74648.5	556.5	111.3
	6 Std_6	Standard	750.0	44514.6	87520.0	775.8	103.4
	7 Std_7	Standard	1000.0	56244.3	84559.3	1015.7	101.3
	8 Std_8	Standard	2500.0	147507.6	112100.1	2013.3	80.5

*Std 8 not eluted for mAb B.

Table 14: *Accuracy of calibration points for mAb B and mAb A, respectively.*

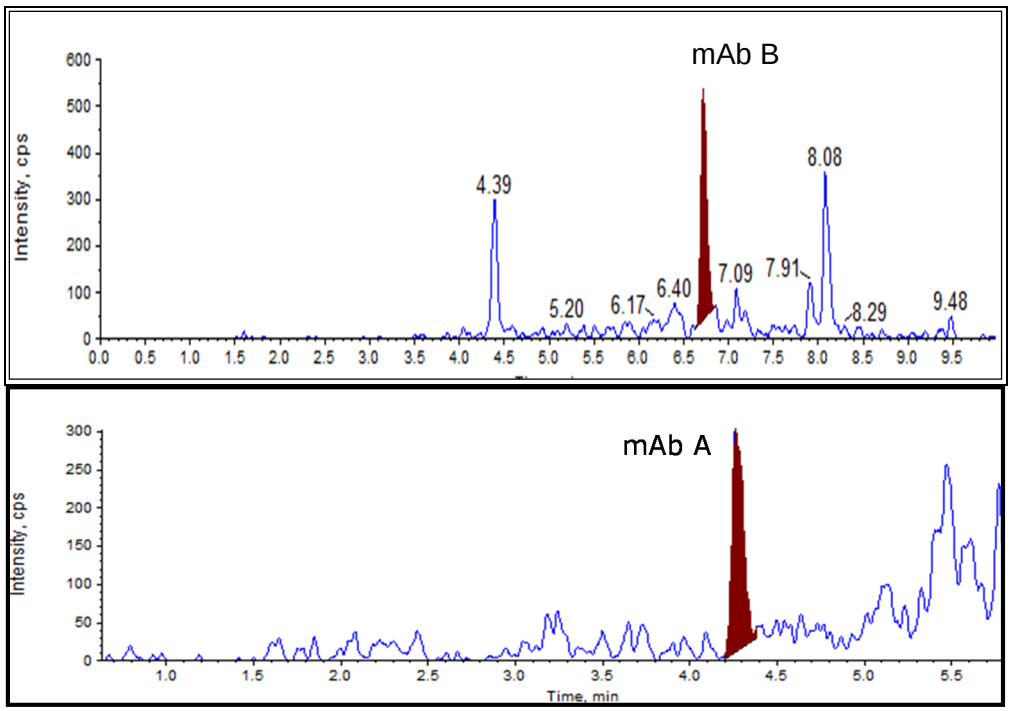

Figure 49: *A representative MRM chromatogram of target peptide (mAb B and mAb A) at LLOQ level obtained after MSIA extraction*

Sample Name	Conc. ng/mL	Sample Type	Analyte Signal To Noise	Sample Name	Conc. ng/mL	Sample Type	Analyte Signal To Noise
DBK	N/A	Double Blank	N/A	DBK	N/A	Double Blank	4.355
STD1	50.0	Standard	4.539	STD1	50.0	Standard	26.515
STD2	75.0	Standard	6.454	STD2	75.0	Standard	43.619
STD3	150.0	Standard	11.038	STD3	150.0	Standard	75.465
STD4	300.0	Standard	23.021	STD4	300.0	Standard	169.919
STD5	500.0	Standard	35.235	STD5	500.0	Standard	271.235
STD6	750.0	Standard	50.868	STD6	750.0	Standard	376.972
STD7	1000.0	Standard	71.656	STD7	1000.0	Standard	512.742

Table 15: *Signal to noise ratio related to mAb B (on the right) and mAb A (on the left) obtained applying the MSIA protocol. N/A= Not Applicable*

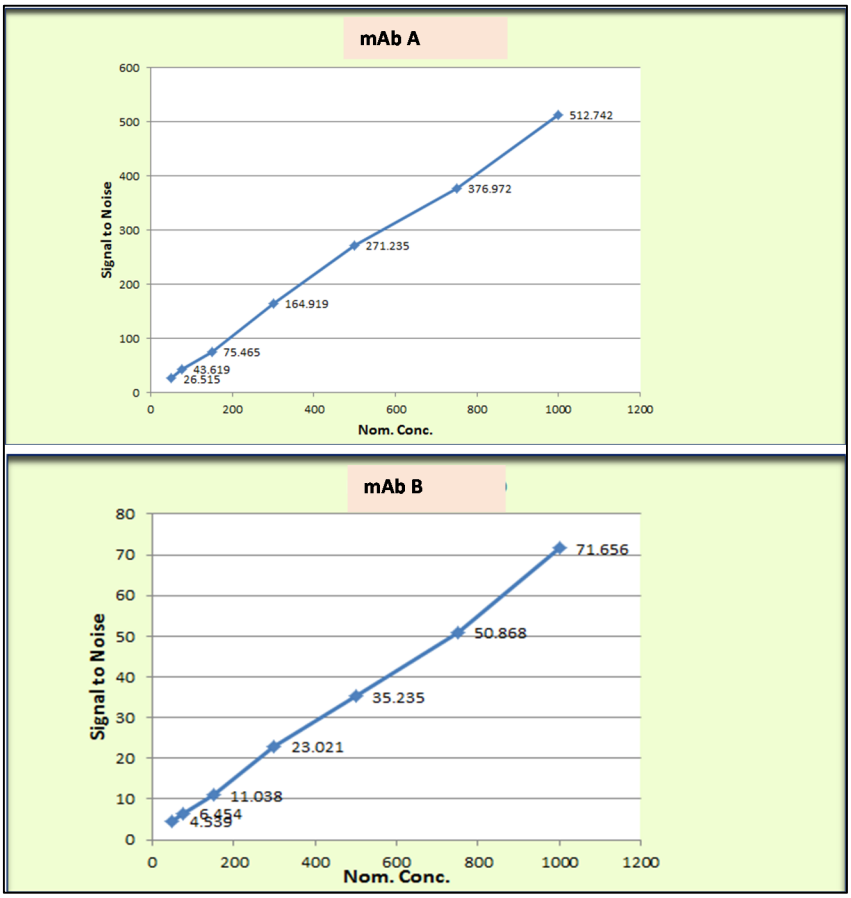

Table 16: *Signal to Noise response correlated to the nominal concentration (Nom. Conc.) of calibration standards*

Results: the back-calculated concentrations of the standard were accurate in the 50.0-1000.0 ng/mL range. As reported in **Table 16** the signal to noise ratio was acceptable. Many sources of noise have been reduced by using this approach and this is particularly evident in our complex sample matrix.

Experiment V:

In order to verify potential competition between the two monoclonal antidobies, cross-selectivity was tested by preparing the mAb B calibration curve (STD 50.0-75.0-100.0-500.0 and 1000.0 ng/mL) spiked at each level with mAb A at ULOQ level and vice-versa. Since the availability of the internal standard was very limited, the experiment was conducted without internal standard. The biotinylated Goat Anti-Human IgG to bind the tips was tested at 0.05 mg/mL, with 100.0 µg/mL BSA.

Sample Name	Sample Type	Analyte Concentration (ng/mL)	Analyte Peak Area (counts)	Calculated Concentration (ng/mL)	Accuracy (%)
1 Prova_DBK	Double Blank	0.0	48.8	18.3	N/A
2 Prova_Std1	Standard	50.0	550.9	52.6	105.2
3 Prova_Std2	Standard	75.0	850.8	73.1	97.5
4 Prova_Std3	Standard	100.0	1107.8	90.7	90.7
5 Prova_Std4	Standard	500.0	8328.7	584.0	116.8
6 Prova_Std5	Standard	1000.0	12938.0	898.9	89.9

Table 17: *Accuracy of mAb B calibration curve spiked with mAb A at ULOQ level. NA= Not Applicable.*

Sample Name	Sample Type	Analyte Concentration (ng/mL)	Analyte Peak Area (counts)	Calculated Concentration (ng/mL)	Accuracy (%)
1 Prova_DBK	Double Blank	0.0	0.0	N/A	N/A
2 Prova_Std1	Standard	50.0	1386.2	48.4	96.7
3 Prova_Std2	Standard	75.0	3609.4	84.9	113.2
4 Prova_Std3	Standard	100.0	3751.5	87.2	87.2
5 Prova_Std4	Standard	500.0	33605.5	577.4	115.5
6 Prova_Std5	Standard	1000.0	51695.2	874.5	87.5

Table 18: *Accuracy of mAb A calibration curve spiked with mAb B at ULOQ level. NA= Not Applicable.*

Results: the cross-selectivity test demonstrated that a high concentration of mAb A monoclonal antibody does not affect the response of mAb B at each level (from 50.0 to 1000.0 ng/mL) and vice-versa. As reported in **Table 17** and **Table 18,** the accuracy (%) of each calibration standard point ranged from 89.9% to 116.8% and from 87.2% to 115.5% for mAb B and mAb A, respectively.

1.2. Conclusions

The experiments carried out showed that affinity purification and mass spectrometry analysis of therapeutic antibodies could constitute a valid alternative to the traditional bioanalytical methodologies for large molecule bioanalysis. The biological complexity of mAbs and the increase in the complexity of constructs requires reliable and unique data. Bioanalytical support is critical to mAbs pharmacokinetic and pharmacodynamic study.

For this reason this technique was introduced in our mass spectrometry laboratory and the preliminary results obtained were very promising. This technique allowed us to significantly reduce interferences from the complex matrix as in our case study. As clearly showed in **Figure 49** (analyte response at LLOQ level in matrix sample), no interfering peaks are present in the processed sample and therefore this approach could provide accurate and precise analytical data. However, MSIA technique requires additional work in order to find the appropriate sample processing conditions due to sample variability and complexity.

MSIA technology is also a challenge as is the traditional Ligand Binding Assay (LBA) for therapeutic antibody analysis. In fact, LBA technique suffers from some deficits such as lack of structural information (e.g. identify drug to antibody ratio), negatively affected by neutralization events (e.g. anti-drug antibody) and may be affected by cross-reactivity and non-specific binding.

The benefits of MSIA & MS platform are enhanced specificity through m/z detection, circumventions needed for LBA Ab reagent, improved data content for therapeutic characterization and ability to counter neutralization events. The deficits of this platform are that data content is limited to detectable peptides, and methods are labor intensive and still require automation. In the near future, our research will be extended to other complex molecules in order to implement this technique in our laboratory.

Chapter VII

1. Antibody-drug conjugates (ADCs)[43]

Antibody–drug conjugates (ADCs) represent a growing segment of therapeutic molecules in development. Therapeutic monoclonal antibodies can be conjugated with a variety of molecules including small-molecule drugs, radionuclides, peptides, other proteins (protein toxins, enzymes, cytokines), and polyethylene glycol (**Figure 50**). Other than polyethylene glycol, the conjugated moiety provides a specific mechanism of action (MOA) resulting in the death of the target cell (**Figure 51**). For these conjugates, the monoclonal antibody (mAb) acts as a drug delivery system as it targets the conjugated moiety specifically to a cell expressing the antigen recognized by the mAb. However, the mAb provides additional functions to the conjugate, such as a typical antibody half-life of several days to several weeks and, in some cases, antibody effector function, or signal transduction triggering cell death.

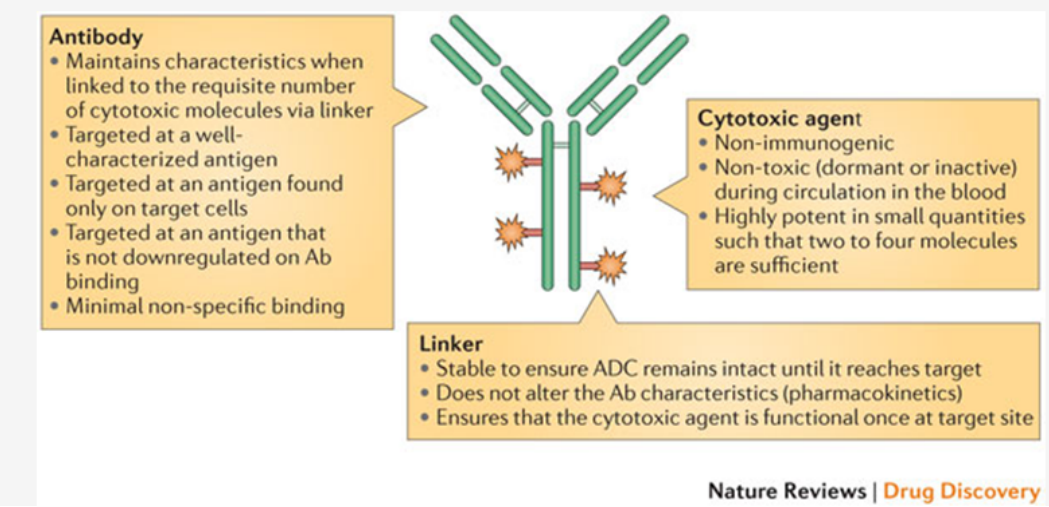

Figure 50: *Second generation ADCs*

[43] Marjorie A. Shapiro, Xiao-Hong Chen. Regulatory Considerations When Developing Assays for the Characterization and Quality Control of Antibody-Drug Conjugate

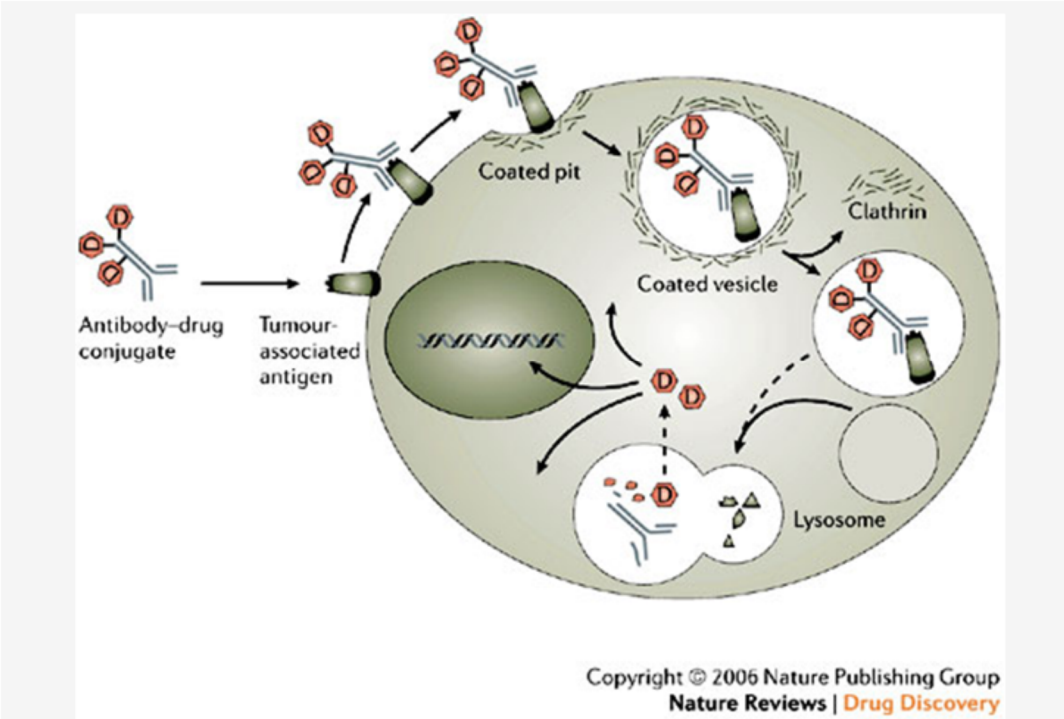

Figure 51*: To regain their cytotoxic activity, the cytotoxic agent has to be cleaved from the chemo-immunoconjugate. Uptake of antibodies predominantly occurs via the clathrin-mediated endocytosis pathway. After binding the respective antigen associated with coated pits, antibody–drug conjugates will be readily endocytosed, from where they transit through several stages of transport and endosomal vesicles and finally end up in a lysosome. There, linkers and antibody will be cleaved releasing the cytotoxic agent which — after exit from the lysosomal compartment — exerts its cytotoxic effect*[44]*.*

Antibody-drug conjugates: Background and components

The first investigational new drug (IND) for an ADC was submitted in the early 1990s. In the past four and a half years, the number of ADC IND submissions has more than doubled the number seen in the previous 15 years. The growth in ADC IND submissions is mainly due to advances in mAb development and methods for characterization, identification of cytotoxic small drugs, and, in particular, advances in linker and conjugation chemistry.

The three components of an ADC include the mAb, the cytotoxic small drug molecule, and the linker. Upon binding the target cell, the ADC is internalized where the drug is released and kills the cell by the mechanism of the small drug. The most frequently used small drugs

[44] David Schrama, Ralph A. Reisfeld & Jürgen C. Becker Nature Reviews Drug Discovery **5**, 147-159 (February 2006)

to date include maytansinoids and auristatins, which disrupt the tubulin network, and calicheamicin and doxorubicin, which intercalate into the minor groove of DNA, but disrupt DNA by different mechanisms. While the linker does not provide activity to the ADC, the design of the linker, its stability, and the conjugation chemistry are crucial for the success of an ADC. The linker should be stable in serum so that the cytotoxic drug is not released into circulation prior to reaching the target cell, but allow cleavage once internalized to permit the cytotoxic drug to reach its target.

Since ADCs are comprised of both drug and biological molecules, the characterization and quality assurance of an ADC need to be relevant both for the small drug and linker components as well as the mAb.

Drug and linker starting materials and intermediates

The drug/linker intermediates may be derived by fermentation, chemical synthesis, or semisynthesis processes (chemically modified fermentation product). They may be either a small chemical compound, large complex molecule, or peptide. The stage of clinical development determines the extent of the description and characterization of these intermediates. A discussion regarding the designation of starting materials from which the drug/linker is produced should be included as part of an End-of-Phase 2 meeting with the Agency. The extent of the characterization and quality control of the drug/linker intermediates is the same as if they were developed as a drug substance, since a complete characterization is difficult after conjugations. Characterization includes the chemical structure as well as the impurity profile.

The impurity profile should include drug/linker-related impurities, process impurities, and a structural characterization of the impurities present at levels that are greater than the ICH Q3A-recommended identification threshold (typically higher than 0.1%). Quality control testing and specifications for the drug/linker intermediates should include appearance, identity, assay (HPLC), and impurities. Stability testing should be performed under long-term (real-time) and accelerated storage conditions to support the intended storage conditions of the drug/linker intermediates.

Monoclonal antibody intermediate

The extent of the characterization and quality control of the mAb intermediate is the same as if it was developed as a drug substance. This includes adventitious agent safety testing of cell banks and unprocessed bulk and endotoxin and bioburden testing of the purified bulk mAb.

The characterization of the mAb includes methods that assess primary, secondary, and higher-order structure; size and charge variants, glycosylation; and other post-translational modifications such as deamidated and oxidized amino acid residues. Product-related impurities can include charge and size variants, which should be identified in order to understand the impact they may have on the in vivo behavior of the ADC. Removal of process-related impurities should be assessed during the mAb manufacture. It may be acceptable to provide risk assessments early in development for some small-molecule process-related impurities. Removal of process-related impurities can be validated and the data provided with the Biologics License Application (BLA).

Antibody function should also be assessed, including antigen binding, signal transduction that may lead to cell death or growth inhibition, antibody effector function, and binding to FcγR and FcRn. Even though cytotoxicity of the small drug component is intended as the major mechanism of action (MOA), several ADCs are reported to have additional MOAs. The best known example of this is T-DM1, a maytansinoid derivative conjugated to trastuzumab for the treatment of HER2 positive breast cancer. The MOA of trastuzumab includes antibody-dependent cellular cytotoxicity and inhibition of cell proliferation by different paths, including prevention of HER2 receptor dimerization, increased endocytic destruction of the receptor, and inhibition of shedding of the extracellular domain.

Characterization of the antibody-drug conjugate

Once conjugated, a structural characterization assessing drug loading is crucial. This characterization includes determining the molar absorption coefficient, the drug load distribution, individual drug load variants, and drug-to-antibody ratio. The ability to characterize individual drug load variants depends on the conjugation chemistry. For example, when conjugation is to cysteine residues of partially reduced mAbs, there will be a small number of cysteine residues available for conjugation commonly resulting in ~4 drug molecules per antibody. Conjugation to lysine residues is more complex, since there are

greater than 50 lysine residues in a mAb, which may lead to greater variation in the drug loading distribution.

Mass spectrometry, hydrophobic interaction chromatography, and reversed-phase HPLC are used to characterize the distribution of drug load variants. Peptide mapping methods enable the identification of the conjugated lysines, but it remains difficult to identify all the drug load variants. The impurity profile of free drug-related substances, quenching agents, residual solvents, and other process-related impurities can be characterized and controlled. Moreover, the impact of conjugation chemistry on the mAb should be determined for important biological functions of the mAb, including binding to antigen and effector function or signal transduction, if relevant.

In addition, a comparison of product-related variants of the ADC should be compared to the unconjugated mAb to determine if the conjugation leads to novel mAb-related variants other than the specific conjugation sites. A comparability study should be performed on the ADC drug substance when manufacturing changes are introduced to either the intermediates or the ADC drug substance processes.

2. Aim of ADC Project

The ADC developed at Merck Serono is a novel second generation ADC candidate. This ADC combines a cytotoxic payload with a biodegradable polymer system. As an example, once loaded with drug(s), the polymer is then attached through a stable linker to the antibody or antibody alternative to create a linker with the antibody. The ADC under investigation provides several key advantages over currently available approaches, including the ability to deliver diverse payloads, the opportunity to significantly increase drug loading per antibody, significantly improved ADC physicochemical properties and easy manufacturing.

The strategy adopted in the NBEs laboratories at Merck Serono Ivrea Site consisted of developing and qualifying bioanalytical methods to:

1. quantify the free fraction of cytotoxic drug in plasma and tumor tissue samples to monitor unconjugated drug-driven (LC-MS/MS technology)
2. quantify the payload (cytotoxic drug conjugated to the linker) drug in plasma and tumor tissue samples to monitor ADC-driven activity (LC-MS/MS technology)
3. quantify the total Ab in plasma and tumor tissue samples to monitor total antibody-driven activity (Generic IgG capture and detection)

Figure 52 shows the possible combinations that can be investigated in order to obtain the maximum quali-quantitative information about an ADC and the assays needed for characterizing ADCs.

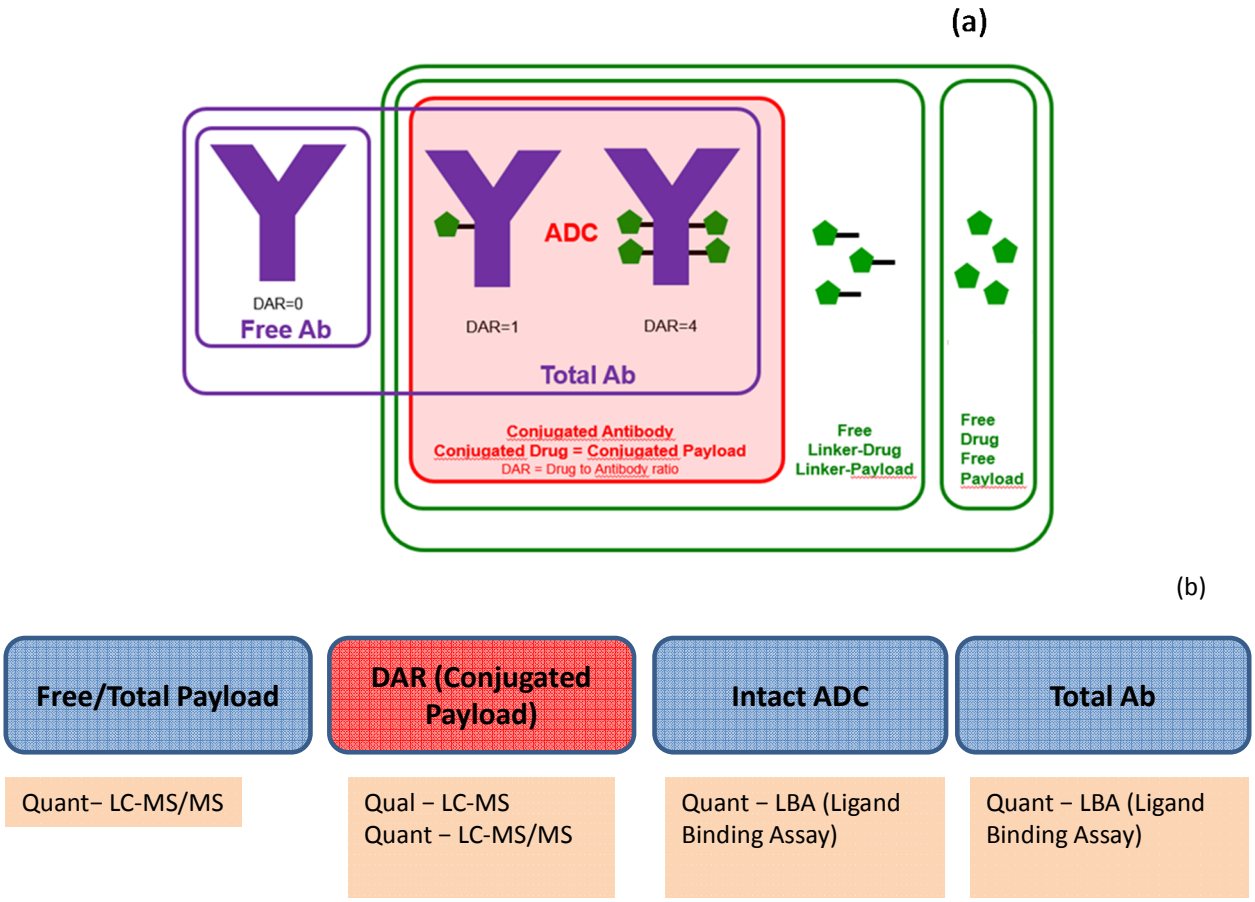

***Figure 52**: (a) Generic ADC structure and some Bioanalytical terms. (b) LC-MS and LBA strategies.*

The ADC-consists of: (I) a monoclonal antibody, which is mainly used to treat cancers, (II) Polymer-Linker-Drug™

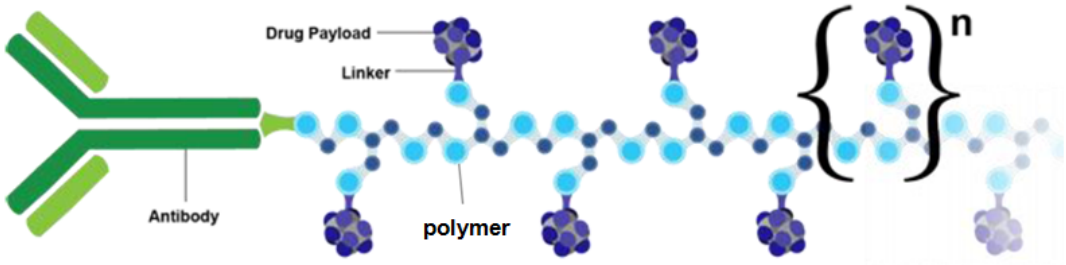

***Figure 53:** Schematic structure of ADC*

Drug release is done by a set of enzymes mainly present in lysosomes. The release is possible at high pH and temperature. Low pH stabilizes the ester bond.

Each analyte provides unique information regarding ADC behavior *in vivo* and, singly or in combination, facilitates understanding of ADC PharmacoKinetics (PK). The significance of PK is provided by different aspects that should be considered and evaluated:

- **Total antibody (t-mAb)**
  a) T-mAb PK profile describes the antibody-related PK behavior of the ADC
  b) Provides the best assessment of the in vivo stability and integrity of the anti body over time
  c) The t-mAb PK profile of ADC serves a key role in ADC optimization
  d) Evaluating the impact of conjugation and selecting a drug load

- **Conjugated antibody (c-mAb)**
  a) Gives an estimate of the active ADC concentration, and is the basis for most ADC PK analyses.
  b) Normally done by LBA
  c) Linked to elimination of intact ADC from circulation and to complete deconjugation processes
  d) Even if the PK properties of ADC species are similar, differences in the composition of the circulating ADC mixture (DAR distribution) could lead to different pharmacologic activities and make it difficult to link concentration to physiological effect

- **Payload**
  a) Describes a mixture of ADC species bearing different amounts of drug
  b) Changes in Payload concentration could reflect both elimination of ADC from systemic circulation and loss of cytotoxic drug from the antibody (similarly to c-mAb)
  c) In contrast to the c-mAb, it provides limited information about the concentration of the antibody to which the drug is bound

d) Done by LC-MS/MS on ADC with cleavable linkers; with uncleavable linkers c-mAb must be done (LBA)
e) Integration of both analytes with DAR analysis can give a full picture of elimination and catabolism (i.e. deconjugation) processes

- **Free Drug and Free linker-conjugated Drug**
  a) Cytotoxic drug released from the ADC is a concern and may be associated with loss of efficacy or increased toxicity
  b) Done by LC-MS/MS
  c) Cytotoxic drug loss from an ADC can occur by multiple chemical and enzymatic processes resulting in different structural products
  d) Knowledge of the identity, including metabolism of the cytotoxic drug, pharmacologic activity, and prevalence of these products
     - In vitro studies and in vivo disposition studies are necessary
     - Not only related to cytotoxic drug, but also to linker-conjugated drug

2.1. Material and methods

Chemicals and reagents

Acetonitrile (LiChrosolv®, Reag. Ph Eur, gradient grade for liquid chromatography), 2-Propanol (LiChrosolv®, gradient grade for liquid chromatography), Methanol (LiChrosolv®, Reag. Ph. Eur., gradient grade for liquid chromatography), Formic Acid (Emsure® ACS, Reag. Ph. Eur., 98-100% for analysis) and Sodium Hydroxide (Pellet pure, assay acidimetric, NaOH), ≥ 99.0%) were purchased from Merck Millipore (Merck KGaA, Darmstadt, Germany). Ultrapure water was from a Millipore Milli-Q system (Merck Millipore, Billerica, MA). Mouse Plasma in Li-heparin was purchased from Charles River Laboratories.

LC–MS/MS Equipment

UPLC–MS/MS analyses were performed by an Acquity UPLC™ (Waters Corporation Milford, MA) system consisting of Binary Solvent Manager, Sample Manager, Sample Organizer and Column oven. An Acquity UPLC CSH™ (Charged Surface Hybrid) C18 column (2.1 × 100 mm, 1.7 μm particle size; Waters, Milford, MA, USA) was used for the separation. The UPLC system was interfaced with an AB SCIEX TripleQuad™ 5500 mass

spectrometer (AB SCIEX, Toronto, Canada) used as the detector. Analyst software v.1.6.2 was used for data acquisition and processing.

2.2. Standard and Quality Control solutions

Stock solution of polymer-linker-drug was prepared in acetonitrile containing 2.5% of Formic Acid at a concentration of 1 mg/mL. Working solutions were prepared by diluting stock solution in order to obtain the final concentrations desired. Polymer-linker-drug calibration standard concentrations were 10.00, 20.00, 50.00, 100.0, 200.0, 500.0, 1000, 2000 and 5000.0 ng/mL for the method performance evaluation runs. SS (Spiked Sample) concentrations were 10.00 (LLOQ level), 30.00, 300.0, 4000 and 5000 (ULOQ level) ng/mL. The polymer-linker-drug labeled working solution was prepared in acetonitrile containing 2.5% of Formic Acid at a concentration of 250.0 ng/mL.

2.3. Method development of Payload

2.3.1. Sample preparation optimization

The method development of payload (toxin conjugated to the mAb via linker) for the determination of the Total drug toxin in Li-heparinized mouse plasma samples and homogenized human tumor tissue was focused on finding the best extraction condition because of the small sample volume available (**sample volume to be used for sample processing/extraction: 5.0 µL**).

The first step consisted of optimizing the chemical hydrolysis of polymer-linker-drug payload that is composed of a polymer that carries toxin A, by a hydroxypropylamino moiety. Toxin A is condensed by an amide bond to the hydroxypropyl amino moiety. This constitutes Toxin A-HPA. The Toxin A-HPA is linked to the polymer by an ester bond (**Figure 54**).

The hydrolysis step generates free Toxin A-HPA (**Figure 54**) that subsequently has to be extracted from the matrix. To avoid any unwanted, premature hydrolysis of polymer linker-

toxin, all the samples were acidified at pH 4.0 by adding an appropriate quantity of citric acid.

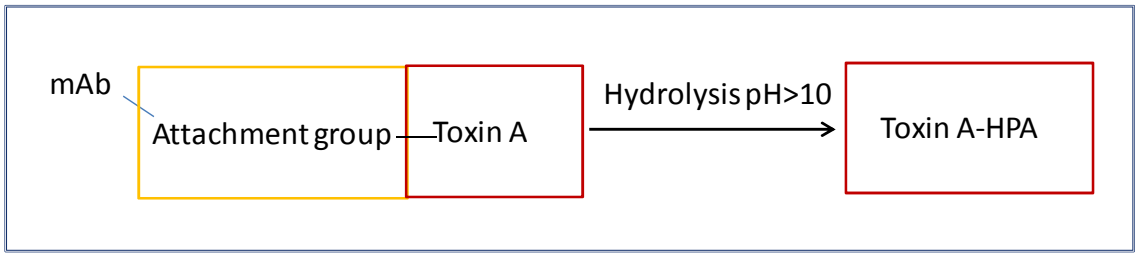

Figure 54: *Schematic representation of the linker-drug conjugate with toxin A and formation of toxin A-HPA upon hydrolysis.*

The hydrolysis step was tested on different media: H_2O with citric acid to mimic the plasma sample, H_2O without citric acid and Phosphate Buffer as plasma surrogate, in order to test the linearity of the Calibration Standard solutions and the accuracy and precision of the Quality Control solutions (working solution check test) before proceeding to plasma sample testing.

The results obtained showed poor linearity in the defined linear dynamic range (from 10.00 ng/mL to 5000 ng/mL).

The curve parameters showed a sort of “broken linear curve” where around 200.0 ng/mL the slopes changes, potentially due to unspecified absorption occurring during the reaction.

As showed in **Table 19**, it is clearly evident as only the QC Low fits the first part of the calibration curve (10.00-200.0 ng/mL) while in **Table 20** the data show that only the QC-Medium and the QC-High fit the second part of the calibration curve.

Sample Name	Sample Type	Analyte Concentration (ng/mL)	Analyte Peak Area (counts)	IS Peak Area (counts)	Area Ratio	Calculated Concentration (ng/mL)	Accuracy (%)
STD-1	Standard	10.00	1368.6	50614.8	0.027	10.73	107.3
STD-2	Standard	20.00	2459.9	55978.6	0.044	17.27	86.4
STD-3	Standard	50.00	6890.1	56157.0	0.123	47.75	95.5
STD-4	Standard	100.0	12322.7	48703.5	0.253	98.19	98.2
STD-5	Standard	200.0	33801.0	58108.9	0.582	225.4	112.7
STD-6	Standard	500.0	92434.5	52772.6	1.752	678.2	**135.6**
STD-7	Standard	1000	284917.5	55694.4	5.116	1980	**198.0**
STD-8	Standard	2000	502449.7	60867.3	8.255	3195	**159.8**
STD-9	Standard	5000	1419982.4	55528.5	25.572	9897	**197.9**
RS_2	Solvent	0.0	43.0	22.8	1.887	N/A	N/A
QC-L	Quality Control	30.00	5017.0	59831.5	0.084	32.72	109.1
QC-M	Quality Control	300.0	58819.4	60069.4	0.979	379.2	**126.4**
QC-H	Quality Control	4000	1278283.3	60529.5	21.118	8174	**204.3**

Table 19: *Calibration curve and QCs prepared in surrogate medium. NA= Not Applicable.*

Sample Name	Sample Type	Analyte Concentration (ng/mL)	Area Ratio	Calculated Concentration (ng/mL)	Accuracy (%)
STD-1	Standard	10.00	0.027	91.79	**917.9**
STD-2	Standard	20.00	0.044	95.25	**476.2**
STD-3	Standard	50.00	0.123	111.4	**222.7**
STD-4	Standard	100.0	0.253	138.0	**138.0**
STD-5	Standard	200.0	0.582	205.3	102.6
STD-6	Standard	500.0	1.752	444.6	88.9
STD-7	Standard	1000	5.116	1133	113.3
STD-8	Standard	2000	8.255	1775	88.8
STD-9	Standard	5000	25.572	5319	106.4
RS_2	Solvent	0.0	1.887	N/A	N/A
QC-L	Quality Control	30.00	0.084	103.4	**344.7**
QC-M	Quality Control	300.0	0.979	286.6	95.5
QC-H	Quality Control	4000	21.118	4407	110.2

Table 20: *Calibration curve and QCs prepared in surrogate medium. NA= Not Applicable.*

A second approach was (I) to spike the calibration standard solutions in the matrix before performing hydrolysis in order to avoid this absorption and (II) to introduce a clean-up step consisting of the Protein Precipitation Technique (PPT).

Under these conditions, good linearity and good quality control accuracy were obtained (**Table 21**).

Sample Name	Sample Type	Analyte Concentration (ng/mL)	Analyte Peak Area (counts)	IS Peak Area (counts)	Area Ratio	Calculated Concentration (ng/mL)	Accuracy (%)
DBK_1	Double Blank	0.0	655.5	1338.6	0.49	N/A	N/A
STD-0	Blank	0.0	530.6	231498.9	0.002	N/A	N/A
STD-1	Standard	10.00	8960.4	261760.5	0.034	9.710	97.1
STD-2	Standard	20.00	15266.9	197840.4	0.077	21.12	105.6
STD-3	Standard	50.00	42857.8	227098.2	0.189	50.77	101.5
STD-4	Standard	100.0	85484.4	236193.1	0.362	96.80	96.8
STD-5	Standard	200.0	186457.5	239755.1	0.778	207.3	103.6
STD-6	Standard	500.0	428643.0	232268.3	1.845	491.1	98.2
STD-7	Standard	1000	856727.5	239777.2	3.573	950.2	95.0
STD-8	Standard	2000	1866023.9	240674.2	7.753	2061	103.1
STD-9	Standard	5000	4611271.6	247533.9	18.629	4951	99.0
DBK_2	Double Blank	0.0	967.7	823.5	1.175	N/A	N/A
QC-L	Quality Control	30.00	31017.2	294937.0	0.105	28.56	95.2
QC-M	Quality Control	300.0	276094.0	254244.1	1.086	289.2	96.4
QC-H	Quality Control	4000	4272796.6	272629.7	15.673	4166	104.1
DBK_3	Double Blank	0.0	374.2	245.4	1.525	N/A	N/A

Table 21: *Calibration curve and QCs prepared in matrix. NA= Not Applicable.*

The PPT technique (see **Figure 55**) with organic solvent (acetonitrile acidified with 2.5% of formic acid) was chosen and tested as preferred extraction technique for the many advantages it can offer:

- State-of-the-art design that maximizes sample recovery
- Elimination of time-consuming sample handling steps
- Increased confidence in results by minimizing sample cross-talk
- Unique valve design controls flow until vacuum is applied
- Maximized Mass Spec uptime by eliminating cloudy filtrates
- Suitability for manual or automated sample processing

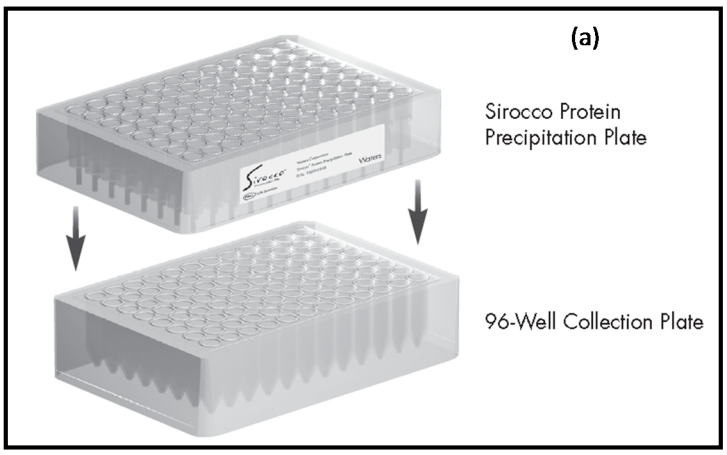

(Sirocco™ Plate from Waters)

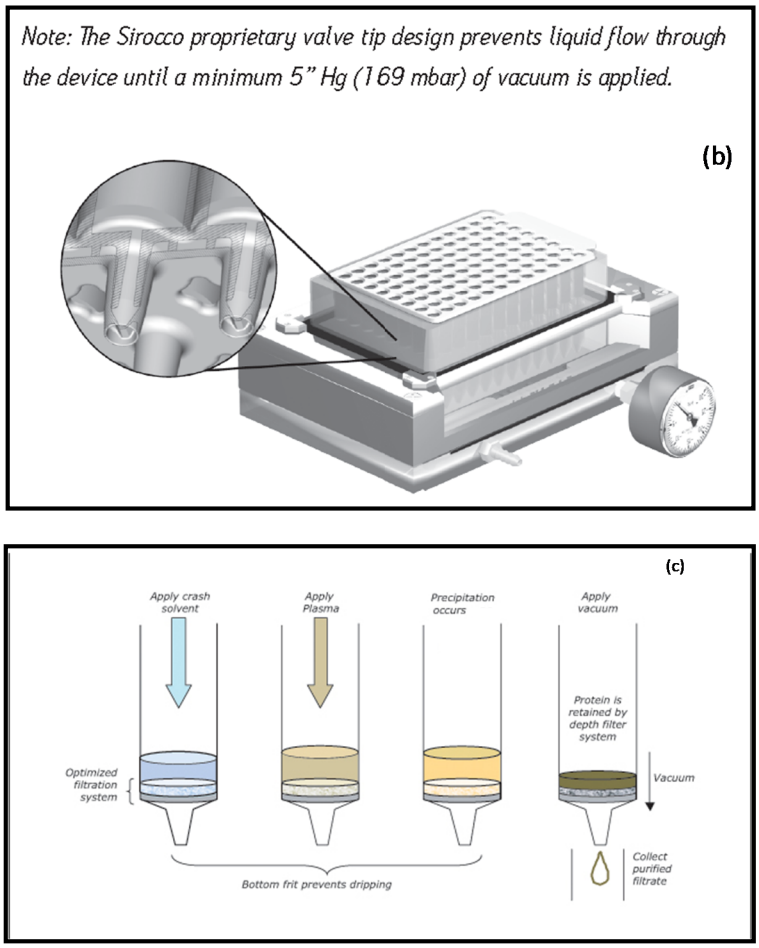

Figure 55: *Waters Sirocco Protein Precipitation plate technology (a and b) and scheme of the Protein Precipitation step (c)*

Initially, samples were prepared by adding the free labeled Internal Standard Toxin A-HPA during the extraction process only and supposing a 100% of hydrolysis reaction. After preliminary tests, it was decided to use the polymer-linker-drug Labelled-IS in order to standardize also the sample hydrolysis step.

The sample preparation was optimized as described in the following procedure:

a) Transfer 30.0 µL of H_2O to the well plate
b) Transfer 5.0 µL of polymer-linker-drug Labeled-IS WS
c) Transfer 5.0 µL of sample (STD, QC or unknown sample)
d) Add 10.0 µL of NaOH 1N
e) Cover the plate
f) Vortex for 5 minutes at room temperature at 850 rpm on a Thermomixer
g) Incubate at 60°C for 2 hours (850 rpm) on a Thermomixer
h) Cool the sample at room temperature
i) Add the samples to a Sirocco plate containing 200.0 µL of Precipitation Reagent
j) Cover the plate and mix gently for approximately 5 minutes on a Thermomixer
k) Filter on a vacuum manifold in a collection well-plate
l) Add 500.0 µL of Recostitution Solvent (water/acetonitrile : 50/50 containing 2.5% of formic acid) to each well and mix gently for approximately 10 minutes on an orbital shaker

2.3.2. Comparison between ADC and polymer-linker-drug hydrolysis

Due to a very small amount of ADC-polymer-linker-drug (antibody conjugated to the polymer), the method development was performed using the polymer-linker-drug compound (polymer conjugated to the toxin).

In order to verify the feasibility of this approach, some ADC-polymer-linker-drug spiked samples were hydrolyzed following the procedure described in paragraph 2.3.1 and the sample concentrations were calculated on the calibration curve prepared using polymer-linker-drug standard.

The results obtained showed that the ADC-polymer-linker-drug releases the expected concentration of Toxin A-HPA (**Table 22**).

This means that the efficiency of the hydrolysis is the same in both types of samples, polymer-linker-drug and ADC-polymer-linker-drug

In conclusion, the polymer-linker-drug standard compound can be used as surrogate of ADC-polymer-linker-drug to qualify the method and to analyze the incurred samples.

Sample Name	Sample Type	Analyte Concentration (ng/mL)	Analyte Peak Area (counts)	IS Peak Area (counts)	Area Ratio	Calculated Concentration (ng/mL)	Accuracy (%)
DBK	Double Blank	0.0	155.0	47.2	3.282	N/A	N/A
Std_0	Blank	0.0	727.4	180088.1	0.004	N/A	N/A
Std_1	Standard	10	4997.3	133378.3	0.037	9.918	99.2
Std_2	Standard	20	9560.5	105889.3	0.09	20.56	102.8
Std_3	Standard	50	28103.3	127620.3	0.22	46.75	93.5
Std_4	Standard	100	61083.6	120083.1	0.509	104.9	104.9
Std_5	Standard	200	131307.6	126016.2	1.042	212.4	106.2
Std_6	Standard	500	303322.2	129346.7	2.345	475.0	95.0
Std_7	Standard	1000	633843.5	125911.8	5.034	1017	101.7
Std_8	Standard	2000	1139005.7	113325.4	10.051	2028	101.4
Std_9	Standard	5000	2961815.5	125228.4	23.651	4769	95.4
DBK	Double Blank	0.0	444.8	0.0	N/A	N/A	N/A
ADC_3	Quality Control	29.00	13430.7	105499.2	0.127	28.02	96.6
ADC_4	Quality Control	519.0	316632.9	122123.6	2.593	524.9	101.1
ADC_5	Quality Control	1083	658024.3	130234.8	5.053	1021	94.3
ADC_8	Quality Control	29.00	9109.5	68485.5	0.133	29.17	100.6
ADC_9	Quality Control	519.0	166042.6	68740.1	2.416	489.2	94.3
ADC_10	Quality Control	1083	254014.3	57322.6	4.431	895.4	82.7

Table 22: *Toxin A-HPA (from ADC-polymer-linker-drug) back-calculated on calibration curve prepared using polymer-linker-drug standard.*

2.3.3. LC-MS/MS Optimization

Three analytical columns were initially tested for their chromatographic performance: 75 mm x 2.1 mm, 1.7 µm particle size Acquity BEH™ C18; 100 mm x 2.1 mm, 1.7 µm particle size Acquity BEH™ C18 and 100 mm x 2.1 mm, 1.7 µm particle size Acquity CSH™ from Waters.

Two eluent systems were tested during method development, water-methanol and water-acetonitrile, both containing 0.1% formic acid, under generic linear gradient conditions based on the chemical structure of the compound (5-95% organic). The water-methanol condition was discarded due to poor sensitivity while the water-acetonitrile condition showed a good analyte signal intensity. The BEH™ C18 columns generated a tailing phenomenon on chromatographic peaks (**Figure 57**) while the CSH column, due to the different interaction mechanism with the analytes, provided a good peak shape (**Figure 56**). Because peak tailing can influence the quality of a separation and also the results, the CSH™ column was selected for this method.

Optimized sensitivity and peak shape were achieved using the 100 mm x 2.1 mm, 1.7 µm d_p Acquity CSH™ column maintained at 40°C and the water-acetonitrile gradient. The autosampler temperature was set at 5°C ±3°C to avoid any sample degradation.

Eluents consisted of 0.1% formic acid in water (eluent A) and 0.1% formic acid in acetonitrile (eluent B).

The following gradient elution was applied at a flow rate of 0.350 mL/min: 5-95% B over 3 minutes, held at 95% for 2 minutes. Eluent B was then returned to 5% over 0.1 min. The system was allowed to re-equilibrate for 2.4 min, giving a total run time of 7.5 minutes. The injection volume was 10.0 µL. A needle wash step using water/acetonitrile: 95/5 containing 0.1% of formic acid (weak wash) and water/acetonitrile/isopropanol/methanol: 25/25/25/25 containing 0.1% of formic acid (strong wash) was included in the method.

The electrospray interface was operated in positive electrospray ionization mode with an ion spray voltage of 5500 V. Nitrogen was used as collision gas. The optimized source conditions were as follows: gas 1:40 psi; gas 2: 45 psi; curtain gas (CUR): 30 psi; collision gas (CAD): 9 arbitrary units (a.u.); and desolvation temperature (TEM): 450°C. The optimized compound conditions were declustering potential (DP): 110 V; collision energy (CE): 42 eV; entrance potential (EP): 10 V; collision cell exit potential (CXP): 15 V for analyte and 14 for internal standard; and dwell time: 150 ms for all analytes. The multiple reaction monitoring (MRM) transitions used were: *m/z* 803.6 (Auristatin F-HPA) → 771.6 (**Figure 58**) and *m/z* 809.6 (Toxin A-HPA- labeled IS) → 777.6.

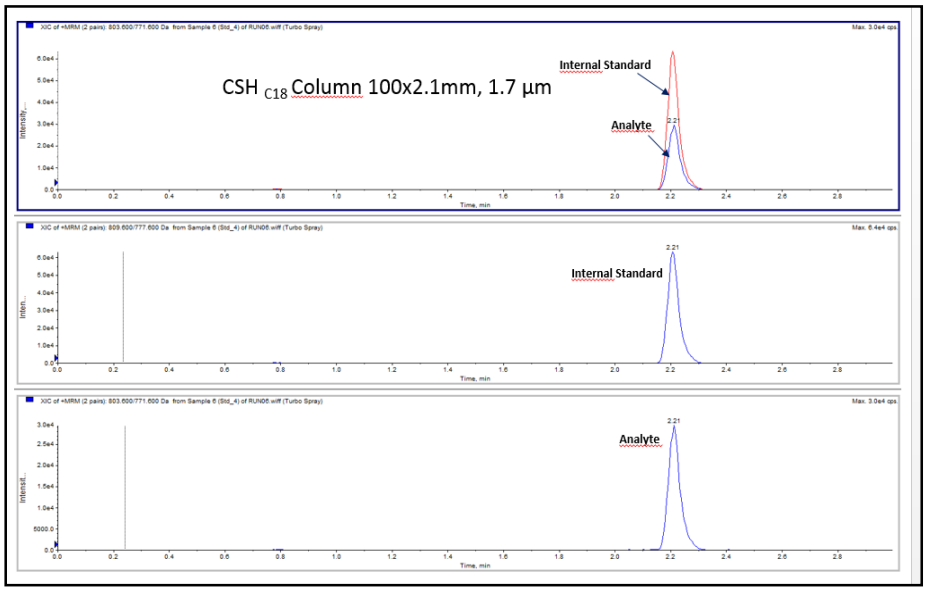

Figure 56: *Chromatographic peak using the CSH column*

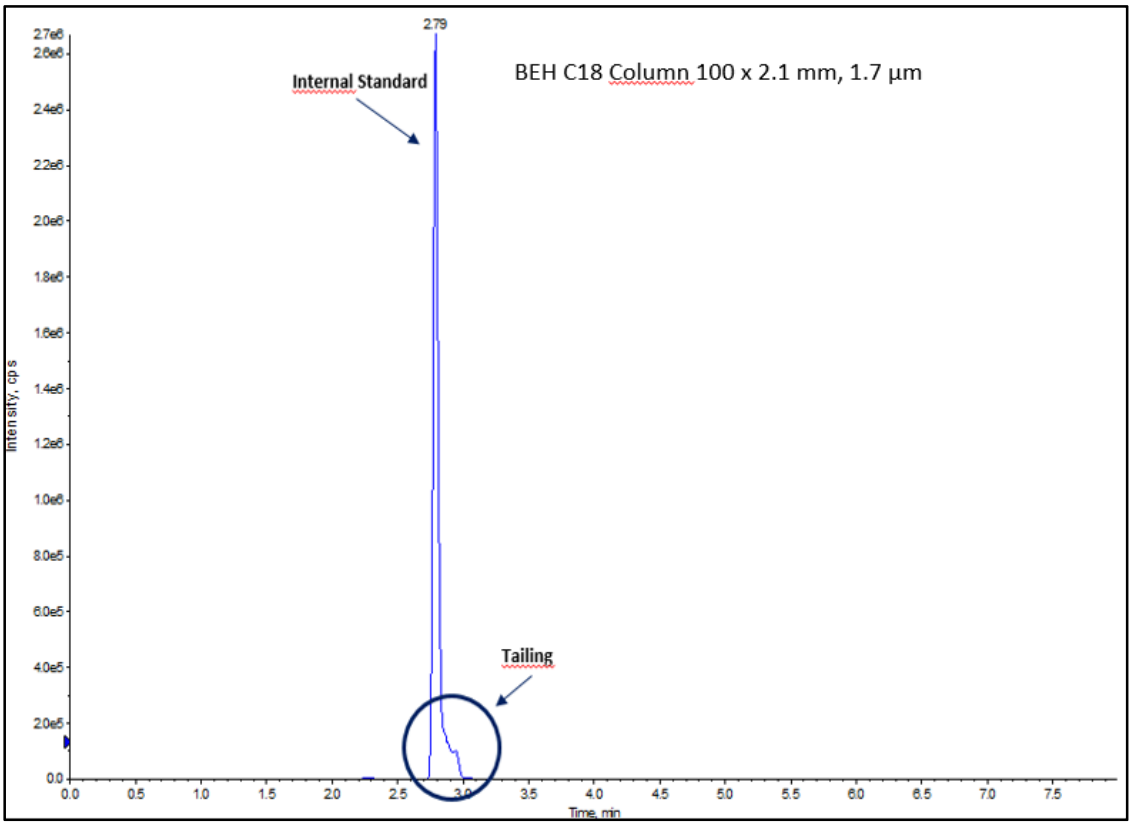

***Figure 57**: Chromatographic peak using the BEH C18 column on Toxin A-HPA- labeled IS*

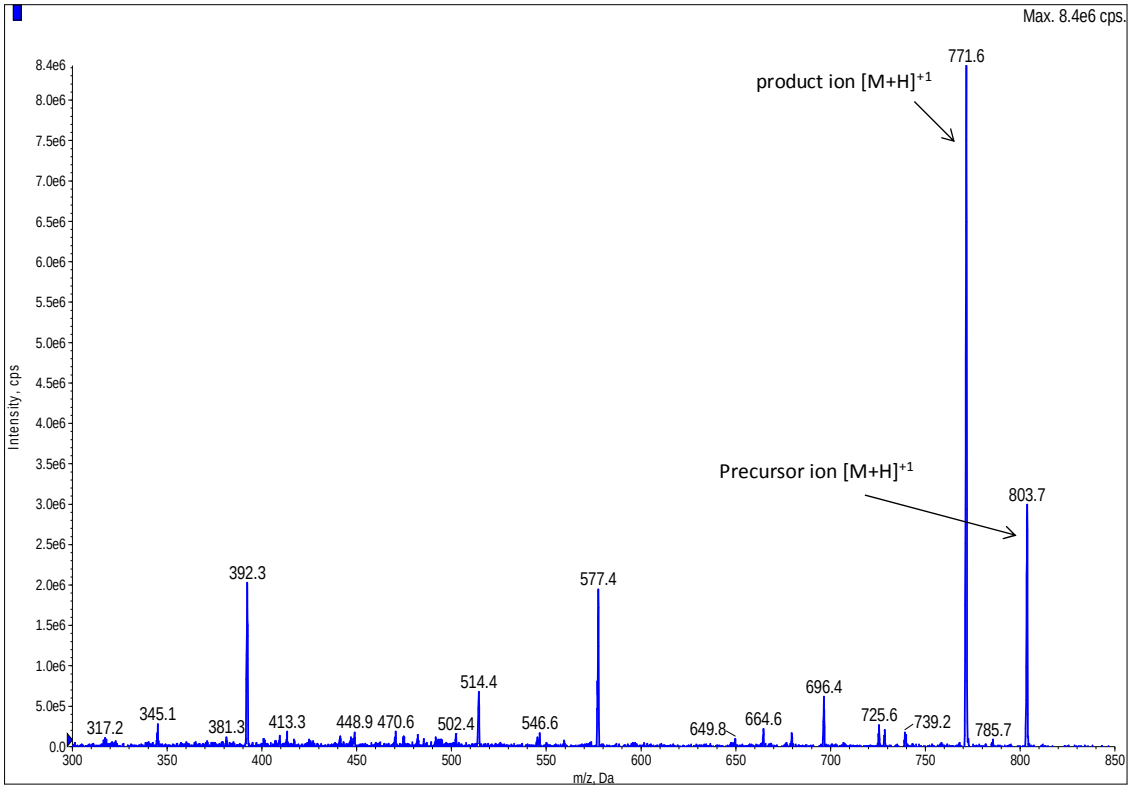

***Figure 58:** Precursor ion of Toxin A-HPA and its main product ion*

2.4. Results and Discussion

The method development provided consistent preliminary results. First, the Protein Precipitation Technique was the appropriate choice for sample clean-up, giving good sensitivity and selectivity. No significant interfering peaks were observed near the main peak from a plasma sample. Second, the LC-MS/MS conditions provided robust and reproducible analytical data.

The LLOQ obtained on the mass spectrometer was the value needed to accomplish Toxin A-HPA measurement in an intravenous single dose toxicity and TK study in CD1 mouse plasma samples.

The second step was to qualify the method according to the required guideline and to the internal requirement for Discovery Phase.

3. Method Qualification

The last step in the method development was method qualification. To this end, the following parameters were tested:

- Linearity
- Intra- and Inter-run Accuracy and Precision
- Selectivity
- Sensitivity
- Effect of dilution
- Carryover
- Autosampler stability
- Freeze / Thaw stability
- Bench-top stability

3.1. Acceptance Criteria

The acceptance criteria for each test performed during qualification are described in the following table:

Method Qualification					
Test	**Parameter**	**Batches**	**Concentration Levels**	**Replicates**	**Acceptance Criteria**
Linearity	Calibration curve	Included in each batch	9, additionally double blank and zero standard	1	Bias (%) within ±15% (±20% at the LLOQ) 75% of all calibration samples must be within the accuracy range
Accuracy & precision	Intra-batch	1	5 (SSL, SSM, SSH and SSLLOQ + SSULOQ)	5	Mean Bias (%) within ±15% (±20% at the LLOQ) Precision (%CV) ≤ 15% (≤ 20% at the LLOQ)
	Inter-batch	3 (2+Intra-batch)	5 (SSL, SSM, SSH and SSLLOQ + SSULOQ)	3 (pooled matrix)	Mean Bias (%) within ±15% (±20% at the LLOQ) Precision (%CV) ≤ 15% (≤ 20% at the LLOQ)
Selectivity	vs. Matrix	1	N.A.	3 (pooled matrix)	Mean Analyte response ≤ 20% LLOQ Mean IS response ≤ 5% of STD0
	vs. Matrix (LLOQ)	1	LLOQ	5 (covered in intra-batch Accuracy and Precision)	Back-calculated conc. within ±20% of nominal conc. (%Bias) and precision (%CV) ≤ 20%. Batch must have at least 80% of the replicates back-calculated conc. within ±20% of nominal conc.(%Bias)
	vs. IS	1	IS	3 (included as zero standard sample in each analytical run)	Mean Analyte response ≤ 20% LLOQ
	vs. Analyte	1	ULOQ	3	Mean IS response ≤ 5% of the average Internal Standard (IS) response in the assay

Method Qualification					
Sensitivity	Covered in intra-batch accuracy & precision				N.A.
Effect of dilution	Dilution Integrity	1	Final dilution applied 1:100 (200.0 µg/mL diluted to 2000 ng/mL)	3	Mean Bias (%) within ±15% Precision (%CV) ≤ 15%
Carryover	Carryover	1	N.A.	One for each batch	Analyte response after ULOQ must be ≤ 20% LLOQ
Stabilities	Freeze/Thaw	1	2 (SSL-SSH)	3 (after 2 cycles of freeze&thaw)	Bias (%) vs. nominal within ±15% Precision (%CV) ≤ 15%
	Autosampler	1	2 (SSL-SSH)	3 (t=72h)	
	Bench-top	1	2 (SSL-SSH)	3 (at 2h, RT)	

Table 23: *List and acceptance criteria of the Method qualification test*

The calculations applied to each test are reported below and were applied for every qualification study:

1. **Linearity**

The %BIAS of the estimated concentration of each standard curve point was calculated as follows:

$$\%\ BIAS = \frac{\text{Estimated Conc.} - \text{Nominal Conc.}}{\text{Nominal Conc.}}\ \text{X}\ 100$$

2. **Carryover**

Carryover assessment was performed in every qualification run. For this test the following parameter was calculated:

- The analyte response in the DBK after the ULOQ sample

$$Carryover\ (\%) = \frac{\text{Analyte Peak Area in DBK}}{\text{Analyte Peak Area in LLOQ}}\ \text{X}\ 100$$

3. Intra-Run and Inter-Run Accuracy and Precision

The %BIAS of each replicate of each SS and the %CV was calculated as follows:

$$\%\ BIAS = \frac{\text{Estimated Conc.} - \text{Nominal Conc.}}{\text{Nominal Conc.}}\ \text{X}\ 100$$

$$\%\ CV = \frac{\text{Standard Deviation}}{\text{Mean Conc.}}\ \text{X}\ 100$$

4. Selectivity

Selectivity vs. matrix: for this test the following parameter was calculated:

- The mean analyte (% AN interference)

$$Selectivity\ vs\ matrix = \frac{\text{Average Analyte Peak Area in matrix samples}}{\text{Area of LLOQ in the assay}}\text{X}\ 100$$

- The mean IS (% IS interference)

$$Selectivity\ vs\ matrix = \frac{\text{Average IS Peak Area in matrix samples}}{\text{Area of IS in the STD0 sample}}\text{X}\ 100$$

Selectivity vs. matrix at LLOQ: for this test the following parameters were calculated:

- The %BIAS and %CV calculated as reported for intra-inter run accuracy and precision

Selectivity vs. IS (% Analyte interference): for this test the following parameters were calculated:

- The mean analyte response in the STD0 samples
- The mean LLOQ area in the corresponding batches

$$Selectivity\ vs\ IS = \frac{\text{Average Analyte Peak Areas in ST0 samples}}{\text{Average Analyte Peak Area in the LLOQ}}\text{X}\ 100$$

Selectivity vs. analyte (% IS interference): for this test the following parameter was calculated:

- The mean IS response

$$Selecivity\ vs\ AN = \frac{\text{Average IS Peak Area in ULOQ samples}}{\text{Average IS Peak Area in the assay}}\ X\ 100$$

5. Sample Dilution

For this test the following parameters were calculated:

- The %BIAS and %CV as reported for intra-inter run accuracy and precision

6. Freeze-Thaw Stability

For this test the following parameters were calculated:

- The %BIAS vs. nominal concentration and %CV calculated as reported for intra-inter run accuracy and precision.

7. Autosampler Stability

For this test the following parameters were calculated:

- The %BIAS vs. nominal concentration and %CV calculated as reported for intra-inter run accuracy and precision.

8. Bench-top stability

For this test the following parameters were calculated:

- The %BIAS vs. nominal concentration and %CV calculated as reported for intra-inter run accuracy and precision.

3.2. Qualification of the UPLC-MS/MS method for the quantitation of Total Toxin A-HPA in mouse plasma samples

3.2.1. Linearity

Good linearity was obtained for the nine-point calibration curve constructed by plotting the peak area ratio of analyte to its internal standard versus the corresponding concentration ratio and fitting the data using linear regression with $1/x^2$ weighting factor. For six consecutive batches, the calibration curves showed an overall accuracy (%) ranging from 96.7% to 103.2% with %CV $\leq$ 6.8% over the concentration range of 10.00 (LLOQ) - 5000 (ULOQ) ng/mL (**Table 24**).

Run ID/Bias (%)	Std1 ng/mL 10.00	Std2 ng/mL 20.00	Std3 ng/mL 50.00	Std4 ng/mL 100.0	Std5 ng/mL 200.0	Std6 ng/mL 500.0	Std7 ng/mL 1000	Std8 ng/mL 2000	Std9 ng/mL 5000
1	9.85	20.18	51.50	104.4	207.4	458.7	1021	1872	5103
Bias (%)	**-1.5**	**0.9**	**3.0**	**4.4**	**3.7**	**-8.3**	**2.1**	**-6.4**	**2.1**
2	10.32	19.09	46.92	102.8	196.4	509.8	1061	2043	4817
Bias (%)	**3.2**	**-4.6**	**-6.2**	**2.8**	**-1.8**	**2.0**	**6.1**	**2.2**	**-3.7**
3	10.43	18.82	47.27	97.3	192.2	550.8	1008	2128	4815
Bias (%)	**4.3**	**-5.9**	**-5.5**	**-2.7**	**-3.9**	**10.2**	**0.8**	**6.4**	**-3.7**
4	9.47	21.73	52.15	102.3	202.0	474.1	996	1909	4961
Bias (%)	**-5.3**	**8.7**	**4.3**	**2.3**	**1.0**	**-5.2**	**-0.4**	**-4.6**	**-0.8**
5	10.42	18.13	49.01	106.7	208.5	502.6	985	2111	4585
Bias (%)	**4.2**	**-9.4**	**-2.0**	**6.7**	**4.3**	**0.5**	**-1.5**	**5.6**	**-8.3**
6	9.79	20.71	49.66	105.9	193.9	507.6	992	2018	4743
Bias (%)	-2.1	3.6	-0.7	5.9	-3.1	1.5	-0.8	0.9	-5.1
Statistics									
Mean	10.05	19.78	49.42	103.2	200.1	500.6	1010	2014	4837
STDEV	0.40	1.34	2.14	3.36	6.96	31.99	27.88	104.35	178.52
CV (%)	4.0	6.8	4.3	3.3	3.5	6.4	2.8	5.2	3.7
Accuracy (%)	100.5	98.9	98.8	103.2	100.1	100.1	101.0	100.7	96.7

Table 24: *Precision and accuracy for the calibration standard of Toxin A-HPA in plasma mouse from six qualification batches*

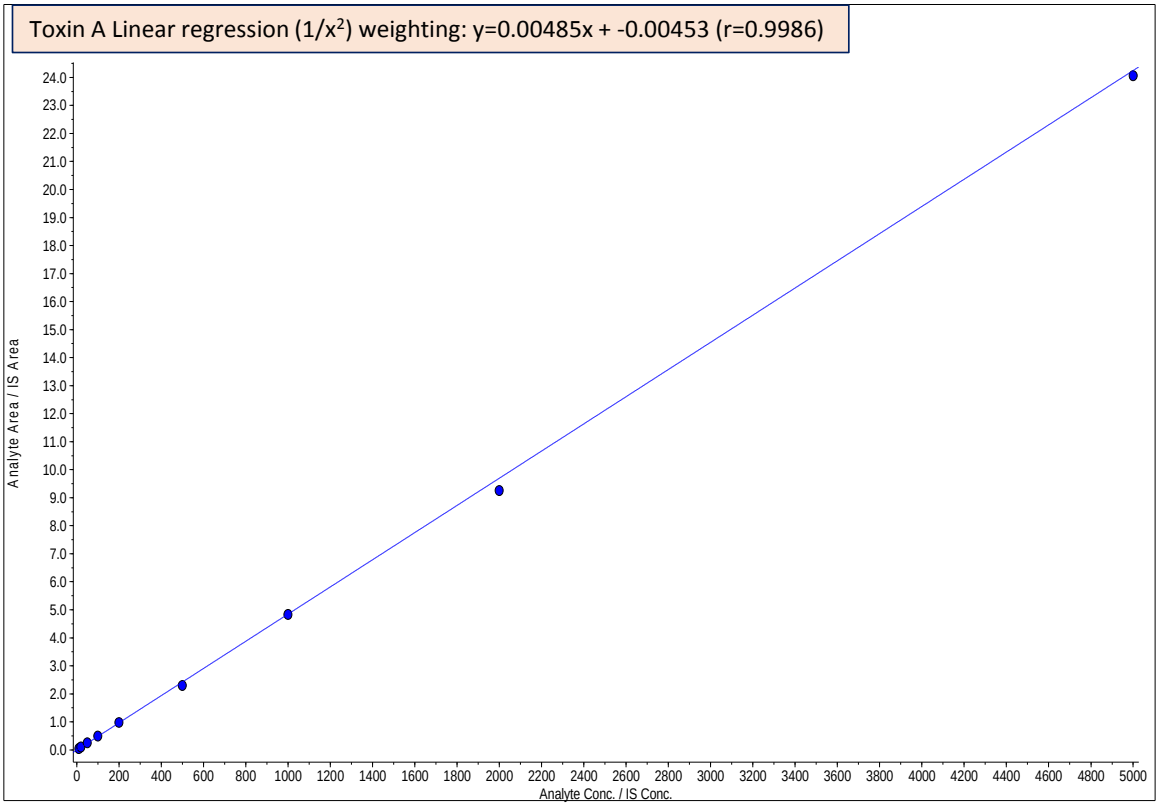

Figure 59: *A representative linear response of Toxin A-HPA in matrix*

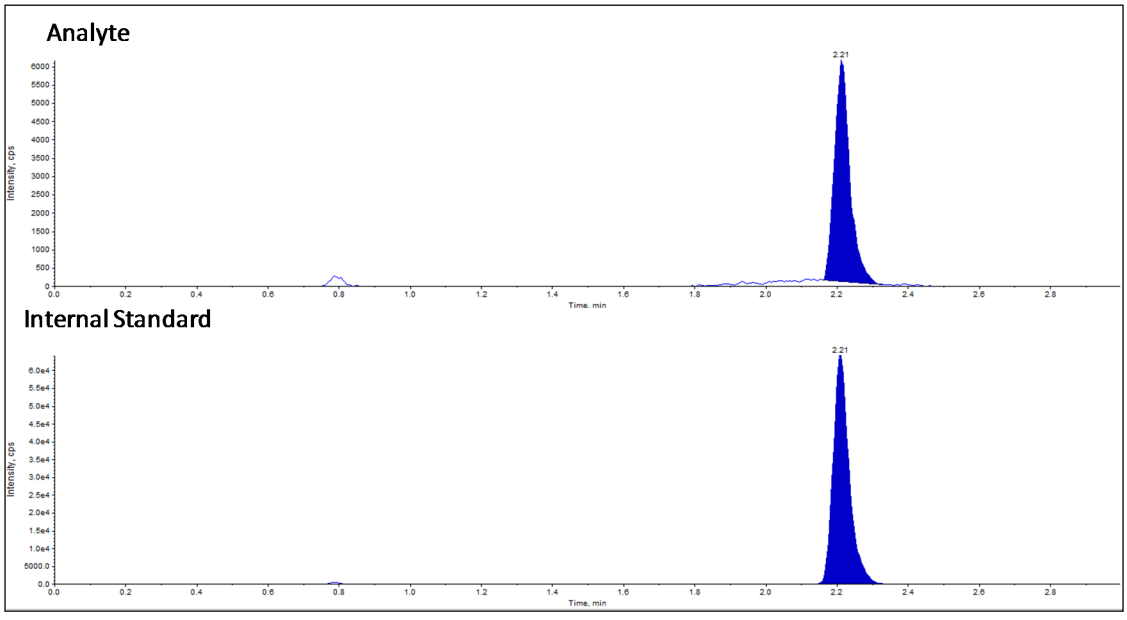

Figure 60: *A representative MRM chromatogram of Toxin A-HPA at LLOQ level and its Internal Standard in matrix sample*

The carryover met the acceptance criteria in each run.

Run ID	AN Peak Area in LLOQ (Std1)	AN Peak Area in DBK after ULOQ	%Carry Over
1	9081.2	501.2	5.5
2	6407.3	318.6	5.0
3	7592.9	427.4	5.6
4	7051.3	295.9	4.2
5	10441.7	442.5	4.2
6	6857.0	399.6	5.8

Table 25: *Carryover evaluation*

The slope value was consistent for six consecutive batches and the slope variation % was ≤ 5.1% over all the runs (**Table 26**).

The correlation coefficient (r) of the linear regression was between 0.9978-0.9993 (**Table 26**).

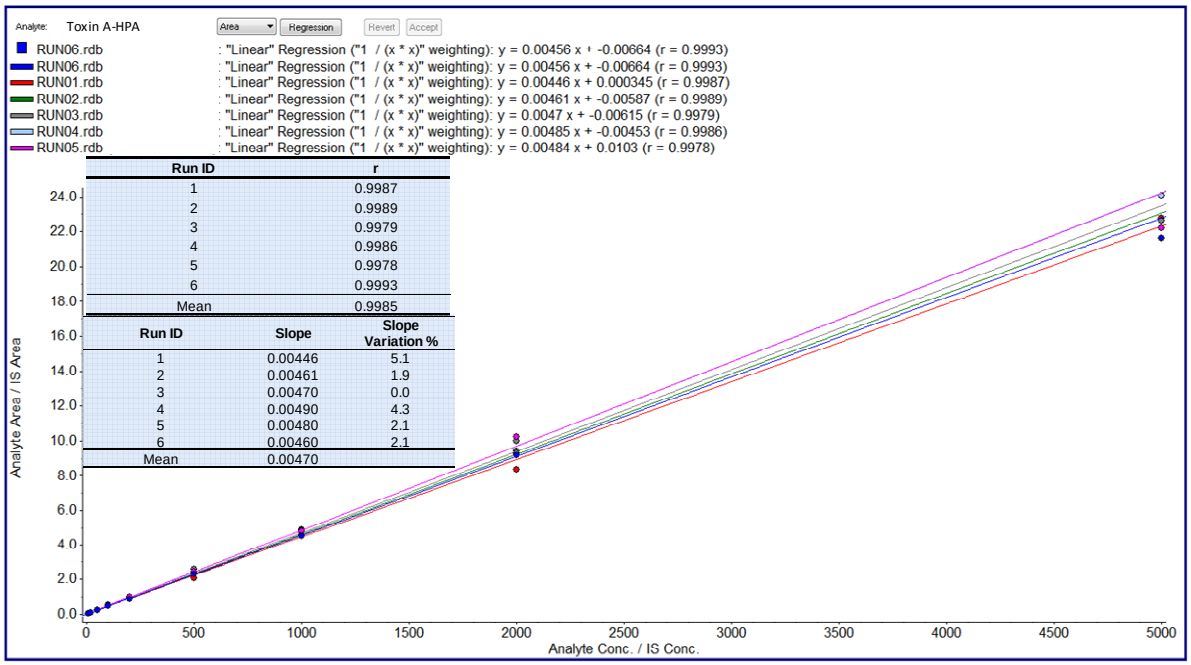

Table 26: *Overlay of the calibration curves of the study showing the reproducibility and good linearity in terms of slope accuracy and correlecion coefficients near to 1.*

The LLOQ was taken as the lowest calibration concentration that passed acceptance criteria with a signal-to-noise (x4 standard deviation) of a least 5:1 (the mean S/N evaluated in each run was about 35).

3.2.2. Intra-Inter Run Accuracy and Precision

Method accuracy and precision were evaluated using Spiked Samples (SS) prepared by spiking polymer-linker-drug standard into blank plasma at five concentration levels (10.00, 30.00, 300.0, 4000 and 5000 ng/mL) to serve as SS LLOQ, SS Low, SS Medium, SS High and SS ULOQ.

Three consecutive batches were prepared and each batch contained a freshly prepared calibration curve and five replicates of SS samples at the five levels.

Intra-assay precision was calculated by obtaining the Coefficient of Variation (CV) % of the five replicates of each SS level, and intra-assay accuracy was calculated by averaging the accuracies (%Bias) of five replicates of each SS level against the fresh curve.

Inter-assay precision was calculated by obtaining the %CV of all 11 replicates at each SS level from all the three batches, with overall accuracy calculated by averaging the accuracies of all 11 replicates at each SS level from all the three batches.

Accuracy (%Bias) ranged from -3.3 to 7.6 and precision (%CV) ranged from 1.7 to 7.0 for intra-assay. Accuracy (%Bias) ranged from -2.9 to 8.7 and precision (%CV) ranged from 2.6 to 12.3 for inter-assay.

Accuracy and precision were evaluated including SS-LLOQ and SS-ULOQ (see **Table 27** and **Figure 61**).

The method was found to be highly accurate and precise.

The statistics on QC samples used for run acceptance and to perform runs 04, 05 and 06 for Selectivity, Freeze and Thaw, Bench-top, dilution integrity and autosampler stability 24 and 72 hours tests are reported in **Table 28**.

Intra-assay (Run ID: 1)	SS-LLOQ ng/mL 10.00	SS-Low ng/mL 30.00	SS-Medium ng/mL 300.0	SS-High ng/mL 4000	SS-ULOQ ng/mL 5000
Mean Conc.	9.88	30.77	305.2	4304	4834
Intra-Run Accuracy (%BIAS)	-1.2	2.6	1.8	7.6	-3.3
SD	0.692	1.29	5.12	304	273
Intra-Run Precision (%CV)	7.0	4.2	1.7	7.1	5.6
n	5	5	5	5	5
Inter-assay (Run ID: 2, 3)	**SS-LLOQ ng/mL 10.00**	**SS-Low ng/mL 30.00**	**SS-Medium ng/mL 300.0**	**SS-High ng/mL 4000**	**SS-ULOQ ng/mL 5000**
Overall Mean Conc.	10.13	30.71	306.3	4348	4853
Inter-Run Accuracy (%BIAS)	1.3	2.4	2.1	8.7	-2.9
Overall SD	1.25	1.86	8.10	313	320
Inter-Run Precision (%CV)	12.3	6.1	2.6	7.2	6.6
n	11	11	11	11	11

Table 27: *Intra-Inter assay accuracy and precision*

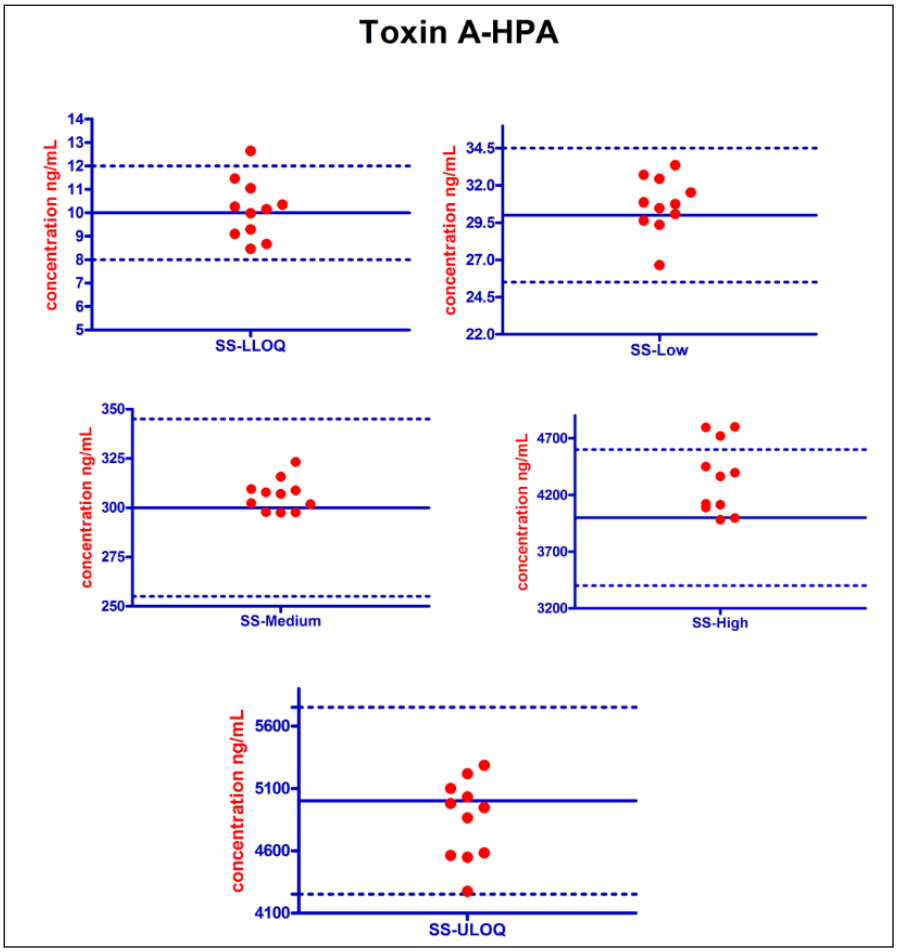

Figure 61*: Scatter plot of the SS samples analyzed for the intra-inter assay accuracy and precision evaluation*

Expected Concentration	Result Table Name	Sample Name	Number Of Values Used	Mean	Standard Deviation	%CV	Accuracy
30.00	RUN06.rdb	QC_L1, QC_L2	2 of 2	32.22	0.435	1.350	107.4
30.00	RUN04.rdb	QC_L1, QC_L2	1 of 2	29.08	N/A	N/A	96.9
30.00	RUN05.rdb	QC_L2	1 of 1	28.05	N/A	N/A	93.5
30.00	All	QC_L1, QC_L2	4 of 5	30.39	2.170	7.141	101.3
30.00	Average	QC_L1, QC_L2	3 of 3	29.78	2.176	7.307	99.3
300.0	RUN06.rdb	QC_M1, QC_M2	2 of 2	315.3	32.43	10.29	105.1
300.0	RUN04.rdb	QC_M1, QC_M2	2 of 2	276.9	1.485	0.5362	92.3
300.0	RUN05.rdb	QC_M1, QC_M2	2 of 2	300.5	3.382	1.126	100.2
300.0	All	QC_M1	6 of 6	397.6	22.65	7.612	99.2
300.0	Average	QC_M1	3 of 3	297.6	19.36	6.507	99.2
4000	RUN06.rdb	QC_H1, QC_H2	2 of 2	4133	22.08	0.5341	103.3
4000	RUN04.rdb	QC_H1, QC_H2	2 of 2	4231	34.17	0.8074	105.8
4000	RUN05.rdb	QC_H1, QC_H2	2 of 2	4175	137.4	3.290	104.4
4000	All	QC_H1	6 of 6	4180	77.69	1.859	104.5
4000	Average	QC_H1	3 of 3	4180	49.13	1.175	104.5

***Table 28**: Individual Concentration and Summary Statistics for the Quality Control Samples used for run acceptance. N/A = Not Applicable.*

3.2.3. Method selectivity

Method selectivity was evaluated by assaying:

- three replicates of blank plasma sample without analyte and internal standard to verify possible interferences at the analyte and internal standard retention time;
- three replicates of blank plasma sample with Internal Standard only to verify possible analyte traces at the analyte retention time;
- three replicates of blank plasma sample with analyte at ULOQ concentration level only to verify possible internal standard traces at internal standard retention time;
- five LLOQ replicates to verify the accuracy and precision of the lowest concentration in plasma samples.

No interfering peaks were detected at the retention time of interest (**Figure 62**, **Figure 63**, and **Table 29**).

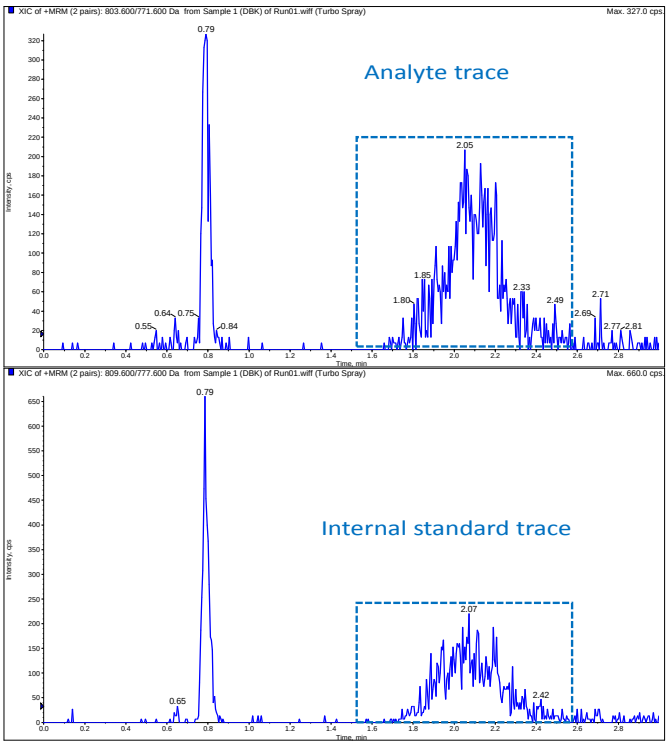

Figure 62: *Internal standard and analyte MRM traces in the extracted blank matrix sample*

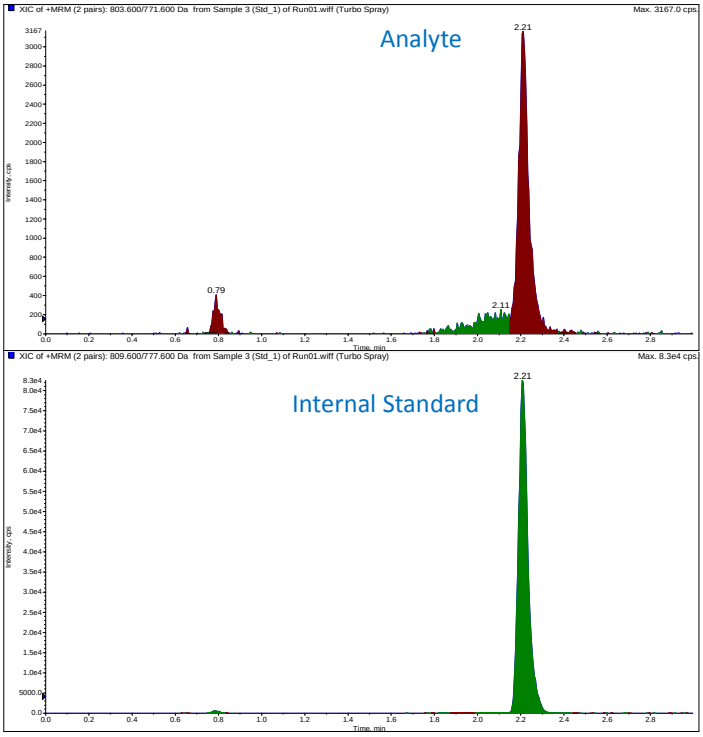

Figure 63: *A representative MRM chromatogram of extracted Internal Standard and analyte at LLOQ level*

Selectivity: • **matrix selectivity** • **selectivity vs AN** • **selectivity vs IS** • **matrix selectivity (LLOQ)**	0.0% IS interference and 0.8% AN interference 0.2% IS interference 3.8% AN interference %BIAS ranged from -13.3 to 3.5 and the %CV was 7.0 (100% of LLOQ replicates passed)

***Table 29**: Selectivity data*

3.2.4. Dilution Test

In order to verify that samples exceeding the calibration range can be analyzed after appropriate dilution, validation/dilution integrity samples were prepared at one level exceeding the calibration range.

Subsequently, samples were diluted with blank matrix in order to bring the concentrations into the calibration range. A spiked sample at 200.0 µg/mL in normal mouse plasma pool was prepared at a concentration level requiring a maximum dilution factor of 100.

The results reported in **Table 30** show that the samples diluted 100 fold correctly fit the calibration curve.

RUN ID 4	Back-Calculated Conc. ng/mL (theoretical 200.0 µg/mL)	Bias (%)
	187.3	-6.4
	218.8	9.4
	169.3	-15.4
Mean Conc.	191.8	
Mean Accuracy (%BIAS)	-4.1	
SD	25.05	
Precision (%CV)	13.1	
n	3	

***Table 30:** Dilution integrity data*

3.2.5. Stability Investigations

Drug stability experiments should mimic conditions under which samples are collected, stored, and processed, as closely as possible. Experiments should be conducted in unaltered representative matrix, including the same type of anticoagulant and cover the time periods of actual or anticipated sample storage under the individual conditions. Stability samples were prepared at both a low and high concentration covering the calibration range (typically, samples should be prepared at the low and high validation level (~3x LLOQ and ~75-80% ULOQ).

The following stability experiments were performed in biological matrix:

- Bench-top stability (during sample preparation without special protection from daylight)
- Post-preparative stability (autosampler stability or re-injection feasibility)
- Freeze and thaw stability (during repeated freezing and thawing cycles). Samples should be stored frozen for at least 12h and thawed applying the same conditions tested for bench-top stability (e.g. if bench-top stability calls for storage on wet ice, freeze/thaw stability samples must be thawed on wet ice as well)

In case of multi-analyte assays, stability must be evaluated in the presence of all analytes (i.e. stability samples spiked with all analytes). This is particularly important for bioequivalence trials. The results reported in **Table 31** show that the spiked samples extracted are stable in the autosampler for 72 hours at 5°C. Additionally, the spiked samples thawed and kept for 2 hours at room temperature (time needed to process the samples) are stable and the spiked samples frozen and thawed for three times are stable under these conditions.

Run ID **5** **Autosampler Stability 72h**	**SS-Low** **(ng/mL)** **30.00**	**SS-High** **(ng/mL)** **4000**
Mean Conc.	29.71	4218
Mean Accuracy (%BIAS)	-1.0	5.5
Precision (%CV)	8.8	4.9
n	3	3
Run ID **4** **Bench-Top Stability 2h at RT**	**SS-Low** **(ng/mL)** **30.00**	**SS-High** **(ng/mL)** **4000**
Mean Conc.	29.13	3968
Mean Accuracy (%BIAS)	-2.9	-0.8
SD	2.3	263.2
Precision (%CV)	7.9	6.6
n	3	3
Run ID **4** **Freeze&Thaw Stability 2 cycles**	**SS-Low** **(ng/mL)**	**SS-High** **(ng/mL)**
Mean Conc.	30.89	4052
Mean Accuracy (%BIAS)	3.0	1.3
SD	1.7	107.1
Precision (%CV)	5.5	2.6
n	3	3

Table 31: *Stability data (Autosampler stability, Bench-top and Freeze&Thaw)*

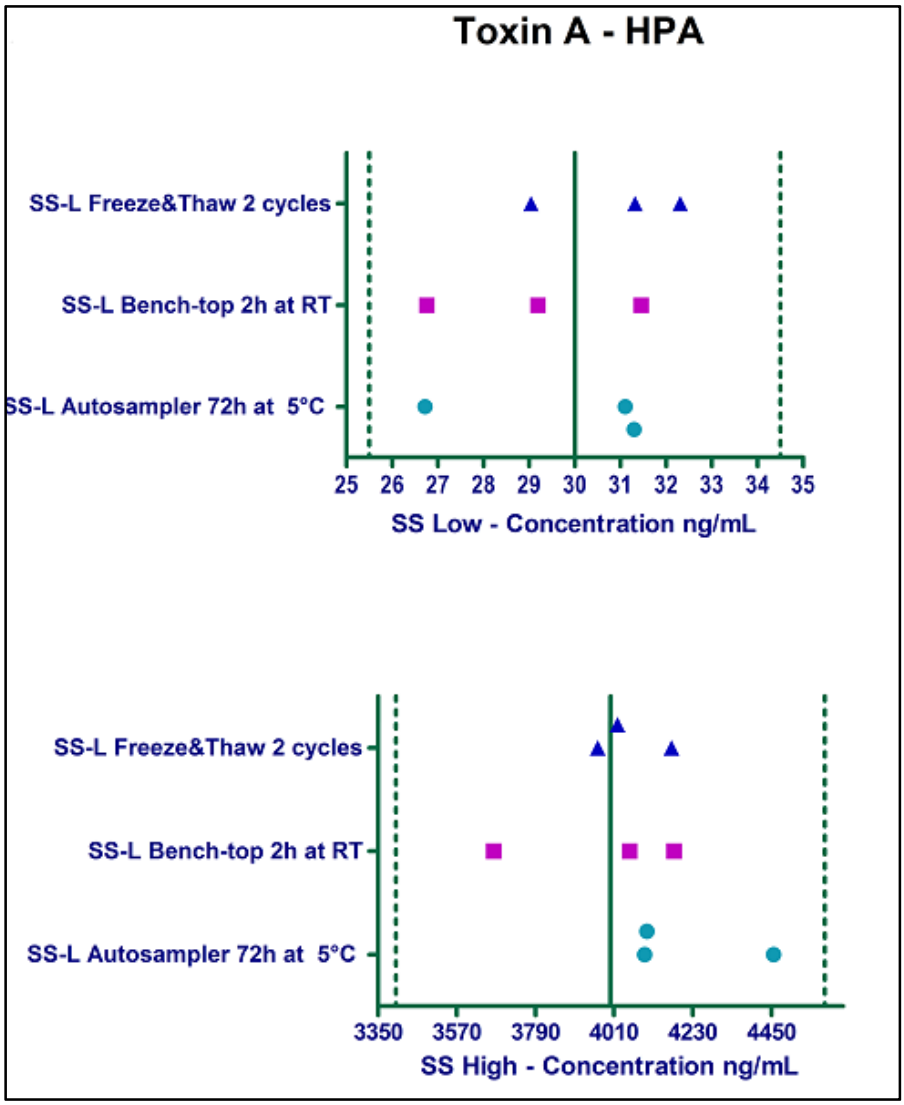

***Figure 64**: Scatter plot of the stability data. The graphic shows that the Spiked Samples are stable under the conditions tested.*

3.3. Conclusion

In summary, the LC–MS/MS method for the quantitation of Toxin A-HPA in mouse plasma was developed and qualified. This method offers significant advantages in terms of sensitivity and selectivity, faster run time (7.5 min) and lower sample requirements.

An Internal Standard is usually required for precise and accurate quantitative determinations in bioanalysis. It should match the structure of the analyte as closely as possible. The ideal Internal Standard used in mass spectrometric quantitation is the stable-isotope-labeled analyte. Amongst others the most important reason to use the isotope-labeled analyte is its coelution with the analyte thus compensating for ion suppression effects which are a common observation in LC–ESI-MS–MS.

With dilution integrity up to 100-fold, it was established that the upper limit of quantification is extendable up to 200.0 µg/mL. Hence, this method is useful for preclinical pharmacokinetic and toxicokinetic studies. The sensitivity could be further improved by sample concentration.

Additionally, the Protein Precipitation assay performed by using a 96 well plate allowed an increase in throughput of sample preparation.

3.4. Qualification of Total Toxin A-HPA in homogenized human tumor tissue

3.4.1. Homogenized human tumor tissue pre-treatment

The homogenized human tumor tissue was obtained by applying a generic method set-up within the NBEs Bionalytical department. The protocol applied was the following:

Critical reagents:

Cell extraction buffer (Invitrogen)
Protein phosphatase inhibitor kit II (Calbiochem)
Complete mini protease inhibitor cocktail tablets (Roche)
BCA protein assay kit (Pierce Thermo Scientific)

Chemicals:

Deionized water (MilliQ, Merck-Millipore)
Phosphate-buffered Saline (PBS Gibco)

Solutions:

Tissue Lysis Buffer: dissolve 1 tablet of complete mini protease inhibitor in 10 mL of cell extraction buffer + 100 µL of protein phosphatase inhibitor (freshly prepared)

10X PBS solution: dissolve 20 tables of PBS in 1 L of MilliQ water (stable 1 month at room temperature)

1X PBS solution: dilute the 10x PBS solution 1:10 using MilliQ water (stable 2 weeks at +4°C)

Procedure:

- Prepare tissue lysis buffer on the day of extraction and store on ice until use
- Cool the precellys homogenizer from -5°C to +4°C
- Weight 80-150 mg of tumor/tissue in precellys tubes, if the weight is not available
- Calculate the lysis buffer volume to be added based on the initial weight (700 µL / 100 mg tissue) and add to the tube
- Homogenize using the following protocol:

  15 sec. at 6500 rpm – 15 sec. Pause – 15 sec. at 6500 rpm
- Centrifuge for 1 minute at 13000 g at +4°C and take the supernatant
- Place the extracts on ice if Bioanalytics determination of drug content is done immediately. Otherwise samples must be stored at -20°C until analysis.

3.4.2. Linearity

Good linearity was obtained for the nine-point calibration curve constructed by plotting the peak area ratio of analyte to its internal standard versus the corresponding concentration ratio and fitting the data using linear regression with $1/x^2$ weighting factor. For six consecutive batches, the calibration curves showed an overall accuracy (%) ranging from 96.7% to 109.5% with CV% ≤ 7.9% over the concentration range of 10.00 - 5000 ng/mL (**Table 32**). The calibration curves were prepared in plasma after testing the equivalence between the response of the curve prepared in plasma vs. curve prepared in homogenized tumor tissue. These curves were used to back-calculate the SS/QCs and sample testing concentration in homogenized tumor tissue. The choice was due to the insufficient amount of homogenized tumor tissue for study conduct.

Run ID - %Bias	Std1 ng/mL 10.00	Std2 ng/mL 20.00	Std3 ng/mL 50.00	Std4 ng/mL 100.0	Std5 ng/mL 200.0	Std6 ng/mL 500.0	Std7 ng/mL 1000	Std8 ng/mL 2000	Std9 ng/mL 5000
3	10.06	19.76	47.57	111.8	193.7	500.0	934	1977	5225
Bias (%)	**0.6**	**-1.2**	**-4.9**	**11.8**	**-3.2**	**0.0**	**-6.6**	**-1.2**	**4.5**
4	10.05	18.90	54.33	104.8	205.7	467.1	1016	1997	4687
Bias (%)	**0.5**	**-5.5**	**8.7**	**4.8**	**2.8**	**-6.6**	**1.6**	**-0.2**	**-6.3**
5	9.94	20.08	49.99	105.1	199.4	484.4	1025	2006	4789
Bias (%)	**-0.6**	**0.4**	**0.0**	**5.1**	**-0.3**	**-3.1**	**2.5**	**0.3**	**-4.2**
6	9.55	21.99	47.25	106.0	206.5	487.5	944	2034	4865
Bias (%)	**-4.5**	**9.9**	**-5.5**	**6.0**	**3.3**	**-2.5**	**-5.6**	**1.7**	**-2.7**
7	9.45	22.36	49.88	126.0	182.6	516.4	1026	1966	4919
Bias (%)	**-5.5**	**11.8**	**-0.2**	**26.0***	**-8.7**	**3.3**	**2.6**	**-1.7**	**-1.6**
8	9.30	22.50	51.26	103.2	198.0	492.5	997	2025	4516
Bias (%)	**-7.0**	**12.5**	**2.5**	**3.2**	**-1.0**	**-1.5**	**-0.3**	**1.3**	**-9.7**
Statistic									
Mean	9.72	20.93	50.05	109.5	197.7	491.3	990	2001	4834
STDEV	0.33	1.54	2.60	8.61	8.81	16.46	41.25	26.48	239.09
CV (%)	3.4	7.4	5.2	7.9	4.5	3.4	4.2	1.3	4.9
Accuracy (%)	97.2	104.65	100.1	109.5	98.9	98.3	99.0	100.1	96.7

Table 32: *Precision and accuracy for the calibration standard of Toxin A-HPA in mouse plasma from six qualification batches*

The carryover met the acceptance criteria in each run.

Run ID	AN Peak Area in LLOQ (Std1)	AN Peak Area in DBK after ULOQ	Carryover (%)
3	8327.1	426.5	5.1
4	11748.8	362.7	3.1
5	8263.6	451.5	5.5
6	4872.3	432.7	8.9
7	8222.8	1580.5	19.2
8	9698.7	1549.9	16.0

***Table 33**: Carryover evaluation*

The slope value was consistent for six consecutive batches and the slope variation was ≤ 4.7 over the runs analyzed. The correlation coefficient (r) of the linear regression was between 0.9975-0.9995.

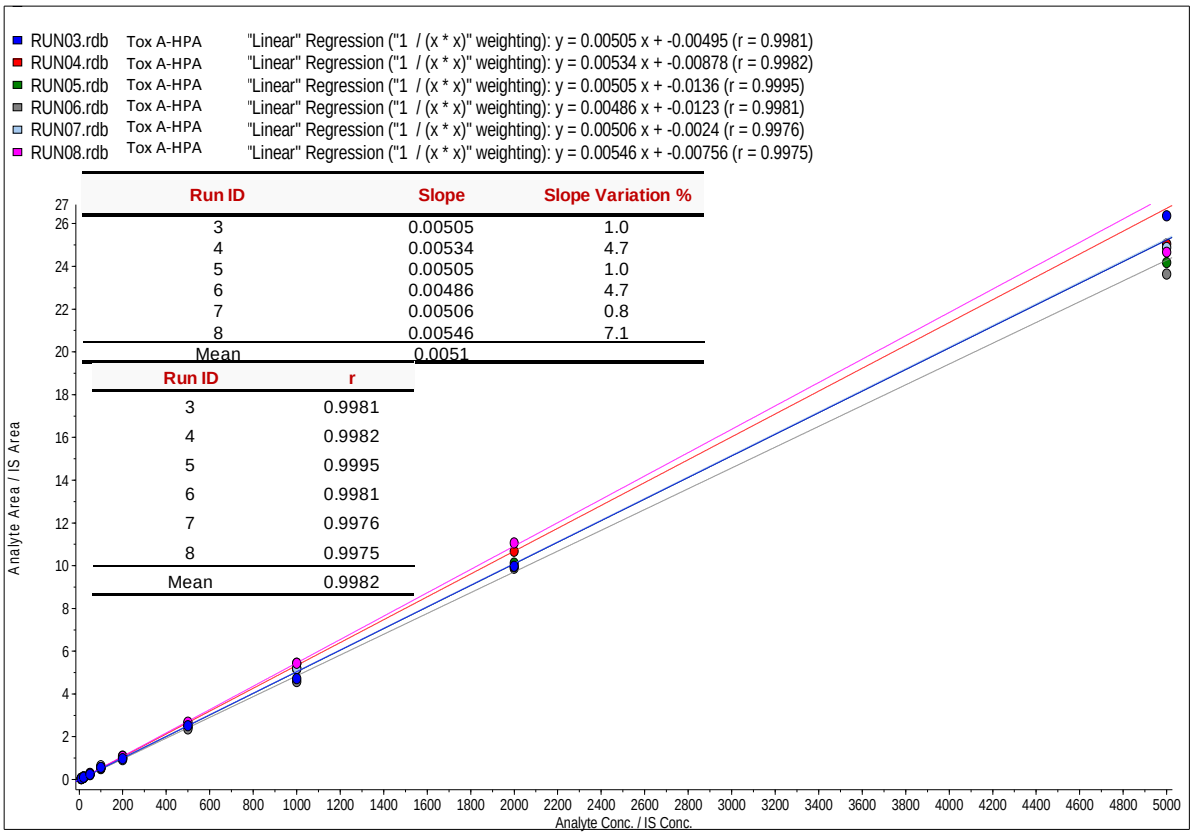

***Table 34:** Overlay of the calibration curves of the study showing the reproducibility and good linearity in terms of slope accuracy and correlecion coefficients near to 1.*

The LLOQ was taken as the lowest calibration concentration that passed acceptance criteria with a signal-to-noise (x4 standard deviation) of a least 5:1.

3.4.3. Intra-Inter Run Accuracy and Precision

Method accuracy and precision were evaluated using Spiked Samples (SS) prepared by spiking polymer-linker-drug Standard into the blank tumor tissue at five concentration levels (10.00, 30.00, 300.0, 4000 and 5000 ng/mL) to serve as SS LLOQ, SS Low, SS Medium, SS High and SS ULOQ.

Three consecutive batches were prepared and each batch contained a freshly prepared calibration curve and five replicates of SS samples at the five levels.

Intra-assay precision was calculated by obtaining the Coefficient of Variation (CV) % of the five replicates of each SS level, and intra-assay accuracy was calculated by averaging the accuracies (% Bias) of five replicates of each SS level against the fresh curve.

Inter-assay precision was calculated by obtaining the %CV of all 11 replicates at each SS level from all the three batches, with overall accuracy calculated by averaging the accuracies of all 11 replicates at each SS level from all the three batches.

Accuracy (%Bias) ranged from -7.5% to 2.4% and precision (%CV) ranged from 1.9% to 8.2% for intra-assay. Accuracy (%Bias) ranged from -6.2% to 1.4% and precision (%CV) ranged from 2.7% to 6.7% for inter-assay.

Accuracy and precision were evaluated including SS-LLOQ and SS-ULOQ (**Table 35** and **Figure 65**). **The method was found to be highly accurate and precise.**

The statistics on QC samples used for run acceptance and to perform runs 04, 05 and 06 for Selectivity, Freeze and Thaw, Bench-top, dilution integrity and autosampler stability 24 and 72 hour tests are reported in **Figure 65**.

Intra-assay	SS-LLOQ (ng/mL) 10.00	SS-Low (ng/mL) 30.00	SS-Medium (ng/mL) 300.0	SS-High (ng/mL) 4000	SS-ULOQ (ng/mL) 5000
Mean Conc.	9.79	30.73	277.5	3832.2	4771
Intra-Run Accuracy (%BIAS)	-2.1	2.4	-7.5	-4.2	-4.6
SD	0.798	1.85	9.40	131	90.0
Intra-Run Precision (%CV)	8.2	6.0	3.4	3.4	1.9
n	5	5	5	5	5
Inter-assay	**SS-LLOQ (ng/mL) 10.00**	**SS-Low (ng/mL) 30.00**	**SS-Medium (ng/mL) 300.0**	**SS-High (ng/mL) 4000**	**SS-ULOQ (ng/mL) 5000**
Overall Mean Conc.	10.06	30.41	281.4	4388	4903
Inter-Run Accuracy (%BIAS)	0.6	1.4	-6.2	-1.1	-1.9
Overall SD	0.670	1.64	16.4	105	182
Inter-Run Precision (%CV)	6.7	5.4	5.8	2.4	3.7
n	11	11	11	11	11

Table 35: *Intra and inter-assay accuracy and precision evaluation*

RUN ID	QC-Low 30.00 (ng/mL)	Bias (%)	QC-Medium 300.0 (ng/mL)	Bias (%)	QC-High 4000 (ng/mL)	Bias (%)
06	31.43	0.5	292.5	-2.5	3780	-5.5
	30.70	2.3	307.3	2.4	3718	-7.1
07	32.45	0.8	303.2	1.1	4239	6.0
	32.59	8.6	322.8	7.6	4522	13.1
08	31.17	3.9	295.2	-1.6	4493	12.3
	33.47	11.6	305.6	1.9	4279	7
Mean	31.97		304.4		4172	
STDEV	1.0		10.7		346.8	
CV (%)	3.1		3.5		8.3	
Accuracy (%)	106.6		101.5		104.3	
Bias (%)	4.6		1.5		4.3	
n	6		6		6	

Table 36*: Individual Concentration and Summary Statistics for the Quality Control Samples*

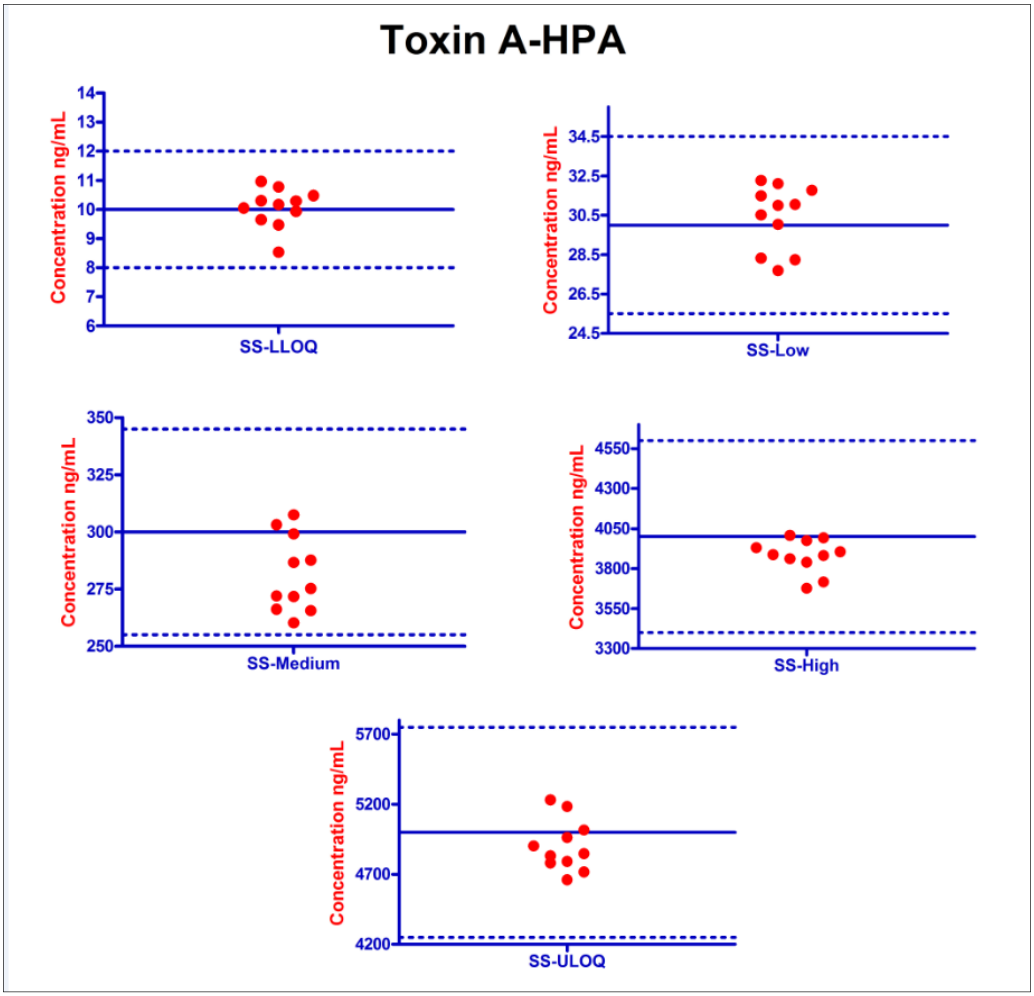

Figure 65: *Scattter plot of the spiked sample analyzed for intra-inter run accuracy and precision evaluation.*

3.4.4. Method selectivity

Method selectivity was evaluated by assaying:

a) three replicates of blank tumor tissue samples without analyte and internal standard to verify possible interferences at the analyte and internal standard retention time;

b) three replicates of blank tumor tissue samples with Internal Standard only to verify possible analyte traces at the analyte retention time;

c) three replicates of blank tumor tissue samples with analyte at ULOQ concentration level only to verify possible internal standard traces at internal standard retention time;

d) five LLOQ replicates to verify the accuracy and precision of the lowest concentration in tumor tissue samples.

No interfering peaks were detected at the retention time of interest as highlighted by the blue bar (**Figure 66** and **Table 37**).

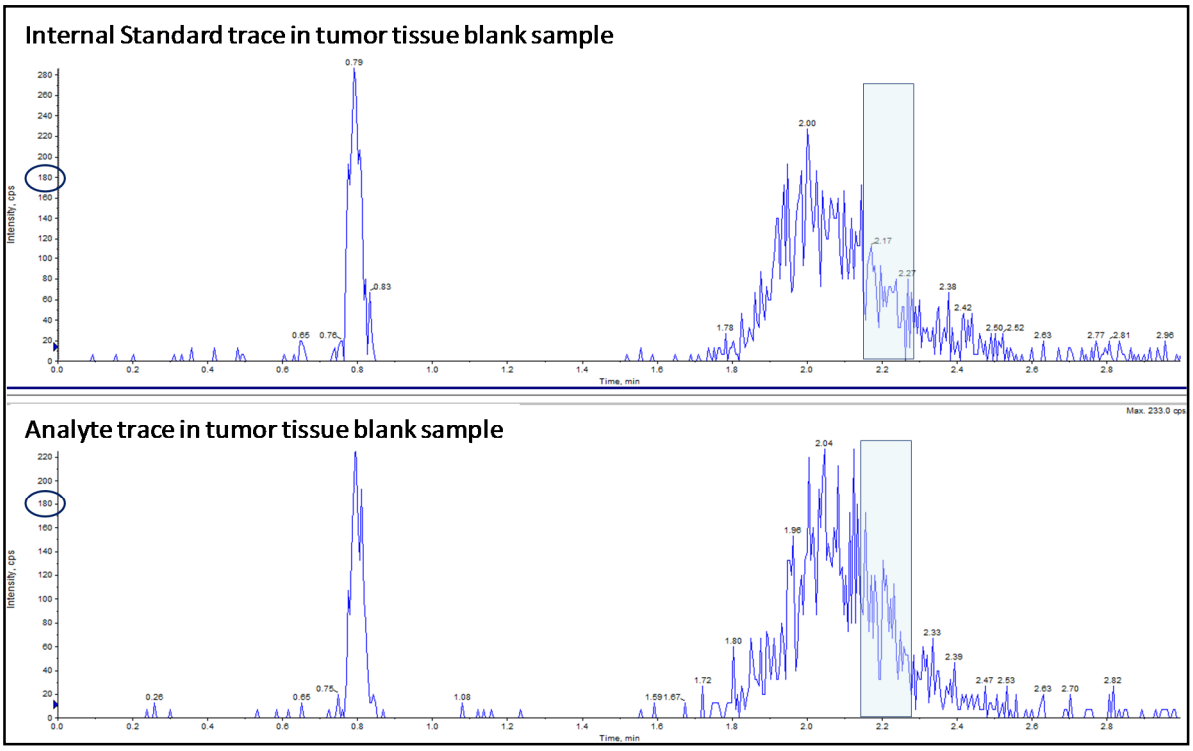

Figure 66: *Analyte and Internal Standard MRM transitions in blank sample*

Selectivity: • **matrix selectivity** • **selectivity vs AN** • **selectivity vs IS** • **matrix selectivity (LLOQ)**	0.0% IS interference and 2.3% AN interference 0.0% IS interference 3.3% AN interference %BIAS ranged from -14.6 to 5.3 and %CV was 8.2 (100% of LLOQ replicates passed)

Table 37: *Selectivity data*

3.4.5. Dilution Test

In order to verify that samples exceeding the calibration range can be analyzed after appropriate dilution, validation/dilution integrity samples were prepared at one level exceeding the calibration range.

Subsequently, samples were diluted with blank matrix in order to bring the concentrations into the calibration range. A spiked sample at 200.0 µg/mL in homogenized human tumor tissue was prepared at a concentration level requiring a maximum dilution factor of 100.

The results reported in **Table 38** show that the samples diluted 100 fold correctly fit the calibration curve.

RUN ID 8	Back-Calculated Conc. ng/mL (theoretical 2000 ng/mL)	Bias (%)
	2133	6.7
	2109	5.5
	2167	8.4
Mean Conc.	2136	
Mean Accuracy (%BIAS)	6.9	
SD	29.1	
Precision (%CV)	1.4	
n	3	

Table 38: *Dilution integrity data*

3.4.6. Stability Investigations

Drug stability experiments should mimic conditions under which samples are collected, stored, and processed, as closely as possible. The experiments should be conducted in unaltered representative matrix, including the same type of anticoagulant and cover the time periods of actual or anticipated sample storage under the individual conditions. Stability samples were prepared at both a low and high concentration covering the calibration range (typically, samples should be prepared at the low and high validation level (~3x LLOQ and ~75-80% ULOQ).

The following stability experiments in biological matrix were performed:

- Bench-top stability (during sample preparation without special protection from daylight)
- Post preparative stability (autosampler stability or re-injection feasibility)
- Freeze and thaw stability (during repeated freezing and thawing cycles). Samples should be stored frozen for at least 12h and thawed applying the same conditions tested for bench-top stability (e.g. if bench-top stability calls for storage on wet ice, freeze/thaw stability samples must be thawed on wet ice as well)

In case of multi-analyte assays, stability must be evaluated in the presence of all analytes (i.e. stability samples spiked with all analytes). This is particularly important for bioequivalence trials.

The results reported in **Table 39** show that the spiked samples extracted are stable in the autosampler for 72 hours at 5°C. Additionally, the spiked samples thawed and kept for 2 hours at room temperature (time needed to process the samples) are stable and the spiked sample frozen and thawed twice are stable under these conditions.

Run ID: 6 **Autosampler Stability 72h**	**SS-Low (ng/mL)** **30.00**	**SS-High (ng/mL)** **4000**
Mean Conc.	32.95	4242
Mean Accuracy (%BIAS)	9.8	6.1
SD	1.77	22.9
Precision (%CV)	5.5	0.5
n	3	3
Run ID: 8 **Bench-Top Stability 2h at RT**	**SS-Low (ng/mL)** **30.00**	**SS-High (ng/mL)** **4000**
Mean Conc.	32.34	4187
Mean Accuracy (%BIAS)	7.8	4.7
SD	0.687	69.6
Precision (%CV)	2.1	1.7
n	3	3
Run ID: 8 **Freeze&Thaw Stability 2 cycles**	**SS-Low (ng/mL)** **30.00**	**SS-High (ng/mL)** **4000**
Mean Conc.	32.77	4284
Mean Accuracy (%BIAS)	9.2	7.1
SD	1.08	120
Precision (%CV)	3.3	2.8
n	3	3

Table 39: *Stability data evaluation*

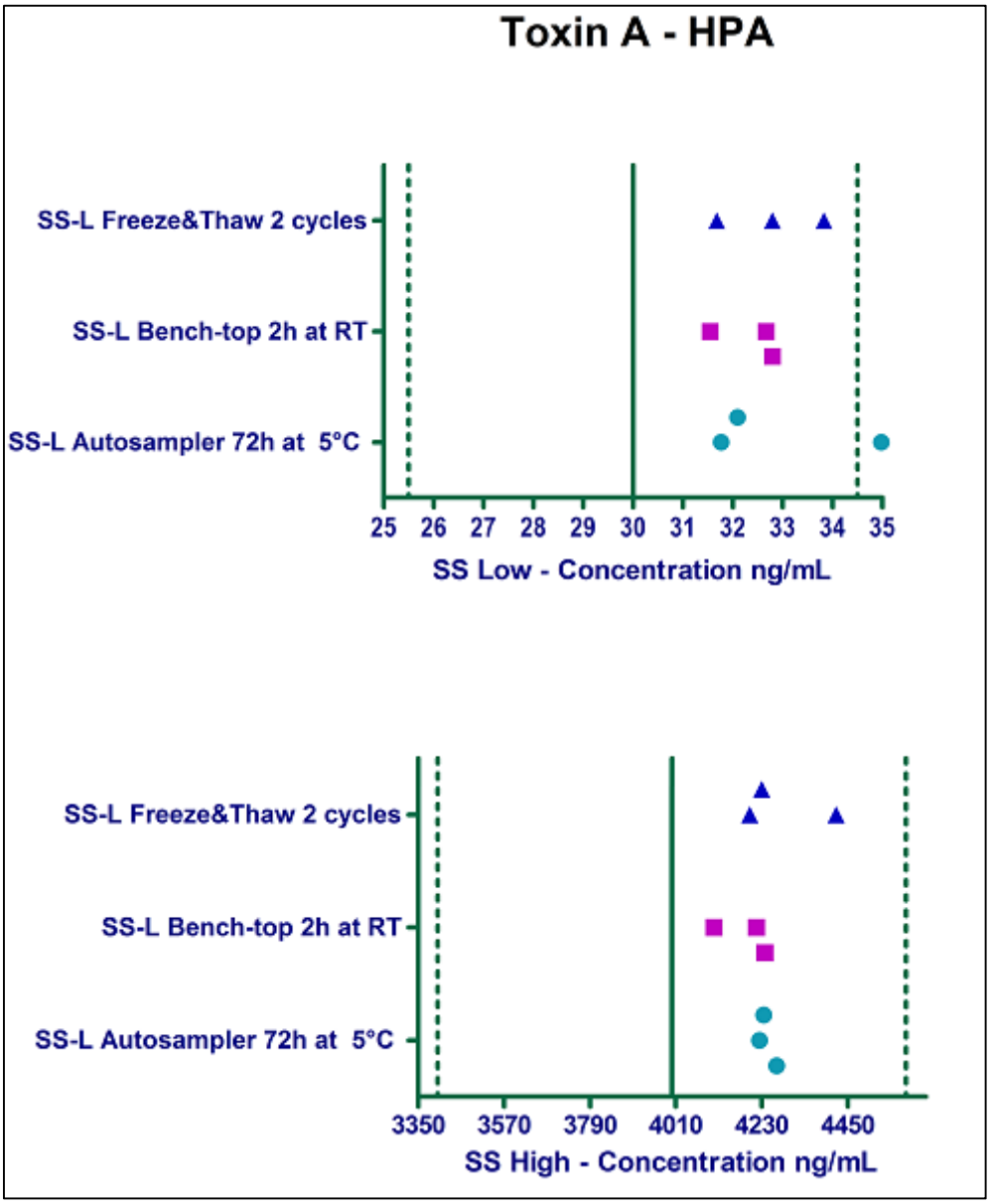

Figure 67: *Scatter plot of the stability data. The graphic shows that the spiked samples are stable under the conditions tested.*

3.5. Conclusion

A reliable LC–MS/MS method for Toxin A-HPA determination in human tumor tissue has been developed and qualified. This method provides selectivity, specificity, accuracy and reproducibility. The assay was able to measure accurately Toxin-A HPA levels from a small sample volume (5.0 µl).

Additionally, the high sensitivity of the triple quadrupole mass spectrometer allowed sample dilution prior to sample analysis and no sample evaporation/concentration was required. Since the sample obtained after the PPT was in organic solvent, samples were diluted with a

mixture of water / acetonitrile (50/50 + 2.5% formic acid) in order to obtain the appropriate condition for injection. The final sample was diluted 140 times.

3.6. Method development of Free Toxin A and free Toxin A-HPA Quantitation in mouse plasma

The method development of the free toxins quantitation was set up on the basis of conditions used for payload determination (see paragraph 2.3).

This means that the chromatographic conditions used for the determination of toxin A-HPA from ADC was maintained and work was focused on optimizing the mass spectrometric conditions in order to improve sensitivity. Since the level of free toxins was estimated to be low in the incurred samples, the method was re-optimized in order to have a calibration curve range from 0.250 ng/mL to 10.0 ng/mL.

The strategy adopted was to select the two main product ions and verify their selectivity in matrix samples (**Figure 68** and **Figure 69**). The product ions were found to be selective in matrix samples and then the MRM transitions were summed as reported in the figure below.

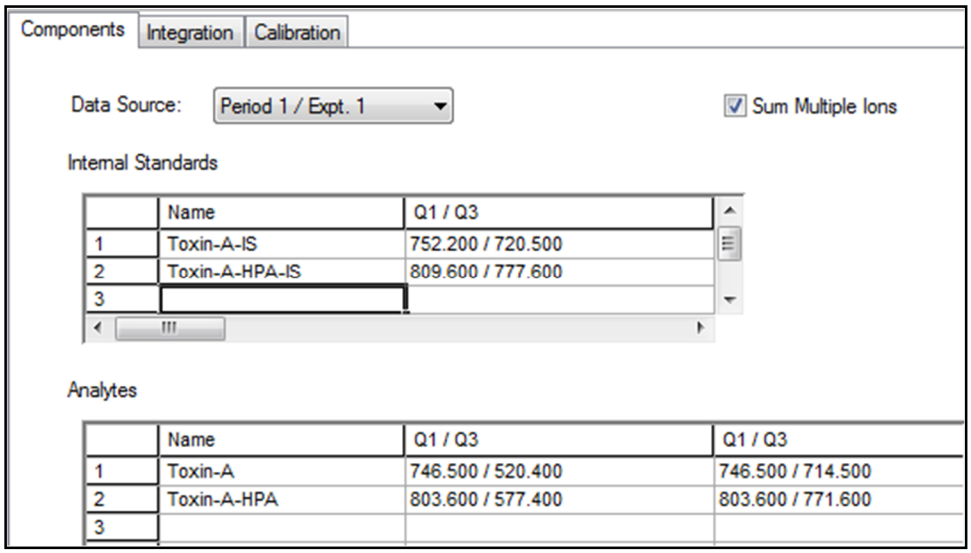

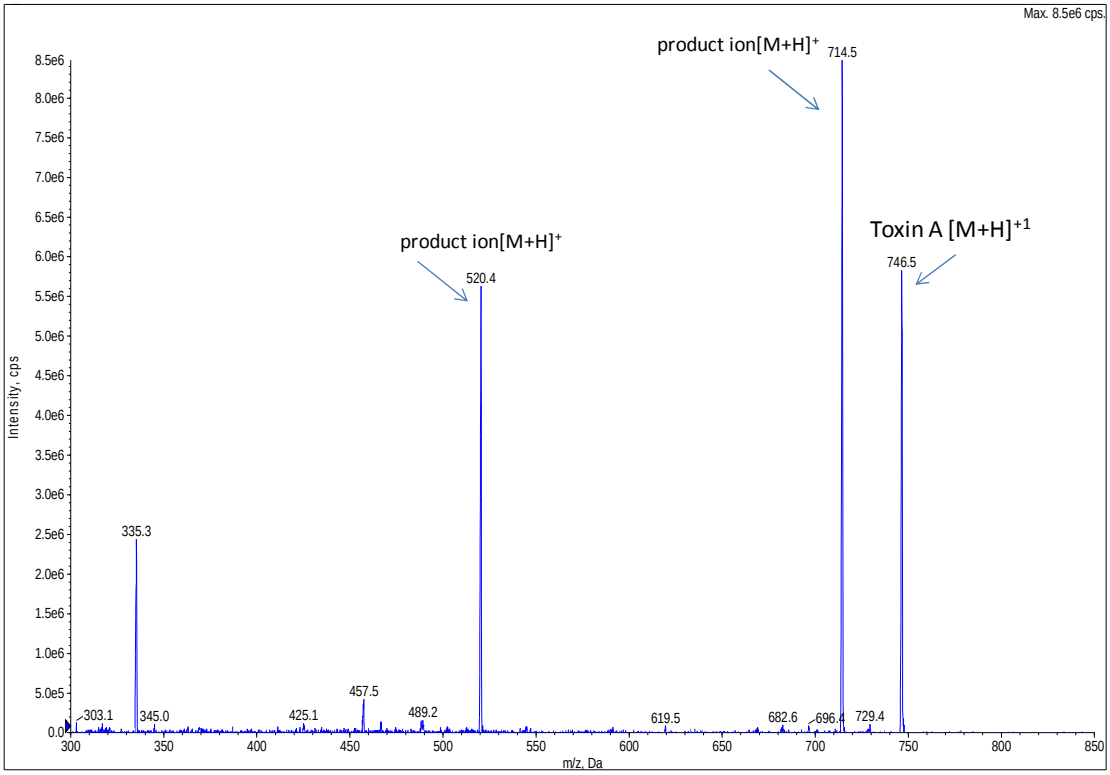

***Figure 68**: Toxin A precursor ion and the selected product ions*

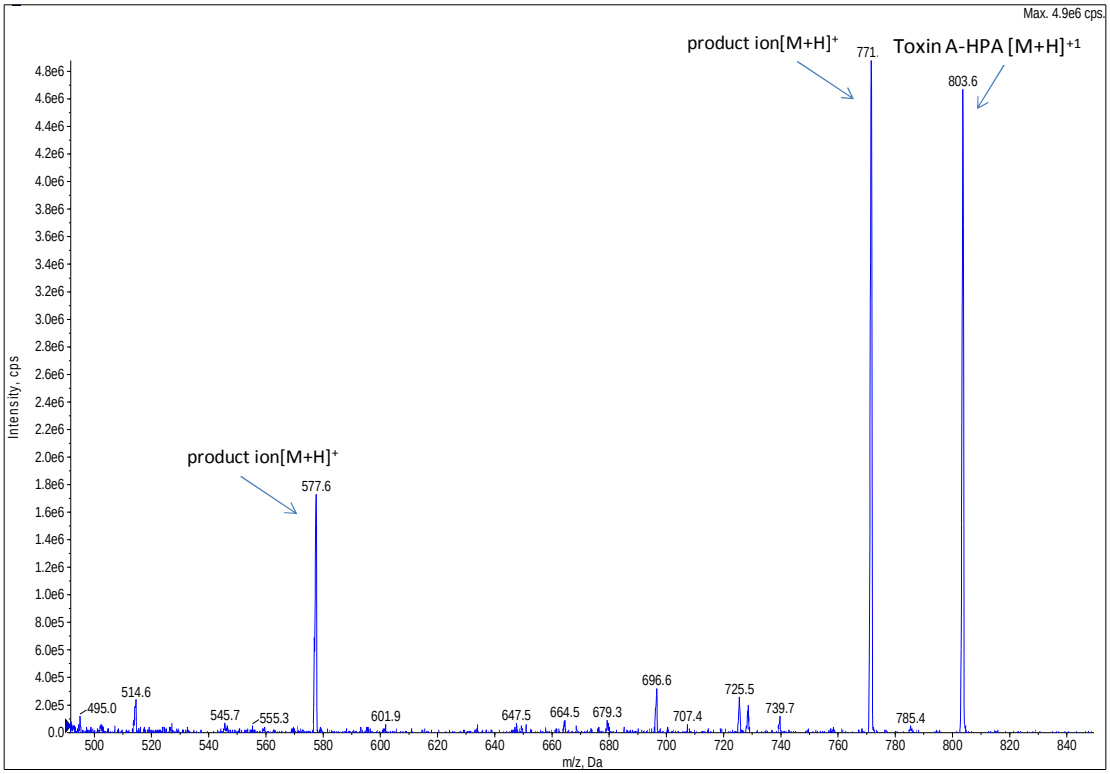

***Figure 69:** Toxin A-HPA precursor ion and the selected product ions*

3.6.1. Sample preparation optimization

Since the sample volume available for the real sample analysis was very limited, efficiency of the protein precipitation technique was verified by using a small volume of sample in a large volume of precipitation reagent (acetonitrile with 2.5% of formic acid). Waters protocol for Sirocco plate recommends a *sample : precipitation reagent* ratio of *1:4* but due to the impossibility of using only 40.0 µL of precipitation reagent (this volume was the dead volume of Sirocco plate and therefore a larger volume was required) two different volumes of precipitation reagent were tried to perform the protein precipitation: (a) precipitation reagent : plasma samples ratio = 150.0 µL : 5.0 µL and (b) precipitation reagent : plasma samples ratio = 100.0 µL : 5.0 µL (**Figure 70, Figure 71, Figure 72** and **Figure 73**). Results showed that the accuracy and precision parameters were consistent for toxin A and toxin A-HPA extracted using 150.0 µL of precipitation reagent, while accuracy and precision of both analytes extracted using 100.0 µL of precipitation reagent were not so consistent. The experiment (b) showed: high variability of internal standard areas (as highlighted in red and reported in **Figure 72** and **Figure 73).** Any sample preparation error was excluded since the samples of experiments (a) and (b) were prepared all together and at the same time, using the same Sirocco plate and pipette. On the basis of these results the final choice was to use 150 µL of precipitation reagent to perform sample clean-up.

Sample Name	Sample Type	Analyte Concentration (ng/mL)	Analyte Peak Area (counts)	IS Peak Area (counts)	Area Ratio	Calculated Concentration (ng/mL)	Accuracy (%)
DBK_1	Double Blank	0.0	0.0	0.0	N/A	N/A	N/A
Std1	Standard	0.250	3577.0	49270.1	0.073	0.229	91.6
Std2	Standard	0.375	7501.9	51616.6	0.145	0.420	112.1
Std3	Standard	0.500	9309.0	49244.4	0.189	0.535	107.1
Std4	Standard	1.00	16591.3	49900.2	0.332	0.913	91.3
Std5	Standard	2.50	42452.8	52614.0	0.807	2.16	86.4
Std6	Standard	5.00	93324.4	48691.1	1.917	5.08	101.6
Std7	Standard	7.50	133997.5	49830.5	2.689	7.11	94.9
Std8	Standard	10.0	188267.5	43245.8	4.353	11.5	114.9
DBK_2	Double Blank	0.0	0.0	0.0	N/A	N/A	N/A
QC_L	Quality Control	0.750	14719.7	47526.1	0.31	0.853	113.7
QC_M	Quality Control	3.75	54673.9	47053.3	1.162	3.10	82.5
QC_H	Quality Control	8.00	138279.5	50025.3	2.764	7.31	91.4

Figure 70: *Toxin A results using 150.0 µL of precipitation reagent. NA= Not Applicable.*

Sample Name	Sample Type	Analyte Concentration (ng/mL)	Analyte Peak Area (counts)	IS Peak Area (counts)	Area Ratio	Calculated Concentration (ng/mL)	Accuracy (%)
DBK_1	Double Blank	0.0	176.6	0.0	N/A	N/A	N/A
Std1	Standard	0.250	2676.6	24258.0	0.11	0.249	99.6
Std2	Standard	0.375	4072.8	26936.9	0.151	0.344	91.7
Std3	Standard	0.500	6162.5	24885.2	0.248	0.567	113.5
Std4	Standard	1.00	11091.8	25381.5	0.437	1.01	100.6
Std5	Standard	2.50	25782.9	26383.4	0.977	2.26	90.4
Std6	Standard	5.00	57687.5	27079.1	2.13	4.93	98.7
Std7	Standard	7.50	83983.3	26762.7	3.138	7.27	96.9
Std8	Standard	10.00	113027.1	24095.00	4.691	10.9	108.7
DBK_2	Double Blank	0.0	298.1	0.0	N/A	N/A	N/A
QC_L	Quality Control	0.750	8632.9	23227.7	0.372	0.855	114.0
QC_M	Quality Control	3.75	35961.3	24760.2	1.452	3.36	89.6
QC_H	Quality Control	8.00	82732.1	24973.3	3.313	7.67	95.9

Figure 71: *Toxin A - HPA results using 150 µL of precipitation reagent. NA= Not Applicable.*

Sample Name	Sample Type	Analyte Concentration (ng/mL)	Analyte Peak Area (counts)	IS Peak Area (counts)	Area Ratio	Calculated Concentration (ng/mL)	Accuracy (%)
Test C_DBK_1	Double Blank	N/A	0.0	0.0	N/A	N/A	N/A
Test C_Std0	Blank	N/A	0.0	24214.3	0.0	No Peak	N/A
Test C_Std1	Standard	0.250	4097.6	15130.2	0.271	0.254	101.6
Test C_Std2	Standard	0.375	2786.3	10920.1	0.255	0.229	61.2
Test C_Std3	Standard	0.500	6439.0	15182.9	0.424	0.494	98.8
Test C_Std4	Standard	1.00	1256.7	5480.7	0.229	0.189	18.9
Test C_Std5	Standard	2.50	19790.3	13447.2	1.472	2.14	85.4
Test C_Std6	Standard	5.00	59819.6	17896.7	3.342	5.07	101.3
Test C_Std7	Standard	7.50	66966.3	12630.9	5.302	8.14	108.5
Test C_Std8	Standard	10.00	107516.5	15892.5	6.765	10.4	104.3
Test C_DBK_2	Double Blank	N/A	0.0	0.0	N/A	N/A	N/A
Test C_QC_L	Quality Control	0.750	10188.6	18087.0	0.563	0.712	95.0
Test C_QC_M	Quality Control	3.75	11590.5	10665.2	1.087	1.53	40.9
Test C_QC_H	Quality Control	8.00	90466.5	17116.0	5.286	8.11	101.4
RS_1	Double Blank	N/A	0.0	0.0	N/A	N/A	N/A

Figure 72: *Toxin A results using 100 µL of precipitation reagent. NA= Not Applicable.*

Sample Name	Sample Type	Analyte Concentration (ng/mL)	Analyte Peak Area (counts)	IS Peak Area (counts)	Area Ratio	Calculated Concentration (ng/mL)	Accuracy (%)
Test C_DBK_1	Double Blank	0.0	0.0	0.0	N/A	N/A	N/A
Test C_Std0	Blank	0.0	0.0	11308.9	0.0	N/A	N/A
Test C_Std1	Standard	0.250	1833.8	7964.4	0.23	0.249	99.4
Test C_Std2	Standard	0.375	1997.9	6033.6	0.331	0.379	101.2
Test C_Std3	Standard	0.500	3628.7	8537.6	0.425	0.501	100.2
Test C_Std4	Standard	1.00	921.8	2825.3	0.326	0.373	37.3
Test C_Std5	Standard	2.50	13192.9	6866	1.921	2.44	97.6
Test C_Std6	Standard	5.00	37379.5	10304.4	3.628	4.65	93.0
Test C_Std7	Standard	7.50	43259.5	6946.7	6.227	8.02	106.9
Test C_Std8	Standard	10.00	66384.9	8421.5	7.883	10.2	101.6
Test C_DBK_2	Double Blank	0.0	0.0	0.0	N/A	N/A	N/A
Test C_QC_L	Quality Control	0.750	5611.8	11011.1	0.51	0.611	81.4
Test C_QC_M	Quality Control	3.75	8572.6	5301.5	1.617	2.05	54.5
Test C_QC_H	Quality Control	8.00	53810.7	8358.6	6.438	8.29	103.7

Figure 73: *Toxin A - HPA results using 100 µL of precipitation reagent. NA= Not Applicable.*

3.7. Qualification of UPLC-MS/MS method for the quantitation of free Toxin A and Toxin A-HPA in mouse plasma samples

3.7.1. Linearity

Good linearity was obtained for the eight-point calibration curve constructed by plotting the peak area ratio of analyte to its internal standard versus the corresponding concentration ratio and fitting the data using linear regression with 1/x weighting factor. For six consecutive batches, the calibration curves showed an overall accuracy (%) ranging from 97.9% to 102.4% with %CV ≤ 5.2% and from 97.4% to 104.8% with %CV ≤ 7.6% for toxin-A and toxin A-HPA respectively, over the concentration range of 10.00-5000 ng/mL (**Table 40** and **Table 41**).

Toxin A	Std1 ng/mL	Std2 ng/mL	Std3 ng/mL	Std4 ng/mL	Std5 ng/mL	Std6 ng/mL	Std7 ng/mL	Std8 ng/mL
Run ID - %Bias	**0.250**	**0.375**	**0.500**	**1.00**	**2.50**	**5.00**	**7.50**	**10.0**
1	0.252	0.374	0.479	0.97	2.61	5.50	6.79	10.2
Bias (%)	**0.8**	**-0.3**	**-4.2**	**-3.0**	**4.4**	**10.0**	**-9.5**	**2.0**
2	0.255	0.376	0.463	0.969	2.60	5.38	7.70	9.38
Bias (%)	**2.0**	**0.3**	**-7.4**	**-3.1**	**4.0**	**7.6**	**2.7**	**-6.2**
3	0.262	0.354	0.495	1.00	2.50	5.07	7.66	9.78
Bias (%)	**4.8**	**-5.6**	**-1.0**	**0.0**	**0.0**	**1.4**	**2.1**	**-2.2**
4	0.267	0.377	0.518	0.946	2.32	4.92	7.72	10.1
Bias (%)	**6.8**	**0.5**	**3.6**	**-5.4**	**-7.2**	**-1.6**	**2.9**	**1.0**
5	0.240	0.380	0.500	0.971	2.65	5.20	7.40	9.79
Bias (%)	**-4.0**	**1.3**	**0.0**	**-2.9**	**6.0**	**4.0**	**-1.3**	**-2.1**
6	0.260	0.341	0.512	1.030	2.44	5.12	7.45	10.0
Bias (%)	**4.0**	**-9.1**	**2.4**	**3.0**	**-2.4**	**2.4**	**-0.7**	**-0.4**
Statistic								
Mean	0.256	0.367	0.495	0.981	2.52	5.20	7.45	9.87
STDEV	0.0094	0.016	0.021	0.030	0.13	0.21	0.35	0.29
CV (%)	3.7	4.4	4.2	3.1	5.2	4.0	4.7	2.9
Accuracy (%)	102.4	97.9	99.0	98.1	100.8	104.0	99.3	98.7

***Table 40**: Precision and accuracy for the calibration standard of free Toxin A in mouse plasma from six qualification batches*

Toxin A-HPA	Std1	Std2	Std3	Std4	Std5	Std6	Std7	Std8
	ng/mL	ng/mL	ng/mL	ng/mL	ng/mL	ng/mL	ng/mL	ng/mL
Run ID - %Bias	**0.250**	**0.375**	**0.500**	**1.00**	**2.50**	**5.00**	**7.50**	**10.0**
1	0.252	0.391	0.493	0.97	2.42	5.34	6.77	10.5
Bias (%)	**0.8**	**4.3**	**-1.4**	**-2.9**	**-3.2**	**6.8**	**-9.7**	**5.0**
2	0.226	0.382	0.499	0.982	2.71	5.20	7.84	9.29
Bias (%)	**-9.6**	**1.9**	**-0.2**	**-1.8**	**8.4**	**4.0**	**4.5**	**-7.1**
3	0.269	0.364	0.493	1.01	2.40	4.90	7.55	10.1
Bias (%)	**7.6**	**-2.9**	**-1.4**	**1.0**	**-4.0**	**-2.0**	**0.7**	**1.0**
4	0.281	0.395	0.514	0.90	2.16	4.83	7.73	10.3
Bias (%)	**12.4**	**5.3**	**2.8**	**-9.6**	**-13.6**	**-3.4**	**3.1**	**3.0**
5	0.279	0.375	0.448	0.98	2.45	4.99	7.93	9.67
Bias (%)	**11.6**	**0.0**	**-10.4**	**-1.6**	**-2.0**	**-0.2**	**5.7**	**-3.3**
6	0.262	0.366	0.474	1.04	2.43	5.11	7.49	10.0
Bias (%)	**4.8**	**-2.4**	**-5.2**	**4.0**	**-2.8**	**2.2**	**-0.1**	**-0.5**
Statistic								
Mean	0.262	0.379	0.487	0.982	2.43	5.06	7.55	10.0
STDEV	0.020	0.013	0.023	0.046	0.17	0.19	0.42	0.44
CV (%)	7.6	3.4	4.7	4.7	7.0	3.8	5.6	4.4
Accuracy (%)	104.8	101.1	97.4	98.2	97.2	101.2	100.7	100.0

Table 41: *Precision and accuracy for the calibration standard of free Toxin A-HPA in mouse plasma from six qualification batches*

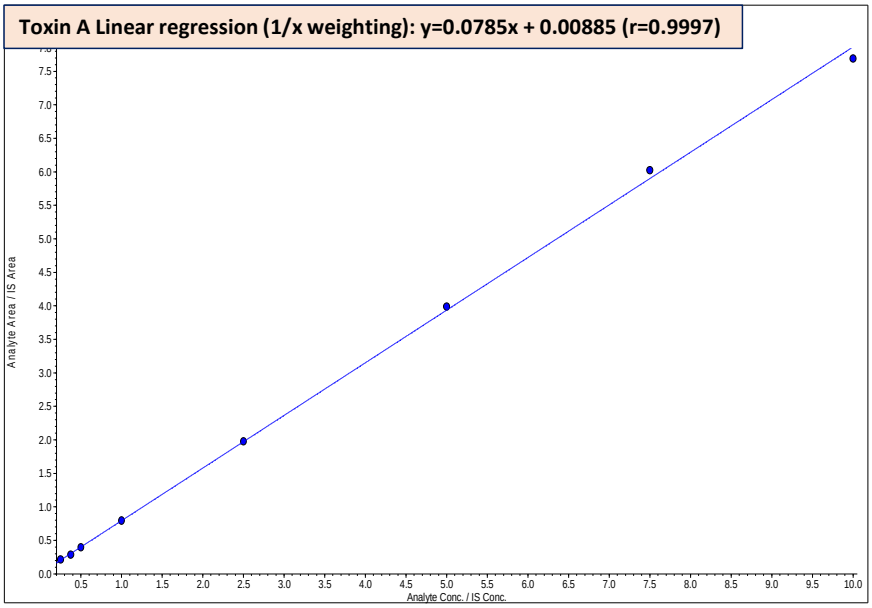

Figure 74: *A representative linear response of free Toxin A in plasma samples*

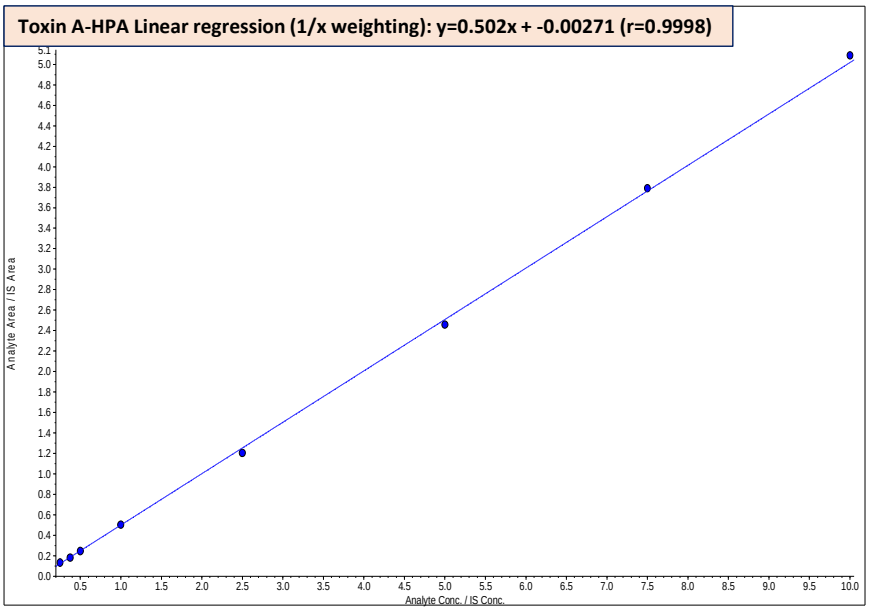

Figure 75**:** *A representative linear response of free Toxin A-HPA in plasma samples*

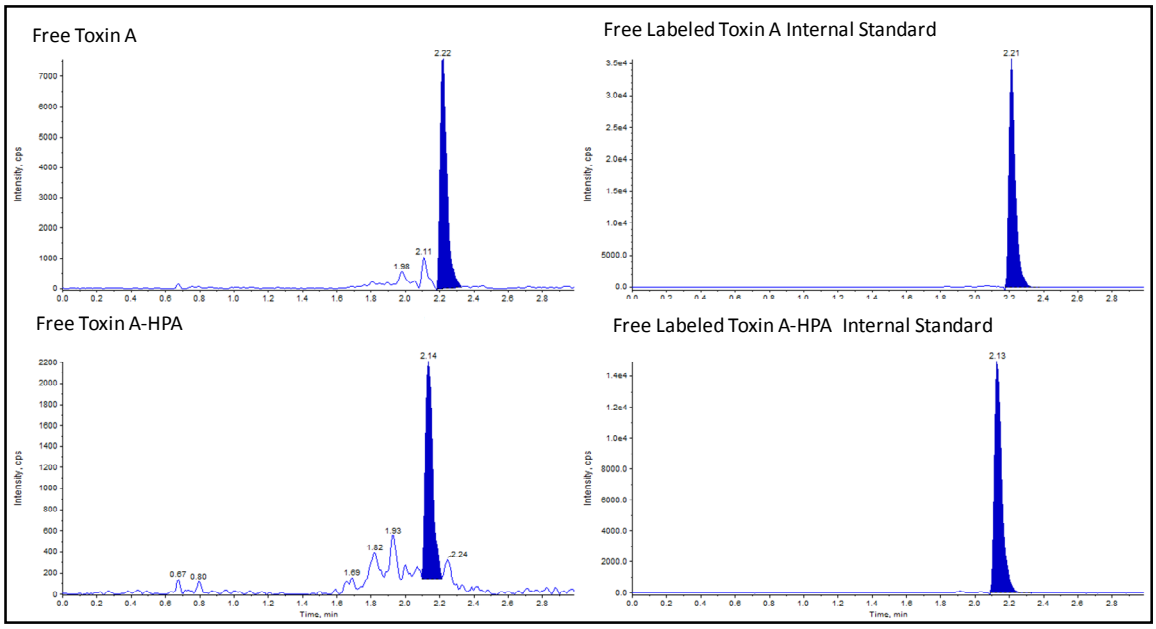

Figure 76: *Representative MRM chromatograms of free Toxin A and A-HPA at LLOQ level in plasma samples*

The carryover met the acceptance criteria in each run for both the analytes.

Toxin A			
Run ID	**AN Peak Area in LLOQ (Std1)**	**AN Peak Area in DBK after ULOQ**	**Carry Over (%)**
1	32937.1	466.5	1.4
2	20299.5	0.0	0.0
3	21430.3	95.8	0.4
4	14857.8	128.8	0.9
5	13190.2	0.0	0.0
6	13797.0	0.0	0.0
Toxin A-HPA			
Run ID	**AN Peak Area in LLOQ (Std1)**	**AN Peak Area in DBK after ULOQ**	**Carry Over (%)**
1	8323.8	0.0	0.0
2	5823.1	761.0	13.1
3	6590.5	106.7	1.6
4	4946.0	61.6	1.2
5	5089.0	660.6	13.0
6	4434.2	0.0	0.0

Table 42*: Carryover evaluation for Toxin A and A-HPA*

The slope value was consistent for six consecutive batches and the slope variation was ≤ 3.5 and ≤ 9.3 for Toxin A and A-HPA respectively, over all the runs. The correlation coefficient (r) of the linear regression was between 0.9970-0.9998 and between 0.99971-0.9998 for Toxin A and A-HPA respectively, over all the runs **(Figure 77** and **Figure 78).**

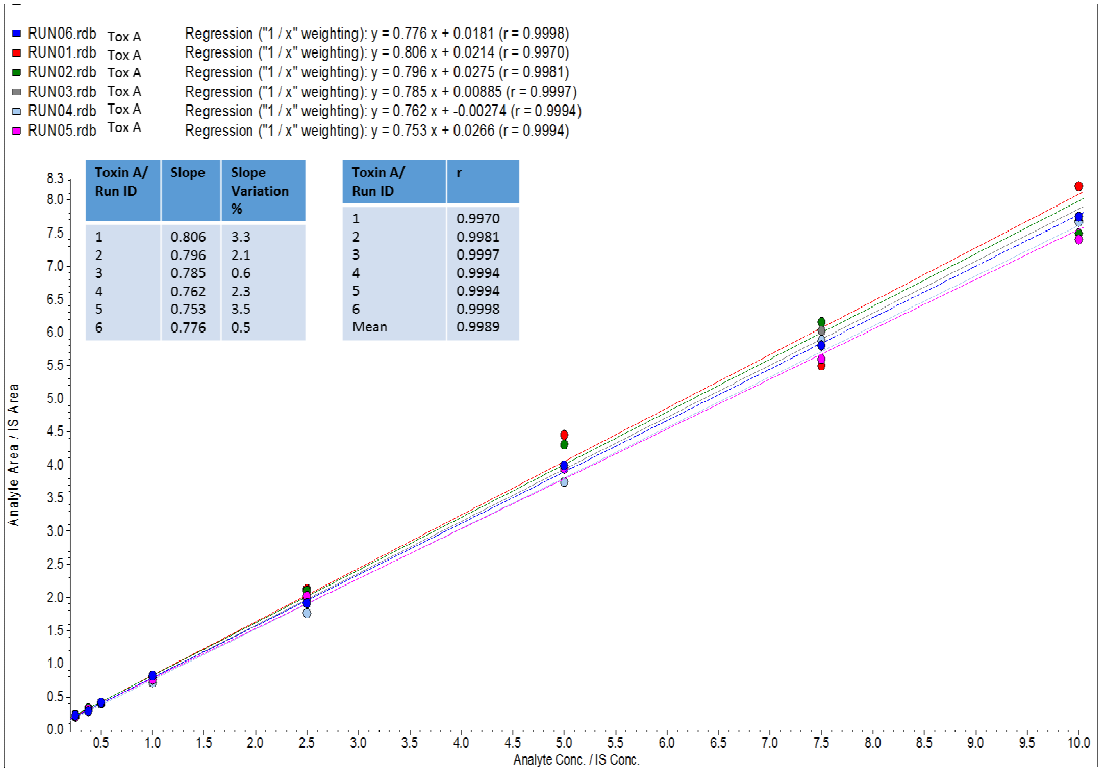

Toxin A/ Run ID	Slope	Slope Variation %
1	0.806	3.3
2	0.796	2.1
3	0.785	0.6
4	0.762	2.3
5	0.753	3.5
6	0.776	0.5

Toxin A/ Run ID	r
1	0.9970
2	0.9981
3	0.9997
4	0.9994
5	0.9994
6	0.9998
Mean	0.9989

Figure 77*: Overlay of the Toxin A calibration curves of the study. The slope variation (%) and the correlaction coefficient data show method reproducibility.*

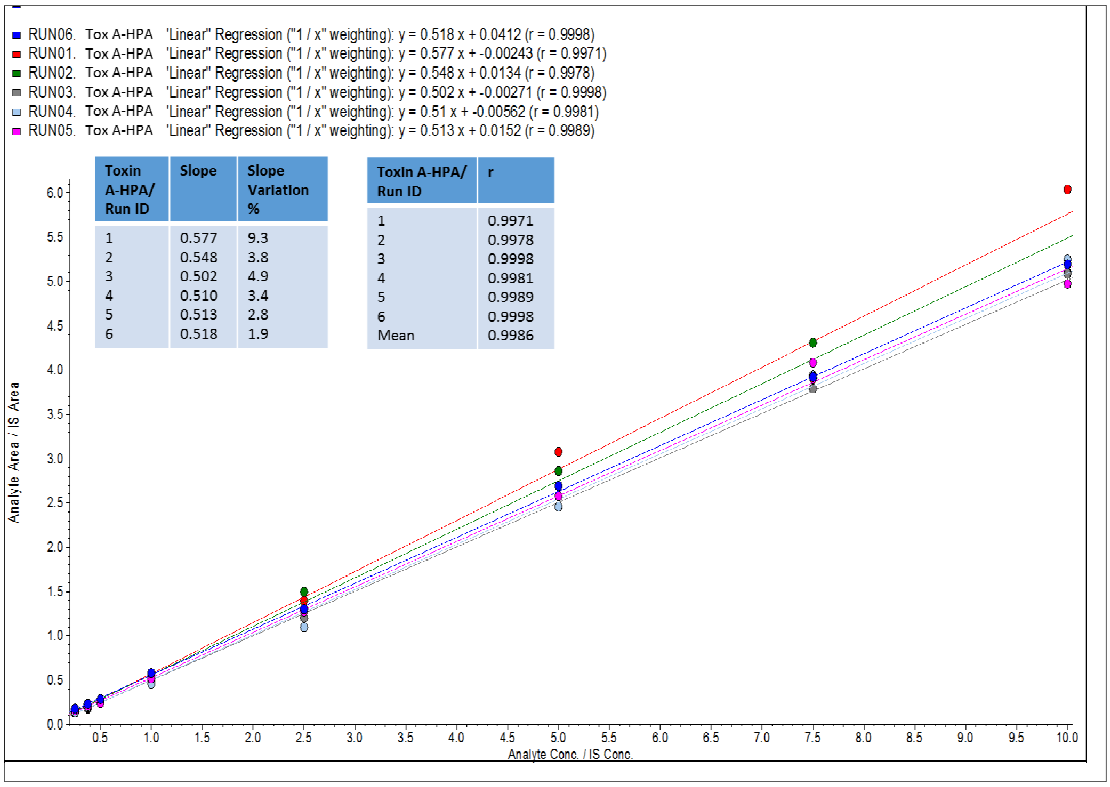

***Figure 78**: Overlay of the Toxin A-HPA calibration curves of the study. The slope variation (%) and the correlaction coefficient data show method reproducibility.*

The LLOQ was taken as the lowest calibration concentration that passed acceptance criteria with a signal-to-noise (x4 standard deviation) of a least 5:1.

3.7.2. Intra-Inter Run Accuracy and Precision

Method accuracy and precision were evaluated using Spiked Samples (SS) prepared by spiking Toxin A and Toxin A-HPA into the blank plasma at five concentration levels (0.250, 0.750, 3.75, 8.00 and 10.0 ng/mL) to serve as SS LLOQ, SS Low, SS Medium, SS High and SS ULOQ.

Three consecutive batches were prepared and each batch contained a freshly prepared calibration curve and five replicates of SS samples at the five levels.

Intra-assay precision was calculated by obtaining the Coefficient of Variation (CV) % of the five replicates of each SS level, and intra-assay accuracy was calculated by averaging the accuracies (Bias%) of five replicates of each SS level against the fresh curve.

Inter-assay precision was calculated by obtaining the %CV of all 11 replicates at each SS level from all the three batches, with overall accuracy calculated by averaging the accuracies of all 11 replicates at each SS level from all the three batches.

Toxin A: accuracy (%Bias) ranged from -9.3% to 3.8% and precision (%CV) ranged from 1.3% to 6.7% for intra-assay. Accuracy (%Bias) ranged from -8.2% to 3.5% and precision (%CV) ranged from 3.8% to 5.5% for inter-assay.

Toxin A-HPA: accuracy (%Bias) ranged from -6.9% to 5.1% and precision (%CV) ranged from 1.8% to 5.1% for intra-assay . Accuracy (%Bias) ranged from -3.0% to 4.9% and precision (%CV) ranged from 3.8% to 6.6% for inter-assay.

Accuracy and precision were evaluated including SS-LLOQ and SS-ULOQ (**Table 43** and **Table 44**, **Figure 79** and **Figure 80**).

In conclusion, **the method was found to be highly accurate and precise.**

The statistics on QC samples used for run acceptance and to perform runs 04, 05 and 06 for Selectivity, Freeze and Thaw, Bench-top, dilution integrity and autosampler stability 24 and 72 hour tests are reported in **Table 45** and **Table 46.**

Toxin A Intra-assay	**SS-LLOQ (ng/mL) 0.250**	**SS-Low (ng/mL) 0.750**	**SS-Medium (ng/mL) 3.75**	**SS-High (ng/mL) 8.00**	**SS-ULOQ (ng/mL) 10.0**
Mean Conc.	0.233	0.779	3.40	7.87	9.80
Intra-Run Accuracy (%BIAS)	-6.0	3.8	-9.3	-1.7	-2.0
SD	0.01	0.04	0.06	0.10	0.66
Intra-Run Precision (%CV)	4.3	5.1	1.8	1.3	6.7
n	5	5	5	5	5
Toxin A Inter-assay	**SS-LLOQ (ng/mL) 0.250**	**SS-Low (ng/mL) 0.750**	**SS-Medium (ng/mL) 3.75**	**SS-High (ng/mL) 8.00**	**SS-ULOQ (ng/mL) 10.0**
Overall Mean Conc.	0.230	0.780	3.44	7.88	9.97
Intra-Run Accuracy (%BIAS)	-6.6	3.5	-8.2	0.3	-0.3
Overall SD	0.01	0.03	0.19	0.37	0.48
Intra-Run Precision (%CV)	4.3	3.8	5.5	4.7	4.8
n	11	11	11	11	11

***Table 43**: Toxin A, Intra-assay and Inter-assay accuracy and precision*

Toxin A-HPA Intra-assay	SS-LLOQ (ng/mL) 0.250	SS-Low (ng/mL) 0.750	SS-Medium (ng/mL) 3.75	SS-High (ng/mL) 8.00	SS-ULOQ (ng/mL) 10.0
Mean Conc.	0.254	0.788	3.49	7.96	9.78
Intra-Run Accuracy (%BIAS)	1.4	5.1	-6.9	-0.5	-2.2
SD	0.01	0.04	0.14	0.14	0.50
Intra-Run Precision (%CV)	3.9	5.1	4.0	1.8	5.1
n	5	5	5	5	5
Toxin A-HPA Inter-assay	**SS-LLOQ (ng/mL) 0.250**	**SS-Low (ng/mL) 0.750**	**SS-Medium (ng/mL) 3.75**	**SS-High (ng/mL) 8.00**	**SS-ULOQ (ng/mL) 10.0**
Overall Mean Conc.	0.248	0.787	3.64	7.98	10.0
Intra-Run Accuracy (%BIAS)	-0.7	4.9	-3	1.4	0.4
Overall SD	0.01	0.03	0.24	0.34	0.5
Intra-Run Precision (%CV)	4.0	3.8	6.6	4.3	5.0
n	11	11	11	11	11

Table 44: *Toxin A-HPA, Intra-assay and Inter-assay accuracy and precision*

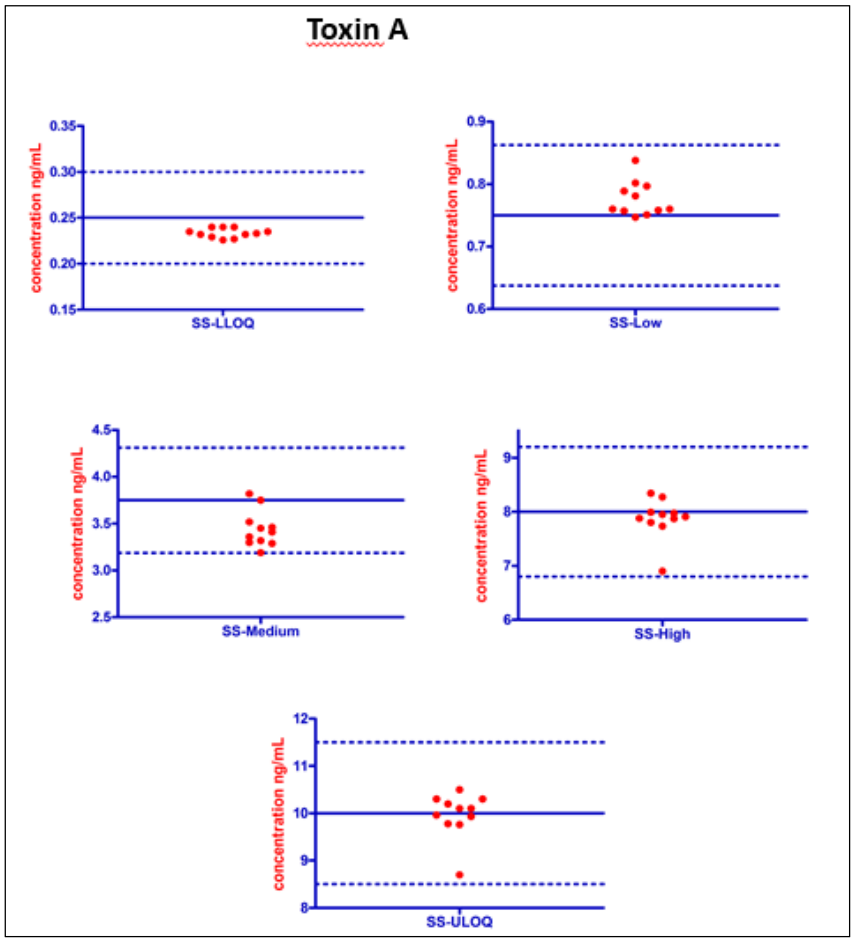

Figure 79: *Scatter plot of the toxin A Spiked Samples analyzed for intra-and inter-run accuracy and precision assessment.*

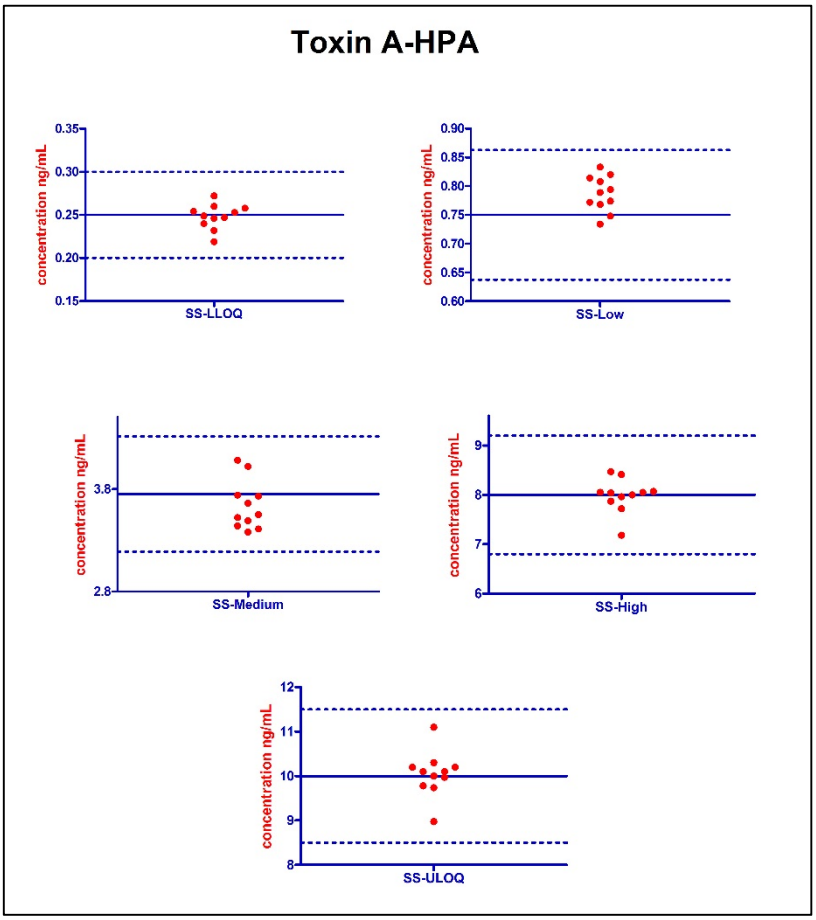

***Figure 80**: Scatter plot of the toxin A-HPA Spiked Samples analyzed for intra-and inter-run accuracy and precision assessment.*

Toxin A						
Run ID	**QC-Low 0.750 (ng/mL)**	**Bias (%)**	**QC-Medium 3.75 (ng/mL)**	**Bias (%)**	**QC-High 8.00 (ng/mL)**	**Bias (%)**
04	0.859	14.5	3.91	4.3	7.21	-9.9
	0.851	13.5	3.97	5.9	7.97	-0.4
05	0.705	-6.0	4.10	9.3	8.35	4.4
	0.820	9.3	3.98	6.1	8.11	1.4
06	0.708	-5.6	3.94	5.1	8.04	0.5
	0.757	0.9	3.80	1.3	8.47	5.9
Mean	0.783		3.95		8.03	
SD	0.1		0.1		0.4	
%CV	12.8		2.5		5.0	
Accuracy (%)	104.4		105.3		100.4	
%Bias	4.4		5.3		0.3	
n	6		6		6	

***Table 45**: Toxin A, Individual Concentration and Summary Statistics for Quality Control Samples*

Toxin A-HPA						
Run ID	**QC-Low 0.750 (ng/mL)**	**Bias (%)**	**QC-Medium 3.75 (ng/mL)**	**Bias (%)**	**QC-High 8.00 (ng/mL)**	**Bias (%)**
04	0.827	10.3	3.74	-0.3	7.04	-12.0
	0.815	8.7	3.91	4.3	7.98	-0.2
05	0.675	-10.0	3.77	0.5	8.16	2.0
	0.831	10.8	3.79	1.1	8.26	3.3
06	0.716	-4.5	3.63	-3.2	8.23	2.9
	0.753	0.4	3.62	-3.5	8.22	2.8
Mean	0.770		3.74		7.98	
SD	0.07		0.11		0.47	
%CV	9.1		2.9		5.9	
Accuracy (%)	102.7		99.7		99.8	
%Bias	2.6		-0.2		-0.2	
n	6		6		6	

Table 46**:** *Toxin A-HPA, Individual Concentration and Summary Statistics for Quality Control Samples*

3.7.3. Method selectivity

Method selectivity was evaluated by assaying:

- three replicates of blank plasma sample without analyte and internal standard to verify possible interferences at the analyte and internal standard retention time;
- three replicates of blank plasma sample with Internal Standard only to verify possible analyte traces at the analyte retention time;
- three replicates of blank plasma sample with analyte at ULOQ concentration level only to verify possible internal standard traces at the internal standard retention time;
- five LLOQ replicates to verify the accuracy and precision of the lowest concentration in plasma samples.

No interfering peaks were detected at the retention time of interest, as highlighted by the blue bar, for each MRM transition in blank matrix (**Table 47**, **Figure 81** and **Figure 82**).

Selectivity for Toxin A: • **matrix selectivity** • **selectivity vs AN** • **selectivity vs IS** • **matrix selectivity (LLOQ)**	 0.1% IS interference and 2.4% AN interference 0.1% IS interference 1.2% AN interference %BIAS ranged from -9.2 to -4.0 and the precision (%CV) was 2.3 (100% of LLOQ replicates passed)
Selectivity for Toxin A-HPA: • **matrix selectivity** • **selectivity vs AN** • **selectivity vs IS** • **matrix selectivity (LLOQ)**	 0.1% IS interference and 4.0% AN interference 0.2% IS interference 2.4% AN interference %BIAS ranged from -4.4 to 8.8 and the precision (%CV) was 5.1 (100% of LLOQ replicates passed)

Table 47: *Toxin A and A-HPA selectivity data*

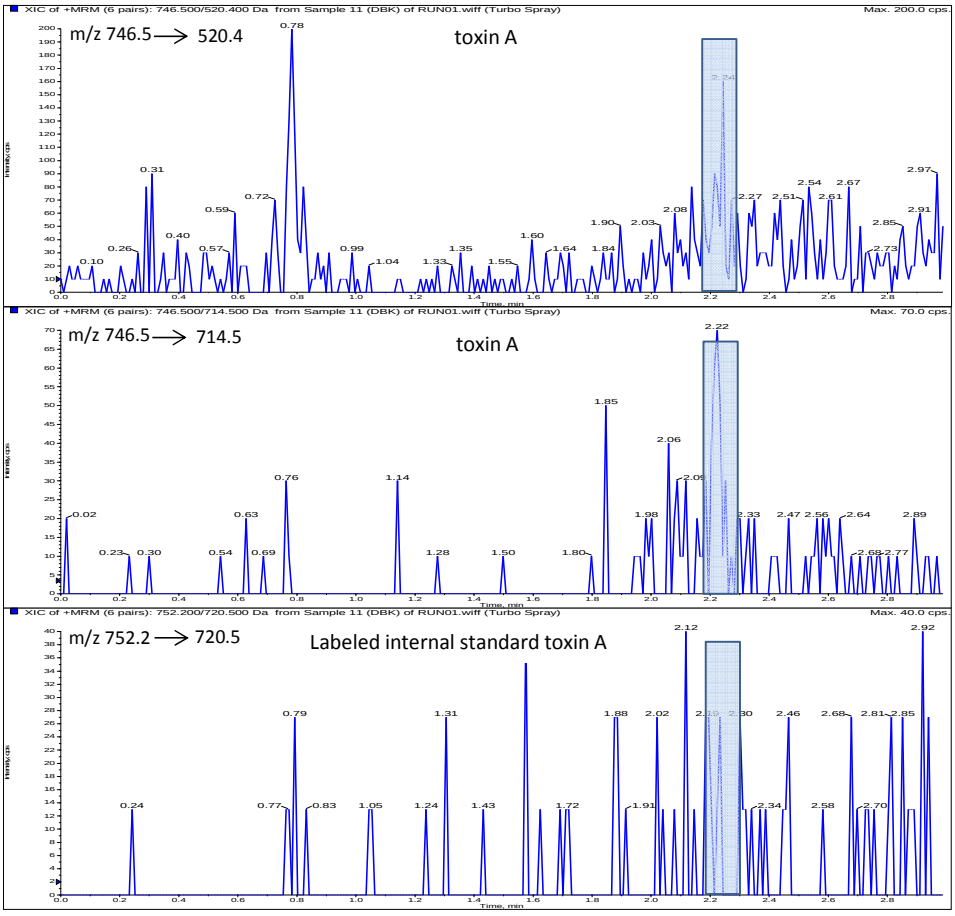

Figure 81: *MRM transitions of toxin A and its labeled internal standard in blank matrix. The blue bar shows that no interfences are present at the analytes retention times.*

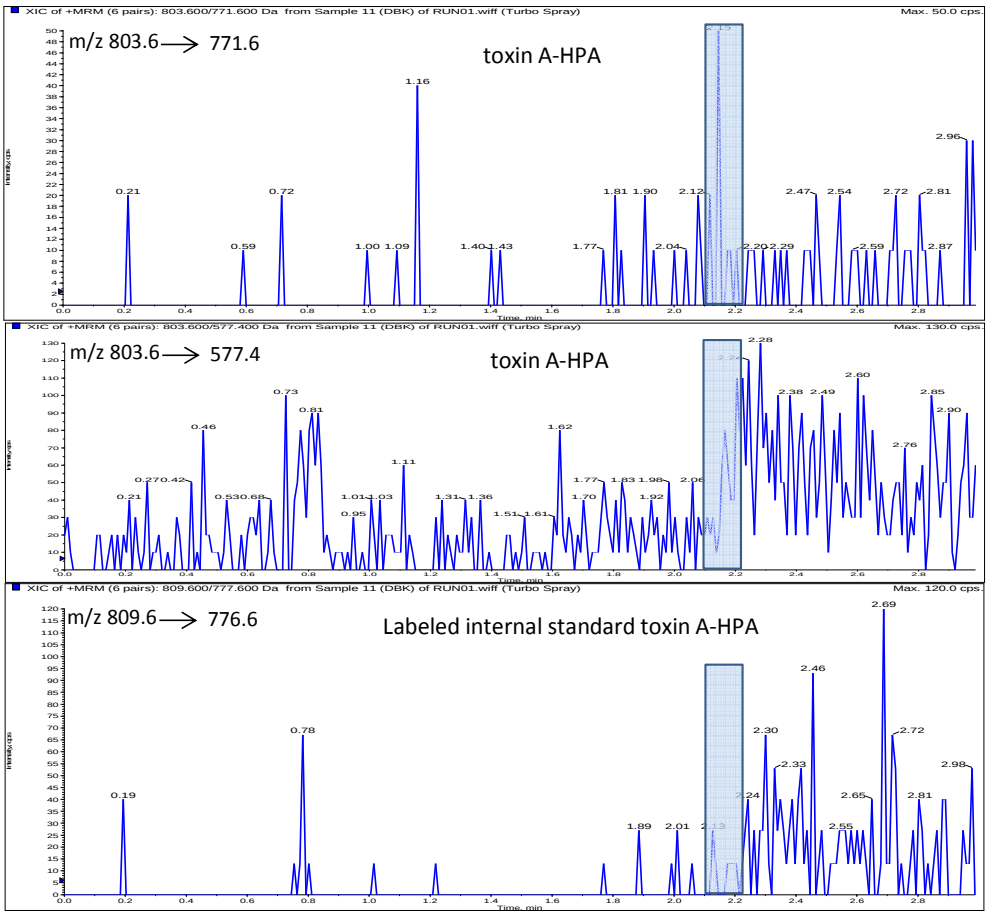

Figure 82: *MRM transitions of toxin A-HPA and its labeled internal standard in blank matrix. The blue bar shows that no interfences are present at the analytes retention times.*

3.7.4. Dilution Test

In order to verify that samples exceeding the calibration range can be analyzed after appropriate dilution, validation/dilution integrity samples were prepared at one level exceeding the calibration range.

Subsequently, samples were diluted with blank matrix in order to bring the concentrations into the calibration range. A spiked sample at 75.0 µg/mL in normal mouse plasma pool was prepared at a concentration level requiring a maximum dilution factor of 100.

Results show that the samples diluted 100 fold correctly fit the calibration curve (**Table 48** and **Table 49**).

Toxin A RUN ID 4 ID	Back Calculated Conc. (nominal value 750 ng/mL
	688 **632** **685**
Mean Conc.	668
Mean Accuracy (%BIAS)	-10.9
SD	31.5
Precision (%CV)	4.7
n	3

Table 48: *Toxin A, dilution test*

Toxin A – HPA RUN ID 4 ID	Back Calculated Conc. (nominal value 750 ng/mL
	639 663 672
Mean Conc.	658
Mean Accuracy (%BIAS)	-12.3
SD	17.1
Precision (%CV)	2.6
n	3

Table 49: *Toxin A-HPA, dilution test*

3.7.5. Stability Investigations

Drug stability experiments should mimic conditions under which samples are collected, stored, and processed, as closely as possible. The experiments should be conducted in unaltered representative matrix, including the same type of anticoagulant and cover the time periods of actual or anticipated sample storage under the individual conditions. Stability samples were prepared at both a low and high concentration covering the calibration range (typically, samples should be prepared at the low and high validation level (~3x LLOQ and ~75-80% ULOQ).

The following stability experiments in biological matrix were performed:

- Bench-top stability (during sample preparation without special protection from daylight)
- Post-preparative stability (autosampler stability or re-injection feasibility)
- Freeze and thaw stability (during repeated freezing and thawing cycles). Samples should be stored frozen for at least 12h and thawed applying the same conditions

tested for bench-top stability (e.g. if bench-top stability calls for storage on wet ice, freeze/thaw stability samples must be thawed on wet ice as well)

In case of multi-analyte assays, stability must be evaluated in the presence of all analytes (i.e. stability samples spiked with all analytes). This is particularly important for bioequivalence trials.

The results reported in **Table 50** and **Table 52** showed that the spiked samples extracted are stable in the autosampler for 72 hours at 5°C. Additionally, the spiked samples thawed and kept for 2 hours at room temperature (time needed to process the samples) are stable and the spiked sample frozen and thawed for three times are stable under these conditions (**Figure 83** and **Figure 84**).

Toxin A - Run ID 6	**SS-Low (ng/mL)**	**SS-High (ng/mL)**
Autosampler Stability at 48h	**0.750**	**8.00**
Mean Conc.	0.774	8.18
Mean Accuracy (%BIAS)	3.2	2.3
SD	0.04	0.09
Precision (%CV)	5.2	1.1
n	3	3
Toxin A - Run ID 6	**SS-Low (ng/mL)**	**SS-High (ng/mL)**
Autosampler Stability at 72h	**0.750**	**8.00**
Mean Conc.	0.752	7.93
Mean Accuracy (%BIAS)	0.3	-0.9
SD	0.03	0.14
Precision (%CV)	4.0	1.8
n	3	3

Table 50: *Toxin A, Autosampler stability test*

Toxin A - Run ID 4 Bench-Top Stability 2h at RT	SS-Low (ng/mL) 0.750	SS-High (ng/mL) 8.00
Mean Conc.	0.809	8.29
Mean Accuracy (%BIAS)	7.8	3.7
SD	0.03	0.07
Precision (%CV)	3.7	0.8
n	3	3
Toxin A - Run ID 4 **Freeze&Thaw Stability 3 cycles**	**SS-Low (ng/mL)** **0.750**	**SS-High (ng/mL)** **8.00**
Mean Conc.	0.784	7.82
Mean Accuracy (%BIAS)	4.5	-2.2
SD	0.046	0.39
Precision (%CV)	5.9	5.0
n	3	3

Table 51**:** *Toxin A, bench-top and Freeze&Thaw stability test*

Toxin A-HPA - Run ID 5 Autosampler Stability at 48h	SS-Low (ng/mL) 0.750	SS-High (ng/mL) 8.00
Mean Conc.	0.776	8.51
Mean Accuracy (%BIAS)	3.5	6.4
SD	0.013	0.067
Precision (%CV)	1.7	0.8
n	3	3
Toxin A-HPA - Run ID 6 **Autosampler Stability at 72h**	**SS-Low (ng/mL)** **0.750**	**SS-High (ng/mL)** **8.00**
Mean Conc.	0.754	8.49
Mean Accuracy (%BIAS)	0.5	6.1
SD	0.029	0.42
Precision (%CV)	3.8	4.9
n	3	3

Table 52: *Toxin A-HPA, autosampler stability test*

Toxin A-HPA -Run ID 4	SS-Low (ng/mL)	SS-High (ng/mL)
	0.750	**8.00**
Bench-Top Stability 2h at RT		
Mean Conc.	0.845	8.48
Mean Accuracy (%BIAS)	12.6	5.9
SD	0.041	0.24
Precision (%CV)	4.9	2.8
n	3	3
Toxin A-HPA -Run ID 4	**SS-Low (ng/mL)**	**SS-High (ng/mL)**
	0.750	**8.00**
Freeze&Thaw Stability 3 cycles		
Mean Conc.	0.782	7.71
Mean Accuracy (%BIAS)	4.3	-3.6
SD	0.071	0.15
Precision (%CV)	9.1	1.9
n	3	3

Table 53: *Toxin A-HPA, Bench-top and Freeze&Thaw stability test*

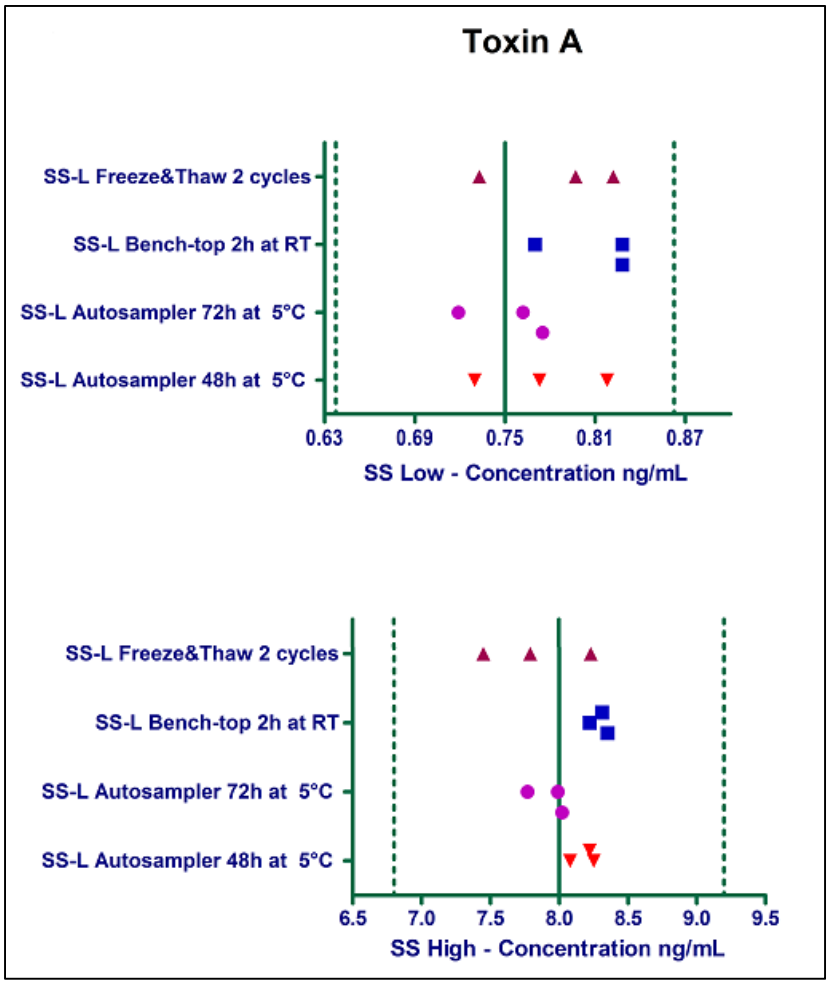

Figure 83: *The scatter plot shows that the toxin A spiked samples are stable under the conditions tested for stability assessment. The SS are within the range (nominal value ± 15%).*

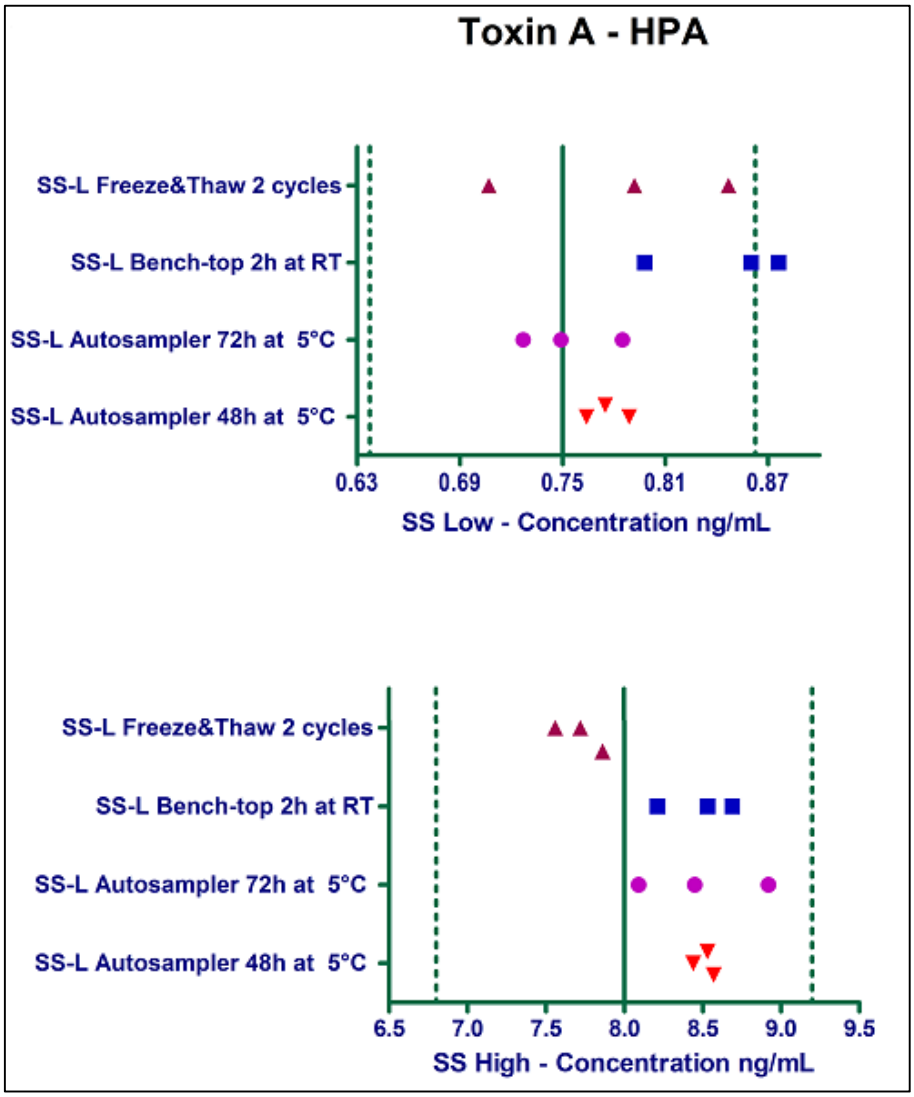

***Figure 84**: The scatter plot shows that the toxin A-HPA spiked samples are stable under the conditions tested for stability assessment. The SS are within the range (nominal value ± 15%).*

3.8. Conclusion

The qualified method for the determination of free toxins in plasma was accurate, precise, selective, linear and without significative matrix interferences. Our goal was to develop (see paragraph 3.6) and quantify a robust, reproducible method using 5.0 µL of sample only, due to the limited availability of blood and consequently of plasma from the *in-vivo* mouse toxicity study.

Both analytes were detected and quantified in the same analytical run with a good chromatographic separation.

3.9. Method development of Free Toxin A and Toxin A-HPA in homogenized tumor tissue samples

The method development of free toxins quantitation in homogenized tumor tissue was set up on the basis of the experiments performed for plasma matrix.

Spiked samples in tumor tissue were analyzed in three batches in order to verify the accuracy and precision of the method in tumor matrix.

The preliminary results obtained showed good precision, accuracy and reproducibility of the method (see **Table 54** and **Table 55**).

Run ID	**LLOQ**	**Low**	**Medium**	**High**	**ULOQ**
Batch 1	**ng/mL**	**ng/mL**	**ng/mL**	**ng/mL**	**ng/mL**
	0.250	**0.750**	**3.75**	**8.00**	**10.0**
Mean	0.239	0.622	3.27	7.31	9.46
Mean %BIAS	-4.3	-17.1	-12.8	-8.7	-5.4
STDEV (%)	0.0104	0.115	0.096	0.362	0.380
%CV	4.4	18.5	2.9	5.0	4.0
Run ID	**LLOQ**	**Low**	**Medium**	**High**	**ULOQ**
Batch 2	**ng/mL**	**ng/mL**	**ng/mL**	**ng/mL**	**ng/mL**
	0.250	**0.750**	**3.75**	**8.00**	**10.0**
Mean	0.255	0.678	3.14	7.51	9.10
Mean %BIAS	2.0	-9.6	-16.2	5.1	-9.5
STDEV (%)	0.0144	0.014	0.040	0.670	0.070
%CV	5.6	2.1	1.3	8.9	0.8
Run ID	**LLOQ**	**Low**	**Medium**	**High**	**ULOQ**
Batch 3	**ng/mL**	**ng/mL**	**ng/mL**	**ng/mL**	**ng/mL**
	0.250	**0.750**	**3.75**	**8.00**	**10.0**
Mean	0.260	0.730	3.36	7.35	9.08
Mean %BIAS	4.1	-2.7	-10.4	-8.1	-9.2
STDEV (%)	0.0160	0.0728	0.190	0.440	1.03
%CV	6.2	10.0	5.7	6.0	11.3
Overall mean	0.252	0.677	3.26	7.39	9.21
Overall mean %BIAS	0.6	-9.8	-13.1	-3.9	-7.9
Overall STDEV (%)	0.0152	0.0830	0.140	0.450	0.620
Overall %CV	6.0	12.3	4.3	6.1	6.7
n	11	11	11	11	11

Table 54**:** *Toxin A accuracy and precision evaluation*

Run ID	LLOQ	Low	Medium	High	ULOQ
Batch 1	**ng/mL**	**ng/mL**	**ng/mL**	**ng/mL**	**ng/mL**
	0.250	**0.750**	**3.75**	**8.00**	**10.0**
Mean	0.210	0.632	3.25	7.30	9.83
Mean %BIAS	-16.0	-15.8	-13.3	-8.8	-1.7
STDEV (%)	0.0114	0.062	0.080	0.394	0.57
%CV	5.4	9.8	2.5	5.4	5.8
Run ID	**LLOQ**	**Low**	**Medium**	**High**	**ULOQ**
Batch 2	**ng/mL**	**ng/mL**	**ng/mL**	**ng/mL**	**ng/mL**
	0.250	**0.750**	**3.75**	**8.00**	**10.0**
Mean	0.231	0.678	3.33	7.53	10.2
Mean %BIAS	-7.7	-9.6	-11.3	4.9	2.0
STDEV (%)	0.0112	0.036	0.23	0.62	0.14
%CV	4.8	5.3	6.9	8.2	1.4
Run ID	**LLOQ**	**Low**	**Medium**	**High**	**ULOQ**
Batch 3	**ng/mL**	**ng/mL**	**ng/mL**	**ng/mL**	**ng/mL**
	0.250	**0.750**	**3.75**	**8.00**	**10.0**
Mean	0.242	0.698	3.58	7.73	9.50
Mean %BIAS	-3.1	-7.0	-4.6	-3.4	-5.0
STDEV (%)	0.0021	0.0522	0.24	0.56	0.63
%CV	0.9	7.5	6.7	7.2	6.6
Overall mean	0.228	0.674	3.39	7.52	9.80
Overall mean %BIAS	-8.9	-10.8	-9.7	-2.4	-1.6
Overall STDEV (%)	0.0163	0.050	0.23	0.50	0.54
Overall %CV	7.1	7.4	6.8	6.6	5.5
n	11	11	11	11	11

Table 55: *Toxin A-HPA accuracy and precision evaluation*

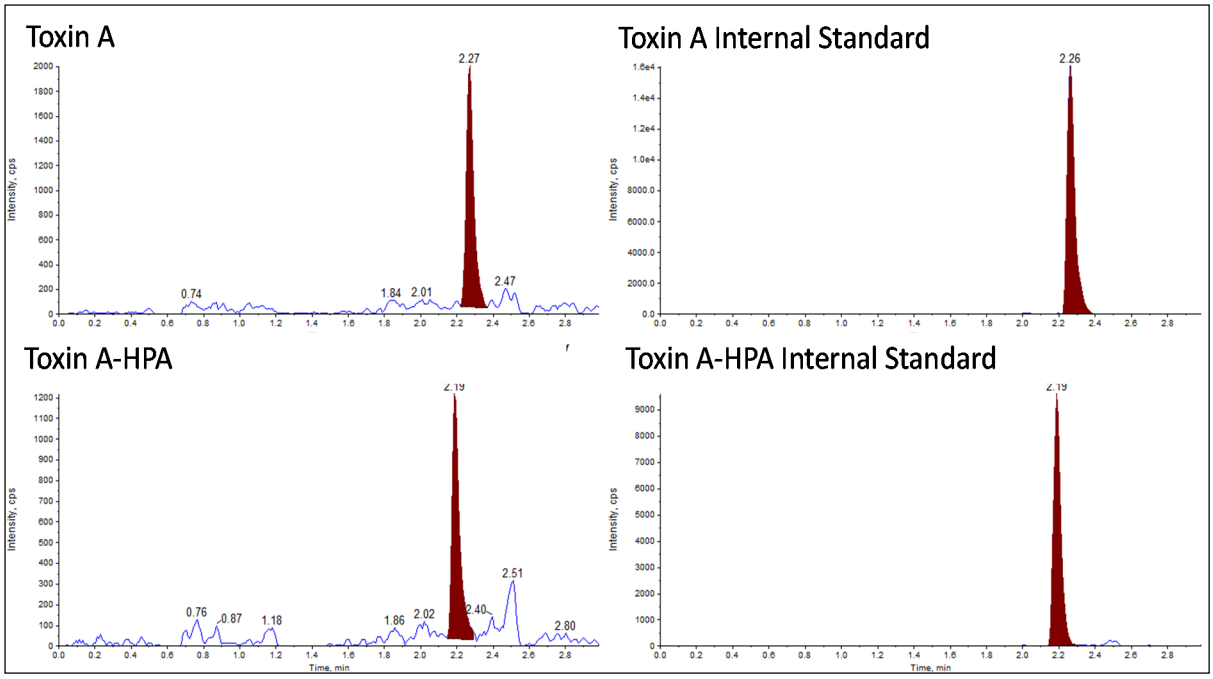

***Figure 85**: The MRM chromatogram of Toxin-A and Toxin-A HPA in human tumor tissue samples*

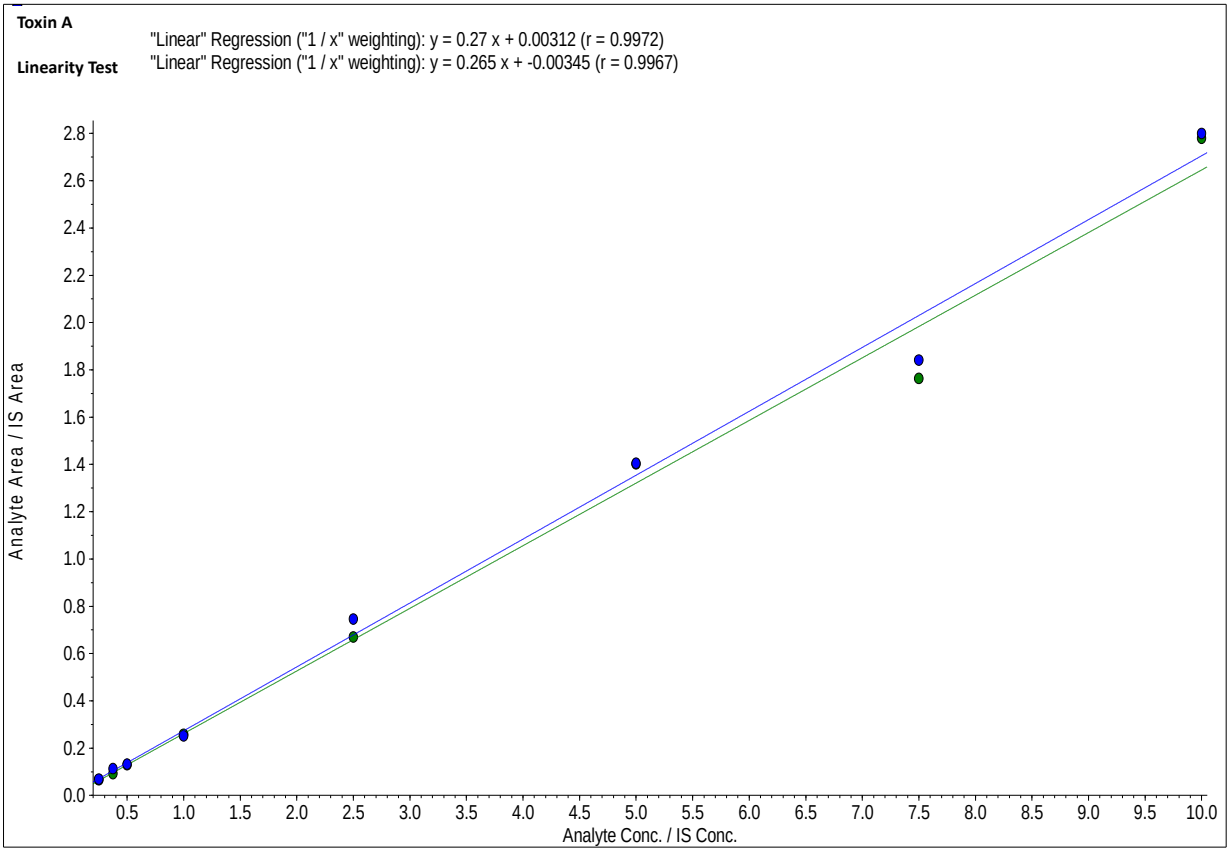

***Figure 86**: Overlay of two Toxin-A calibration curves*

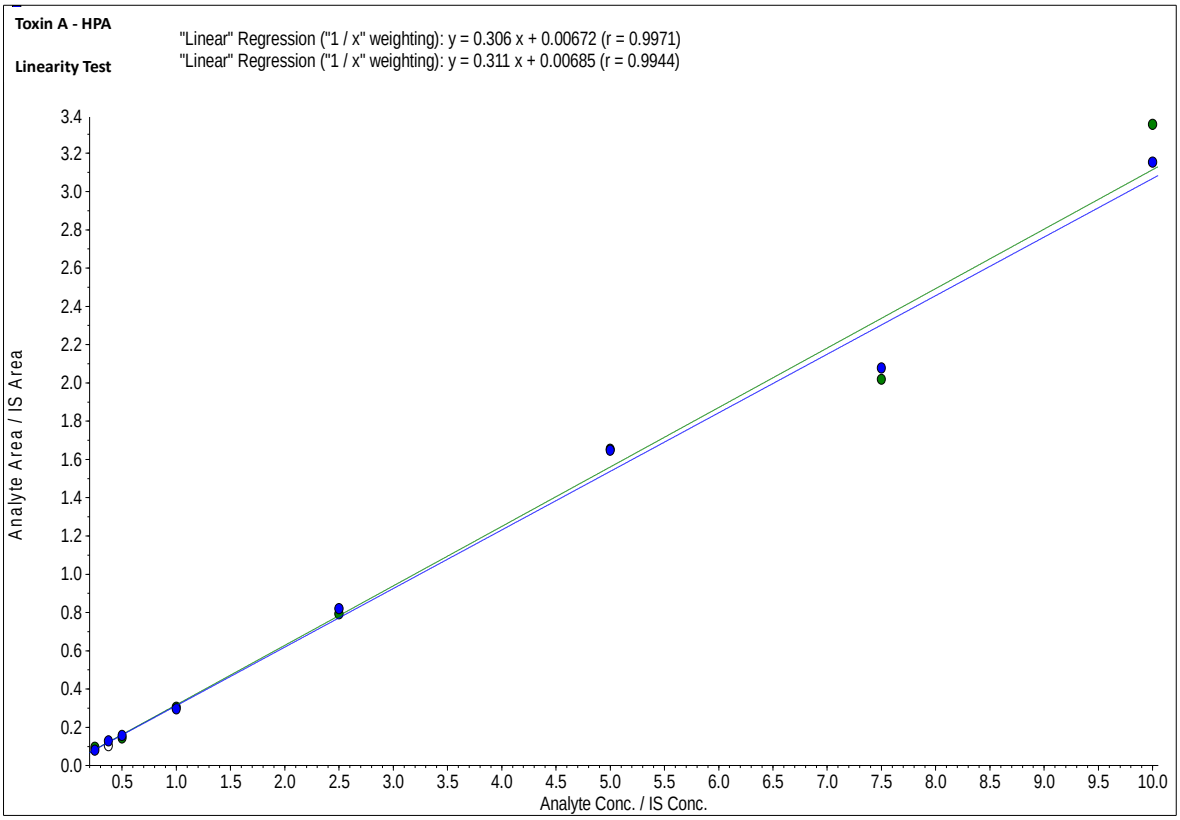

***Figure 87**: Overlay of two Toxin-A HPA calibration curves*

3.10. Conclusion

The results obtained during the preliminary experiment were promising.The next step will be to qualify the method in homogenized tumor tissue samples according to the experimental plan already applied to the other methods.

When cytotoxic drug is sequestered in tissues (non-circulating), the ability to quantitatively measure it in tissue compartments becomes particularly important.

Application of this bioanalytical method will provide information about the efficacy of the ADC in the tumor tissue. Comparison of free cytotoxin amount and total cytotoxin amount in tumor tissue will provide a more consistent data as the amount of total cytotoxin measured (obtained after sample hydrolysis) substracted to the amount of free toxin should be near to zero.

3.11. Qualification of the UPLC-MS/MS method for the Quantitation of Total Toxin A-HPA, Free Toxin A and Free Toxin A-HPA in monkey plasma samples

The payload and free drug UPLC-MS/MS methods were qualified also in monkey plasma samples. No changes in the UPLC-MS/MS conditions were introduced and therefore only the qualification summary tables are reported (see **Table 56** and **Table 57**).

The analytes response at LLOQ level was acceptable and no interfering peaks were detected in blank monkey extracted plasma samples (see **Figure 88** and **Figure 89**).

These methods were successfully applied to analysis of samples from a "*dose range-finding study by intravenouse administration in cynomolgus monkeys"*.
The study was conducted to obtain preliminary information on the local and systemic exposure of ADC-linker-drug after intravenouse administration to cynomolgus monkey, in order to establish the range of doses for a subsequent GLP-regulated toxicity study in the same species.

General Information	
Analytes	Toxin A and Toxin A-HPA
Internal Standard	Isotopically Labeled Toxin A and Toxin A-HPA
LLOQ	0.250 ng/mL
ULOQ	10.0 ng/mL
Sample matrix	Li –heparinized monkey plasma with citric acid
Toxin A	
Linearity	Accuracy (%) of all calibration standard points within ± 20% for LLOQ level and ± 15% for the other calibration standard points level
Intra-run accuracy and precision	Mean accuracy (%BIAS) ranged from -4.1% to 5.1% Precision (%CV) ranged from 2.3% to 5.8%
Inter-run accuracy and precision	Overall accuracy (%BIAS) ranged from -2.4% to 3.6% Overall precision (%CV) ranged from 4.4% to 8.0%
Selectivity: • matrix selectivity • selectivity vs AN • selectivity vs IS • matrix selectivity (LLOQ)	0.1% IS interference and 3.3% AN interference 0.1% IS interference 1.1% AN interference %BIAS ranged from -7.6% to -1.6% and the precision (%CV) was 2.3% (100% of LLOQ replicates passed)
AN carryover	≤ 20% of LLOQ peak area
Extended range after dilution	750 ng/mL
Autosampler stability at 5℃	72 hours
Bench-Top Stability	2 hours
Freeze&Thaw Stability	2 cycles
Toxin A - HPA	
Linearity	Accuracy (%) of all calibration standard points within ± 20% for LLOQ level and ± 15% for the other calibration standard points level
Intra-run accuracy and precision	Mean accuracy (%BIAS) ranged from -5.4% to 1.4% Precision (%CV) ranged from 3.1% to 7.2%
Inter-run accuracy and precision	Overall accuracy (%BIAS) ranged from -4.7% to 2.1% Overall precision (%CV) ranged from 3.3% to 9.1%
Selectivity: matrix selectivity selectivity vs AN selectivity vs IS matrix selectivity (LLOQ)	0.1% IS interference and 2.4% AN interference 0.0% IS interference 1.1% AN interference %BIAS ranged from -14.8 to 2 and the precision (%CV) was 7.2% (100% of LLOQ replicates passed)
AN carryover	≤ 20% of LLOQ peak area
Extended range after dilution	750 ng/mL
Autosampler stability at 5℃	24 hours
Bench-Top Stability	2 hours
Freeze & Thaw Stability	2 cycles

Table 56: Qualification summary table for free Toxin A and free Toxin A-HPA method

General Information	
Analyte	Linker-drug conjugate that after hydrolysis step generates free Toxin A-HPA
Internal Standard	Linker-drug conjugate that after hydrolysis step generates free Toxin A-HPA-labeled (it contains Isotopically labeled Toxin A -Val-^{15}N-^{13}C5 (Toxin A-IS)
LLOQ	10.00 ng/mL
ULOQ	5000 ng/mL
Sample matrix	Li –heparinized mouse plasma with citric acid
Parameters	
Linearity	Accuracy (%) of all calibration standard points within ± 20% for LLOQ level and ± 15% for the other calibration standard points level
Intra-run accuracy and precision	Mean accuracy (%BIAS) ranged from -6.0% to -0.1% Precision (%CV) ranged from 1.5% to 9.2%
Inter-run accuracy and precision	Overall accuracy (%BIAS) ranged from -5.9% to 1.6% Overall precision (%CV) ranged from 3.0% to 7.4%
Selectivity: • matrix selectivity • selectivity vs AN • selectivity vs IS • matrix selectivity (LLOQ)	0.0% IS interference and 8.6% AN interference 0.0% IS interference 6.6% AN interference %BIAS ranged from -5.9 to 3.5 and the precision (%CV) was 3.5% (100% of LLOQ replicates passed)
AN carryover	≤ 20% of LLOQ peak area
Extended range after dilution	200.0 µg/mL
Autosampler stability at 5℃	72 hours
Bench-Top Stability	2 hours
Freeze & Thaw Stability	3 cycles

Table 57: *Qualification summary table for Total Toxin A-HPA method*

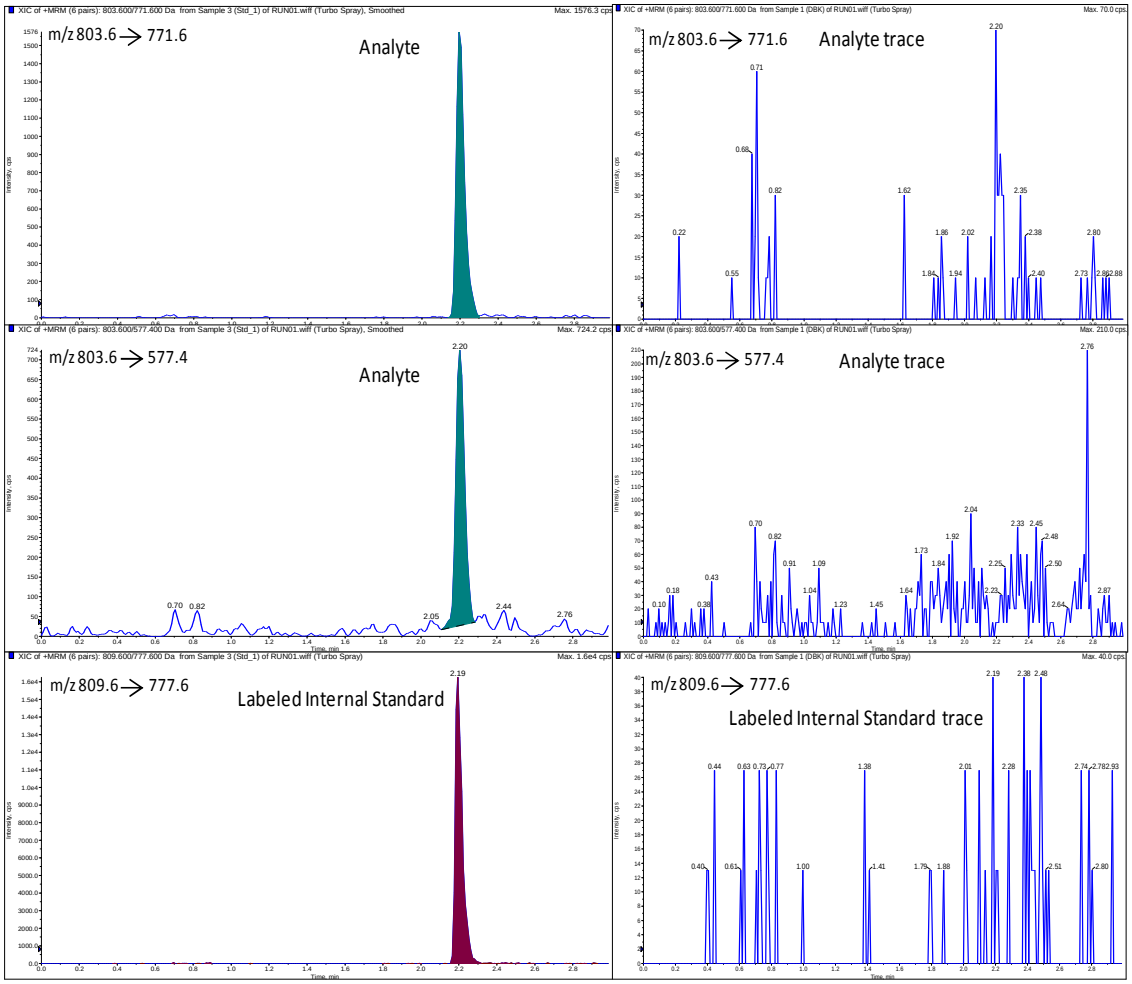

***Figure 88*:** *A representative MRM chromatogram of Toxin A-HPA and its labeled Internal Standard at LLOQ level and, on the left, MRM chromatogram of the extracted blank matrix showing no peak interferences*

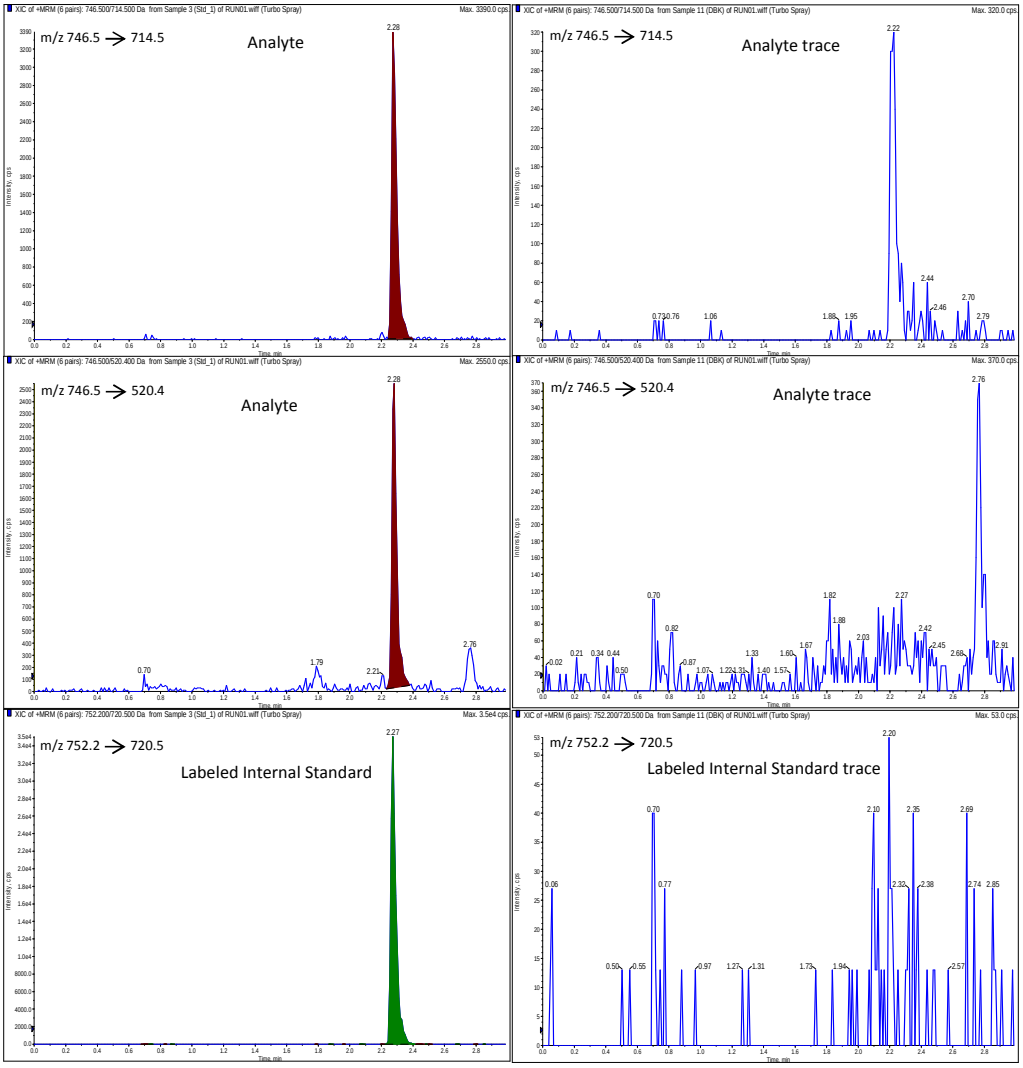

***Figure 89**: A representative MRM chromatogram of Toxin A and its labeled Internal Standard at LLOQ level and, on the left, MRM chromatogram of the extracted blank matrix showing no peak interferences*

3.12. Conclusion

The results of this study showed that the qualified LC-MS/MS method proved to be a robust, reliable, selective, and sensitive assay sufficient for simultaneous monitoring of pharmacokinetic parameters of free Toxin A and free Toxin A-HPA and Total Toxin A-HPA after sample hydrolysis.

A small plasma sample volume and LLOQ were sufficiently sensitive to detect terminal phase concentrations of the drugs.

The next step will be to determine the average drug-to-antibody ratio (DAR) and the total antibody (naked and conjugated) by using the LC-MS platform. This approach could introduce an orthogonal method to the conventional method (i.e ELISA method, commonly used for large molecule analysis for a single analyte).

Appendix I

Works published by the candidate

LC-MS method for the quantitation of two monoclonal antibodies by multiple signature peptides in monkey serum

By: Rita Mastroianni*, Marina Feroggio, Barbara Marsiglia, Clarissa Porzio Vernino, Simona Riva and Luca Barbero*

JOURNAL OF ANALYTICAL & BIOANALYTICAL TECHNIQUES
Volume: 6
Issue: 4
DOI: 10.4172/2155-9872.1000252
Published July 02, 2015
View Journal Information

Abstract

Evaluation of the in vivo concentration of a monoclonal antibody (mAb) mixture is a challenging task. Here we report the application of an LC-MS bioanalytical method in monkey serum to quantify Sym004, an equimolar mixture of two monoclonal antibodies, 992mAb and 1024mAb. This method has been validated according to industry standards and it is based on the determination of two specific signature peptides that report the single mAbs concentrations and on another peptide, common to the two mAbs, that measures the total concentration of the two target proteins.

It is shown that the total concentration is in agreement with the sum of the two single concentrations measured in spiked monkey serum samples. The consistency of the results will allow monitoring of the metabolic fate of different parts of the mAbs, at least in the central body compartment. This can then help to rationalize the design of the protein therapeutics modulating their stability accordingly.

Ultra-high performance liquid chromatography tandem high-resolution mass spectrometry study of tricyclazole photodegradation products in water

By: Gosetti, F (Gosetti, Fabio)[1]; Chiuminatto, U (Chiuminatto, Ugo)[2]; Mazzucco, E (Mazzucco, Eleonora)[1]; Mastroianni, R (Mastroianni, Rita)[3];Bolfi, B (Bolfi, Bianca)[1]; Marengo, E (Marengo, Emilio)[1]

ENVIRONMENTAL SCIENCE AND POLLUTION RESEARCH
Volume: 22
Issue: 11
Pages: 8288-8295
DOI: 10.1007/s11356-014-3983-4
Published: JUN 2015
View Journal Information

Abstract

This paper reports the study of the photodegradation reactions that tricyclazole can naturally undergo, under the action of sunlight, in aqueous solutions of standard tricyclazole and of the commercial BEAM(TM) formulation. The analyses are carried out by ultra-high performance liquid chromatography technique coupled with high-resolution tandem mass spectrometry. Analysis of both tricyclazole and BEAM(TM) water solutions undergone to hydrolysis does not evidence new chromatographic peaks with respect to the not treated solutions. On the contrary, analysis of the same samples subjected to sunlight irradiation shows a decreased intensity of tricyclazole signal and the presence of new chromatographic peaks. Two photodegradation products of tricyclazole have been identified, one of which has been also quantified, being the commercial standard available. The pattern is similar for the solutions of the standard fungicide and of the BEAM(TM) formulation. The results obtained from eco-toxicological tests show that toxicity of tricyclazole standard solutions is greater than that of the irradiated ones, whereas toxicity levels of all the BEAM(TM) solutions investigated (non-irradiated, irradiated, and hydrolyzed) are comparable and lower than those shown by tricyclazole standard solutions. Experiments performed in paddy water solution show that there is no difference in the degradation products formed.

Retrospective analysis for the identification of 4-aminocarminic acid photo-degradation products in beverages

By: Gosetti, F (Gosetti, Fabio)[1]; Chiuminatto, U (Chiuminatto, Ugo)[2]; Mastroianni, R (Mastroianni, Rita)[3]; Mazzucco, E (Mazzucco, Eleonora)[1];Manfredi, M (Manfredi, Marcello)[1,4]; Marengo, E (Marengo, Emilio)[1]

FOOD ADDITIVES AND CONTAMINANTS PART A-CHEMISTRY ANALYSIS CONTROL EXPOSURE & RISK ASSESSMENT
Volume: 32
Issue: 3
Pages: 285-292
DOI: 10.1080/19440049.2014.1003615
Published: MAR 4 2015
View Journal Information

Abstract

This article deals with the identification of the photo-degradation products of 4-aminocarminic acid potentially present in commercial beverages. Sixteen beverages of different composition but all containing the E120 dye were previously analysed by ultra-high-performance liquid chromatography (UHPLC) coupled with quadrupole-time of flight mass spectrometry to identify the common degradation products of the E120 dye. Since it is plausible to find unauthorised 4-aminocarminic acid in beverages which report generic E120 dye on the label, retrospective analysis was employed here not only to search for the possible presence of 4-aminocarminic acid but also to investigate the potential formation of photo-degradation products derived from this compound. For this purpose, a statistical approach based on Student's t-test was used to compare the degraded beverages containing 4-aminocarminic acid with all the others. Five degradation products were identified and their structures were elucidated on the basis of the high-accuracy and high-resolution of mass and mass/mass spectra. The toxicity of the degradation products was evaluated through the Ames Salmonella/microsome mutagenicity assay. No evidence of mutagenicity was obtained for the beverages subjected or not to irradiation, whereas a toxic effect of the 4-aminocarminic acid standard solution already at 100.0 ugL^{-1} was found. This leads, once again, to the conclusion that the toxicity study must be carried out on the beverages in order to take into account of all the possible masking/protection interactions among the ingredients.

Ultra-high-performance liquid chromatography/tandem high-resolution mass spectrometry analysis of sixteen red beverages containing carminic acid: Identification of degradation products by using principal component analysis/discriminant analysis

By: Gosetti, F (Gosetti, Fabio)[1]; Chiuminatto, U (Chiuminatto, Ugo)[2]; Mazzucco, E (Mazzucco, Eleonora)[1]; Mastroianni, R (Mastroianni, Rita)[3];Marengo, E (Marengo, Emilio)[1]

FOOD CHEMISTRY
Volume: 167
Pages: 454-462
DOI: 10.1016/j.foodchem.2014.07.026
Published: JAN 15 2015
View Journal Information

Abstract

The study investigates the sunlight photodegradation process of carminic acid, a natural red colourant used in beverages. For this purpose, both carminic acid aqueous standard solutions and sixteen different commercial beverages, ten containing carminic acid and six containing E120 dye, were subjected to photirradiation. The results show different patterns of degradation, not only between the standard solutions and the beverages, but also from beverage to beverage. Due to the different beverage recipes, unpredictable reactions take place between the dye and the other ingredients.

To identify the dye degradation products in a very complex scenario, a methodology was used, based on the combined use of principal component analysis with discriminant analysis and ultra-high-performance liquid chromatography coupled with tandem high resolution mass spectrometry. The methodology is unaffected by beverage composition and allows the degradation products of carminic acid dye to be identified for each beverage.

Acknowledgments

I would like to extend my grateful, sincere thanks to Merck for their financial and scientific support. My gratitude goes also to my colleagues and support staff.

I would like to thank the Department of “Scienze e Innovazione Tecnologica of the “Piemonte Orientale A. Avogadro" University for their scientific proficiency, guidance and understanding during my PhD.

Finally, and most importantly, I would like to thank my family and in particular my mother for all their support and encouragement.